A Nondegenerate Three-level Cascade Laser Coupled to a Two-mode Squeezed Vacuum Reservoir

A Dissertation Submitted to the
School of Graduate Studies
Addis Ababa University

In Partial Fulfilment
of the Requirement for the degree
of Doctor of Philosophy in Physics

Sintayehu Tesfa

February 2008

Acknowledgement

First and foremost I would like to express my deepest and heart felt thanks to Dr. Fesseha Kassahun, the thesis supervisor, for drawing my attention to the intricacy of three-level laser. Particularly, his invaluable guidance, relentless attention during our encounters, and meticulous evaluation of the entire work are indispensable in producing the dissertation in this extent and depth. The goodwill and assistance graciously offered by the staffs of the Department of Physics, specially W/ro Tilat and Ato Bogale, are so generous and satisfying. I am also grateful for the assistance of Dr. Mulugeta in sharing his views and materials in the early stage of the work. I wish to extend my deepest respect for the discussion I had with Prof. Singh that casted unprecedent effect on the shaping of my attitude towards scientific research. The brotherly advice and console of Dr. Tilahun during the most challenging moments of the work would not be forgotten. Word cannot express the effort of my friends and colleagues here in Physics Department and elsewhere by being behind me during those trying moments to be sane and complete the task. I only can say thank you, since the list too long to include. I wish that my heart felt thanks reach Kassahun and Melkamu for shouldering the most difficult responsibility in my behave. It would be unjust if I failed to express my appreciation to Dilla University for granting me the study leave. My sincere thanks go to my beloved family Tesfa, Firdawok, Fantu, Tayech, and Misrak for the financial and morale support they have rendered me. In the long ups and downs full of sorry saga the understanding, comfort, and love from Mekdes, Abel, and Bezawit that I gratefully enjoyed outshine all the rest.

Abstract

Detailed analysis of the squeezing of the cavity as well as the output radiation and statistical properties of the cavity radiation of a nondegenerate three-level cascade laser, in which the top and bottom levels of the injected atoms are coupled by an external coherent radiation, and whose cavity is coupled to a two-mode squeezed vacuum reservoir is presented. The generated radiation exhibits a high degree of squeezing in the minus quadrature either for a weak or strong driving radiation. In general, the degree of squeezing and mean number of photon pairs increase with the linear gain coefficient and squeeze parameter. The driving radiation leads to squeezing of the cavity radiation even when $\eta = 0$ and $\eta = 1$. Moreover, it is found that there is no distinct difference between the probability for finding odd and even number of photon pairs in the cavity. In addition, the mean number of photons in mode a turns out to be greater than that in mode b.

Contents

1

Introduction

The interaction of atoms with radiation is one of the central problems in quantum optics. In particular the interaction of three-level atoms, in different configurations, with radiation has attracted a great deal of interest for the last 20 years or so [1, 2, 3, 4]. In these studies, atomic coherence is found to be responsible for various important features of the emitted radiation. In recent years, a three-level cascade laser has drawn a considerable attention in connection with its potential as a source of squeezed light [4, 5, 6, 7, 8, 9, 10, 11]. The squeezing feature of the emitted radiation is due to atomic coherence that can be induced either by preparing the atoms initially in a coherent superposition of the top and bottom levels [4, 5, 6] or coupling these levels by an external radiation [7, 8, 9] or using these mechanisms simultaneously [10, 12, 13, 14].

The top, intermediate, and bottom levels of a three-level cascade atom can be conveniently denoted by $|a\rangle$, $|b\rangle$, and $|c\rangle$, respectively. A direct transition between levels $|a\rangle$ and $|c\rangle$ is taken to be dipole forbidden. When a three-level cascade atom decays from the top level to the bottom level via the intermediate level, two photons are emitted. If the two photons have the same frequency, the three-level atom is called degenerate otherwise nondegenerate. We define a three-level cascade laser as a quantum optical system in which three-level atoms in a cascade configuration and initially prepared in a coherent superposition of the top and bottom levels are injected at a constant rate into a cavity coupled to a vacuum reservoir. These atoms are removed from the cavity after sometime, which is long enough for the atoms to decay spontaneously to levels other than the middle or bottom.

A three-level laser has been studied by some authors [4, 5, 6] and the cavity radiation is found to be in a squeezed state under certain conditions. In addition, the mean and variance of the photon number for a degenerate three-level cascade laser have been calculated [15]. It is found that the mean photon number of the cavity radiation increases with the linear gain coefficient and the cavity radiation exhibits super-Poissonian photon statistics. Recently, a three-level laser whose cavity contains a parametric amplifier has been studied [16]. It is found that the parametric amplifier enhances the degree of squeezing of the cavity radiation. Furthermore, a three-level laser in which atomic coherence is induced by coupling the top and bottom levels by an external radiation has been studied by different authors [8, 11]. It is found that for a strong driving radiation this three-level cascade laser resembles a parametric oscillator. The atomic coherence induced by initially preparing the atoms in a coherent superposition of the top and bottom levels and by coupling these levels by a coherent radiation do not generally lead to the same degree of squeezing. Moreover, the cavity radiation of a degenerate three-level cascade laser in which the top and bottom levels are coupled by a strong coherent radiation has been investigated [10, 12, 13]. It is found that the cavity radiation exhibits second-order squeezing and the photon number distribution does not show different features in finding even and odd number of photons [10].

Although the degenerate three-level cascade scheme is mathematically more attractive, the study of the nondegenerate case has also attracted attention over the years. In this regard, An and Sargent III [17] developed a quantum theory of a nondegenerate multi-wave mixing for a three-level system in the presence of a two-mode radiation in the cavity. These authors predicted that this quantum system can be a source of a two-mode squeezed radiation. Recently Villas-Boas and Mousa [18] showed that a single driven nondegenerate three-level atom in a cascade configuration which is initially prepared in the coherent superposition of the top and bottom levels and placed in a cavity can be used to generate superposition of highly squeezed two-mode radiation in a weak driving limit and they also found that squeezing is relatively better in a strong driving limit. Moreover, Hu and Xu [19] most recently have extensively studied a collection of N nondegenerate three-level atoms in the cascade configuration confined in a cavity when the atoms are excited by two step external driving radiation. After calculating the Mandel Q-parameter and intensity fluctuations spectrum they found that due to the coherent excitation the laser intensity fluctuations are suppressed up to 50% below the shot noise limit and the laser line width is reduced below the ordinary laser. Furthermore, recent experiment by Buhner and Tamm [20] shows that there is an additional narrow peak due to an electron shelving in a driven nondegenerate three-level cascade atomic system. The theoretical explanation of this experimental result was given by Evers and Keitel [21] via calculating the resonance fluorescence spectrum using numerical analysis.

Nondegenerate three-level cascade laser is a source of a two-mode squeezed radiation that is characterized by a strong correlation of the modes at two different frequencies. The squeezing does not exist in each mode, but in the correlated state formed by the two modes. Due to the strong correlation between the modes, the two-mode squeezed radiation generally violates certain classical inequalities and hence can be applied in preparing Einstein-Podolsky-Rosen (EPR) [22] type entanglement [18], in quantum teleportation of continuous variables [23], and in testing of quantum nonlocality [24, 25] among others. Nondegenerate parametric oscillator [26], nondegenerate four-wave mixing [27], and optical kerr medium [28] are some sources of the two-mode squeezed radiation. In these quantum systems the optical losses and extra noise sources fundamentally associated with the optical nonlinearity required to generate squeezing limit the maximum achievable squeezing. For instance, the maximum two-mode squeezing produced by a nondegenerate parametric oscillator is limited to 50% [26]. However, we expect that the squeezing can be substantially improved for the nondegenerate three-level cascade laser, since the atoms left the cavity after sometime which is usually short.

In this dissertation, we seek to analyze a radiation generated by a nondegenerate three-level cascade laser in which the top and bottom levels of the three-level atoms are coupled by a strong coherent radiation. And the two-mode cavity radiation is coupled to a two-mode squeezed vacuum reservoir via a single-port mirror. We study the squeezing of the cavity radiation as well as the output radiation and the statistical properties of the cavity radiation. We carry out our analysis applying the solutions of the pertinent stochastic differential equations associated with the normal ordering. These differential equations are obtained following the procedure introduced by Fesseha [16]. We calculate in particular the quadrature variances, squeezing spectrum, mean and variance of the photon number pairs, photon number distribution, and variance of the photon number difference. To this end, we first derive the master equation for the quantum optical system under consideration in the linear and adiabatic approximation schemes following the approach described in Ref. [29]. Applying this master equation, we obtain stochastic differential equations associated with the normal ordering. We then find the solutions of these stochastic differential equations and the correlation properties of the associated noise forces following the procedure described in Refs. [30] and [16], respectively.

2

Master Equation

The Hamiltonian describing the coupling of the upper and bottom levels by coherent radiation at resonance can be expressed as

$$\hat{H}_C = i\frac{\Omega}{2}[|c\rangle\langle a| - |a\rangle\langle c|], \tag{2.1}$$

where Ω is a constant proportional to the amplitude of the coherent radiation. In addition, the interaction of a three-level cascade atom with a two-mode cavity radiation can be described in the interaction picture by the Hamiltonian

$$\hat{H}_I = ig[\hat{a}|a\rangle\langle b| - |b\rangle\langle a|\hat{a}^\dagger + \hat{b}|b\rangle\langle c| - |c\rangle\langle b|\hat{b}^\dagger], \tag{2.2}$$

where g is the coupling constant, taken to be the same for both transitions, and $(\hat{a}, \hat{b})$ are the annihilation operators for the two cavity modes. On the basis of Eqs. (2.1) and (2.2) the interaction of a three-level cascade atom, whose top and bottom levels are initially prepared in an arbitrary coherent superposition and also coupled by external coherent radiation, with two-mode cavity radiation can be described in the interaction picture by the Hamiltonian

$$\hat{H} = ig[\hat{a}|a\rangle\langle b| - |b\rangle\langle a|\hat{a}^\dagger + \hat{b}|b\rangle\langle c| - |c\rangle\langle b|\hat{b}^\dagger] + i\frac{\Omega}{2}[|c\rangle\langle a| - |a\rangle\langle c|]. \tag{2.3}$$

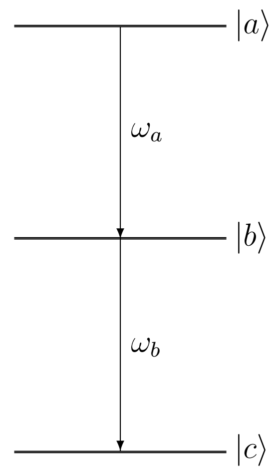

Fig. 2.1. Schematic representation of a nondegenerate three-level atom in a cascade configuration.

We take the initial state of a three-level atom to be

$$|\Psi_A(0)\rangle \ = C_a(0)|a\rangle + C_c(0)|c\rangle, \tag{2.4}$$

where $C_a(0) = \langle a|\Psi_A(0)\rangle$ and $C_c(0) = \langle c|\Psi_A(0)\rangle$ are probability amplitudes for the atom to be initially in the top and bottom levels, respectively. Hence the corresponding initial density operator is

$$\hat{\rho}_A(0) = \rho_{aa}^{(0)}|a\rangle\langle a| + \rho_{ac}^{(0)}|a\rangle\langle c| + \rho_{ca}^{(0)}|c\rangle\langle a| + \rho_{cc}^{(0)}|c\rangle\langle c|, \tag{2.5}$$

where $\rho_{aa}^{(0)} = |C_a(0)|^2$, $\rho_{ac}^{(0)} = C_a(0)C_c^*(0)$, $\rho_{ca}^{(0)} = C_c(0)C_a^*(0)$, and $\rho_{cc}^{(0)} = |C_c(0)|^2$.

Here we wish to consider the case in which three-level atoms in a cascade configuration and initially prepared in a coherent superposition of the top and bottom levels are injected into a cavity at constant rate r_a and removed after sometime τ, which is long enough for the atoms to spontaneously decay to levels other than the middle or the bottom level. We denote the density operator for the cavity radiation plus a single atom injected into the cavity at time t_j by $\rho_{AR}(t, t_j)$, in which $t - \tau \leq t_j \leq t$. The density operator for all the atoms in the cavity plus the cavity radiation at time t can be expressed as

$$\hat{\rho}_{AR}(t) = r_a \sum_j \hat{\rho}_{AR}(t, t_j)\Delta t_j, \tag{2.6}$$

where $r_a\Delta t_j$ represents the number of atoms injected into the cavity in a time interval of Δt_j. Assuming that the atoms are continuously injected into the cavity and taking the limit that $\Delta t_j \to 0$, the summation over j can be converted into integration with respect to t':

$$\hat{\rho}_{AR}(t) = r_a \int_{t-\tau}^{t} \hat{\rho}_{AR}(t,t')dt'. \tag{2.7}$$

Now differentiating Eq. (2.7) with respect to t and then applying the identity,

$$\frac{d}{dx}\int_a^x f(x,y)dy = f(x,x) - f(x,a) + \int_a^x \frac{\partial}{\partial x} f(x,y)dy, \tag{2.8}$$

we obtain

$$\frac{d}{dt}\hat{\rho}_{AR}(t) = r_a[\rho_{AR}(t,t) - \hat{\rho}_{AR}(t,t-\tau)] + r_a \int_{t-\tau}^{t} \frac{\partial}{\partial t}\hat{\rho}_{AR}(t,t')dt'. \tag{2.9}$$

We notice that $\hat{\rho}_{AR}(t,t)$ represents the density operator for an atom plus the cavity radiation at a time when the atom is injected into the cavity, whereas $\hat{\rho}_{AR}(t,t-\tau)$ represents the density operator when the atom is removed from the cavity. Since the atomic and radiation variables are not correlated at the instant the atoms are injected into or removed from the cavity,

$$\hat{\rho}_{AR}(t,t) = \hat{\rho}_A(0)\hat{\rho}(t), \tag{2.10}$$

$$\hat{\rho}_{AR}(t,t-\tau) = \hat{\rho}_A(t-\tau)\hat{\rho}(t), \tag{2.11}$$

where

$$\hat{\rho}_A(0) = \hat{\rho}_A(t). \tag{2.12}$$

With the aid of (2.10) and (2.11), Eq. (2.9) can be put in the form

$$\frac{d}{dt}\hat{\rho}_{AR}(t) = r_a[\hat{\rho}_A(0) - \hat{\rho}_A(t-\tau)]\hat{\rho}(t) + r_a \int_{t-\tau}^{t} \frac{\partial}{\partial t}\hat{\rho}_{AR}(t,t')dt'. \tag{2.13}$$

On the other hand, the density operator $\hat{\rho}_{AR}(t,t')$ evolves in time according to

$$\frac{\partial}{\partial t}\hat{\rho}_{AR}(t,t') = -i[\hat{H},\ \hat{\rho}_{AR}(t,t')]. \tag{2.14}$$

In view of (2.7) and (2.14), Eq. (2.13) takes the form

$$\frac{d}{dt}\hat{\rho}_{AR}(t) = r_a[\hat{\rho}_A(0) - \hat{\rho}_A(t-\tau)]\hat{\rho}(t) - i[\hat{H},\ \hat{\rho}_{AR}(t)]. \tag{2.15}$$

Moreover, taking the trace over the atomic variables and using the fact that

$$Tr_A(\hat{\rho}_A(0)) = Tr_A(\hat{\rho}_A(t-\tau)) = 1, \tag{2.16}$$

we see that

$$\frac{d\hat{\rho}(t)}{dt} = -iTr_A[\hat{H},\ \hat{\rho}_{AR}(t)]. \tag{2.17}$$

Employing Eqs. (2.3) and (2.17), the time development of the reduced density operator for radiation is found to be

$$\frac{d\hat{\rho}(t)}{dt} = g[\hat{\rho}_{ab}\hat{a}^\dagger - \hat{a}^\dagger\hat{\rho}_{ab} - \hat{b}^\dagger\hat{\rho}_{bc} + \hat{\rho}_{bc}\hat{b}^\dagger + \hat{a}\hat{\rho}_{ba} - \hat{\rho}_{ba}\hat{a} + \hat{b}\hat{\rho}_{cb} - \hat{\rho}_{cb}\hat{b}], \tag{2.18}$$

in which

$$\hat{\rho}_{\alpha\beta} = \langle\alpha|\hat{\rho}_{AR}|\beta\rangle, \tag{2.19}$$

with $\alpha, \beta = a, b, c$.

On the basis of Eqs. (2.15) and (2.19), one can write

$$\frac{d}{dt}\hat{\rho}_{\alpha\beta}(t) = r_a\langle\alpha|\hat{\rho}_A(0)|\beta\rangle\hat{\rho} - r_a\langle\alpha|\hat{\rho}_A(t-\tau)|\beta\rangle\hat{\rho} - i\langle\alpha|[\hat{H},\ \hat{\rho}_{AR}(t)]|\beta\rangle - \gamma\hat{\rho}_{\alpha\beta}, \tag{2.20}$$

where the last term is included to account for the decay of the atoms due to spontaneous emission. Here γ is the atomic decay rate taken to be the same for the three levels. Assuming the atoms to be removed from the cavity after they have decayed to levels other than the middle or the bottom level, we notice that

$$\langle\alpha|\hat{\rho}_A(t-\tau)|\beta\rangle = 0. \tag{2.21}$$

On account of Eqs. (2.3), (2.5), (2.20), and (2.21), we get

$$\begin{aligned}\frac{d}{dt}\hat{\rho}_{\alpha\beta}(t) &= r_a[\rho_{aa}^{(0)}\delta_{\alpha a}\delta_{a\beta} + \rho_{ac}^{(0)}\delta_{\alpha a}\delta_{c\beta} + \rho_{ca}^{(0)}\delta_{\alpha c}\delta_{a\beta} + \rho_{cc}^{(0)}\delta_{\alpha c}\delta_{c\beta}]\hat{\rho}(t)\\ &\quad - g[\hat{a}^\dagger\hat{\rho}_{a\beta}\delta_{\alpha b} + \hat{b}^\dagger\hat{\rho}_{b\beta}\delta_{\alpha c} - \hat{a}\hat{\rho}_{b\beta}\delta_{\alpha a} - \hat{b}\hat{\rho}_{c\beta}\delta_{\alpha b} + \hat{\rho}_{\alpha a}\hat{a}\delta_{b\beta} + \hat{\rho}_{\alpha b}\hat{b}\delta_{c\beta}\\ &\quad - \hat{\rho}_{\alpha b}\hat{a}^\dagger\delta_{a\beta} - \hat{\rho}_{\alpha c}\hat{b}^\dagger\delta_{b\beta}] - \frac{\Omega}{2}[\hat{\rho}_{c\beta}\delta_{a\alpha} - \hat{\rho}_{a\beta}\delta_{c\alpha} - \hat{\rho}_{\alpha a}\delta_{c\beta} + \hat{\rho}_{\alpha c}\delta_{a\beta}] - \gamma\hat{\rho}_{\alpha\beta}.\end{aligned} \tag{2.22}$$

It then follows that

$$\frac{d}{dt}\hat{\rho}_{aa}(t) = r_a\rho^{(0)}_{aa}\hat{\rho}(t) + g(\hat{a}\hat{\rho}_{ba} + \hat{\rho}_{ab}\hat{a}^\dagger) - \frac{\Omega}{2}(\hat{\rho}_{ac} + \hat{\rho}_{ca}) - \gamma\hat{\rho}_{aa}, \tag{2.23}$$

$$\frac{d}{dt}\hat{\rho}_{bb}(t) = -g(\hat{a}^\dagger\hat{\rho}_{ab} + \hat{\rho}_{ba}\hat{a} - \hat{b}\hat{\rho}_{cb} - \hat{\rho}_{bc}\hat{b}^\dagger) - \gamma\hat{\rho}_{bb}, \tag{2.24}$$

$$\frac{d}{dt}\hat{\rho}_{cc}(t) = r_a\rho^{(0)}_{cc}\hat{\rho}(t) - g(\hat{b}^\dagger\hat{\rho}_{bc} + \hat{\rho}_{cb}\hat{b}) + \frac{\Omega}{2}(\hat{\rho}_{ac} + \hat{\rho}_{ca}) - \gamma\hat{\rho}_{cc}, \tag{2.25}$$

$$\frac{d}{dt}\hat{\rho}_{ab}(t) = g(\hat{a}\hat{\rho}_{bb} - \hat{\rho}_{aa}\hat{a} + \hat{\rho}_{ac}\hat{b}^\dagger) - \frac{\Omega}{2}\hat{\rho}_{cb} - \gamma\hat{\rho}_{ab}, \tag{2.26}$$

$$\frac{d}{dt}\hat{\rho}_{ac}(t) = r_a\hat{\rho}^{(0)}_{ac}\hat{\rho} + g(\hat{a}\hat{\rho}_{bc} - \hat{\rho}_{ab}\hat{b}) - \frac{\Omega}{2}(\hat{\rho}_{cc} - \hat{\rho}_{aa}) - \gamma\hat{\rho}_{ac}, \tag{2.27}$$

$$\frac{d}{dt}\hat{\rho}_{cb}(t) = -g(\hat{\rho}_{ca}\hat{a} - \hat{\rho}_{cc}\hat{b}^\dagger + \hat{b}^\dagger\hat{\rho}_{bb}) + \frac{\Omega}{2}\hat{\rho}_{ab} - \gamma\hat{\rho}_{cb}. \tag{2.28}$$

In the good cavity limit ($\gamma \gg \kappa$), the cavity mode variables change slowly when compared to the atomic variables. Hence the atomic variables will reach steady state in a relatively short time. The time derivative of such variables can then be set equal to zero, while keeping the remaining atomic and cavity mode variables at time t. This procedure is referred to as the adiabatic approximation scheme. Confining ourselves to linear analysis, which amounts to dropping the terms containing g in Eqs. (2.23), (2.24), (2.25), and (2.27), and applying the adiabatic approximation scheme, we have

$$r_a\rho^{(0)}_{aa}\hat{\rho}(t) - \frac{\Omega}{2}(\hat{\rho}_{ac} + \hat{\rho}_{ca}) - \gamma\hat{\rho}_{aa} = 0, \tag{2.29}$$

$$\hat{\rho}_{bb} = 0, \tag{2.30}$$

$$r_a\rho^{(0)}_{cc}\hat{\rho}(t) + \frac{\Omega}{2}(\hat{\rho}_{ac} + \hat{\rho}_{ca}) - \gamma\hat{\rho}_{cc} = 0, \tag{2.31}$$

$$r_a\rho^{(0)}_{ac}\hat{\rho}(t) - \frac{\Omega}{2}(\hat{\rho}_{cc} - \hat{\rho}_{aa}) - \gamma\hat{\rho}_{ac} = 0. \tag{2.32}$$

Upon setting $\rho_{ac}^{(0)} = \rho_{ca}^{(0)}$, we see from Eq. (2.32) that

$$\hat{\rho}_{ac} = \hat{\rho}_{ca}. \tag{2.33}$$

Thus in view of Eqs. (2.29), (2.31), (2.32), and (2.33), we find

$$\hat{\rho}_{aa} = \frac{r_a\hat{\rho}}{2\gamma(\gamma^2+\Omega^2)}\left[(2\gamma^2+\Omega^2)\rho_{aa}^{(0)} - 2\gamma\Omega\rho_{ac}^{(0)} + \Omega^2\rho_{cc}^{(0)}\right], \tag{2.34}$$

$$\hat{\rho}_{cc} = \frac{r_a\hat{\rho}}{2\gamma(\gamma^2+\Omega^2)}\left[\Omega^2\rho_{aa}^{(0)} + 2\gamma\Omega\rho_{ac}^{(0)} + (2\gamma^2+\Omega^2)\rho_{cc}^{(0)}\right], \tag{2.35}$$

$$\hat{\rho}_{ac} = \frac{r_a\hat{\rho}}{2(\gamma^2+\Omega^2)}\left[\Omega(\rho_{aa}^{(0)} - \rho_{cc}^{(0)}) + 2\gamma\rho_{ac}^{(0)}\right], \tag{2.36}$$

with $\hat{\rho} = \hat{\rho}(t)$. Now making use of Eqs. (2.26), (2.28), (2.30), (2.34), (2.35), and (2.36), we obtain applying the adiabatic approximation scheme once again that

$$\begin{aligned}\hat{\rho}_{ab} = -&\frac{gr_a\hat{\rho}}{(4\gamma^2+\Omega^2)(\gamma^2+\Omega^2)}\left[\hat{a}[(4\gamma^2+\Omega^2)\rho_{aa}^{(0)} - 6\gamma\Omega\rho_{ac}^{(0)} + 3\Omega^2\rho_{cc}^{(0)}]\right.\\ &\left.+\hat{b}^\dagger\left[-\frac{\Omega(2\gamma^2-\Omega^2)}{\gamma}\rho_{aa}^{(0)} + 2(\Omega^2-2\gamma^2)\rho_{ac}^{(0)} + \frac{\Omega(\Omega^2+4\gamma^2)}{\gamma}\rho_{cc}^{(0)}\right]\right],\end{aligned} \tag{2.37}$$

$$\begin{aligned}\hat{\rho}_{cb} = &\frac{gr_a\hat{\rho}}{(4\gamma^2+\Omega^2)(\gamma^2+\Omega^2)}\left[\hat{a}\left[-\frac{\Omega(4\gamma^2+\Omega^2)}{\gamma}\rho_{aa}^{(0)} - 2(2\gamma^2-\Omega^2)\rho_{ac}^{(0)}\right.\right.\\ &\left.\left.-\frac{\Omega(\Omega^2-2\gamma^2)}{\gamma}\rho_{cc}^{(0)}\right] + \hat{b}^\dagger\left[3\Omega^2\rho_{aa}^{(0)} + 6\Omega\gamma\rho_{ac}^{(0)} + (\Omega^2+4\gamma^2)\rho_{cc}^{(0)}\right]\right].\end{aligned} \tag{2.38}$$

Employing Eqs. (2.37) and (2.38), Eq. (2.18) can be put in the form

$$\begin{aligned}\frac{d\hat{\rho}}{dt} = &\frac{AC}{2B}\left[2\hat{a}^\dagger\hat{\rho}\hat{a} - \hat{\rho}\hat{a}\hat{a}^\dagger - \hat{a}\hat{a}^\dagger\hat{\rho}\right] + \frac{AD}{2B}\left[2\hat{b}\hat{\rho}\hat{b}^\dagger - \hat{\rho}\hat{b}^\dagger\hat{b} - \hat{b}^\dagger\hat{b}\hat{\rho}\right]\\ &+\frac{AE}{2B}\left[\hat{a}^\dagger\hat{\rho}\hat{b}^\dagger - \hat{\rho}\hat{b}^\dagger\hat{a}^\dagger + \hat{b}\hat{\rho}\hat{a} - \hat{a}\hat{b}\hat{\rho}\right] + \frac{AF}{2B}\left[\hat{a}^\dagger\hat{\rho}\hat{b}^\dagger - \hat{b}^\dagger\hat{a}^\dagger\hat{\rho} + \hat{b}\hat{\rho}\hat{a} - \hat{\rho}\hat{a}\hat{b}\right],\end{aligned} \tag{2.39}$$

where

$$A = \frac{2r_a g^2}{\gamma^2}, \tag{2.40}$$

is the linear gain coefficient and

$$B = \left(1+\frac{\Omega^2}{\gamma^2}\right)\left(1+\frac{\Omega^2}{4\gamma^2}\right), \tag{2.41}$$

$$C = \rho_{aa}^{(0)}\left(1+\frac{\Omega^2}{4\gamma^2}\right) - \rho_{ac}^{(0)}\frac{3\Omega}{2\gamma} + \rho_{cc}^{(0)}\frac{3\Omega^2}{4\gamma^2}, \tag{2.42}$$

$$D = \rho_{aa}^{(0)}\frac{3\Omega^2}{4\gamma^2} + \rho_{ac}^{(0)}\frac{3\Omega}{2\gamma} + \rho_{cc}^{(0)}\left(1+\frac{\Omega^2}{4\gamma^2}\right), \tag{2.43}$$

$$E = -\rho_{aa}^{(0)}\frac{\Omega}{2\gamma}\left(1-\frac{\Omega^2}{2\gamma^2}\right) - \rho_{ac}^{(0)}\left(1-\frac{\Omega^2}{2\gamma^2}\right) + \rho_{cc}^{(0)}\frac{\Omega}{\gamma}\left(1+\frac{\Omega^2}{4\gamma^2}\right), \tag{2.44}$$

$$F = -\rho_{aa}^{(0)}\frac{\Omega}{\gamma}\left(1+\frac{\Omega^2}{4\gamma^2}\right) - \rho_{ac}^{(0)}\left(1-\frac{\Omega^2}{2\gamma^2}\right) + \rho_{cc}^{(0)}\frac{\Omega}{2\gamma}\left(1-\frac{\Omega^2}{2\gamma^2}\right). \tag{2.45}$$

We next seek to obtain the time evolution of the density operator for a two-mode cavity radiation coupled to a two-mode squeezed vacuum reservoir via a single-port mirror. In general, the time evolution of the reduced density operator for the cavity radiation coupled to a reservoir has, in the Born approximation [33], the form

$$\begin{aligned}\frac{d\hat{\rho}(t)}{dt} &= -i[\hat{H}_S,\ \hat{\rho}(t)] - i[\langle\hat{H}_{SR}(t)\rangle_R,\ \hat{\rho}(0)] - \int_0^t [\langle\hat{H}_{SR}(t)\rangle_R,\ [\hat{H}_S(t'),\ \hat{\rho}(t')]]dt' \\ &- \int_0^t Tr_R[\hat{H}_{SR}(t),\ [\hat{H}_{SR}(t'),\ \hat{\rho}(t')\hat{R}]]dt',\end{aligned} \tag{2.46}$$

where S and R refer to the system and reservoir variables. Furthermore, the interaction of a two-mode cavity radiation with a two-mode reservoir can be described in the interaction picture by the Hamiltonian

$$\hat{H}_{SR}(t) = i\sum_k \lambda_k[\hat{a}^\dagger\hat{a}_k e^{i(\omega_0-\omega_k)t} - \hat{a}\hat{a}_k^\dagger e^{-i(\omega_0-\omega_k)t} + \hat{b}^\dagger\hat{b}_k e^{i(\omega_0-\omega_k)t} - \hat{b}\hat{b}_k^\dagger e^{-i(\omega_0-\omega_k)t}], \tag{2.47}$$

where $\omega_0 = \frac{\omega_a+\omega_b}{2}$, with ω_a and ω_b representing the frequencies and $(\hat{a},\hat{b})$ being the annihilation operators for the cavity modes. In addition, $(\hat{a}_k,\hat{b}_k)$ are the annihilation operators, w_k is the frequency, and λ_k is the cavity damping constant for the kth mode representing the reservpor. In view of Eq. (2.47), we can write

$$\begin{aligned}\langle\hat{H}_{SR}(t)\rangle_R = i\sum_k \lambda_k[\hat{a}^\dagger\langle\hat{a}_k\rangle_R e^{i(\omega_0-\omega_k)t} - \hat{a}\langle\hat{a}_k^\dagger\rangle_R e^{-i(\omega_0-\omega_k)t} \\ + \hat{b}^\dagger\langle\hat{b}_k\rangle_R e^{i(\omega_0-\omega_k)t} - \hat{b}\langle\hat{b}_k^\dagger\rangle_R e^{-i(\omega_0-\omega_k)t}].\end{aligned} \tag{2.48}$$

For a two-mode squeezed vacuum reservoir (See Appendix 7.1), we find

$$\langle \hat{a}_k \rangle_R = \langle \hat{b}_k \rangle_R = 0. \tag{2.49}$$

Hence one can easily see that

$$\langle \hat{H}_{SR} \rangle_R = 0. \tag{2.50}$$

We therefore see that

$$[\langle \hat{H}_{SR} \rangle_R,\ \hat{\rho}(0)] = 0, \tag{2.51}$$

$$[\langle \hat{H}_{SR} \rangle_R,\ [\hat{H}(t'),\ \hat{\rho}(t')]] = 0. \tag{2.52}$$

On account of (2.51) and (2.52), Eq. (2.46) can be put in the form

$$\begin{aligned} \frac{d\hat{\rho}(t)}{dt} &= -i[\hat{H}_S,\ \hat{\rho}(t)] - \int_0^t Tr_R(\hat{R}\hat{H}_{SR}(t)\hat{H}_{SR}(t'))\hat{\rho}(t')dt' \\ &- \int_0^t \hat{\rho}(t')Tr_R(\hat{R}\hat{H}_{SR}(t')\hat{H}_{SR}(t))dt' + \int_0^t Tr_R(\hat{H}_{SR}(t)\hat{\rho}(t')\hat{R}\hat{H}_{SR}(t'))dt' \\ &+ \int_0^t Tr_R(\hat{H}_{SR}(t')\hat{\rho}(t')\hat{R}\hat{H}_{SR}(t))dt'. \end{aligned} \tag{2.53}$$

Making use of Eq. (2.47) and the fact that the cavity and reservoir operators commute, we find

$$\begin{aligned} Tr_R(\hat{R}\hat{H}_{SR}(t)\hat{H}_{SR}(t')) &= I_1\hat{a}\hat{a}^\dagger + I_2\hat{a}^\dagger\hat{a} + I_3\hat{a}^{\dagger 2} + I_4\hat{a}^2 + I_5\hat{b}\hat{b}^\dagger + I_6\hat{b}^\dagger\hat{b} + I_7\hat{b}^{\dagger 2} \\ &+ I_8\hat{b}^2 + I_9 2\hat{a}^\dagger\hat{b}^\dagger + I_{10}2\hat{a}\hat{b} + I_{11}2\hat{a}^\dagger\hat{b} + I_{12}2\hat{a}\hat{b}^\dagger, \end{aligned} \tag{2.54}$$

where

$$I_1 = \sum_{kj} \lambda_k\lambda_j \langle \hat{a}_k^\dagger \hat{a}_j \rangle_R e^{-i(\omega_0-\omega_k)t+i(\omega_0-\omega_j)t'}, \tag{2.55}$$

$$I_2 = \sum_{kj} \lambda_k\lambda_j \langle \hat{a}_k \hat{a}_j^\dagger \rangle_R e^{i(\omega_0-\omega_k)t-i(\omega_0-\omega_j)t'}, \tag{2.56}$$

$$I_3 = -\sum_{kj} \lambda_k\lambda_j \langle \hat{a}_k \hat{a}_j \rangle_R e^{i(\omega_0-\omega_k)t+i(\omega_0-\omega_j)t'}, \tag{2.57}$$

$$I_4 = -\sum_{kj} \lambda_k \lambda_j \langle \hat{a}_k^\dagger \hat{a}_j^\dagger \rangle_R e^{-i(\omega_0-\omega_k)t - i(\omega_0-\omega_j)t'}, \tag{2.58}$$

$$I_5 = \sum_{kj} \lambda_k \lambda_j \langle \hat{b}_k^\dagger \hat{b}_j \rangle_R e^{-i(\omega_0-\omega_k)t + i(\omega_0-\omega_j)t'}, \tag{2.59}$$

$$I_6 = \sum_{kj} \lambda_k \lambda_j \langle \hat{b}_k \hat{b}_j^\dagger \rangle_R e^{i(\omega_0-\omega_k)t - i(\omega_0-\omega_j)t'}, \tag{2.60}$$

$$I_7 = -\sum_{kj} \lambda_k \lambda_j \langle \hat{b}_k \hat{b}_j \rangle_R e^{i(\omega_0-\omega_k)t + i(\omega_0-\omega_j)t'}, \tag{2.61}$$

$$I_8 = -\sum_{kj} \lambda_k \lambda_j \langle \hat{b}_k^\dagger \hat{b}_j^\dagger \rangle_R e^{-i(\omega_0-\omega_k)t - i(\omega_0-\omega_j)t'}, \tag{2.62}$$

$$I_9 = -\sum_{kj} \lambda_k \lambda_j \langle \hat{a}_k \hat{b}_j \rangle_R e^{i(\omega_0-\omega_k)t + i(\omega_0-\omega_j)t'}, \tag{2.63}$$

$$I_{10} = -\sum_{kj} \lambda_k \lambda_j \langle \hat{a}_k^\dagger \hat{b}_j^\dagger \rangle_R e^{-i(\omega_0-\omega_k)t - i(\omega_0-\omega_j)t'}, \tag{2.64}$$

$$I_{11} = \sum_{kj} \lambda_k \lambda_j \langle \hat{a}_k \hat{b}_j^\dagger \rangle_R e^{i(\omega_0-\omega_k)t - i(\omega_0-\omega_j)t'}, \tag{2.65}$$

$$I_{12} = \sum_{kj} \lambda_k \lambda_j \langle \hat{a}_k^\dagger \hat{b}_j \rangle_R e^{-i(\omega_0-\omega_k)t + i(\omega_0-\omega_j)t'}. \tag{2.66}$$

We note with the aid of Eqs. (A21), (A25), and (A29) (See Appendix 7.1) that

$$I_3 = I_4 = I_7 = I_8 = I_{11} = I_{12} = 0. \tag{2.67}$$

On the other hand, using Eqs. (A17), (A20), (A23), (A24), and (A31) one can easily see that

$$I_1 = I_5 = N \sum_k \lambda_k^2 e^{-i(\omega_0-\omega_k)(t-t')}, \tag{2.68}$$

$$I_2 = I_6 = (N+1) \sum_k \lambda_k^2 e^{i(\omega_0 - \omega_k)(t-t')}, \tag{2.69}$$

$$I_9 = -M \sum_k \lambda_k \lambda_{\kappa_a + \kappa_b - k} e^{i(\omega_0 - \omega_k)(t-t')}, \tag{2.70}$$

$$I_{10} = -M \sum_k \lambda_k \lambda_{\kappa_a + \kappa_b - k} e^{-i(\omega_0 - \omega_k)(t-t')}, \tag{2.71}$$

where

$$N = \sinh^2 r \tag{2.72}$$

is the mean photon number of the squeezed vacuum modes and

$$M = \sinh r \cosh r. \tag{2.73}$$

Assuming the reservoir mode frequencies (ω_k's to be closely spaced, a summation over k can be converted into an integration over ω. In view of this fact, one can write

$$\sum_k \lambda_k^2 e^{\pm i(\omega_0 - \omega_k)(t-t')} = \int_0^\infty g(\omega)\lambda^2(\omega) e^{\pm i(\omega_0 - \omega)(t-t')} d\omega, \tag{2.74}$$

where $g(\omega)$ is the density of the modes for which the frequency lies between ω and $\omega + d\omega$. We assume that ω varies very little around ω_0. In view of this, we can replace $g(\omega)$ and $\lambda^2(\omega)$ by $g(\omega_0)$ and $\lambda^2(\omega_0)$ and extend the lower limit of the integration to $-\infty$. Consequently, we have

$$\sum_k \lambda_k^2 e^{\pm i(\omega_0 - \omega_k)(t-t')} = g(\omega_0)\lambda^2(\omega_0) \int_{-\infty}^\infty e^{\pm i(\omega_0 - \omega)(t-t')} d\omega. \tag{2.75}$$

Moreover, upon setting $\omega' = \omega - \omega_0$ we notice that

$$\sum_k \lambda_k^2 e^{\pm i(\omega_0 - \omega_k)(t-t')} = g(\omega_0)\lambda^2(\omega_0) \int_{-\infty}^\infty e^{\mp i\omega'(t-t')} d\omega'. \tag{2.76}$$

It then follows that

$$\sum_k \lambda_k^2 e^{\pm i(\omega_0 - \omega_k)(t-t')} = \kappa \delta(t-t'), \tag{2.77}$$

where

$$\kappa = 2\pi g(\omega_0)\lambda^2(\omega_0), \tag{2.78}$$

is defined as the cavity damping constant. Following the same procedure, it is possible to write

$$\sum_k \lambda_k \lambda_{k_a+k_b-k} e^{\pm i(\omega_0-\omega_k)(t-t')} = g(\omega_0)\lambda^2(\omega_0)\int_{-\infty}^{\infty} e^{\mp i\omega'(t-t')}d\omega'. \tag{2.79}$$

On the basis of Eqs. (2.76), (2.77), and (2.78), we see that

$$\sum_k \lambda_k \lambda_{k_a+k_b-k} e^{\pm i(\omega_0-\omega_k)(t-t')} = \kappa\delta(t-t'). \tag{2.80}$$

Hence on account of Eqs. (2.77) and (2.80), one can put Eqs. (2.68), (2.69), (2.70), and (2.71) in the form

$$I_1 = I_5 = N\kappa\delta(t-t'), \tag{2.81}$$

$$I_2 = I_6 = (N+1)\kappa\delta(t-t'), \tag{2.82}$$

$$I_9 = I_{10} = -M\kappa\delta(t-t'). \tag{2.83}$$

Furthermore, applying Eqs. (2.67), (2.81), (2.82), and (2.83), we can express Eq. (2.54) as

$$\begin{aligned} Tr_R(\hat{R}\hat{H}_{SR}(t)\hat{H}_{SR}(t')) = \{&\kappa[(N+1)\hat{a}^\dagger\hat{a} + N\hat{a}\hat{a}^\dagger] + \kappa[(N+1)\hat{b}^\dagger\hat{b} + N\hat{b}\hat{b}^\dagger] \\ &- 2M\kappa(\hat{a}^\dagger\hat{b}^\dagger + \hat{a}\hat{b})\}\delta(t-t'). \end{aligned} \tag{2.84}$$

We easily see that

$$\begin{aligned} \int_0^t Tr_R(\hat{R}\hat{H}_{SR}(t)\hat{H}_{SR}(t'))\hat{\rho}(t')dt' = &\frac{\kappa}{2}[(N+1)\hat{a}^\dagger\hat{a}\hat{\rho} + N\hat{a}\hat{a}^\dagger\hat{\rho}] \\ &+ \frac{\kappa}{2}[(N+1)\hat{b}^\dagger\hat{b}\hat{\rho} + N\hat{b}\hat{b}^\dagger\hat{\rho}] - M\kappa(\hat{a}^\dagger\hat{b}^\dagger\hat{\rho} + \hat{a}\hat{b}\hat{\rho}), \end{aligned} \tag{2.85}$$

with $\hat{\rho} = \hat{\rho}(t)$. We also see that

$$\int_0^t \hat{\rho}(t')Tr_R(\hat{R}\hat{H}_{SR}(t)\hat{H}_{SR}(t'))dt' = \frac{\kappa}{2}[(N+1)\hat{\rho}\hat{a}^\dagger\hat{a} + N\hat{\rho}\hat{a}\hat{a}^\dagger] + \frac{\kappa}{2}[(N+1)\hat{\rho}\hat{b}^\dagger\hat{b} + N\hat{\rho}\hat{b}\hat{b}^\dagger] - M\kappa(\hat{\rho}\hat{a}^\dagger\hat{b}^\dagger + \hat{\rho}\hat{a}\hat{b}). \tag{2.86}$$

Using Eq. (2.47) and the cyclic property of the trace operation, one can verify that

$$Tr_R(\hat{H}_{SR}(t)\hat{\rho}(t')\hat{R}\hat{H}_{SR}(t')) = I_1\hat{a}^\dagger\hat{\rho}\hat{a} + I_2\hat{a}\hat{\rho}\hat{a}^\dagger + I_3\hat{a}^\dagger\hat{\rho}\hat{a}^\dagger + I_4\hat{a}\hat{\rho}\hat{a} + I_5\hat{b}^\dagger\hat{\rho}\hat{b} + I_6\hat{b}\hat{\rho}\hat{b}^\dagger + I_7\hat{b}^\dagger\hat{\rho}\hat{b}^\dagger + I_8\hat{b}\hat{\rho}\hat{b} + I_9(\hat{a}^\dagger\hat{\rho}\hat{b}^\dagger + \hat{b}^\dagger\hat{\rho}\hat{a}^\dagger) + I_{10}(\hat{a}\hat{\rho}\hat{b} + \hat{b}\hat{\rho}\hat{a}) + I_{11}(\hat{a}^\dagger\hat{\rho}\hat{b} + \hat{b}\hat{\rho}\hat{a}^\dagger) + I_{12}(\hat{a}\hat{\rho}\hat{b}^\dagger + \hat{b}^\dagger\hat{\rho}\hat{a}). \tag{2.87}$$

Hence in view of Eqs. (2.67), (2.81), (2.82), and (2.83), we note that

$$Tr_R(\hat{H}_{SR}(t)\hat{\rho}(t')\hat{R}\hat{H}_{SR}(t')) = \{\kappa[(N+1)\hat{a}\hat{\rho}(t')\hat{a}^\dagger + N\hat{a}^\dagger\hat{\rho}(t')\hat{a}] + \kappa[(N+1)\hat{b}\hat{\rho}(t')\hat{b}^\dagger + N\hat{b}^\dagger\hat{\rho}(t')\hat{b}] - M\kappa[\hat{a}^\dagger\hat{\rho}\hat{b}^\dagger + \hat{b}^\dagger\hat{\rho}\hat{a}^\dagger + \hat{a}\hat{\rho}\hat{b} + \hat{b}\hat{\rho}\hat{a}]\}\delta(t-t'), \tag{2.88}$$

from which follows

$$\int_0^t Tr_R(\hat{H}_{SR}(t)\hat{\rho}(t')\hat{R}\hat{H}_{SR}(t')) = \frac{\kappa}{2}[(N+1)\hat{a}\hat{\rho}\hat{a}^\dagger + N\hat{a}^\dagger\hat{\rho}\hat{a}] + \frac{\kappa}{2}[(N+1)\hat{b}\hat{\rho}\hat{b}^\dagger + N\hat{b}^\dagger\hat{\rho}\hat{b}] - \frac{M\kappa}{2}[\hat{a}^\dagger\hat{\rho}\hat{b}^\dagger + \hat{b}^\dagger\hat{\rho}\hat{a}^\dagger + \hat{a}\hat{\rho}\hat{b} + \hat{b}\hat{\rho}\hat{a}] \tag{2.89}$$

and

$$\int_0^t Tr_R(\hat{H}_{SR}(t')\hat{\rho}(t)\hat{R}\hat{H}_{SR}(t)) = \frac{\kappa}{2}[(N+1)\hat{a}\hat{\rho}\hat{a}^\dagger + N\hat{a}^\dagger\hat{\rho}\hat{a}] + \frac{\kappa}{2}[(N+1)\hat{b}\hat{\rho}\hat{b}^\dagger + +N\hat{b}^\dagger\hat{\rho}\hat{b}] - \frac{M\kappa}{2}[\hat{a}^\dagger\hat{\rho}\hat{b}^\dagger + \hat{b}^\dagger\hat{\rho}\hat{a}^\dagger + \hat{a}\hat{\rho}\hat{b} + \hat{b}\hat{\rho}\hat{a}]. \tag{2.90}$$

Substitution of Eqs. (2.85), (2.86), (2.89), and (2.90) into Eq. (2.53) results in

$$\frac{d\hat{\rho}(t)}{dt} = -i[\hat{H}_S(t), \hat{\rho}(t)] + \frac{\kappa(N+1)}{2}[2\hat{a}\hat{\rho}\hat{a}^\dagger - \hat{a}^\dagger\hat{a}\hat{\rho} - \hat{\rho}\hat{a}^\dagger\hat{a}] + \frac{\kappa N}{2}[2\hat{a}^\dagger\hat{\rho}\hat{a} - \hat{a}\hat{a}^\dagger\hat{\rho} - \hat{\rho}\hat{a}\hat{a}^\dagger] + \frac{\kappa(N+1)}{2}[2\hat{b}\hat{\rho}\hat{b}^\dagger - \hat{b}^\dagger\hat{b}\hat{\rho} - \hat{\rho}\hat{b}^\dagger\hat{b}] + \frac{\kappa N}{2}[2\hat{b}^\dagger\hat{\rho}\hat{b} - \hat{b}\hat{b}^\dagger\hat{\rho} - \hat{\rho}\hat{b}\hat{b}^\dagger] - M\kappa[\hat{a}^\dagger\hat{\rho}\hat{b}^\dagger + \hat{b}^\dagger\hat{\rho}\hat{a}^\dagger + \hat{a}\hat{\rho}\hat{b} + \hat{b}\hat{\rho}\hat{a} - \hat{a}^\dagger\hat{b}^\dagger\hat{\rho} - \hat{a}\hat{b}\hat{\rho} - \hat{\rho}\hat{a}^\dagger\hat{b}^\dagger - \hat{\rho}\hat{a}\hat{b}]. \tag{2.91}$$

On account of Eqs. (2.39) and (2.91), the master equation for the cavity radiation of the quantum optical system under consideration finally turns out to be

$$\begin{aligned}\frac{d\hat{\rho}(t)}{dt} &= \frac{\kappa(N+1)}{2}[2\hat{a}\hat{\rho}\hat{a}^\dagger - \hat{a}^\dagger\hat{a}\hat{\rho} - \hat{\rho}\hat{a}^\dagger\hat{a}] + \frac{1}{2}\left(\frac{AC}{B} + \kappa N\right)[2\hat{a}^\dagger\hat{\rho}\hat{a} - \hat{a}\hat{a}^\dagger\hat{\rho} - \hat{\rho}\hat{a}\hat{a}^\dagger] \\ &+ \frac{1}{2}\left(\frac{AD}{B} + \kappa(N+1)\right)[2\hat{b}\hat{\rho}\hat{b}^\dagger - \hat{b}^\dagger\hat{b}\hat{\rho} - \hat{\rho}\hat{b}^\dagger\hat{b}] + \frac{\kappa N}{2}[2\hat{b}^\dagger\hat{\rho}\hat{b} - \hat{b}\hat{b}^\dagger\hat{\rho} - \hat{\rho}\hat{b}\hat{b}^\dagger] \\ &+ \frac{AE}{2B}[\hat{a}^\dagger\hat{\rho}\hat{b}^\dagger - \hat{a}\hat{b}\hat{\rho} - \hat{\rho}\hat{a}^\dagger\hat{b}^\dagger + \hat{b}\hat{\rho}\hat{a}] + \frac{AF}{2B}[\hat{a}^\dagger\hat{\rho}\hat{b}^\dagger - \hat{a}^\dagger\hat{b}^\dagger\hat{\rho} - \hat{\rho}\hat{a}\hat{b} + \hat{b}\hat{\rho}\hat{a}] \\ &- M\kappa[\hat{a}^\dagger\hat{\rho}\hat{b}^\dagger + \hat{b}^\dagger\hat{\rho}\hat{a}^\dagger + \hat{a}\hat{\rho}\hat{b} + \hat{b}\hat{\rho}\hat{a} - \hat{a}^\dagger\hat{b}^\dagger\hat{\rho} - \hat{a}\hat{b}\hat{\rho} - \hat{\rho}\hat{a}^\dagger\hat{b}^\dagger - \hat{\rho}\hat{a}\hat{b}].\end{aligned} \tag{2.92}$$

3

Stochastic Differential Equations

We now seek to obtain the stochastic differential equations associated with the normal ordering for the cavity mode variables applying the pertinent master equation. To this end, employing Eq. (2.92) it can be verified that

$$\frac{d}{dt}\langle\hat{a}(t)\rangle = -\frac{\mu_a}{2}\langle\hat{a}(t)\rangle + \frac{AE}{2B}\langle\hat{b}^\dagger(t)\rangle, \tag{3.1}$$

$$\frac{d}{dt}\langle\hat{b}^\dagger(t)\rangle = -\frac{\mu_b}{2}\langle\hat{b}^\dagger(t)\rangle - \frac{AF}{2B}\langle\hat{a}(t)\rangle, \tag{3.2}$$

$$\frac{d}{dt}\langle\hat{a}^\dagger(t)\hat{a}(t)\rangle = -\mu_a\langle\hat{a}^\dagger(t)\hat{a}(t)\rangle + \frac{AE}{2B}[\langle\hat{a}^\dagger(t)\hat{b}^\dagger(t)\rangle + \langle\hat{a}(t)\hat{b}(t)\rangle] + \frac{AC}{B} + \kappa N, \tag{3.3}$$

$$\frac{d}{dt}\langle\hat{b}^\dagger(t)\hat{b}(t)\rangle = -\mu_b\langle\hat{b}^\dagger(t)\hat{b}(t)\rangle - \frac{AF}{2B}[\langle\hat{a}^\dagger(t)\hat{b}^\dagger(t)\rangle + \langle\hat{a}(t)\hat{b}(t)\rangle] + \kappa N, \tag{3.4}$$

$$\frac{d}{dt}\langle\hat{a}^2(t)\rangle = -\mu_a\langle\hat{a}^2(t)\rangle + \frac{AE}{B}\langle\hat{b}^\dagger(t)\hat{a}(t)\rangle, \tag{3.5}$$

$$\frac{d}{dt}\langle\hat{b}^{\dagger 2}(t)\rangle = -\mu_b\langle\hat{b}^{\dagger 2}(t)\rangle - \frac{AF}{B}\langle\hat{a}(t)\hat{b}^\dagger(t)\rangle, \tag{3.6}$$

$$\frac{d}{dt}\langle\hat{a}(t)\hat{b}(t)\rangle = -\frac{\mu_b+\mu_a}{2}\langle\hat{a}(t)\hat{b}(t)\rangle - \frac{AF}{2B}\langle\hat{a}^\dagger(t)\hat{a}(t)\rangle + \frac{AE}{2B}\langle\hat{b}^\dagger(t)\hat{b}(t)\rangle - \frac{AF}{2B} + \kappa M, \tag{3.7}$$

$$\frac{d}{dt}\langle\hat{a}^\dagger(t)\hat{b}(t)\rangle = -\frac{\mu_b+\mu_a}{2}\langle\hat{a}^\dagger(t)\hat{b}(t)\rangle - \frac{AF}{2B}\langle\hat{a}^{\dagger 2}(t)\rangle + \frac{AE}{2B}\langle\hat{b}^2(t)\rangle, \tag{3.8}$$

in which

$$\mu_a = \kappa - \frac{AC}{B}, \tag{3.9}$$

$$\mu_b = \kappa + \frac{AD}{B}. \tag{3.10}$$

We note that the operators in the above equations are in the normal order. The c-number equations corresponding to (3.1), (3.2), (3.3), (3.4), (3.5), (3.6), (3.7), and (3.8) are

$$\frac{d}{dt}\langle\alpha(t)\rangle = -\frac{\mu_a}{2}\langle\alpha(t)\rangle + \frac{AE}{2B}\langle\beta^*(t)\rangle, \tag{3.11}$$

$$\frac{d}{dt}\langle\beta^*(t)\rangle = -\frac{\mu_b}{2}\langle\beta^*(t)\rangle - \frac{AF}{2B}\langle\alpha(t)\rangle, \tag{3.12}$$

$$\frac{d}{dt}\langle\alpha^*(t)\alpha(t)\rangle = -\mu_a\langle\alpha^*(t)\alpha(t)\rangle + \frac{AE}{2B}(\langle\alpha^*(t)\beta^*(t)\rangle + \langle\alpha(t)\beta(t)\rangle) + \frac{AC}{B} + \kappa N, \tag{3.13}$$

$$\frac{d}{dt}\langle\beta^*(t)\beta(t)\rangle = -\mu_b\langle\beta^*(t)\beta(t)\rangle - \frac{AF}{2B}[\langle\alpha^*(t)\beta^*(t)\rangle + \langle\alpha(t)\beta(t)\rangle] + \kappa N, \tag{3.14}$$

$$\frac{d}{dt}\langle\alpha^2(t)\rangle = -\mu_a\langle\alpha^2(t)\rangle + \frac{AE}{B}\langle\beta^*(t)\alpha(t)\rangle, \tag{3.15}$$

$$\frac{d}{dt}\langle\beta^{*^2}(t)\rangle = -\mu_b\langle\beta^{*^2}(t)\rangle - \frac{AF}{B}\langle\alpha(t)\beta^*(t)\rangle, \tag{3.16}$$

$$\frac{d}{dt}\langle\alpha(t)\beta(t)\rangle = -\frac{\mu_b + \mu_a}{2}\langle\alpha(t)\beta(t)\rangle - \frac{AF}{2B}\langle\alpha^*(t)\alpha(t)\rangle + \frac{AE}{2B}\langle\beta^*(t)\beta(t)\rangle$$
$$- \frac{AF}{2B} + \kappa M, \tag{3.17}$$

$$\frac{d}{dt}\langle\alpha^*(t)\beta(t)\rangle = -\frac{\mu_b + \mu_a}{2}\langle\alpha^*(t)\beta(t)\rangle - \frac{AF}{2B}\langle\alpha^{*^2}(t)\rangle + \frac{AE}{2B}\langle\beta^2(t)\rangle. \tag{3.18}$$

On the basis of Eqs. (3.11) and (3.12), one can write

$$\frac{d}{dt}\alpha(t) = -\frac{\mu_a}{2}\alpha(t) + \frac{AE}{2B}\beta^*(t) + f_a(t), \tag{3.19}$$

$$\frac{d}{dt}\beta^*(t) = -\frac{\mu_b}{2}\beta^*(t) - \frac{AF}{2B}\alpha(t) + f_b^*(t), \tag{3.20}$$

where $f_a(t)$ and $f_b^*(t)$ are noise forces the properties of which remain to be determined. The expectation values of Eqs. (3.19) and (3.20) would be identical to (3.11) and (3.12) provided that

$$\langle f_a(t)\rangle = 0, \tag{3.21}$$

$$\langle f_b^*(t)\rangle = 0. \tag{3.22}$$

On the other hand, making use of the fact that

$$\frac{d}{dt}\langle\alpha^*(t)\alpha(t)\rangle = \left\langle \alpha(t)\frac{d}{dt}\alpha^*(t)\right\rangle + \left\langle \alpha^*(t)\frac{d}{dt}\alpha(t)\right\rangle \tag{3.23}$$

along with Eq. (3.19), we find

$$\frac{d}{dt}\langle\alpha^*(t)\alpha(t)\rangle = -\mu_a\langle\alpha^*(t)\alpha(t)\rangle + \frac{AE}{2B}[\langle\alpha^*(t)\beta^*(t)\rangle + \langle\alpha(t)\beta(t)\rangle]$$
$$+ \langle\alpha^*(t)f_a(t)\rangle + \langle\alpha(t)f_a^*(t)\rangle. \tag{3.24}$$

Upon comparing Eqs. (3.13) and (3.24), one can see that

$$\langle\alpha^*(t)f_a(t)\rangle + \langle\alpha(t)f_a^*(t)\rangle = \frac{AC}{B} + \kappa N. \tag{3.25}$$

It can also be verified following a similar procedure that

$$\langle\beta^*(t)f_b(t)\rangle + \langle\beta(t)f_b^*(t)\rangle = \kappa N, \tag{3.26}$$

$$\langle\alpha(t)f_a(t)\rangle = 0, \tag{3.27}$$

$$\langle\beta^*(t)f_b^*(t)\rangle = 0, \tag{3.28}$$

$$\langle\beta(t)f_a(t)\rangle + \langle\alpha(t)f_b(t)\rangle = -\frac{AF}{2B} + \kappa M, \tag{3.29}$$

$$\langle\beta(t)f_a^*(t)\rangle + \langle\alpha^*(t)f_b(t)\rangle = 0. \tag{3.30}$$

Furthermore, the formal solutions of Eqs. (3.19) and (3.20) can be written as

$$\alpha(t) = \alpha(0)e^{-\frac{\mu_a}{2}t} + \int_0^t e^{-\frac{\mu_a}{2}(t-t')}\left(f_a(t') + \frac{AE}{2B}\beta^*(t')\right)dt', \tag{3.31}$$

$$\beta^*(t) = \beta^*(0)e^{-\frac{\mu_b}{2}t} + \int_0^t e^{-\frac{\mu_b}{2}(t-t')}\left(f_b^*(t') - \frac{AF}{2B}\alpha(t')\right)dt'. \tag{3.32}$$

Applying Eq. (3.31), we get

$$\begin{aligned}\langle\alpha(t)f_a^*(t)\rangle &= \langle\alpha(0)f_a^*(t)\rangle e^{-\frac{\mu_a}{2}t}\\ &+ \int_0^t e^{-\frac{\mu_a}{2}(t-t')}\left(\langle f_a(t')f_a^*(t)\rangle + \frac{AE}{2B}\langle\beta^*(t')f_a^*(t)\rangle\right)dt',\end{aligned} \tag{3.33}$$

$$\begin{aligned}\langle\alpha^*(t)f_a(t)\rangle &= \langle\alpha^*(0)f_a(t)\rangle e^{-\frac{\mu_a}{2}t}\\ &+ \int_0^t e^{-\frac{\mu_a}{2}(t-t')}\left(\langle f_a^*(t')f_a(t)\rangle + \frac{AE}{2B}\langle\beta(t')f_a(t)\rangle\right)dt'.\end{aligned} \tag{3.34}$$

Based on the fact that the noise force at time t does not affect the cavity mode variables at earlier times, we have

$$\langle\alpha(0)f_a^*(t)\rangle = \langle\beta^*(t')f_a^*(t)\rangle = 0. \tag{3.35}$$

Now making use of Eqs. (3.33), (3.34), and (3.35), we obtain

$$\begin{aligned}\langle\alpha^*(t)f_a(t)\rangle + \langle\alpha(t)f_a^*(t)\rangle &= \int_0^t e^{-\frac{\mu_a}{2}(t-t')}\langle f_a(t')f_a^*(t)\rangle dt'\\ &+ \int_0^t e^{-\frac{\mu_a}{2}(t-t')}\langle f_a^*(t')f_a(t)\rangle dt'.\end{aligned} \tag{3.36}$$

Hence on account of Eqs. (3.25) and (3.36), we see that

$$\int_0^t e^{-\frac{\mu_a}{2}(t-t')}\langle f_a(t')f_a^*(t)\rangle dt' + \int_0^t e^{-\frac{\mu_a}{2}(t-t')}\langle f_a^*(t')f_a(t)\rangle dt' = \frac{AC}{B} + \kappa N. \tag{3.37}$$

Claiming

$$\langle f_a(t')f_a^*(t)\rangle = \langle f_a^*(t')f_a(t)\rangle, \tag{3.38}$$

we have

$$\int_0^t e^{-\frac{\mu_a}{2}(t-t')}\langle f_a(t')f_a^*(t)\rangle dt' = \frac{1}{2}\left(\frac{AC}{B} + \kappa N\right). \tag{3.39}$$

Now on the basis of the relation

$$\int_0^t e^{-a(t-t')}\langle f(t')g(t)\rangle dt' = c, \tag{3.40}$$

it can be asserted that

$$\langle f(t')g(t)\rangle = 2c\delta(t-t'), \tag{3.41}$$

with a being a constant. Therefore, in view of Eqs. (3.38), (3.40), and (3.41), we get

$$\langle f_a(t')f_a^*(t)\rangle = \left(\frac{AC}{B} + \kappa N\right)\delta(t-t'). \tag{3.42}$$

One can also readily establish following a similar procedure that

$$\langle f_a(t')f_a(t)\rangle = 0, \tag{3.43}$$

$$\langle f_b(t')f_b^*(t)\rangle = \kappa N\delta(t-t'), \tag{3.44}$$

$$\langle f_b(t')f_b(t)\rangle = 0. \tag{3.45}$$

Moreover, with the aid of Eqs. (3.31) and (3.32), we find

$$\begin{aligned}\langle\alpha(t)f_b(t)\rangle &= \langle\alpha(0)f_b(t)\rangle e^{-\frac{\mu_a}{2}t}\\ &+ \int_0^t e^{-\frac{\mu_a}{2}(t-t')}\left(\langle f_a(t')f_b(t)\rangle + \frac{AE}{2B}\langle\beta^*(t')f_b(t)\rangle\right)dt',\end{aligned} \tag{3.46}$$

$$\begin{aligned}\langle\beta(t)f_a(t)\rangle &= \langle\beta(0)f_a(t)\rangle e^{-\frac{\mu_b}{2}t}\\ &+ \int_0^t e^{-\frac{\mu_b}{2}(t-t')}\left(\langle f_b(t')f_a(t)\rangle - \frac{AF}{2B}\langle\alpha^*(t')f_a(t)\rangle\right)dt',\end{aligned} \tag{3.47}$$

so that taking into account Eqs. (3.29) and (3.35), we have

$$\int_0^t e^{-\frac{\mu_a}{2}(t-t')}\langle f_a(t')f_b(t)\rangle dt' + \int_0^t e^{-\frac{\mu_b}{2}(t-t')}\langle f_b(t')f_a(t)\rangle dt' = -\left(\frac{AF}{2B} - \kappa M\right). \tag{3.48}$$

Assuming

$$\langle f_a(t')f_b(t)\rangle = \langle f_b(t')f_a(t)\rangle, \tag{3.49}$$

and taking into account Eqs. (3.40) and (3.41), we get

$$\langle f_b(t')f_a(t)\rangle = -\left(\frac{AF}{2B} - \kappa M\right)\delta(t-t'). \tag{3.50}$$

It can also be shown in a similar manner that

$$\langle f_b^*(t')f_a(t)\rangle = 0. \tag{3.51}$$

We notice that Eqs. (3.21), (3.22), (3.42), (3.43), (3.44), (3.45), (3.50), and (3.51) describe various correlation properties of the noise forces.

We now introduce a variable defined by

$$\rho_{aa}^{(0)} = \frac{1-\eta}{2}, \tag{3.52}$$

with $-1 \leq \eta \leq 1$. It then follows, for three-level atoms are initially prepared to be in a coherent superposition of the top and bottom levels, that

$$\rho_{cc}^{(0)} = \frac{1+\eta}{2}, \tag{3.53}$$

$$\rho_{ac}^{(0)} = \frac{\sqrt{1-\eta^2}}{2}, \tag{3.54}$$

where we have taken that $\rho_{ac}^{(0)} = \rho_{ac}^{*(0)}$. Hence employing (2.42), (2.43), (2.44), (3.9), (3.10), (3.52), (3.53), and (3.54), it is possible to express Eqs. (3.19) and (3.20) as

$$\frac{d}{dt}\alpha(t) = -a_+\alpha(t) - b_+\beta^*(t) + f_a(t), \tag{3.55}$$

$$\frac{d}{dt}\beta^*(t) = -a_-\beta^*(t) - b_-\alpha(t) + f_b^*(t), \tag{3.56}$$

where

$$a_\pm = \frac{\kappa}{2} + \frac{A}{4B}\left[\frac{3\Omega}{2\gamma}\sqrt{1-\eta^2} + \eta\left(1 - \frac{\Omega^2}{2\gamma^2}\right) \mp \left(1 + \frac{\Omega^2}{\gamma^2}\right)\right], \tag{3.57}$$

$$b_\pm = -\frac{A}{4B}\left[\frac{\Omega}{2\gamma}\left(1 + \frac{\Omega^2}{\gamma^2}\right) \pm \left[\frac{3\eta\Omega}{2\gamma} - \sqrt{1-\eta^2}\left(1 - \frac{\Omega^2}{2\gamma^2}\right)\right]\right]. \tag{3.58}$$

We realize that Eqs. (3.55) and (3.56) are coupled differential equations. In order to solve these differential equations, we introduce a matrix equation of the form

$$\frac{d}{dt}\mathcal{A}(t) = -\mathcal{B}\mathcal{A}(t) + \mathcal{C}(t), \tag{3.59}$$

where

$$\mathcal{A}(t) = \begin{pmatrix} \alpha(t) \\ \beta^*(t) \end{pmatrix}, \tag{3.60}$$

$$\mathcal{B} = \begin{pmatrix} a_+ & b_+ \\ b_- & a_- \end{pmatrix}, \tag{3.61}$$

$$\mathcal{C}(t) = \begin{pmatrix} f_a(t) \\ f_b^*(t) \end{pmatrix}. \tag{3.62}$$

We next determine the eigenvalues and eigenvectors of the matrix $\mathcal{B}$ applying the relation

$$\mathcal{B}\mathcal{V}_i = \lambda_i \mathcal{V}_i, \tag{3.63}$$

in which

$$\mathcal{V}_i = \begin{pmatrix} x_i \\ y_i \end{pmatrix}, \tag{3.64}$$

with the normalization condition

$$x_i^2 + y_i^2 = 1, \tag{3.65}$$

where $i = 1, 2$. Eq. (3.63) has a nontrivial solution provided that

$$\begin{vmatrix} a_+ - \lambda & b_+ \\ b_- & a_- - \lambda \end{vmatrix} = 0, \tag{3.66}$$

from which follows

$$\lambda_1 = \left(\frac{a_+ + a_-}{2}\right) + \sqrt{b_+ b_- + \left(\frac{a_+ - a_-}{2}\right)^2}, \tag{3.67}$$

$$\lambda_2 = \left(\frac{a_+ + a_-}{2}\right) - \sqrt{b_+ b_- + \left(\frac{a_+ - a_-}{2}\right)^2}. \tag{3.68}$$

Now we proceed to determine the corresponding eigenvectors. To this end, using Eqs. (3.63) and (3.64), we see that

$$a_+ x_1 + b_+ y_1 = \lambda_1 x_1, \tag{3.69}$$

$$b_- x_1 + a_- y_1 = \lambda_1 y_1. \tag{3.70}$$

In addition, upon solving simultaneously Eqs. (3.65) and (3.69) with $i = 1$, we get

$$x_1 = \frac{b_+}{\sqrt{b_+^2 + (\lambda_1 - a_+)^2}}, \tag{3.71}$$

$$y_1 = \frac{\lambda_1 - a_+}{\sqrt{b_+^2 + (\lambda_1 - a_+)^2}}. \tag{3.72}$$

It can also be verified in a similar manner that

$$x_2 = \frac{b_+}{\sqrt{b_+^2 + (\lambda_2 - a_+)^2}}, \tag{3.73}$$

$$y_2 = \frac{\lambda_2 - a_+}{\sqrt{b_+^2 + (\lambda_2 - a_+)^2}}. \tag{3.74}$$

Thus on account of Eqs. (3.71), (3.72), (3.73), and (3.74), the vector defined by

$$\mathcal{V} = \begin{pmatrix} x_1 & x_2 \\ y_1 & y_2 \end{pmatrix} \tag{3.75}$$

is expressible as

$$\mathcal{V} = \begin{pmatrix} \frac{b_+}{\sqrt{b_+^2 + (\lambda_1 - a_+)^2}} & \frac{b_+}{\sqrt{b_+^2 + (\lambda_2 - a_+)^2}} \\ \frac{\lambda_1 - a_+}{\sqrt{b_+^2 + (\lambda_1 - a_+)^2}} & \frac{\lambda_2 - a_+}{\sqrt{b_+^2 + (\lambda_2 - a_+)^2}} \end{pmatrix}. \tag{3.76}$$

In order to determine the inverse of the matrix (3.76), we first obtain its characteristic equation, which is

$$\lambda^2 - \lambda\left(\frac{b_+}{\sqrt{b_+^2 + (\lambda_1 - a_+)^2}} + \frac{\lambda_2 - a_+}{\sqrt{b_+^2 + (\lambda_2 - a_+)^2}}\right) - \frac{b_+(\lambda_1 - \lambda_2)}{\sqrt{b_+^2 + (\lambda_1 - a_+)^2}\sqrt{b_+^2 + (\lambda_2 - a_+)^2}} = 0. \tag{3.77}$$

Thus using the fact that a matrix satisfies its own characteristic equation, we notice that

$$\mathcal{V}\left[\mathcal{V}-\mathcal{I}\left(\frac{b_+}{\sqrt{b_+^2+(\lambda_1-a_+)^2}}+\frac{\lambda_2-a_+}{\sqrt{b_+^2+(\lambda_2-a_+)^2}}\right)\right]$$
$$=\frac{b_+(\lambda_1-\lambda_2)\mathcal{I}}{\sqrt{b_+^2+(\lambda_1-a_+)^2}\sqrt{b_+^2+(\lambda_2-a_+)^2}}, \tag{3.78}$$

from which follows

$$\mathcal{V}^{-1}=\frac{\sqrt{b_+^2+(\lambda_1-a_+)^2}\sqrt{b_+^2+(\lambda_2-a_+)^2}}{b_+(\lambda_1-\lambda_2)}$$
$$\times\left[\mathcal{V}-\mathcal{I}\left(\frac{b_+}{\sqrt{b_+^2+(\lambda_1-a_+)^2}}+\frac{\lambda_2-a_+}{\sqrt{b_+^2+(\lambda_2-a_+)^2}}\right)\right]. \tag{3.79}$$

Hence making use of Eq. (3.76), one can readily obtain

$$\mathcal{V}^{-1}=\frac{1}{\lambda_1-\lambda_2}\begin{pmatrix}-\frac{\lambda_2-a_+}{b_+}\sqrt{b_+^2+(\lambda_1-a_+)^2} & \sqrt{b_+^2+(\lambda_1-a_+)^2}\\ \frac{\lambda_1-a_+}{b_+}\sqrt{b_+^2+(\lambda_2-a_+)^2} & -\sqrt{b_+^2+(\lambda_2-a_+)^2}\end{pmatrix}. \tag{3.80}$$

Furthermore, employing the fact that

$$\mathcal{V}^{-1}\mathcal{V}=\mathcal{V}\mathcal{V}^{-1}=\mathcal{I}, \tag{3.81}$$

we can rewrite Eq. (3.59) as

$$\frac{d}{dt}\mathcal{A}(t)=-\mathcal{V}\mathcal{V}^{-1}\mathcal{B}\mathcal{V}\mathcal{V}^{-1}\mathcal{A}(t)+\mathcal{C}(t). \tag{3.82}$$

Upon multiplying Eq. (3.82) from left by $\mathcal{V}^{-1}$, we get

$$\frac{d}{dt}(\mathcal{V}^{-1}\mathcal{A}(t))=-\mathcal{R}(\mathcal{V}^{-1}\mathcal{A})(t)+\mathcal{V}^{-1}\mathcal{C}(t), \tag{3.83}$$

where

$$\mathcal{R}=\mathcal{V}^{-1}\mathcal{B}\mathcal{V}=\begin{pmatrix}\lambda_1 & 0\\ 0 & \lambda_2\end{pmatrix}. \tag{3.84}$$

We observe that Eq. (3.83) has a well-behaved solution provided that the matrix $\mathcal{R}$ is positive. We thus see from Eq. (3.84) that $\mathcal{R}$ is positive if both λ_1 and λ_2 are positive.

The formal solution of Eq. (3.83) can be written as

$$\mathcal{V}^{-1}\mathcal{A}(t+\tau)=e^{-\mathcal{R}\tau}\mathcal{V}^{-1}\mathcal{A}(t)+\int_0^\tau e^{-\mathcal{R}(\tau-\tau')}\mathcal{V}^{-1}\mathcal{C}(t+\tau')d\tau'. \tag{3.85}$$

Hence multiplying Eq. (3.85) from the left by $\mathcal{V}$ results in

$$\mathcal{A}(t+\tau) = \mathcal{V}e^{-\mathcal{R}\tau}\mathcal{V}^{-1}\mathcal{A}(t) + \int_0^\tau \mathcal{V}e^{-\mathcal{R}(\tau-\tau')}\mathcal{V}^{-1}\mathcal{C}(t+\tau')d\tau'. \tag{3.86}$$

We note that

$$e^{-\mathcal{R}\tau} = \begin{pmatrix} e^{-\lambda_1\tau} & 0 \\ 0 & e^{-\lambda_2\tau} \end{pmatrix}. \tag{3.87}$$

In addition, using Eqs. (3.59), (3.76), (3.80), and (3.87), we find

$$\mathcal{V}e^{-\mathcal{R}\tau}\mathcal{V}^{-1}\mathcal{A}(t) = \frac{1}{\lambda_1-\lambda_2} \times \begin{pmatrix} ((\lambda_1-a_+)e^{-\lambda_2\tau} - (\lambda_2-a_+)e^{-\lambda_1\tau})\alpha(t) + b_+(e^{-\lambda_1\tau} - e^{-\lambda_2\tau})\beta^*(t) \\ \frac{(\lambda_1-a_+)(\lambda_2-a_+)}{b_+}(e^{-\lambda_2\tau} - e^{-\lambda_1\tau})\alpha(t) + ((\lambda_1-a_+)e^{-\lambda_1\tau} - (\lambda_2-a_+)e^{-\lambda_2\tau})\beta^*(t) \end{pmatrix}. \tag{3.88}$$

And applying Eq. (3.62), (3.76), and (3.80), we get

$$\mathcal{V}e^{-\mathcal{R}(\tau-\tau')}\mathcal{V}^{-1}\mathcal{C}(t+\tau') = \frac{1}{\lambda_1-\lambda_2}\begin{pmatrix} r \\ s \end{pmatrix}, \tag{3.89}$$

where

$$\begin{aligned} r = &((\lambda_1-a_+)e^{-\lambda_2(\tau-\tau')} - (\lambda_2-a_+)e^{-\lambda_1(\tau-\tau')})f_a(t+\tau') \\ &+ b_+(e^{-\lambda_1(\tau-\tau')} - e^{-\lambda_2(\tau-\tau')})f_b^*(t+\tau'), \end{aligned} \tag{3.90}$$

$$\begin{aligned} s = &\frac{(\lambda_1-a_+)(\lambda_2-a_+)}{b_+}(e^{-\lambda_2(\tau-\tau')} - e^{-\lambda_1(\tau-\tau')})f_a(t+\tau') \\ &+ ((\lambda_1-a_+)e^{-\lambda_1(\tau-\tau')} - (\lambda_2-a_+)e^{-\lambda_2(\tau-\tau')})f_b^*(t+\tau'). \end{aligned} \tag{3.91}$$

Now with the aid of Eqs. (3.60), (3.62), (3.86), (3.88), and (3.89), we obtain

$$\alpha(t+\tau) = A_+(\tau)\alpha(t) + B_+(\tau)\beta^*(t) + F_+(t+\tau) + G_+(t+\tau), \tag{3.92}$$

$$\beta(t+\tau) = A_-(\tau)\beta(t) + B_-(\tau)\alpha^*(t) + F_-(t+\tau) + G_-(t+\tau), \tag{3.93}$$

where

$$A_{\pm}(\tau) = \frac{1}{2}\left[(1 \pm p)e^{-\lambda_2 \tau} + (1 \mp p)e^{-\lambda_1 \tau}\right], \tag{3.94}$$

$$B_{\pm}(\tau) = \frac{q_{\pm}}{2}[e^{-\lambda_1 \tau} - e^{-\lambda_2 \tau}], \tag{3.95}$$

$$F_{+}(t+\tau) = \frac{1}{2}\int_0^{\tau} [(1+p)e^{-\lambda_2(\tau-\tau')} + (1-p)e^{-\lambda_1(\tau-\tau')}] f_a(t+\tau') d\tau', \tag{3.96}$$

$$F_{-}(t+\tau) = \frac{1}{2}\int_0^{\tau} [(1-p)e^{-\lambda_2(\tau-\tau')} + (1+p)e^{-\lambda_1(\tau-\tau')}] f_b(t+\tau') d\tau', \tag{3.97}$$

$$G_{+}(t+\tau) = \frac{q_{+}}{2}\int_0^{\tau} [e^{-\lambda_1(\tau-\tau')} - e^{-\lambda_2(\tau-\tau')}] f_b^{*}(t+\tau') d\tau', \tag{3.98}$$

$$G_{-}(t+\tau) = \frac{q_{-}}{2}\int_0^{\tau} [e^{-\lambda_1(\tau-\tau')} - e^{-\lambda_2(\tau-\tau')}] f_a^{*}(t+\tau') d\tau', \tag{3.99}$$

with

$$p = \frac{1+\frac{\Omega^2}{\gamma^2}}{\left[\left(1+\frac{\Omega^2}{\gamma^2}\right)^2\left(1+\frac{\Omega^2}{4\gamma^2}\right) - \left(\frac{3\eta\Omega}{2\gamma} - \sqrt{1-\eta^2}\left(1-\frac{\Omega^2}{2\gamma^2}\right)\right)^2\right]^{\frac{1}{2}}}, \tag{3.100}$$

$$q_{\pm} = \frac{-\frac{\Omega}{2\gamma}(1+\frac{\Omega^2}{\gamma^2}) \mp \left[\frac{3\eta\Omega}{2\gamma} - \sqrt{1-\eta^2}\left(1-\frac{\Omega^2}{2\gamma^2}\right)\right]}{\left[\left(1+\frac{\Omega^2}{\gamma^2}\right)^2\left(1+\frac{\Omega^2}{4\gamma^2}\right) - \left(\frac{3\eta\Omega}{2\gamma} - \sqrt{1-\eta^2}\left(1-\frac{\Omega^2}{2\gamma^2}\right)\right)^2\right]^{\frac{1}{2}}}, \tag{3.101}$$

Upon setting $t = 0$ and then replacing τ by t in Eqs. (3.92) and (3.93), we see that

$$\alpha(t) = A_{+}(t)\alpha(0) + B_{+}(t)\beta^{*}(0) + F_{+}(t) + G_{+}(t), \tag{3.102}$$

$$\beta(t) = A_{-}(t)\beta(0) + B_{-}(t)\alpha^{*}(0) + F_{-}(t) + G_{-}(t), \tag{3.103}$$

where

$$A_{\pm}(t) = \frac{1}{2}\left[(1 \pm p)e^{-\lambda_2 t} + (1 \mp p)e^{-\lambda_1 t}\right], \tag{3.104}$$

$$B_{\pm}(t) = \frac{q_{\pm}}{2}[e^{-\lambda_1 t} - e^{-\lambda_2 t}], \tag{3.105}$$

$$F_{+}(t) = \frac{1}{2}\int_0^t [(1+p)e^{-\lambda_2(t-t')} + (1-p)e^{-\lambda_1(t-t')}] f_a(t')dt', \tag{3.106}$$

$$F_{-}(t) = \frac{1}{2}\int_0^t [(1-p)e^{-\lambda_2(t-t')} + (1+p)e^{-\lambda_1(t-t')}] f_b(t')dt', \tag{3.107}$$

$$G_{+}(t) = \frac{q_{+}}{2}\int_0^t [e^{-\lambda_1(t-t')} - e^{-\lambda_2(t-t')}] f_b^{*}(t')dt', \tag{3.108}$$

$$G_{-}(t) = \frac{q_{-}}{2}\int_0^t [e^{-\lambda_1(t-t')} - e^{-\lambda_2(t-t')}] f_a^{*}(t')dt'. \tag{3.109}$$

It is perhaps worth mentioning that Eqs. (3.92), (3.93), (3.102), and (3.103) will be used to calculate various quantities of interest in the forth coming Sections.

4

Quadrature Fluctuations

4.1 Quadrature variances

A two-mode cavity radiation can be described by an operator

$$\hat{c} = \frac{1}{\sqrt{2}}\big(\hat{a} + \hat{b}\big), \tag{4.1}$$

where $\hat{a}$ and $\hat{b}$ represent the separate modes. We notice that the c-number equation corresponding to (4.1) can be expressed as

$$\gamma = \frac{1}{\sqrt{2}}\big(\alpha + \beta\big). \tag{4.2}$$

On the other hand, employing the commutation relations

$$\big[\hat{a},\ \hat{a}^{\dagger}\big] = \big[\hat{b},\ \hat{b}^{\dagger}\big] = 1, \tag{4.3}$$

$$\big[\hat{a},\ \hat{b}\big] = \big[\hat{a}^{\dagger},\ \hat{b}\big] = 0, \tag{4.4}$$

we get

$$\big[\hat{c},\ \hat{c}^{\dagger}\big] = 1, \tag{4.5}$$

$$\big[\hat{c},\ \hat{c}\big] = 0. \tag{4.6}$$

The squeezing of the two-mode cavity radiation can be studied applying the quadrature operators defined by

$$\hat{c}_{+} = \hat{c}^{\dagger} + \hat{c}, \tag{4.7}$$

$$\hat{c}_- = i(\hat{c}^\dagger - \hat{c}). \tag{4.8}$$

Using Eqs. (4.5) and (4.6), one can verify that

$$\left[\hat{c}_+,\ \hat{c}_-\right] = 2i. \tag{4.9}$$

We now seek to calculate the variance of the quadrature operators (4.7) and (4.8). To begin with, making use of the commutation relations (4.5), we find

$$\Delta c_\pm^2 = 1 \pm \left[\langle \hat{c}^{\dagger^2}\rangle + \langle \hat{c}^2\rangle \pm 2\langle \hat{c}^\dagger \hat{c}\rangle + \langle \hat{c}^\dagger\rangle^2 + \langle \hat{c}\rangle^2 \pm 2\langle \hat{c}\rangle\langle \hat{c}^\dagger\rangle\right]. \tag{4.10}$$

We notice that all operators in Eq. (4.10) are in the normal order. Therefore, the c-number equation corresponding to (4.10) can be expressed in a more appealing form as

$$\Delta c_\pm^2 = 1 \pm \left[\langle \gamma_\pm^2(t)\rangle + \langle \gamma_\pm(t)\rangle^2\right], \tag{4.11}$$

where

$$\gamma_\pm(t) = \gamma^*(t) \pm \gamma(t). \tag{4.12}$$

Hence in view of Eqs. (4.2) and (4.12), we note that

$$\begin{aligned}\Delta c_\pm^2 = 1 + \frac{1}{2}\big[&2\langle \alpha^*\alpha\rangle \pm \langle \alpha^{*^2}\rangle \pm \langle \alpha^2\rangle - \langle \alpha^*\rangle^2 - \langle \alpha\rangle^2 \pm \langle \beta^{*^2}\rangle \pm \langle \beta^2\rangle \\ &+ 2\langle \beta^*\beta\rangle - \langle \beta^*\rangle^2 - \langle \beta\rangle^2\big] \pm \langle \alpha^*\beta^*\rangle + \langle \alpha^*\beta\rangle + \langle \alpha\beta^*\rangle \pm \langle \alpha\beta\rangle \\ &\mp \langle \alpha^*\rangle\langle \alpha\rangle - \langle \alpha^*\rangle\langle \beta^*\rangle \mp \langle \alpha^*\rangle\langle \beta\rangle \mp \langle \alpha\rangle\langle \beta^*\rangle - \langle \alpha\rangle\langle \beta\rangle \mp \langle \beta^*\rangle\langle \beta\rangle.\end{aligned} \tag{4.13}$$

The various expectation values in Eq. (4.13) can be determined using Eqs. (3.102) and (3.103). Thus on account of Eqs. (3.102) and (3.103), and assuming the cavity modes to be initially in a two-mode vacuum state, one can readily verify that

$$\langle \alpha(t)\rangle = \langle \beta(t)\rangle = 0, \tag{4.14}$$

as a result

$$\begin{aligned}\Delta c_\pm^2 = 1 &+ \langle \alpha^*\alpha\rangle + \langle \beta^*\beta\rangle + \langle \alpha^*\beta\rangle + \langle \alpha\beta^*\rangle \\ &\pm \left[\langle \alpha^*\beta^*\rangle + \langle \alpha\beta\rangle + \frac{1}{2}\left(\langle \alpha^{*^2}\rangle + \langle \alpha^2\rangle + \langle \beta^{*^2}\rangle + \langle \beta^2\rangle\right)\right].\end{aligned} \tag{4.15}$$

We now proceed to obtain the expectation values involved in (4.15). To this effect, taking Eq. (3.102) into account, we write

$$\langle \alpha^*(t)\alpha(t)\rangle = A_+(t)\langle \alpha^*(t)\alpha(0)\rangle + B_+(t)\langle \alpha^*(t)\beta^*(0)\rangle + \langle \alpha^*(t)F_+(t)\rangle + \langle \alpha^*(t)G_+(t)\rangle. \tag{4.16}$$

Using the complex conjugate of Eq. (3.102), we easily see that

$$\langle \alpha^*(t)\alpha(0)\rangle = A_+(t)\langle \alpha^*(0)\alpha(0)\rangle + B_+(t)\langle \alpha(0)\beta(0)\rangle + \langle \alpha(0)F_+^*(t)\rangle + \langle \alpha(0)G_+^*(t)\rangle. \tag{4.17}$$

With the aid of the assumption that the noise force at time t does not affect the cavity mode variables at earlier times and taking the cavity modes to be initially in a vacuum state, we get

$$\langle \alpha^*(t)\alpha(0)\rangle = 0. \tag{4.18}$$

It is also possible to show in a similar manner that

$$\langle \alpha^*(t)\beta(0)\rangle = 0, \tag{4.19}$$

$$\langle \alpha^*(t)F_+(t)\rangle = \langle F_+^*(t)F_+(t) + \langle G_+^*(t)F_+(t), \tag{4.20}$$

$$\langle \alpha^*(t)G_+(t)\rangle = \langle F_+^*(t)G_+(t) + \langle G_+^*(t)G_+(t). \tag{4.21}$$

Hence on substituting Eqs. (4.18), (4.19), (4.20), and (4.21) into (4.16), we obtain

$$\langle \alpha^*(t)\alpha(t)\rangle = \langle F_+^*(t)F_+(t)\rangle + \langle G_+^*(t)G_+(t)\rangle + \langle F_+^*(t)G_+(t)\rangle + \langle G_+^*(t)F_+(t)\rangle. \tag{4.22}$$

Next we evaluate the correlation functions in (4.22). To this end, on the basis of Eq. (3.106), we have

$$\langle F_+^*(t)F_+(t)\rangle = \frac{1}{4}\int_0^t\int_0^t [(1-p)e^{-\lambda_1(t-t')} + (1+p)e^{-\lambda_2(t-t')}] \\ \times [(1-p)e^{-\lambda_1(t-t'')} + (1+p)e^{-\lambda_2(t-t'')}]\langle f_a(t'')f_a^*(t')\rangle dt'dt''. \tag{4.23}$$

It then follows on account of Eq. (3.42) that

$$\langle F_+^*(t)F_+(t)\rangle = \frac{\frac{AC}{B}+\kappa N}{4}\int_0^t\int_0^t[(1-p)^2e^{-\lambda_1(2t-t'-t'')}+(1+p)^2e^{-\lambda_2(2t-t'-t'')}$$
$$+(1-p^2)e^{-(\lambda_1(t-t')+\lambda_2(t-t''))}+(1-p^2)e^{-(\lambda_2(t-t')+\lambda_1(t-t''))}]\delta(t'-t'')dt'dt''. \tag{4.24}$$

On carrying out the integrations, one gets

$$\langle F_+^*(t)F_+(t)\rangle = \left(\frac{AC}{B}+\kappa N\right)\left[\frac{(1-p)^2(1-e^{-2\lambda_1 t})}{8\lambda_1}+\frac{(1+p)^2(1-e^{-2\lambda_2 t})}{8\lambda_2}\right.$$
$$\left.+\frac{(1-p^2)(1-e^{-(\lambda_1+\lambda_2)t})}{2(\lambda_1+\lambda_2)}\right]. \tag{4.25}$$

It is also possible to verify in a similar manner that

$$\langle G_+^*(t)G_+(t)\rangle = \kappa N q_+^2\left[\frac{(1-e^{-2\lambda_1 t})}{8\lambda_1}+\frac{(1-e^{-2\lambda_2 t})}{8\lambda_2}-\frac{(1-e^{-(\lambda_1+\lambda_2)t})}{2(\lambda_1+\lambda_2)}\right], \tag{4.26}$$

$$\langle F_+^*(t)G_+(t)\rangle = \langle G_+^*(t)F_+(t)\rangle = -\left(\frac{AF}{2B}-\kappa M\right)q_+\times\left[\frac{(1-p)(1-e^{-2\lambda_1 t})}{8\lambda_1}\right.$$
$$\left.-\frac{(1+p)(1-e^{-2\lambda_2 t})}{8\lambda_2}+\frac{p(1-e^{-(\lambda_1+\lambda_2)t})}{2(\lambda_1+\lambda_2)}\right]. \tag{4.27}$$

In view of Eqs. (4.22), (4.25), (4.26), and (4.27), we find

$$\langle\alpha^*(t)\alpha(t)\rangle = \left[\frac{(\frac{AC}{B}+\kappa N)(1-p)^2+\kappa N q_+^2-(\frac{AF}{B}-2\kappa M)q_+(1-p)}{8\lambda_1}\right][1-e^{-2\lambda_1 t}]$$
$$+\left[\frac{(\frac{AC}{B}+\kappa N)(1+p)^2+\kappa N q_+^2+(\frac{AF}{B}-2\kappa M)q_+(1+p)}{8\lambda_2}\right][1-e^{-2\lambda_2 t}]$$
$$+\left[\frac{(\frac{AC}{B}+\kappa N)(1-p^2)-\kappa N q_+^2-(\frac{AF}{B}-2\kappa M)q_+p}{2(\lambda_1+\lambda_2)}\right][1-e^{-(\lambda_1+\lambda_2)t}]. \tag{4.28}$$

It can also be established following a similar procedure that

$$\langle\beta^*(t)\beta(t)\rangle = \left[\frac{(\frac{AC}{B}+\kappa N)q_-^2+\kappa N(1+p)^2-(\frac{AF}{B}-2\kappa M)q_-(1+p)}{8\lambda_1}\right][1-e^{-2\lambda_1 t}]$$
$$+\left[\frac{(\frac{AC}{B}+\kappa N)q_-^2+\kappa N(1-p)^2+(\frac{AF}{B}-2\kappa M)q_-(1-p)}{8\lambda_2}\right][1-e^{-2\lambda_2 t}]$$
$$-\left[\frac{(\frac{AC}{B}+\kappa N)q_-^2-\kappa N(1-p^2)-(\frac{AF}{B}-2\kappa M)q_-p}{2(\lambda_1+\lambda_2)}\right][1-e^{-(\lambda_1+\lambda_2)t}]. \tag{4.29}$$

In addition, applying Eq. (3.102) it is easy to check that

$$\langle \alpha^2(t) \rangle = \langle F_+^2(t) \rangle + \langle G_+^2(t) \rangle + 2\langle F_+(t) G_+(t) \rangle. \tag{4.30}$$

Now taking into account Eq. (3.106), we can write

$$\langle F_+^2(t) \rangle = \frac{1}{4} \int_0^t \int_0^t [(1-p)e^{-\lambda_1(t-t')} + (1+p)e^{-\lambda_2(t-t')}]^2 \langle f_a(t'') f_a(t') \rangle dt' dt'', \tag{4.31}$$

so that employing (3.43), we have

$$\langle F_+^2(t) \rangle = 0. \tag{4.32}$$

It can also be verified in a similar manner that

$$\langle G_+^2(t) \rangle = \langle G_+(t) F_+(t) \rangle = 0. \tag{4.33}$$

On the basis of Eqs. (4.30), (4.32), and (4.33), we note that

$$\langle \alpha^2(t) \rangle = 0. \tag{4.34}$$

It can also be shown in a similar way that

$$\langle \beta^2(t) \rangle = 0. \tag{4.35}$$

Furthermore, making use of Eqs. (3.102) and (3.103), we obtain

$$\langle \alpha(t)\beta(t) \rangle = \langle F_+(t) F_-(t) \rangle + \langle G_+(t) G_-(t) \rangle + \langle F_+(t) G_-(t) \rangle + \langle G_+(t) F_-(t) \rangle. \tag{4.36}$$

We see that

$$\begin{aligned} \langle F_+(t) F_-(t) \rangle = \frac{1}{4} \int_0^t \int_0^t & [(1-p)e^{-\lambda_1(t-t')} + (1+p)e^{-\lambda_2(t-t')}] \\ & \times [(1+p)e^{-\lambda_1(t-t'')} + (1-p)e^{-\lambda_2(t-t'')}] \langle f_a(t'') f_b(t') \rangle dt' dt''. \end{aligned} \tag{4.37}$$

Thus on account of Eq. (3.49), we get

$$\begin{aligned} \langle F_+(t) F_-(t) \rangle = -\left(\frac{\frac{AF}{2B} - \kappa M}{4} \right) \int_0^t \int_0^t & [(1-p^2)e^{-\lambda_1(2t-t'-t'')} + (1-p^2)e^{-\lambda_2(2t-t'-t'')} \\ & + (1-p)^2 e^{-(\lambda_1(t-t') + \lambda_2(t-t''))} + (1+p)^2 e^{-(\lambda_2(t-t') + \lambda_1(t-t''))}] \delta(t'-t'') dt' dt''. \end{aligned} \tag{4.38}$$

Therefore, on carrying out the integrations, we find

$$\langle F_+(t)F_-(t)\rangle = -\left(\frac{AF}{2B} - \kappa M\right)\left[\frac{(1-p^2)(1-e^{-2\lambda_1 t})}{8\lambda_1} + \frac{(1-p^2)(1-e^{-2\lambda_2 t})}{8\lambda_2} + \frac{(1+p^2)(1-e^{-(\lambda_1+\lambda_2)t})}{2(\lambda_1+\lambda_2)}\right]. \tag{4.39}$$

One can also show in a similar manner that

$$\langle G_+(t)G_-(t)\rangle = -\left(\frac{AF}{2B} - \kappa M\right) q_- q_+ \left[\frac{(1-e^{-2\lambda_1 t})}{8\lambda_1} + \frac{(1-e^{-2\lambda_2 t})}{8\lambda_2} - \frac{(1-e^{-(\lambda_1+\lambda_2)t})}{2(\lambda_1+\lambda_2)}\right], \tag{4.40}$$

$$\langle F_+(t)G_-(t)\rangle = \left(\frac{AC}{B} + \kappa N\right) q_- \left[\frac{(1-p)(1-e^{-2\lambda_1 t})}{8\lambda_1} - \frac{(1+p)(1-e^{-2\lambda_2 t})}{8\lambda_2} + \frac{p(1-e^{-(\lambda_1+\lambda_2)t})}{2(\lambda_1+\lambda_2)}\right], \tag{4.41}$$

$$\langle G_+(t)F_-(t)\rangle = \kappa N q_+ \left[\frac{(1+p)(1-e^{-2\lambda_1 t})}{8\lambda_1} - \frac{(1-p)(1-e^{-2\lambda_2 t})}{8\lambda_2} - \frac{p(1-e^{-(\lambda_1+\lambda_2)t})}{2(\lambda_1+\lambda_2)}\right]. \tag{4.42}$$

Hence using Eqs. (4.36), (4.39), (4.40), (4.41), and (4.42), we reach at

$$\begin{aligned}\langle \alpha(t)\beta(t)\rangle = &\left[\frac{(\frac{AC}{B}+\kappa N)q_-(1-p) + \kappa N q_+(1+p)}{8\lambda_1}\right][1-e^{-2\lambda_1 t}] \\ &- \left[\frac{(\frac{AF}{2B}-\kappa M)(1-p^2+q_-q_+)}{8\lambda_1}\right][1-e^{-2\lambda_1 t}] \\ &- \left[\frac{(\frac{AC}{B}+\kappa N)q_-(1+p) + \kappa N q_+(1-p)}{8\lambda_2}\right][1-e^{-2\lambda_2 t}] \\ &- \left[\frac{(\frac{AF}{2B}-\kappa M)(1-p^2+q_-q_+)}{8\lambda_2}\right][1-e^{-2\lambda_2 t}] \\ &+ \left[\frac{(\frac{AC}{B}+\kappa N)q_- p - \kappa N q_+ p - (\frac{AF}{2B}-\kappa M)(1+p^2-q_-q_+)}{2(\lambda_1+\lambda_2)}\right][1-e^{-(\lambda_1+\lambda_2)t}].\end{aligned} \tag{4.43}$$

Besides, we see from Eq. (4.43) that

$$\langle \alpha^*(t)\beta^*(t)\rangle = \langle \alpha(t)\beta(t)\rangle. \tag{4.44}$$

Following a similar procedure, one can verify that

$$\langle \alpha^*(t)\beta(t)\rangle = 0. \tag{4.45}$$

Now with the aid of Eqs. (4.15), (4.28), (4.29), (4.34), (4.35), (4.43), and (4.45), we arrive at

$$\begin{aligned}
\Delta c_{\pm}^2 = 1 + \Bigg[&\left(\frac{AC}{B} + \kappa N\right)\left[(1-p)^2 + q_-^2 \pm 2q_-(1-p)\right] \\
&+\kappa N\left[(1+p)^2 + q_+^2 \pm 2q_+(1+p)\right] \\
&-\left(\frac{AF}{2B} - \kappa M\right)\left[q_+(1-p) + q_-(1+p) \pm 2(1-p^2+q_-q_+)\right]\Bigg]\left[\frac{1-e^{-2\lambda_1 t}}{8\lambda_1}\right] \\
&+\Bigg[\left(\frac{AC}{B} + \kappa N\right)\left[(1+p)^2 + q_-^2 \mp 2q_-(1+p)\right] + \kappa N\left[(1-p)^2 + q_+^2 \mp 2q_+(1-p)\right] \\
&+\left(\frac{AF}{2B} - \kappa M\right)\left[q_+(1+p) + q_-(1-p) \mp 2(1-p^2+q_-q_+)\right]\Bigg]\left[\frac{1-e^{-2\lambda_2 t}}{8\lambda_2}\right] \\
&+\Bigg[\left(\frac{AC}{B} + \kappa N\right)\left[1-p^2-q_-^2 \pm 2q_-p\right] + \kappa N\left[1-q_+^2-p^2 \mp 2q_+p\right] \\
&-\left(\frac{AF}{2B} - \kappa M\right)\left[p(q_+-q_-) \pm 2(1+p^2-q_-q_+)\right]\Bigg]\left[\frac{1-e^{-(\lambda_1+\lambda_2)t}}{2(\lambda_1+\lambda_2)}\right].
\end{aligned} \tag{4.46}$$

We see that Eq. (4.46) takes at steady state the form

$$\begin{aligned}
\Delta c_{\pm}^2 = 1 + &\left[\frac{A}{B}(C \mp F) + 2\kappa(N \pm M)\right]\frac{(\lambda_1+\lambda_2)^2 + 4\lambda_1\lambda_2}{8\lambda_1\lambda_2(\lambda_1+\lambda_2)} \\
&+\Bigg[\left(\frac{AC}{B} + \kappa N\right)\left(p^2 + q_-^2 \mp 2q_-p\right) + \kappa N\left(p^2 + q_+^2 \pm 2q_+p\right) \\
&+\left(\frac{AF}{B} - 2\kappa M\right)\left(p(q_+-q_-) \pm (p^2 - q_-q_+)\right)\Bigg]\frac{(\lambda_1+\lambda_2)^2 - 4\lambda_1\lambda_2}{8\lambda_1\lambda_2(\lambda_1+\lambda_2)} \\
&+\left[\left(\frac{AC}{B} + \kappa N\right)(p \mp q_-) - \kappa N(p \pm q_+) + \left(\frac{AF}{2B} - \kappa M\right)(q_+ + q_-)\right]\frac{\lambda_1-\lambda_2}{4\lambda_1\lambda_2},
\end{aligned} \tag{4.47}$$

in which

$$C = \frac{1-\eta}{2} + \frac{\Omega^2}{4\gamma^2}(2+\eta) - \frac{3\Omega}{4\gamma}\sqrt{1-\eta^2}, \tag{4.48}$$

$$F = -\frac{\Omega}{4\gamma}\left(1 + \frac{\Omega^2}{\gamma^2}\right) + \frac{3\eta\Omega}{4\gamma} - \frac{\sqrt{1-\eta^2}}{2}\left(1 - \frac{\Omega^2}{2\gamma^2}\right), \tag{4.49}$$

$$\lambda_1 = \frac{\kappa}{2} + \frac{A}{4B}\left[\frac{3\Omega}{2\gamma}\sqrt{1-\eta^2} + \eta\left(1-\frac{\Omega^2}{2\gamma^2}\right) + \chi\right], \tag{4.50}$$

$$\lambda_2 = \frac{\kappa}{2} + \frac{A}{4B}\left[\frac{3\Omega}{2\gamma}\sqrt{1-\eta^2} + \eta\left(1-\frac{\Omega^2}{2\gamma^2}\right) - \chi\right], \tag{4.51}$$

$$\begin{aligned} p^2 + q_-^2 \mp 2q_- p = \frac{1}{\chi^2}\Bigg[&\left(1+\frac{\Omega^2}{\gamma^2}\right)^2\left[1+\frac{\Omega}{\gamma}\left(\frac{\Omega}{4\gamma}\pm 1\right)\right] - \left[\frac{3\eta\Omega}{2\gamma} - \sqrt{1-\eta^2}\left(1-\frac{\Omega^2}{2\gamma^2}\right)\right] \\ &\times\left[-\frac{3\eta\Omega}{2\gamma} + \sqrt{1-\eta^2}\left(1-\frac{\Omega^2}{2\gamma^2}\right) + \left(1+\frac{\Omega^2}{\gamma^2}\right)\left(\frac{\Omega}{\gamma}\pm 2\right)\right]\Bigg], \end{aligned} \tag{4.52}$$

$$\begin{aligned} p^2 + q_+^2 \pm 2q_+ p = \frac{1}{\chi^2}\Bigg[&\left(1+\frac{\Omega^2}{\gamma^2}\right)^2\left[1+\frac{\Omega}{\gamma}\left(\frac{\Omega}{4\gamma}\mp 1\right)\right] - \left[\frac{3\eta\Omega}{2\gamma} - \sqrt{1-\eta^2}\left(1-\frac{\Omega^2}{2\gamma^2}\right)\right] \\ &\times\left[-\frac{3\eta\Omega}{2\gamma} + \sqrt{1-\eta^2}\left(1-\frac{\Omega^2}{2\gamma^2}\right) - \left(1+\frac{\Omega^2}{\gamma^2}\right)\left(\frac{\Omega}{\gamma}\mp 2\right)\right]\Bigg], \end{aligned} \tag{4.53}$$

$$\begin{aligned} p(q_+ - q_-) \pm (p^2 - q_+ q_-) = \frac{1}{\chi^2}\Bigg[&\left[-\frac{3\eta\Omega}{2\gamma} + \sqrt{1-\eta^2}\left(1-\frac{\Omega^2}{2\gamma^2}\right)\right]\Bigg[2\left(1+\frac{\Omega^2}{\gamma^2}\right) \\ &\mp\left(\frac{3\eta\Omega}{2\gamma} - \sqrt{1-\eta^2}\left(1-\frac{\Omega^2}{2\gamma^2}\right)\right)\Bigg] \\ &\pm\left(1+\frac{\Omega^2}{\gamma^2}\right)^2\left(1-\frac{\Omega^2}{4\gamma^2}\right)\Bigg], \end{aligned} \tag{4.54}$$

$$p \mp q_- = \frac{1}{\chi}\left[\left(1+\frac{\Omega^2}{\gamma^2}\right)\left(1\pm\frac{\Omega}{2\gamma}\right) \mp \left[\frac{3\eta\Omega}{2\gamma} - \sqrt{1-\eta^2}\left(1-\frac{\Omega^2}{2\gamma^2}\right)\right]\right], \tag{4.55}$$

$$p \pm q_+ = \frac{1}{\chi}\left[\left(1+\frac{\Omega^2}{\gamma^2}\right)\left(1\mp\frac{\Omega}{2\gamma}\right) \mp \left[\frac{3\eta\Omega}{2\gamma} - \sqrt{1-\eta^2}\left(1-\frac{\Omega^2}{2\gamma^2}\right)\right]\right], \tag{4.56}$$

$$q_+ + q_- = -\frac{\Omega}{\chi\gamma}\left(1+\frac{\Omega^2}{\gamma^2}\right), \tag{4.57}$$

where

$$\chi = \left[\left(1+\frac{\Omega^2}{\gamma^2}\right)^2\left(1+\frac{\Omega^2}{4\gamma^2}\right) - \left[\frac{3\eta\Omega}{2\gamma} - \sqrt{1-\eta^2}\left(1-\frac{\Omega^2}{2\gamma^2}\right)\right]^2\right]^{\frac{1}{2}}. \tag{4.58}$$

In order to investigate the dependence of the squeezing on the amplitude of the driving radiation, initial preparation of the atoms, and linear gain coefficient more closely, we plot the minus quadrature variance versus these parameters. We also obtain the maximum squeezing for various cases considered along with the values of the parameters for which the maximum squeezing occurs. To this end, we first consider the dependence of the squeezing on the amplitude of the driving radiation and initial preparation of the atoms while the linear gain coefficient, squeeze parameter, and cavity damping constant are fixed. In view of the discussion given in chapter 3, Eqs. (3.55) and (3.56) have a well-behaved solutions for $\lambda_2 \geq 0$. It is found using Eq. (4.51) that $\lambda_2 \geq 0$ for $0 \leq \eta \leq 1$, $0 \leq \Omega \leq 10\gamma$, and $A \leq 1.3$. Based on this, we plot the quadrature variance given by Eq. (4.47) versus Ω/γ and η in which the linear gain coefficient is taken to be $A = 1.3$.

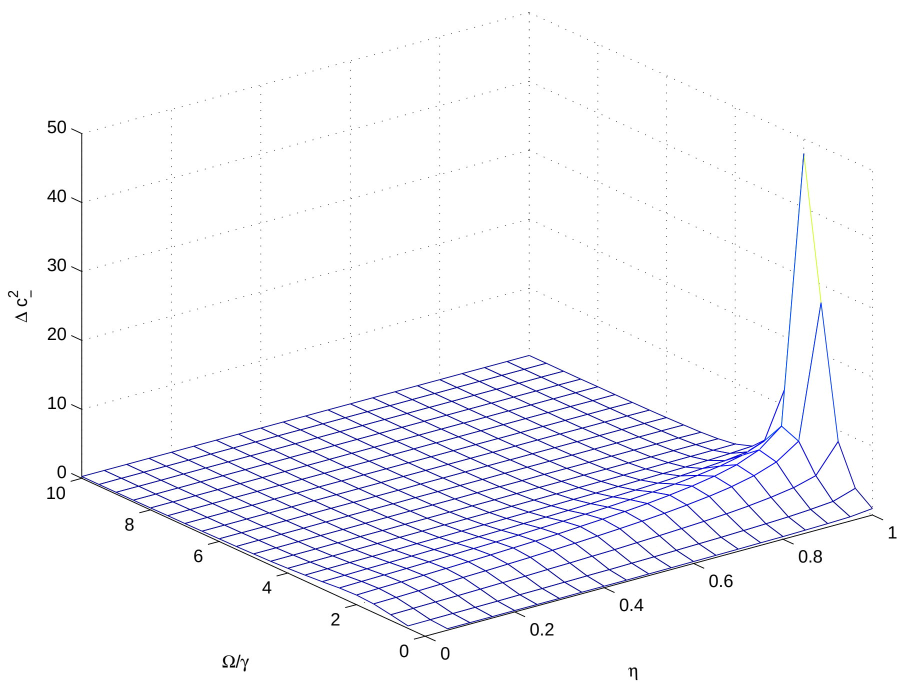

Fig. 4.1: Plot of the quadrature variance Δc_-^2 (Eq. (4.47)) of the two-mode cavity radiation at steady state for $r = 0.75$, $\kappa = 0.5$, and $A = 1.3$.

We clearly see from Fig. 4.1 that the two-mode cavity radiation does not exhibit squeezing for certain values of Ω/γ and η even when it is coupled to a two-mode squeezed vacuum reservoir. It is found, for example when $\eta = 1$, $r = 0.75$, $\kappa = 0.5$, and $A = 1.3$, that there is no squeezing for values of Ω ranging between 0.1γ and 4.1γ. However, a maximum squeezing of 81% occurs for $\eta = 0$ and $\Omega = 0.1\gamma$.

We next plot the quadrature variance versus A and η in which the squeeze parameter and cavity damping constant are fixed at the previous values. We also take the amplitude of the driving radiation for which the maximum squeezing occurs in the previous case ($\Omega = 0.1\gamma$).

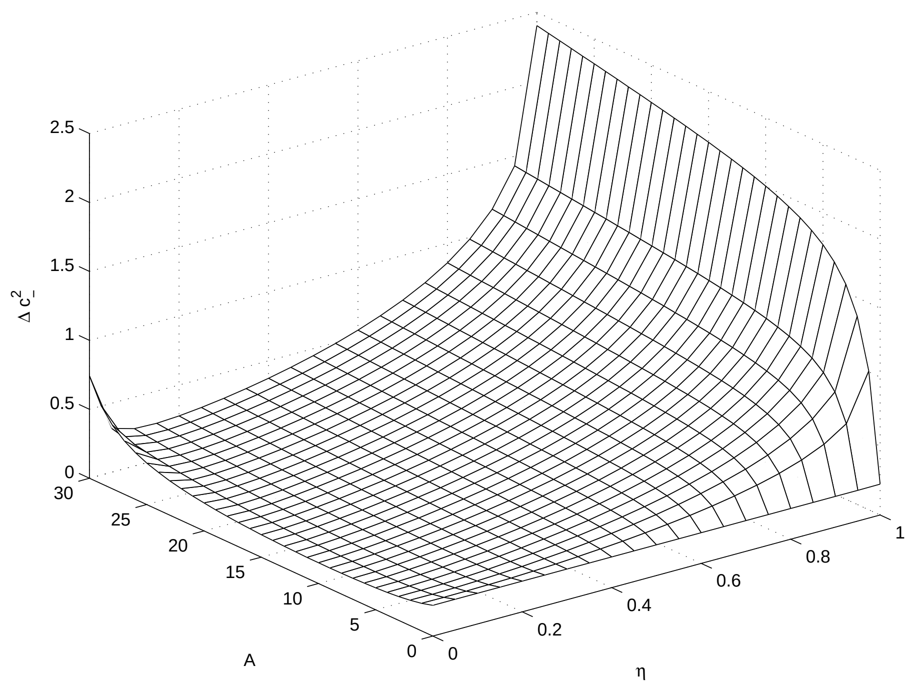

Fig. 4.2: Plot of the quadrature variance Δc_-^2 (Eq. (4.47)) of the two-mode cavity radiation at steady state for $r = 0.75$, $\kappa = 0.5$, and $\Omega = 0.1\gamma$.

It is not difficult to observe from Fig. 4.2 that the two-mode cavity radiation exhibits squeezing for certain values of A and η. It is also possible to see that the degree of squeezing decreases with the linear gain coefficient for some values of η. Moreover, a maximum squeezing of 85% is found to occur for $\eta = 0$ and $A = 9.2$.

We next plot the quadrature variance versus A and Ω/γ for $\eta = 0.1$ and for the same values of r and κ as in the previous case.

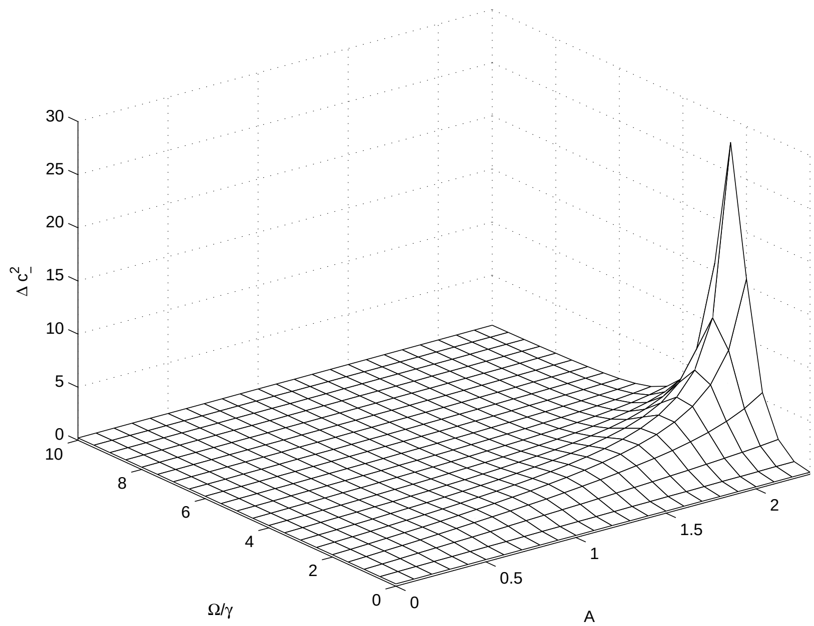

Fig. 4.3: Plot of the quadrature variance Δc_-^2 (Eq. (4.47)) of the two-mode cavity radiation at steady state for $r = 0.75$, $\kappa = 0.5$, and $\eta = 0.1$.

Fig. 4.3 clearly indicates that the two-mode cavity radiation does not exhibit squeezing for certain values of A and Ω/γ. It is also possible to verify that the degree of squeezing decreases with the linear gain coefficient for some values of Ω/γ. In addition, a maximum squeezing of 82% is obtained for $\Omega = 0.1\gamma$ and $A = 2.3$ (the maximum possible value).

As we can infer from Figs. 4.1, 4.2, and 4.3 the quadrature variance of the two-mode cavity radiation strongly depends on the linear gain coefficient A, amplitude of the driving radiation Ω, and initial preparation of the atoms η. However, the explicit dependence of the degree of squeezing on these parameters is not directly evident from these figures. We hence seek to consider various specific cases to study the dependence of the squeezing of the two-mode cavity radiation on these parameters. To this end, we consider the dependence of the squeezing on the squeeze parameter as well as the linear gain coefficient, amplitude of the driving radiation, and initial preparation of the atoms by alternatively fixing two of these parameters. As in the previous cases we also find the maximum squeezing and values of the parameters at which the maximum squeezing occurs. Moreover, we generate data from Eq. (4.47) and present it in a tabular form. We first plot the quadrature variance versus the linear gain coefficient for different values of the squeeze parameter while the values of the amplitude of the driving radiation and initial preparation of the atoms are fixed based on the previous results.

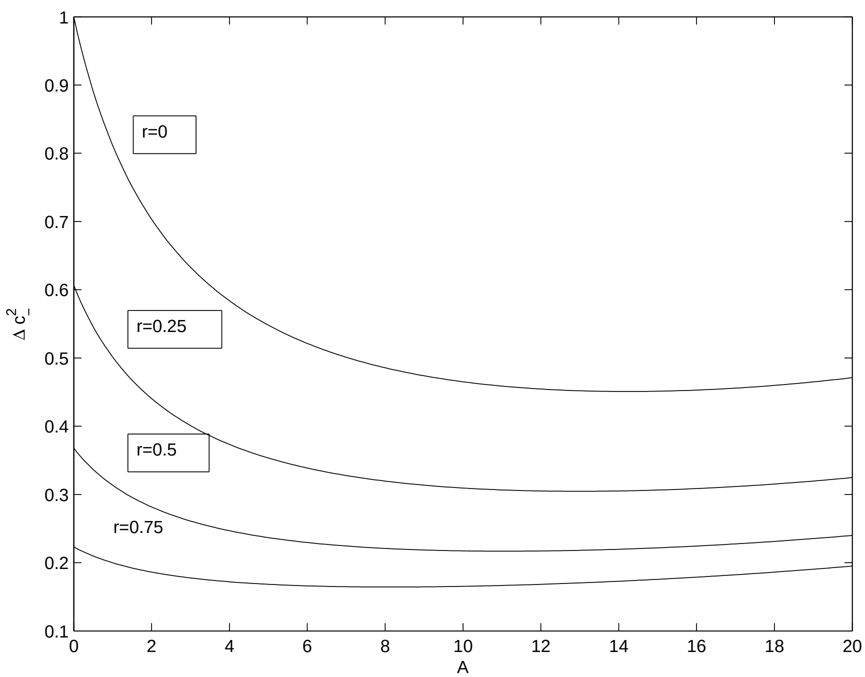

Fig. 4.4: Plots of the quadrature variance Δc_-^2 (Eq. (4.47)) of the cavity radiation at steady state for $\eta = 0.1$, $\kappa = 0.5$, $\Omega = 0.1\gamma$, and different values of r.

In order to see the maximum squeezing and values of A for which the maximum squeezing occurs for each value of r, we generate the data shown in Table (4.1) from Eq. (4.47).

r	Maximum squeezing	Maximum squeezing occurs for
0.00	55%	A=14
0.25	70%	A=13
0.50	78%	A=11
0.75	84%	A=8

Table 4.1: Maximum squeezing for $\eta = 0.1$, $\kappa = 0.5$, $\Omega = 0.1\gamma$, and different values of r.

We see from Fig. 4.4 that the degree of squeezing increases with the squeeze parameter. We also notice from the data given in Table (4.1) that the maximum squeezing occurs for different values A corresponding to different values of r. Closer observation of Fig. 4.4 reveals that the variation in the degree of squeezing of the two-mode radiation due to the squeeze parameter decreases with the linear gain coefficient. We notice that the number of photons emitted by the atoms for smaller values of A is smaller. But the number of photons of the squeezed light entering the cavity is independent of A. Hence the degree of squeezing of the cavity radiation would be dominated by the squeezed light entering the cavity when A is small, which must be the reason for the difference in the variation of the degree of squeezing shown in Fig. 4.4.

Next we plot the quadrature variance versus η for $A = 14$ and different values of r.

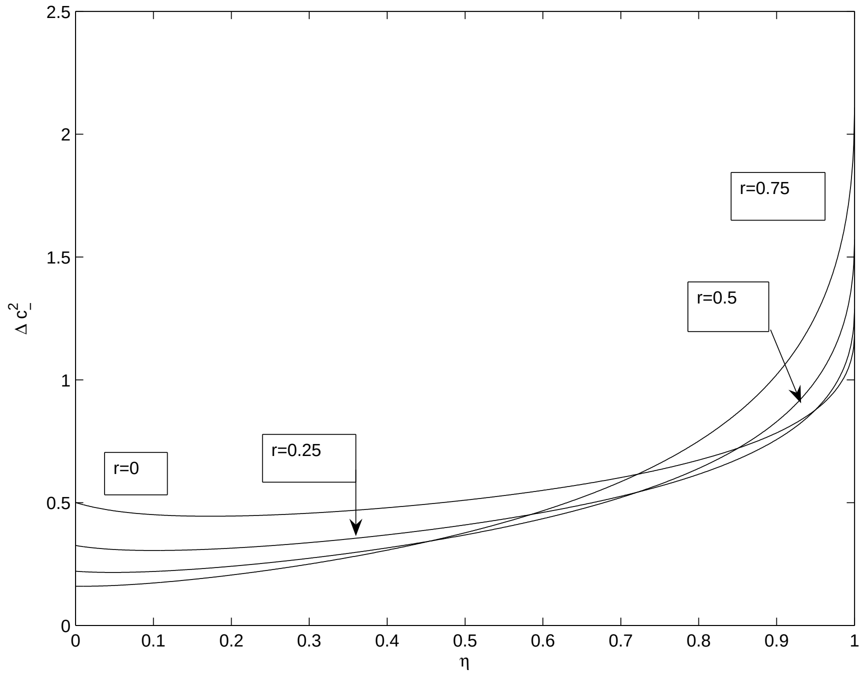

Fig. 4.5: Plots of the quadrature variance Δc_-^2 (Eq. (4.47)) of the cavity radiation at steady state for $A = 14$, $\kappa = 0.5$, $\Omega = 0.1\gamma$, and different values of r.

Following the same procedure the maximum squeezing, values of η for which the maximum squeezing occurs, and values of η for which the squeezing occurs are generated from Eq. (4.47).

r	Max. squeezing	Max. Squeezing occurs for	Squeezing occurs for
0.00	56%	η=0.17	$\eta < 0.98$
0.25	70%	η=0.10	$\eta < 0.97$
0.50	78%	η=0.05	$\eta < 0.95$
0.75	84%	η=0.00	$\eta < 0.89$

Table 4.2: Maximum squeezing for $A = 14$, $\kappa = 0.5$, $\Omega = 0.1\gamma$, and different values of r.

As shown in Fig. 4.5 the cavity radiation exhibits squeezing for certain values of η. We realize that the degree of squeezing increases with the squeeze parameter for smaller values of η, but decreases for larger values. Based on the definition of η (3.52) we note that larger values of η means larger number of the atoms are initially prepared to be in the bottom level. These atoms can absorb one of the modes in the cavity to make a transition to the next upper level. Since the two-mode squeezing is associated with the correlation between the modes, this process undoubtedly affects the squeezing. It is good to note that these excited atoms may not emit radiation that contribute to the squeezing, which may lead to the depletion in the degree of squeezing. We also notice from Table (4.2) that the maximum squeezing occurs for different values of η corresponding to different r. We hence infer from the results shown in Tables (4.1) and (4.2) that a higher degree of squeezing can be obtained by altering the values of A and η for a given value of r.

Now we plot the quadrature variance versus Ω/γ for different values of the linear gain coefficient. Here we take $\eta = 0.1$.

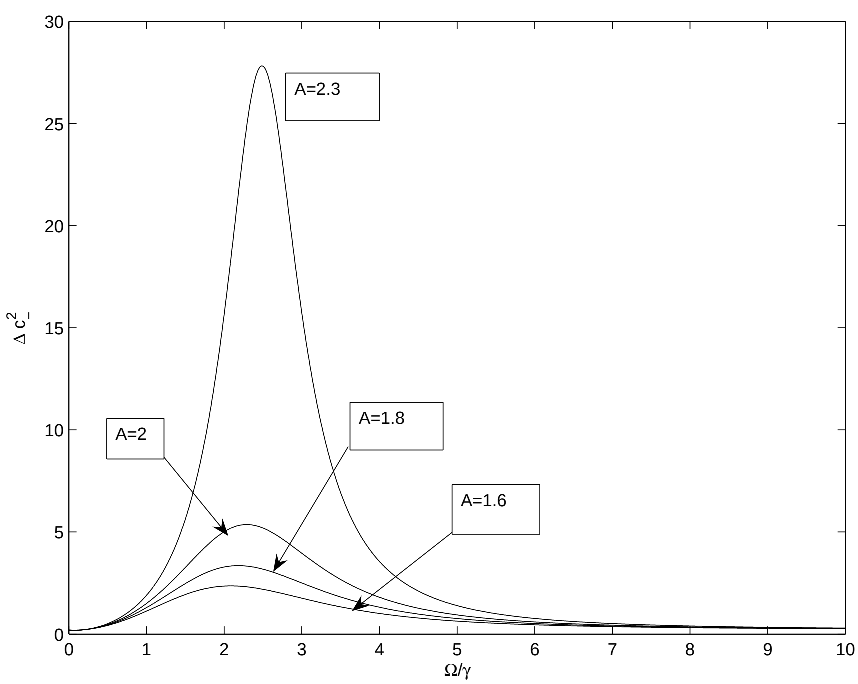

Fig. 4.6: Plots of the quadrature variance Δc_-^2 (Eq. (4.47)) of the cavity radiation at steady state for $\eta = 0.1$, $\kappa = 0.5$, $r = 0.75$, and different values of A.

In a similar manner the maximum squeezing, values of Ω/γ for which the maximum squeezing occurs as well as values of Ω/γ for which the squeezing does not occur are generated from Eq. (4.47).

A	Max. squeezing	Max. Squeezing occurs for	Squeezing does not occur for
1.6	81.0%	$\Omega = 0.07\gamma$	$0.84 < \Omega/\gamma < 4.11$
1.8	81.2%	$\Omega = 0.07\gamma$	$0.85 < \Omega/\gamma < 4.47$
2.0	81.6%	$\Omega = 0.07\gamma$	$0.81 < \Omega/\gamma < 4.89$
2.3	82.1%	$\Omega = 0.07\gamma$	$0.73 < \Omega/\gamma < 5.51$

Table 4.3: Maximum squeezing for $\eta = 0.1$, $\kappa = 0.5$, $r = 0.75$, and different values of A.

As clearly indicated in Fig. 4.6, the cavity radiation exhibits squeezing either for smaller or larger values of Ω/γ. We find that the maximum degree of squeezing increases with the linear gain coefficient in both cases. We also see from the result shown in Table (4.3) that the range of the values of Ω/γ for which the squeezing does not exist increases with the linear gain coefficient.

We next plot the quadrature variance versus Ω/γ for different values of r. The steady state consideration ($\lambda_2 \geq 0$) is found to hold for $A \leq 2.3$ when $\eta = 0.1$ and $0 \leq \Omega \leq 10\gamma$.

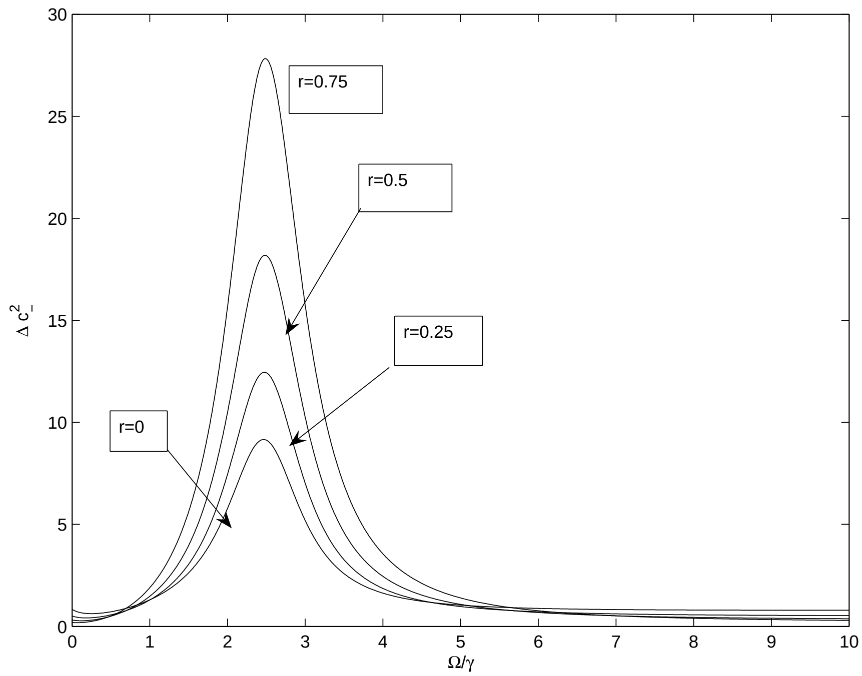

Fig. 4.7: Plots of the quadrature variance Δc_-^2 (Eq. (4.47)) of the cavity radiation at steady state for $A = 2.3$, $\kappa = 0.5$, $\eta = 0.1$, and different values of r.

Following a similar method the maximum squeezing, values of Ω/γ for which the maximum squeezing occurs, and values of Ω/γ for which the squeezing does not occur are generated from Eq. (4.47).

r	Max. squeezing	Max. Squeezing occurs for	Squeezing does not occur for
0.00	38%	$\Omega = 0.25\gamma$	$0.79 < \Omega/\gamma < 5.17$
0.25	59%	$\Omega = 0.18\gamma$	$0.84 < \Omega/\gamma < 4.93$
0.50	73%	$\Omega = 0.12\gamma$	$0.81 < \Omega/\gamma < 5.12$
0.75	82%	$\Omega = 0.07\gamma$	$0.73 < \Omega/\gamma < 5.51$

Table 4.4: Maximum squeezing for $\eta = 0.1$, $\kappa = 0.5$, $A = 2.3$, and different values of r.

We see from Fig. 4.7 that the cavity radiation exhibits squeezing either for smaller or larger values of Ω/γ. We also find that the degree of squeezing increases with the squeeze parameter in both cases.

We gather from what we have seen so far that it is possible to get radiation with a substantial degree of squeezing by properly choosing the linear gain coefficient, amplitude of the driving radiation, and initial preparation of the atoms. Nonetheless, we observe that the degree of squeezing does not increase for all cases with the linear gain coefficient and squeeze parameter as generally expected. In order to study the degree of squeezing of the two-mode cavity radiation more closely, we next consider special cases of interest.

4.1.1 When half of the atoms are initially in the top level

When half of the atoms are initially prepared to be in the top level ($\eta = 0$), Eq. (4.47) takes the form

$$\begin{aligned}\Delta c_{\pm}^2 = 1 &+ \left[\frac{A}{B}(C' \mp F') + 2\kappa(N \pm M)\right]\frac{(\lambda_1' + \lambda_2')^2 + 4\lambda_1'\lambda_2'}{8\lambda_1'\lambda_2'(\lambda_1' + \lambda_2')} \\ &+ \left[\left(\frac{AC'}{B} + \kappa N\right)\left(p'^2 + q_-'^2 \mp 2q_-'p'\right) + \kappa N\left(p'^2 + q_+'^2 \pm 2q_+'p'\right)\right. \\ &+ \left.\left(\frac{AF'}{B} - 2\kappa M\right)\left(p'(q_+' - q_-') \pm (p'^2 - q_-'q_+')\right)\right]\frac{(\lambda_1' + \lambda_2')^2 - 4\lambda_1'\lambda_2'}{8\lambda_1'\lambda_2'(\lambda_1' + \lambda_2')} \\ &+ \left[\left(\frac{AC'}{B} + \kappa N\right)\left(p' \mp q_-'\right) - \kappa N\left(p' \pm q_+'\right)\right. \\ &+ \left.\left(\frac{AF'}{2B} - \kappa M\right)(q_+' + q_-')\right]\frac{\lambda_1' - \lambda_2'}{4\lambda_1'\lambda_2'}, \end{aligned} \tag{4.59}$$

with

$$C' = \frac{1}{2} + \frac{\Omega^2}{2\gamma^2} - \frac{3\Omega}{4\gamma}, \tag{4.60}$$

$$F' = -\frac{\Omega}{4\gamma}\left(1 + \frac{\Omega^2}{\gamma^2}\right) - \left(1 - \frac{\Omega^2}{2\gamma^2}\right), \tag{4.61}$$

$$\lambda_1' = \frac{\kappa}{2} + \frac{A}{4B}\left[\frac{3\Omega}{2\gamma} + \chi'\right], \tag{4.62}$$

$$\lambda_2' = \frac{\kappa}{2} + \frac{A}{4B}\left[\frac{3\Omega}{2\gamma} - \chi'\right], \tag{4.63}$$

$$\begin{aligned} p'^2 + q_-'^2 \mp 2q_-'p' = \frac{1}{\chi'^2}&\left[\left(1 + \frac{\Omega^2}{\gamma^2}\right)^2\left[1 + \frac{\Omega}{\gamma}\left(\frac{\Omega}{4\gamma} \pm 1\right)\right]\right. \\ &+ \left.\left(1 - \frac{\Omega^2}{2\gamma^2}\right)\left[\left(1 - \frac{\Omega^2}{2\gamma^2}\right) + \left(1 + \frac{\Omega^2}{\gamma^2}\right)\left(\frac{\Omega}{\gamma} \pm 2\right)\right]\right], \end{aligned} \tag{4.64}$$

$$p'^2 + q_+'^2 \pm 2q_+'p' = \frac{1}{\chi'^2}\left[\left(1+\frac{\Omega^2}{\gamma^2}\right)^2\left[1+\frac{\Omega}{\gamma}\left(\frac{\Omega}{4\gamma}\mp 1\right)\right]\right.$$
$$\left. + \left(1-\frac{\Omega^2}{2\gamma^2}\right)\left[\left(1-\frac{\Omega^2}{2\gamma^2}\right) - \left(1+\frac{\Omega^2}{\gamma^2}\right)\left(\frac{\Omega}{\gamma}\mp 2\right)\right]\right], \tag{4.65}$$

$$p'(q_+' - q_-') \pm (p'^2 - q_+'q_-') = \frac{1}{\chi'^2}\left[\left(1-\frac{\Omega^2}{2\gamma^2}\right)\left[2\left(1+\frac{\Omega^2}{\gamma^2}\right) \pm \left(1-\frac{\Omega^2}{2\gamma^2}\right)\right]\right.$$
$$\left. \pm \left(1+\frac{\Omega^2}{\gamma^2}\right)^2\left(1-\frac{\Omega^2}{4\gamma^2}\right)\right], \tag{4.66}$$

$$p' \mp q_-' = \frac{1}{\chi'}\left[\left(1+\frac{\Omega^2}{\gamma^2}\right)\left(1\pm\frac{\Omega}{2\gamma}\right) \pm \left(1-\frac{\Omega^2}{2\gamma^2}\right)\right], \tag{4.67}$$

$$p' \pm q_+' = \frac{1}{\chi'}\left[\left(1+\frac{\Omega^2}{\gamma^2}\right)\left(1\mp\frac{\Omega}{2\gamma}\right) \pm \left(1-\frac{\Omega^2}{2\gamma^2}\right)\right], \tag{4.68}$$

$$q_+' + q_-' = -\frac{\Omega}{\chi'\gamma}\left(1+\frac{\Omega^2}{\gamma^2}\right), \tag{4.69}$$

and

$$\chi' = \left[\left(1+\frac{\Omega^2}{\gamma^2}\right)^2\left(1+\frac{\Omega^2}{4\gamma^2}\right) - \left(1-\frac{\Omega^2}{2\gamma^2}\right)^2\right]^{\frac{1}{2}}. \tag{4.70}$$

We now seek to analyze the squeezing of the radiation generated when half of the atoms are initially prepared to be in the top level. In this case, we notice from Eqs. (3.52), (3.53), and (3.54) that $\rho_{aa}^{(0)} = \rho_{cc}^{(0)} = \rho_{ac}^{(0)} = 1/2$. It is also possible to see from Eq. (3.54) that $\rho_{ac}^{(0)}$ can attain a maximum value of 1/2. Therefore, the case for which $\eta = 0$ corresponds to the maximum atomic coherence. In order to study the dependence of the squeezing on the amplitude of the driving radiation, linear gain coefficient, and squeeze parameter more closely, we first plot the quadrature variance versus Ω/γ for different values of A where r is arbitrarily fixed. We consider when Ω/γ is very small.

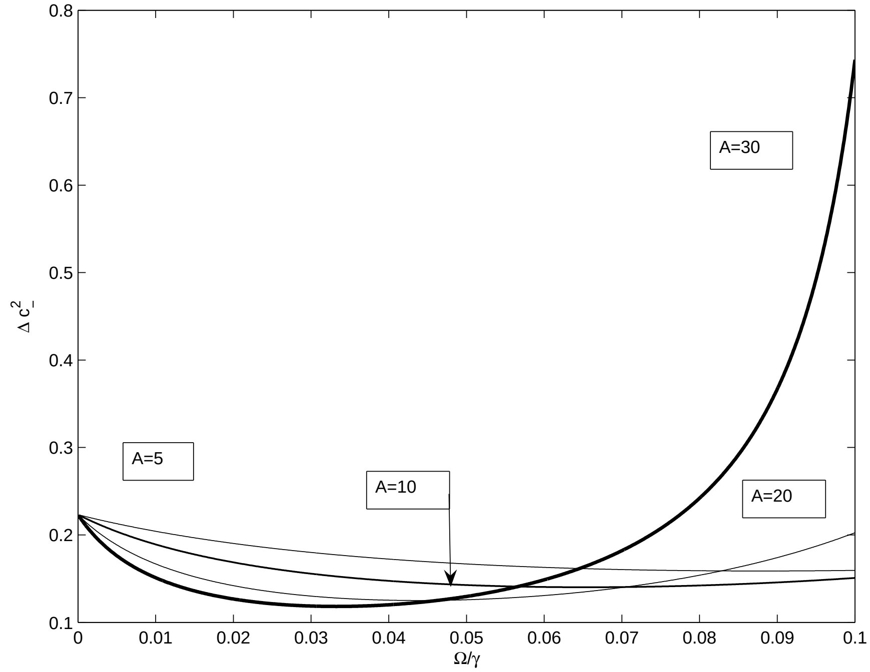

Fig. 4.8: Plots of the quadrature variance Δc_-^2 (Eq. (4.59)) of the two-mode cavity radiation at steady state for $r = 0.75$, $\kappa = 0.5$, $\eta = 0$, and different values of A.

The maximum squeezing and values of Ω/γ for which the maximum squeezing occurs are generated from Eq. (4.59).

A	Maximum squeezing	Maximum squeezing occurs for
1	80%	$\Omega = 0.10\gamma$
10	86%	$\Omega = 0.06\gamma$
20	87%	$\Omega = 0.04\gamma$
30	88%	$\Omega = 0.03\gamma$

Table 4.5: Maximum squeezing for $\eta = 0$, $\kappa = 0.5$, $r = 0.75$, and different values of A.

As clearly indicated in Fig. 4.8, the cavity radiation exhibits squeezing when half of the atoms are initially prepared to be in the top level for smaller values of Ω/γ. We notice that the degree of squeezing increases with the linear gain coefficient for relatively smaller values of Ω/γ, but decreases for larger values. It is also found that the maximum obtainable squeezing increases with the linear gain coefficient. Moreover, it is not difficult to see from Table (4.5) that driving radiation of smaller amplitude is required to generate radiation with a higher degree of squeezing for larger values of the linear gain coefficient.

We next plot the quadrature variance versus Ω/γ for different values of r. Since the steady state consideration ($\lambda_2' \geq 0$) is found using Eq. (4.63) to be valid for $A \leq 30$ when $0 \leq \Omega \leq 0.1\gamma$ and $\eta = 0$, we take $A = 30$.

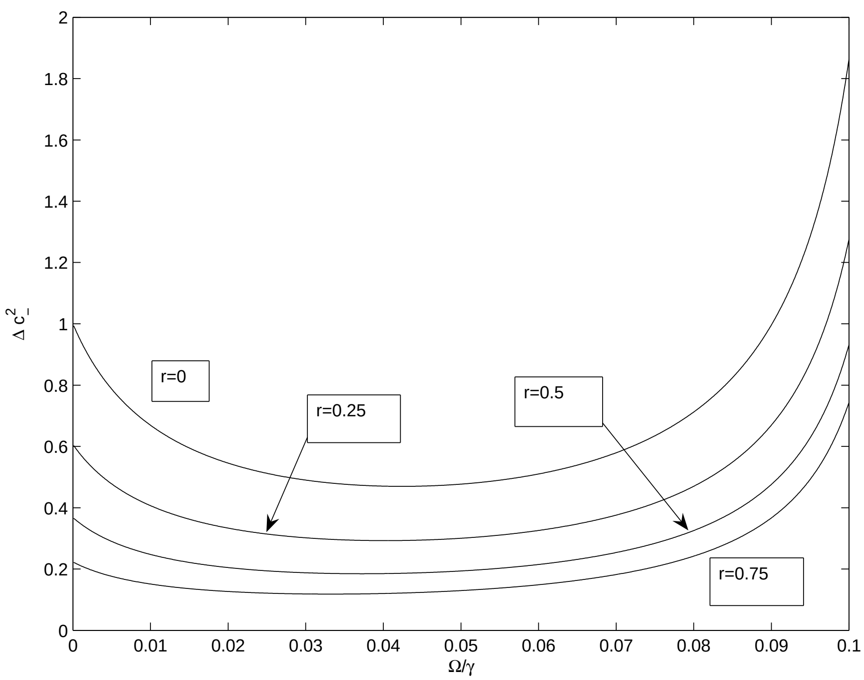

Fig. 4.9: Plots of the quadrature variance Δc_-^2 (Eq. (4.59)) of the two-mode cavity radiation at steady state for $A = 30$, $\kappa = 0.5$, $\eta = 0$, and different values of r.

Following a similar approach, the maximum squeezing and values of Ω/γ for which the maximum squeezing occurs are generated from Eq. (4.59).

r	Maximum squeezing	Maximum squeezing occurs for
0.00	53%	$\Omega = 0.05\gamma$
0.25	71%	$\Omega = 0.04\gamma$
0.50	82%	$\Omega = 0.04\gamma$
0.75	88%	$\Omega = 0.03\gamma$

Table 4.6: Maximum squeezing for $\eta = 0$, $\kappa = 0.5$, $A = 30$, and different values of r.

We see from Fig. 4.9 that the degree of squeezing increases with the squeeze parameter. We also notice from Table (4.6) that the maximum squeezing occurs for almost the same value of Ω/γ for different values of r. As clearly shown in Figs. 4.1 and 4.6 the squeezing is found to occur either for smaller or larger values of Ω/γ, as a result we in the following plot the quadrature variance versus Ω/γ for larger values of Ω/γ.

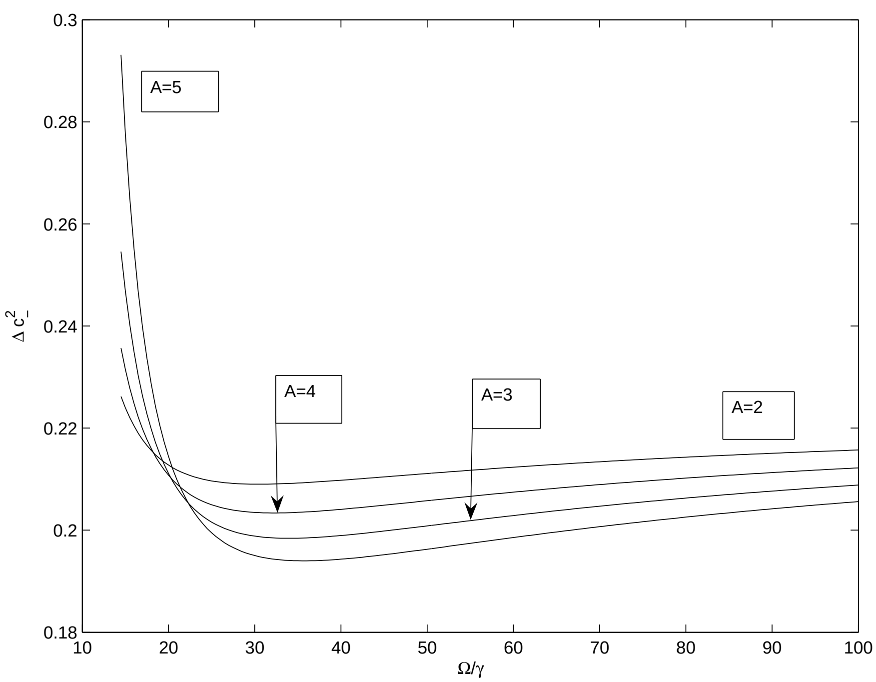

Fig. 4.10: Plots of the quadrature variance Δc_-^2 (Eq. (4.59)) of the two-mode cavity radiation at steady state for $r = 0.75$, $\kappa = 0.5$, $\eta = 0$, and different values of A.

In a similar manner the maximum squeezing and values of Ω/γ for which the maximum squeezing occurs for different values of A are generated from Eq. (4.59).

A	Maximum squeezing	Maximum squeezing occurs for
2	79%	$\Omega = 31\gamma$
3	80%	$\Omega = 33\gamma$
4	80%	$\Omega = 35\gamma$
5	81%	$\Omega = 37\gamma$

Table 4.7: Maximum squeezing for $\eta = 0$, $\kappa = 0.5$, $r = 0.75$, and different values of A.

One can easily see from Fig. 4.10, the cavity radiation exhibits a significant degree of squeezing. We also notice that the degree of squeezing increases with the linear gain coefficient for relatively larger values of Ω/γ, but decreases for smaller values. Moreover, according to the data given in Table (4.7) a strong external radiation is required to generate a radiation with a higher degree of squeezing when the linear gain coefficient is taken to be large.

We now plot the quadrature variance versus Ω/γ for different values of r. We take the linear gain coefficient to be $A = 5$, the maximum value for which the steady state consideration remains to be valid for the intended range of Ω/γ.

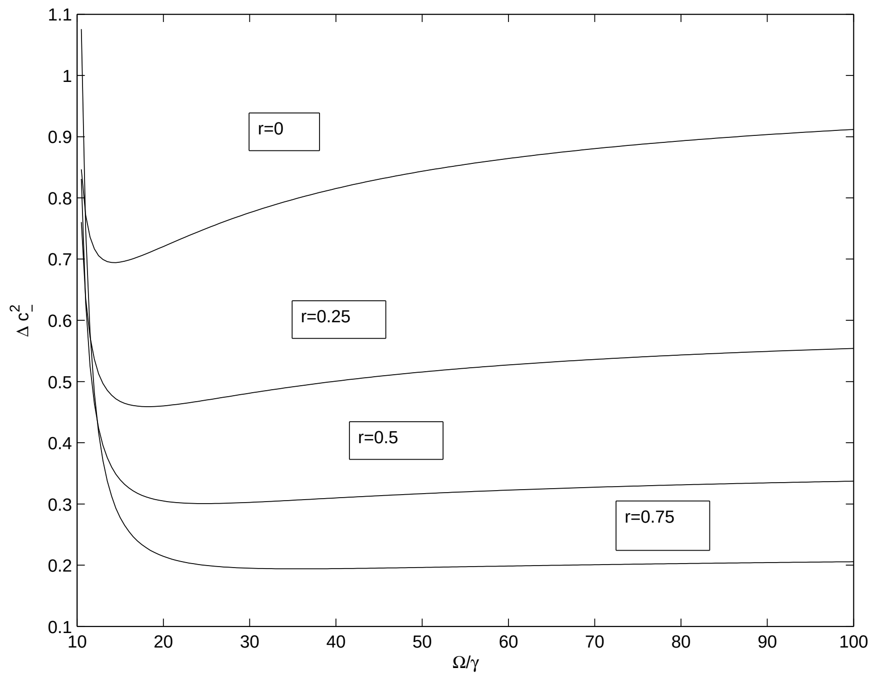

Fig. 4.11: Plots of the quadrature variance Δc_-^2 (Eq. (4.59)) of the two-mode cavity radiation at steady state for $A = 5$, $\kappa = 0.5$, $\eta = 0$, and different values of r.

The maximum squeezing and values of Ω/γ for which the maximum squeezing occurs are generated from Eq. (4.59) following the same approach.

r	Maximum squeezing	Maximum squeezing occurs for
0.00	31%	$\Omega = 15\gamma$
0.25	54%	$\Omega = 20\gamma$
0.50	70%	$\Omega = 27\gamma$
0.75	81%	$\Omega = 37\gamma$

Table 4.8: Maximum squeezing for $\eta = 0$, $\kappa = 0.5$, $A = 5$, and different values of r.

As one can easily see from Fig. 4.11, the degree of squeezing increases with the squeeze parameter. It is also clearly indicated in Table (4.8) that the realizable maximum squeezing occurs for larger values of Ω/γ when r is taken to be large, contrary to the result given in Table (4.6) for smaller values of Ω/γ. Comparing the results shown in Figs. 4.8 and 4.10 as well as Tables (4.5) and (4.7) reveals that for $\eta = 0$ a higher degree of squeezing occurs for very small values of Ω/γ. Though the squeezing is found to increase with the linear gain coefficient, we cannot use arbitrarily large values of A.

4.1.2 When all the atoms are initially in the bottom level

When all the atoms are initially prepared to be in the bottom level ($\eta = 1$), it is possible to put Eq. (4.47) in the form

$$\begin{aligned}
\Delta c_{\pm}^2 = 1 &+ \left[\frac{A}{B}\left(C'' \mp F''\right) + 2\kappa(N \pm M)\right] \frac{(\lambda_1'' + \lambda_2'')^2 + 4\lambda_1''\lambda_2''}{8\lambda_1''\lambda_2''(\lambda_1'' + \lambda_2'')} \\
&+ \left[\left(\frac{AC''}{B} + \kappa N\right)\left(p''^2 + q_-''^2 \mp 2q_-''p''\right) + \kappa N\left(p''^2 + q_+''^2 \pm 2q_+''p''\right)\right. \\
&+ \left.\left(\frac{AF''}{B} - 2\kappa M\right)\left(p''(q_+'' - q_-'') \pm (p''^2 - q_-''q_+'')\right)\right] \frac{(\lambda_1'' + \lambda_2'')^2 - 4\lambda_1''\lambda_2''}{8\lambda_1''\lambda_2''(\lambda_1'' + \lambda_2'')} \\
&+ \left[\left(\frac{AC''}{B} + \kappa N\right)\left(p'' \mp q_-''\right) - \kappa N\left(p'' \pm q_+''\right)\right. \\
&+ \left.\left(\frac{AF''}{2B} - \kappa M\right)\left(q_+'' + q_-''\right)\right] \frac{\lambda_1'' - \lambda_2''}{4\lambda_1''\lambda_2''},
\end{aligned} \tag{4.71}$$

in which

$$C'' = \frac{3\Omega^2}{4\gamma^2}, \tag{4.72}$$

$$F'' = -\frac{\Omega}{4\gamma}\left(1 + \frac{\Omega^2}{\gamma^2}\right) + \frac{3\Omega}{4\gamma}, \tag{4.73}$$

$$\lambda_1'' = \frac{\kappa}{2} + \frac{A}{4B}\left[\left(1 - \frac{\Omega^2}{2\gamma^2}\right) + \chi''\right], \tag{4.74}$$

$$\lambda_2'' = \frac{\kappa}{2} + \frac{A}{4B}\left[\left(1 - \frac{\Omega^2}{2\gamma^2}\right) - \chi''\right], \tag{4.75}$$

$$\begin{aligned}
p''^2 + q_-''^2 \mp 2q_-''p'' = \frac{1}{\chi''^2}&\left[\left(1 + \frac{\Omega^2}{\gamma^2}\right)^2\left[1 + \frac{\Omega}{\gamma}\left(\frac{\Omega}{4\gamma} \pm 1\right)\right]\right. \\
&\left. - \frac{3\Omega}{2\gamma}\left[-\frac{3\Omega}{2\gamma} + \left(1 + \frac{\Omega^2}{\gamma^2}\right)\left(\frac{\Omega}{\gamma} \pm 2\right)\right]\right],
\end{aligned} \tag{4.76}$$

$$p''^2 + q_+''^2 \pm 2q_+''p'' = \frac{1}{\chi''^2}\left[\left(1+\frac{\Omega^2}{\gamma^2}\right)^2\left[1+\frac{\Omega}{\gamma}\left(\frac{\Omega}{4\gamma}\mp 1\right)\right]\right.$$
$$\left.+\frac{3\Omega}{2\gamma}\left[\frac{3\Omega}{2\gamma}+\left(1+\frac{\Omega^2}{\gamma^2}\right)\left(\frac{\Omega}{\gamma}\mp 2\right)\right]\right], \tag{4.77}$$

$$p''(q_+'' - q_-'') \pm (p''^2 - q_+''q_-'') = -\frac{1}{\chi''^2}\left[\frac{3\Omega}{2\gamma}\left[2\left(1+\frac{\Omega^2}{\gamma^2}\right)\mp\frac{3\Omega}{2\gamma}\right]\right.$$
$$\left.\mp\left(1+\frac{\Omega^2}{\gamma^2}\right)^2\left(1-\frac{\Omega^2}{4\gamma^2}\right)\right], \tag{4.78}$$

$$p'' \mp q_-'' = \frac{1}{\chi''}\left[\left(1+\frac{\Omega^2}{\gamma^2}\right)\left(1\pm\frac{\Omega}{2\gamma}\right)\mp\frac{3\Omega}{2\gamma}\right], \tag{4.79}$$

$$p'' \pm q_+'' = \frac{1}{\chi''}\left[\left(1+\frac{\Omega^2}{\gamma^2}\right)\left(1\mp\frac{\Omega}{2\gamma}\right)\mp\frac{3\Omega}{2\gamma}\right], \tag{4.80}$$

$$q_+'' + q_-'' = -\frac{\Omega}{\chi''\gamma}\left(1+\frac{\Omega^2}{\gamma^2}\right), \tag{4.81}$$

with

$$\chi'' = \left[\left(1+\frac{\Omega^2}{\gamma^2}\right)^2\left(1+\frac{\Omega^2}{4\gamma^2}\right)-\frac{3\Omega}{2\gamma}\right]^{\frac{1}{2}}. \tag{4.82}$$

We now seek to analyze the degree of squeezing of the cavity radiation when the atoms are initially prepared to be in the bottom level. In this case, it is possible to see from Eqs. (3.52), (3.53), and (3.54) that $\rho_{aa}^{(0)} = \rho_{ac}^{(0)} = 0$ and $\rho_{cc}^{(0)} = 1$, which corresponds to the minimum atomic coherence. In order to study the dependence of the squeezing on the amplitude of the driving radiation, linear gain coefficient, and squeeze parameter, we first plot the quadrature variance versus Ω/γ for different values of A. We consider the case when Ω/γ is large.

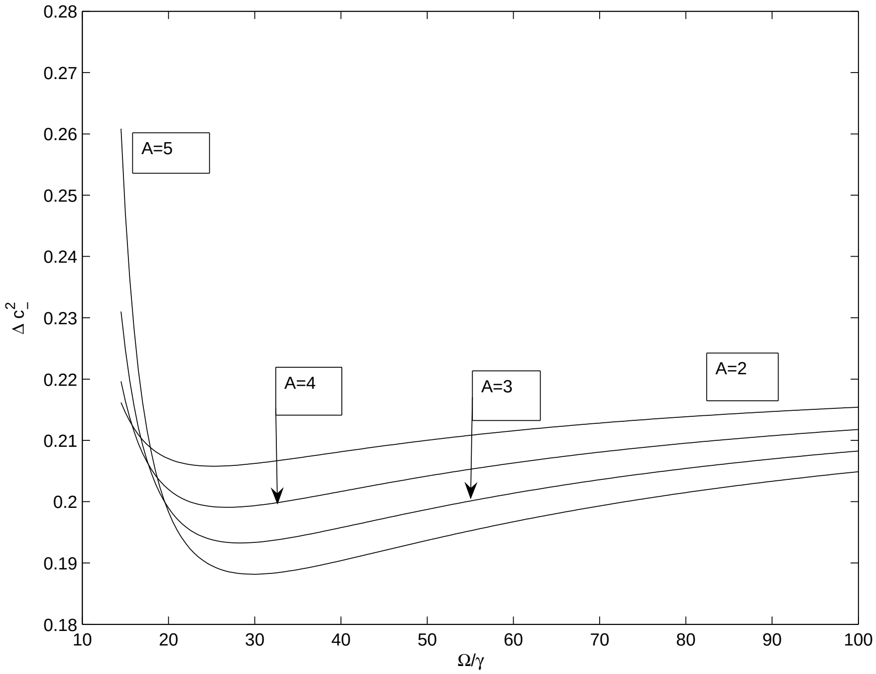

Fig. 4.12: Plots of the quadrature variance Δc_{-}^{2} (Eq. (4.71)) of the two-mode cavity radiation at steady state for $r = 0.75$, $\kappa = 0.5$, $\eta = 1$, and different values of A.

Following a similar procedure the maximum squeezing and values of Ω/γ for which the maximum squeezing occurs are generated from Eq. (4.71).

A	Maximum squeezing	Maximum squeezing occurs for
2	79%	$\Omega = 27\gamma$
3	80%	$\Omega = 28\gamma$
4	81%	$\Omega = 30\gamma$
5	81%	$\Omega = 31\gamma$

Table 4.9: Maximum squeezing for $\eta = 1$, $\kappa = 0.5$, $r = 0.75$, and different values of A.

It is clearly shown in Fig. 4.12 that the cavity radiation exhibits a significant degree of squeezing. Like in the case of $\eta = 0$ (See Fig. 4.10), the degree of squeezing increases with the linear gain coefficient for relatively larger values of Ω/γ, but decreases for smaller values. Moreover, it is possible to see from Figs. 4.10 and 4.12 that the dependence of the degree of squeezing on Ω/γ for $\eta = 0$ and $\eta = 1$ is almost the same, however as shown in Table (4.7) and (4.9) the maximum squeezing for $\eta = 1$ occurs for comparably smaller values of Ω/γ.

We next plot the quadrature variance versus Ω/γ for different values of r. We take $A = 5$ so that a comparison between the results for $\eta = 0$ and $\eta = 1$ can be made.

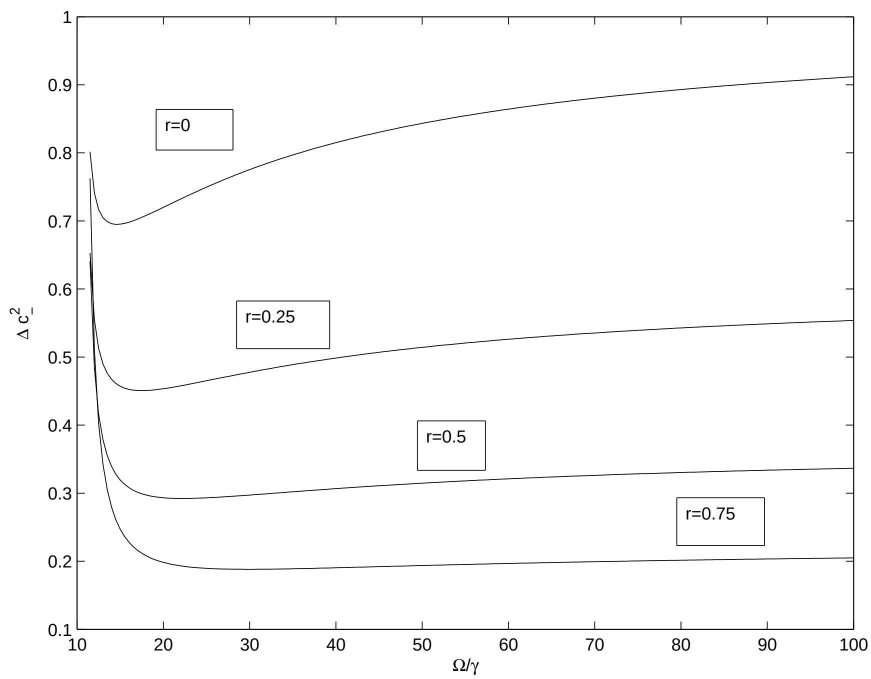

Fig. 4.13: Plots of the quadrature variance Δc_-^2 (Eq. (4.71)) of the two-mode cavity radiation at steady state for $A = 5$, $\kappa = 0.5$, $\eta = 1$, and different values of r.

Following a similar approach the maximum squeezing and values of Ω/γ for which the maximum squeezing occurs are generated from Eq. (4.71).

r	Maximum squeezing	Maximum squeezing occurs for
0.00	31%	$\Omega = 15\gamma$
0.25	55%	$\Omega = 18\gamma$
0.50	71%	$\Omega = 23\gamma$
0.75	81%	$\Omega = 30\gamma$

Table 4.10: Maximum squeezing for $\eta = 1$, $\kappa = 0.5$, $A = 5$, and different values of r.

As we can see from Fig. 4.13, the degree of squeezing increases with the squeeze parameter. Now comparison of the results indicated in Figs. 4.11 and 4.13 as well as Tables (4.8) and (4.10) shows that the dependence of the degree of squeezing on the squeeze parameter is almost the same for $\eta = 0$ and $\eta = 1$, but a maximum degree of squeezing is realizable for relatively smaller values of Ω/γ for $\eta = 1$.

4.1.3 In the absence of the external driving radiation

Next we consider the case when the top and bottom levels of the atoms are not coupled externally by a coherent radiation. We note for $\Omega = 0$ that

$$B = 1, \tag{4.83}$$

$$C = \frac{1-\eta}{2}, \tag{4.84}$$

$$F = -\frac{\sqrt{1-\eta^2}}{2}, \tag{4.85}$$

$$\lambda_1 = \frac{\kappa + A\eta}{2}, \tag{4.86}$$

$$\lambda_2 = \frac{\kappa}{2}, \tag{4.87}$$

$$p^2 + q_-^2 \mp 2q_- p = \frac{2(1 \pm \sqrt{1-\eta^2})}{\eta^2} - 1, \tag{4.88}$$

$$p^2 + q_+^2 \pm 2q_+p = \frac{2(1 \pm \sqrt{1-\eta^2})}{\eta^2} - 1, \tag{4.89}$$

$$p(q_+ - q_-) \pm (p^2 - q_-q_+) = \pm\left[\frac{2(1 \pm \sqrt{1-\eta^2})}{\eta^2} - 1\right], \tag{4.90}$$

$$p \mp q_- = \frac{1 \pm \sqrt{1-\eta^2}}{\eta}, \tag{4.91}$$

$$p \pm q_+ = \frac{1 \pm \sqrt{1-\eta^2}}{\eta}, \tag{4.92}$$

$$q_+ + q_- = 0. \tag{4.93}$$

Employing Eqs. (4.86) and (4.87), we obtain

$$\frac{(\lambda_1+\lambda_2)^2 + 4\lambda_1\lambda_2}{8\lambda_1\lambda_2(\lambda_1+\lambda_2)} = \frac{8\kappa(\kappa+A\eta) + A^2\eta^2}{4\kappa(2\kappa+A\eta)(\kappa+A\eta)}, \tag{4.94}$$

$$\frac{(\lambda_1+\lambda_2)^2 - 4\lambda_1\lambda_2}{8\lambda_1\lambda_2(\lambda_1+\lambda_2)} = \frac{A^2\eta^2}{4\kappa(2\kappa+A\eta)(\kappa+A\eta)}, \tag{4.95}$$

$$\frac{\lambda_1-\lambda_2}{4\lambda_1\lambda_2} = \frac{A\eta}{2\kappa(\kappa+A\eta)}. \tag{4.96}$$

Hence on the basis of Eqs. (4.47), (4.83), (4.84), (4.85), (4.88), (4.89), (4.90), (4.91), (4.92), (4.93), (4.94), (4.95), and (4.96), we find

$$\begin{aligned}\Delta c_\pm^2 &= 1 + A(1-\eta)\frac{4\kappa(\kappa+A\eta) + A[A(1+\eta)+2\kappa](1 \pm \sqrt{1-\eta^2})}{4\kappa(2\kappa+A\eta)(\kappa+A\eta)} \\ &\pm A\sqrt{1-\eta^2}\frac{4\kappa(\kappa+A\eta) + A^2(\eta^2 - 1 \mp \sqrt{1-\eta^2})}{4\kappa(2\kappa+A\eta)(\kappa+A\eta)} \\ &+ (N \pm M)\frac{4\kappa(\kappa+A\eta) + A^2(1 \pm \sqrt{1-\eta^2})}{(2\kappa+A\eta)(\kappa+A\eta)}.\end{aligned} \tag{4.97}$$

Now we seek to analyze the dependence of the squeezing on the linear gain coefficient, initial preparation of the atoms, and squeeze parameter when there is no external driving radiation more closely. To this end, we first plot the quadrature variance versus η for different values of the linear gain coefficient when $r = 0$. We observe that there is no limit in the value of A if $\Omega = 0$ and $\eta \geq 0$.

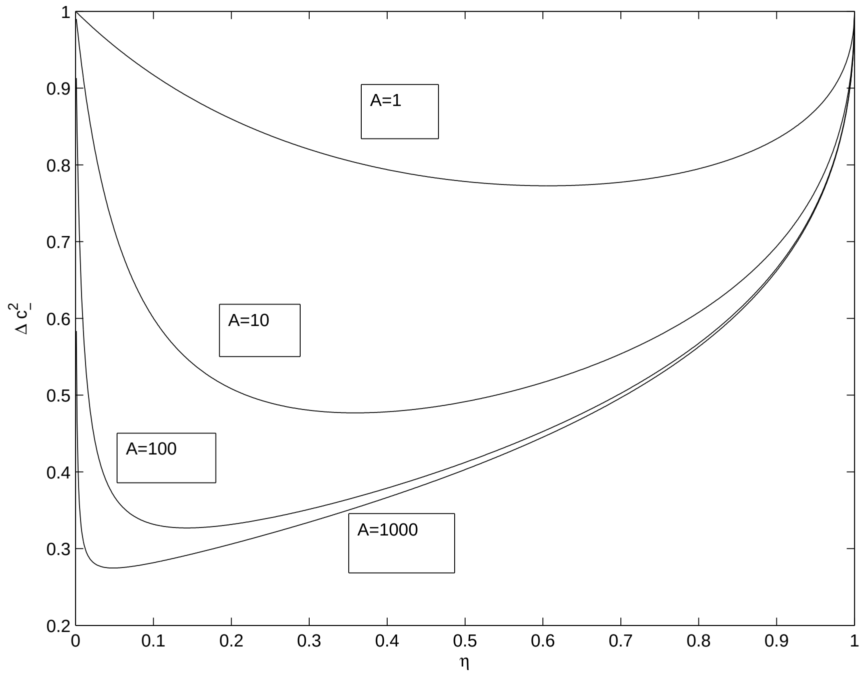

Fig. 4.14: Plots of the quadrature variance Δc_-^2 (Eq. (4.97)) of the two-mode cavity radiation at steady state for $\Omega = 0$, $\kappa = 0.5$, $r = 0$, and different values of A.

The maximum squeezing and values of η for which the maximum squeezing occurs are generated from Eq. (4.97) in the same manner.

A	Maximum squeezing	Maximum squeezing occurs for
1	27%	η=0.63
10	52%	η=0.30
100	67%	η=0.15
1000	73%	η=0.05

Table 4.11: Maximum squeezing for $\Omega = 0$, $\kappa = 0.5$, $r = 0$, and different values of A.

It is clearly shown in Fig. 4.14 that the cavity radiation of a system under consideration exhibits squeezing for values of η between 0 and 1 when there is no external driving radiation. This corresponds to when the atoms are initially prepared in such a way that there are more atoms in the bottom level than the top level. We notice that the degree of squeezing increases with the linear gain coefficient. We also realize that a higher degree of squeezing is observed for smaller values of η and larger values of A. Besides, it is not difficult to see from Fig. 4.14 that squeezing is not exhibited when the atoms are initially prepared with a maximum or minimum atomic coherence. Hence the degree of squeezing of the cavity radiation shown in Figs. 4.9, 4.11, and 4.13 for $r = 0$ is entirely attributed to driving mechanism due to the external coherent radiation.

We next plot the quadrature variance versus η for different values of r. The linear gain coefficient is arbitrarily fixed at $A = 1000$.

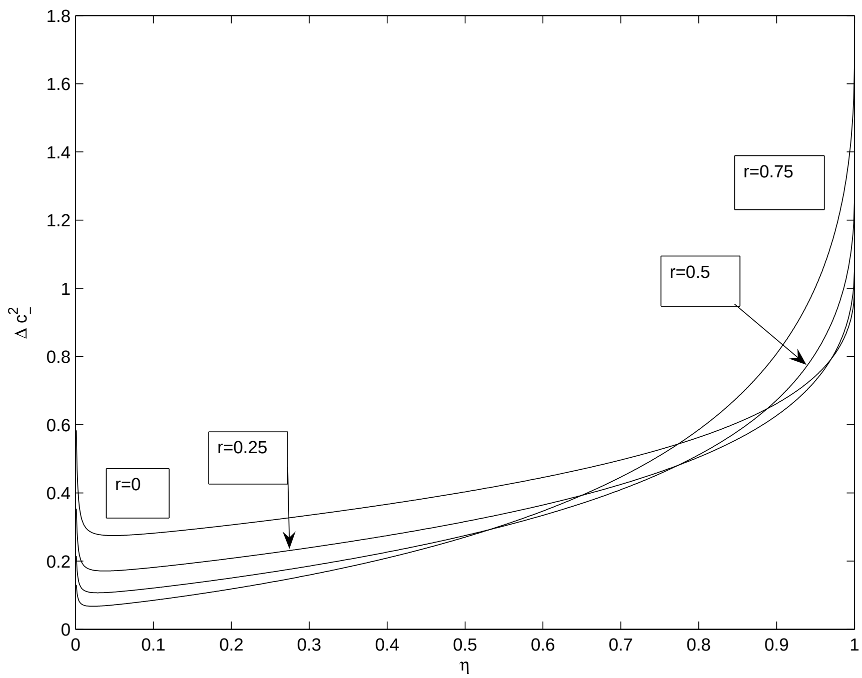

Fig. 4.15: Plots of the quadrature variance Δc_-^2 (Eq. (4.97)) of the two-mode cavity radiation at steady state for $\Omega = 0$, $\kappa = 0.5$, $A = 1000$, and different values of r.

Following a similar approach the maximum squeezing and values of η for which the maximum squeezing occurs are generated from Eq. (4.97).

r	Maximum squeezing	Max. squeezing occurs for	Squeezing occurs for
0.00	73%	η=0.05	$\eta < 0.99$
0.25	83%	η=0.04	$\eta < 0.99$
0.50	89%	η=0.03	$\eta < 0.98$
0.75	93%	η=0.02	$\eta < 0.94$

Table 4.12: Maximum squeezing for $\Omega = 0$, $\kappa = 0.5$, $A = 1000$, and different values of r.

We see from Fig. 4.15 that the cavity radiation of the system under consideration exhibits squeezing for certain values of η. We observe that the degree of squeezing is substantially enhanced by the squeezed radiation that enters the cavity for smaller values of η. However, it is found that the degree of squeezing decreases with the squeeze parameter for values of η close to 1. As shown in Fig. 4.5, the same dependence of the squeezing on the r and η is observed for $\Omega = 0.1\gamma$. As we have already discussed the degree of squeezing decreases with the squeeze parameter near $\eta = 1$, since the atoms in the bottom level absorb the squeezed radiation in the cavity and then emit radiation that does not contribute to the squeezing.

4.1.4 For a weak driving radiation

Next we consider when the amplitude of the driving radiation is taken to be very small ($\Omega \ll \gamma$). In this case, the quadrature variance (4.47) can be written as

$$\begin{aligned}\Delta c_\pm^2 = 1 &+ \left[\frac{A}{B'''}\left(C''' \mp F'''\right) + 2\kappa(N \pm M)\right]\frac{(\lambda_1''' + \lambda_2''')^2 + 4\lambda_1'''\lambda_2'''}{8\lambda_1'''\lambda_2'''(\lambda_1''' + \lambda_2''')} \\ &+ \left[\left(\frac{AC'''}{B'''} + \kappa N\right)\left(p'''^2 + q_-'''^2 \mp 2q_-'''p'''\right) + \kappa N\left(p'''^2 + q_+'''^2 \pm 2q_+'''p'''\right)\right. \\ &+ \left.\left(\frac{AF'''}{B'''} - 2\kappa M\right)\left(p'''(q_+''' - q_-''') \pm (p'''^2 - q_-'''q_+''')\right)\right]\frac{(\lambda_1''' + \lambda_2''')^2 - 4\lambda_1'''\lambda_2'''}{8\lambda_1'''\lambda_2'''(\lambda_1''' + \lambda_2''')} \\ &+ \left[\left(\frac{AC'''}{B'''} + \kappa N\right)\left(p''' \mp q_-'''\right) - \kappa N\left(p''' \pm q_+'''\right)\right. \\ &+ \left.\left(\frac{AF'''}{2B'''} - \kappa M\right)\left(q_+''' + q_-'''\right)\right]\frac{\lambda_1''' - \lambda_2'''}{4\lambda_1'''\lambda_2'''},\end{aligned} \tag{4.98}$$

with

$$B''' = 1, \tag{4.99}$$

$$C''' = \frac{1-\eta}{2} - \frac{3\Omega}{4\gamma}\sqrt{1-\eta^2}, \tag{4.100}$$

$$F''' = -\frac{\Omega}{4\gamma}(1-3\eta) - \frac{\sqrt{1-\eta^2}}{2}, \tag{4.101}$$

$$\lambda_1''' = \frac{\kappa}{2} + \frac{A}{4}\left[\frac{3\Omega}{2\gamma}\sqrt{1-\eta^2} + \eta + \sqrt{\eta^2 + \frac{3\Omega}{\gamma}\eta\sqrt{1-\eta^2}}\right], \tag{4.102}$$

$$\lambda_2''' = \frac{\kappa}{2} + \frac{A}{4}\left[\frac{3\Omega}{2\gamma}\sqrt{1-\eta^2} + \eta - \sqrt{\eta^2 + \frac{3\Omega}{\gamma}\eta\sqrt{1-\eta^2}}\right], \tag{4.103}$$

$$p'''^2 + q_-'''^2 \mp 2q_-'''p''' = \frac{2\left(1 \pm \sqrt{1-\eta^2}\right) - \eta^2 - \frac{\Omega}{\gamma}(3\eta - 1)\left(\sqrt{1-\eta^2} \pm 1\right)}{\eta^2 + \frac{3\Omega}{\gamma}\eta\sqrt{1-\eta^2}}, \tag{4.104}$$

$$p'''^2 + q_+'''^2 \pm 2q_+'''p''' = \frac{2\left(1 \pm \sqrt{1-\eta^2}\right) - \eta^2 - \frac{\Omega}{\gamma}(3\eta + 1)\left(\sqrt{1-\eta^2} \pm 1\right)}{\eta^2 + \frac{3\Omega}{\gamma}\eta\sqrt{1-\eta^2}}, \tag{4.105}$$

$$p'''(q_+''' - q_-''') \pm (p'''^2 - q_+'''q_-''') = \frac{-\frac{3\eta\Omega}{\gamma}\left(1 \pm \sqrt{1-\eta^2}\right) \pm \left[2\left(1 \pm \sqrt{1-\eta^2}\right) - \eta^2\right]}{\eta^2 + \frac{3\Omega}{\gamma}\eta\sqrt{1-\eta^2}}, \tag{4.106}$$

$$p''' \mp q_-''' = \frac{1 \pm \frac{\Omega}{2\gamma} \mp \left(\frac{3\eta\Omega}{2\gamma} - \sqrt{1-\eta^2}\right)}{\left[\eta^2 + \frac{3\Omega}{\gamma}\eta\sqrt{1-\eta^2}\right]^{\frac{1}{2}}}, \tag{4.107}$$

$$p''' \pm q_+''' = \frac{1 \mp \frac{\Omega}{2\gamma} \mp \left(\frac{3\eta\Omega}{2\gamma} - \sqrt{1-\eta^2}\right)}{\left[\eta^2 + \frac{3\Omega}{\gamma}\eta\sqrt{1-\eta^2}\right]^{\frac{1}{2}}}, \tag{4.108}$$

$$q_+''' + q_-''' = -\frac{\Omega}{\gamma\left[\eta^2 + \frac{3\Omega}{\gamma}\eta\sqrt{1-\eta^2}\right]^{\frac{1}{2}}}. \tag{4.109}$$

In order to study the squeezing of the cavity radiation in the weak driving limit more closely, we plot the quadrature variance versus Ω/γ and η. It is found using Eq. (4.103) that $\lambda_2''' \geq 0$ for $0 \leq \eta \leq 1$ and $0 \leq \Omega \leq 0.1\gamma$ when $A \leq 32$, in view of which the linear gain coefficient is taken to be $A = 32$.

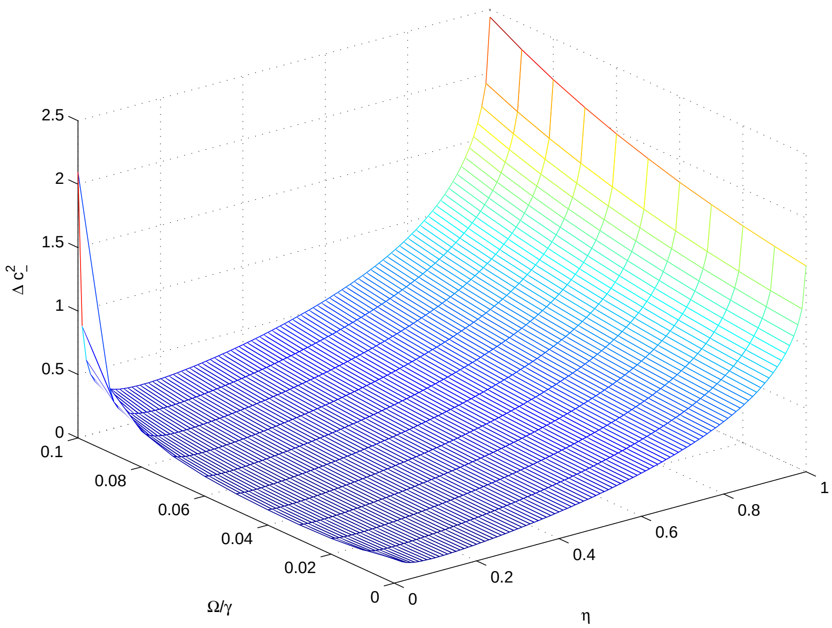

Fig. 4.16: Plot of the quadrature variance Δc_-^2 (Eq. (4.98)) of the two-mode cavity radiation at steady state for $\Omega \ll \gamma$, $r = 0.75$, $\kappa = 0.5$, and $A = 32$.

One can clearly see from Fig. 4.16 that the squeezing exists for certain values of Ω/γ and η. We also notice that the degree of squeezing significantly depends on the initial preparation of the atoms. It is found that a maximum squeezing of 89% occurs for $\eta = 0.06$ and $\Omega = 0.02\gamma$.

We next plot the quadrature variance versus Ω/γ and A. Here η is fixed to the value for which the squeezing is maximum in the previous case ($\eta = 0.06$).

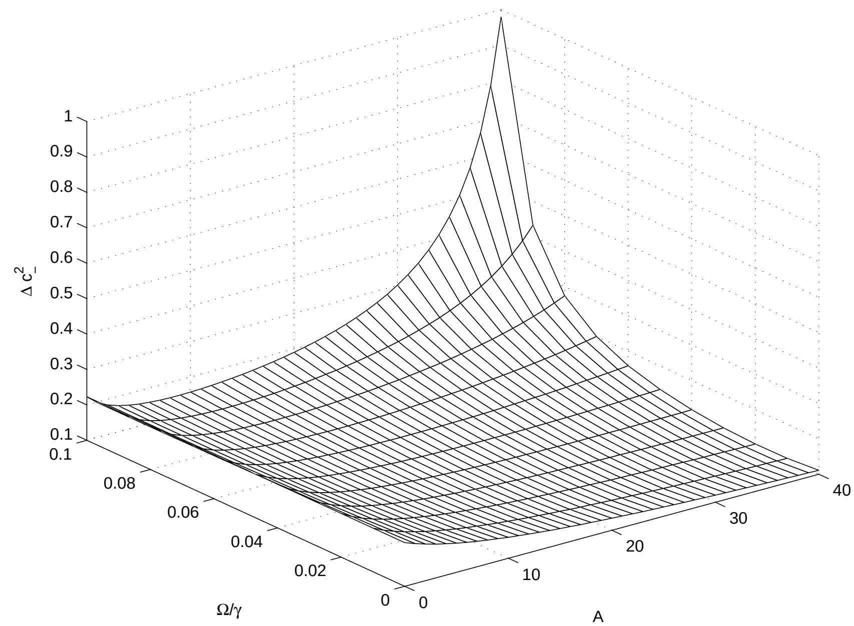

Fig. 4.17: Plot of the quadrature variance Δc_-^2 (Eq. (4.98)) of the two-mode cavity radiation at steady state for $\Omega \ll \gamma$, $r = 0.75$, $\kappa = 0.5$, and $\eta = 0.06$.

For $\eta = 0.06$ a maximum squeezing of 90% occurs for $A = 40$ and $\Omega = 0.02\gamma$ when $r = 0.75$. It is not difficult to see from Fig. 4.17 that the degree of squeezing decreases with the linear gain coefficient for some values of Ω/γ, although it is found to increase with the linear gain coefficient for values of Ω/γ near 0.

We now plot the quadrature variance versus Ω/γ for different values of r. A and η are fixed to the values for which the squeezing is found to be maximum in the previous cases.

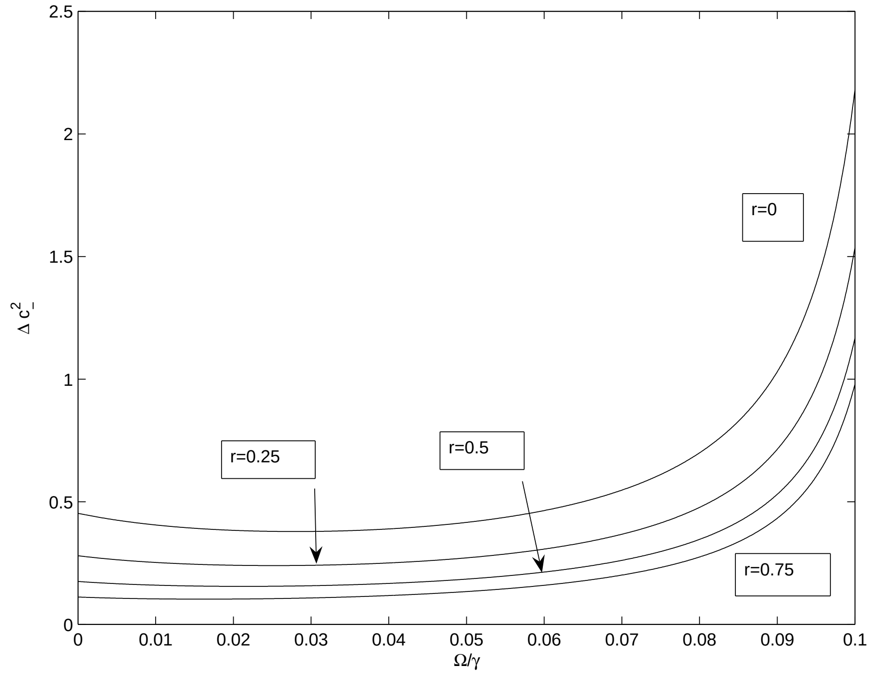

Fig. 4.18: Plots of the quadrature variance Δc_{-}^{2} (Eq. (4.98)) of the two-mode cavity radiation at steady state for $\Omega \ll \gamma$, $A = 40$, $\kappa = 0.5$, $\eta = 0.06$, and different values of r.

In the same manner the maximum squeezing, values of Ω/γ for which the maximum squeezing occurs, and values of Ω/γ for which the squeezing does not occur are generated from Eq. (4.98).

r	Max. squeezing	Max. squeezing occurs for	Squeezing does not occur for
0.00	63%	$\Omega = 0.028\gamma$	$\Omega > 0.087\gamma$
0.25	76%	$\Omega = 0.024\gamma$	$\Omega > 0.092\gamma$
0.50	85%	$\Omega = 0.019\gamma$	$\Omega > 0.098\gamma$
0.75	90%	$\Omega = 0.015\gamma$	-

Table 4.13: Maximum squeezing for $A = 40$, $\kappa = 0.5$, $\eta = 0.06$, and different values of r.

As shown in Fig. 4.18, the squeezing exists for certain values of Ω/γ for smaller values of r. We notice that the degree of squeezing increases with the squeeze parameter.

4.1.5 For a strong driving radiation

On the other hand, when the amplitude of the driving radiation is taken to be very large ($\Omega \gg \gamma$), we see that

$$B = \frac{\Omega^4}{4\gamma^4}, \tag{4.110}$$

$$C = \frac{\Omega^2}{4\gamma^2}(2+\eta), \tag{4.111}$$

$$F = -\frac{\Omega^3}{4\gamma^3}, \tag{4.112}$$

$$\lambda_1 = \frac{\kappa}{2} + \frac{A\gamma}{2\Omega}, \tag{4.113}$$

$$\lambda_2 = \frac{\kappa}{2} - \frac{A\gamma}{2\Omega}, \tag{4.114}$$

$$p^2 + q_-^2 \mp 2q_- p = 1, \tag{4.115}$$

$$p^2 + q_+^2 \pm 2q_+ p = 1, \tag{4.116}$$

$$p(q_+ - q_-) \pm (p^2 - q_- q_+) = \mp 1, \tag{4.117}$$

$$p \mp q_- = \mp 1, \tag{4.118}$$

$$p \pm q_+ = \pm 1, \tag{4.119}$$

$$q_+ + q_- = -2. \tag{4.120}$$

Using Eqs. (4.113) and (4.114), we obtain

$$\frac{(\lambda_1+\lambda_2)^2 + 4\lambda_1\lambda_2}{8\lambda_1\lambda_2(\lambda_1+\lambda_2)} = \frac{2\kappa^2\Omega^2 - A^2\gamma^2}{2\kappa[\kappa^2\Omega^2 - A^2\gamma^2]}, \tag{4.121}$$

$$\frac{(\lambda_1+\lambda_2)^2-4\lambda_1\lambda_2}{8\lambda_1\lambda_2(\lambda_1+\lambda_2)}=\frac{A^2\gamma^2}{2\kappa[\kappa^2\Omega^2-A^2\gamma^2]}, \tag{4.122}$$

$$\frac{\lambda_1-\lambda_2}{4\lambda_1\lambda_2}=\frac{A\gamma\Omega}{\kappa^2\Omega^2-A^2\gamma^2}. \tag{4.123}$$

Hence application of Eqs. (4.110), (4.111), (4.112), (4.115), (4.116), (4.117), (4.118), (4.119), (4.120), (4.121), (4.122), and (4.123) leads to

$$\Delta c_{\pm}^2 = 1+\left[\frac{A\gamma}{\Omega}\left[\frac{\gamma}{\Omega}(2+\eta)\pm 1\right]+2\kappa(N\pm M)\right]\frac{\kappa\Omega^2}{\kappa^2\Omega^2-A^2\gamma^2}$$
$$+\left[\frac{A\gamma}{\Omega}\left[1\mp\frac{\gamma}{\Omega}(2+\eta)\right]+2\kappa\left(M\mp N\right)\right]\frac{A\gamma\Omega}{\kappa^2\Omega^2-A^2\gamma^2}. \tag{4.124}$$

To study the squeezing properties of the cavity radiation in the strong driving limit in detail, we first plot the quadrature variance versus Ω/γ and η. The linear gain coefficient is taken to be $A=48$.

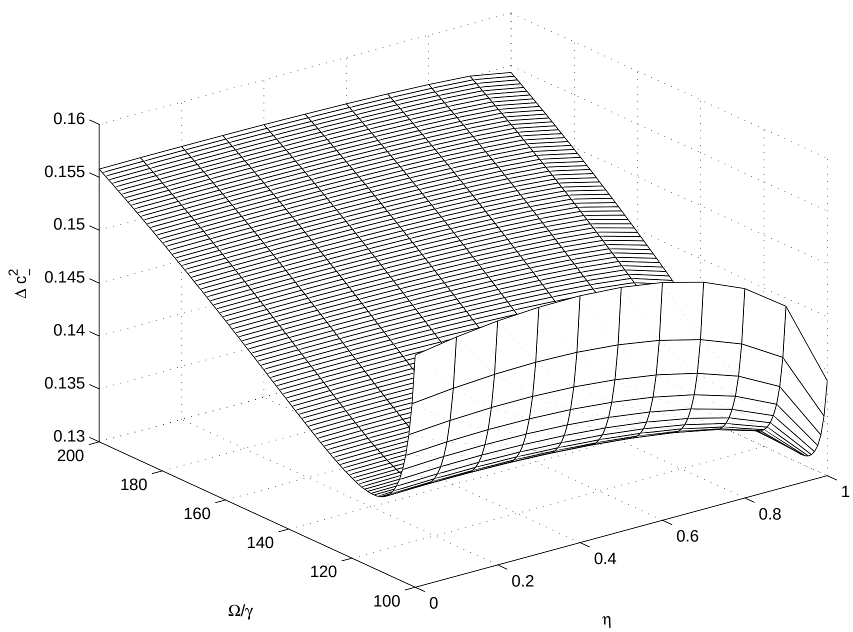

Fig. 4.19: Plot of the quadrature variance Δc_-^2 (Eq. (4.124)) of the cavity radiation at steady state for $\Omega \gg \gamma$, $\kappa=0.5$, $r=0.75$, and $A=48$.

We see from Fig. 4.19 that a significant degree of squeezing can be obtained when $\Omega \gg \gamma$. It is found that a maximum squeezing of 87% occurs for $\eta = 1$ and $\Omega = 108\gamma$. Moreover, comparison of Figs. 4.16 and 4.19 reveals that the squeezing varies more slowly with the initial preparation of the atoms in the strong driving limit than in the weak driving limit.

We next plot the quadrature variance versus Ω/γ and A, where η is fixed to the value for which the squeezing is maximum in the previous case ($\eta = 1$).

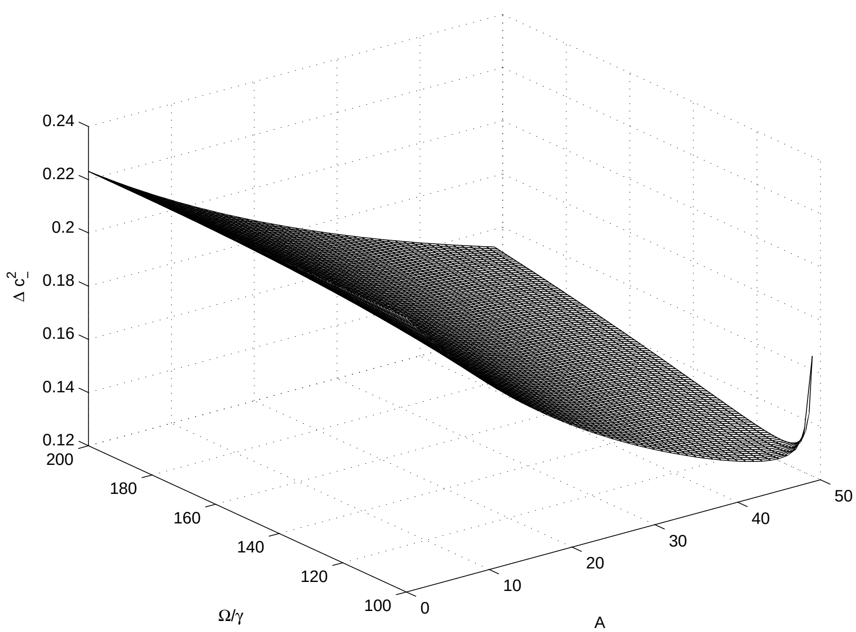

Fig. 4.20: Plot of the quadrature variance Δc_-^2 (Eq. (4.124)) of the cavity radiation at steady state for $\Omega \gg \gamma$, $\kappa = 0.5$, $r = 0.75$, and $\eta = 1$.

Fig. 4.20 clearly indicates that for $\Omega \gg \gamma$, the degree of squeezing decreases with the linear gain coefficient for some values of Ω/γ. It is found that the maximum squeezing of 87% occurs for $A = 48$ and $\Omega = 108\gamma$.

We next plot the quadrature variance versus Ω/γ for different values of r. Here η is fixed to the value for which the maximum squeezing is obtained in the previous case and the linear gain coefficient on the other hand is taken to be $A = 49.4$.

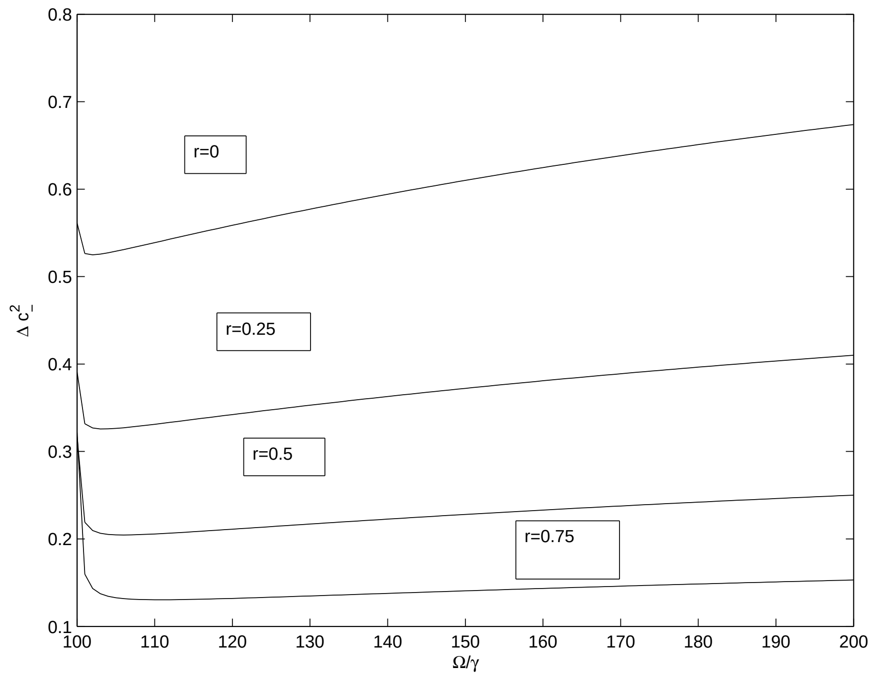

Fig. 4.21: Plots of the quadrature variance Δc_{-}^2 (Eq. (4.124)) of the cavity radiation at steady state for $\Omega \gg \gamma$, $\kappa = 0.5$, $\eta = 1$, $A = 49.4$, and different values of r.

Following a similar procedure the maximum squeezing and values of Ω/γ for which the maximum squeezing occurs are generated from Eq. (4.124).

r	Maximum squeezing	Maximum squeezing occurs for
0.00	48%	$\Omega = 102\gamma$
0.25	68%	$\Omega = 104\gamma$
0.50	80%	$\Omega = 106\gamma$
0.75	87%	$\Omega = 110\gamma$

Table 4.14: Maximum squeezing for $\kappa = 0.5$, $\eta = 1$, $A = 49.4$, and different values of r.

One can clearly see from Fig. 4.21 that for $\Omega \gg \gamma$ the degree of squeezing increases with the squeeze parameter. We also notice from Table (4.14) that the maximum squeezing occurs for nearly the same values of Ω/γ when different values of r are taken. It is found that when there is no initial atomic coherence a squeezing close to 50% can be obtained for $r = 0$. This result agrees with the claim of Xiong *et al.* [11] that a nondegenerate three-level cascade laser in which the atoms are initially prepared in the lower level and externally driven by a strong radiation resembles parametric oscillator.

4.2 Squeezing spectrum

The squeezing spectrum of a two-mode light is expressed as

$$S_{\pm}^{out}(\omega) = 2Re\int_0^{\infty} \langle \hat{c}_{\pm}^{out}(t),\ \hat{c}_{\pm}^{out}(t+\tau)\rangle_{ss} e^{i\omega\tau} d\tau, \tag{4.125}$$

where the quadrature operators $\hat{c}_+(t)$ and $\hat{c}_-(t)$ are defined by Eqs. (4.7) and (4.8), and

$$\langle \hat{c}_{\pm}^{out}(t),\ \hat{c}_{\pm}^{out}(t+\tau)\rangle = \langle \hat{c}_{\pm}^{out}(t)\hat{c}_{\pm}^{out}(t+\tau)\rangle - \langle \hat{c}_{\pm}^{out}(t)\rangle\langle \hat{c}_{\pm}^{out}(t+\tau)\rangle. \tag{4.126}$$

With the aid of the commutation relation

$$\left[\hat{c}_{out}(t),\ \hat{c}_{out}^{\dagger}(t+\tau)\right] = \delta(\tau), \tag{4.127}$$

Eq. (4.125) can be put in the form

$$S_{\pm}^{out}(\omega) = 1 + 2Re\int_0^{\infty} \langle :\hat{c}_{\pm}^{out}(t),\ \hat{c}_{\pm}^{out}(t+\tau):\rangle_{ss} e^{i\omega\tau} d\tau, \tag{4.128}$$

where :: denotes that the operators are put in the normal order. The squeezing spectrum can also be written in terms of c-number variables associated with the normal ordering as

$$S_{\pm}^{out}(\omega) = 1 \pm 2Re\int_0^{\infty} \langle \gamma_{\pm}^{out}(t),\ \gamma_{\pm}^{out}(t+\tau)\rangle_{ss} e^{i\omega\tau} d\tau, \tag{4.129}$$

in which

$$\gamma_{\pm}^{out}(t) = \gamma_{out}^{*}(t) \pm \gamma_{out}(t). \tag{4.130}$$

Hence in view of Eq. (4.2), we see that

$$\gamma_{\pm}^{out}(t) = \frac{1}{\sqrt{2}}\left[\alpha_{out}^{*}(t) + \beta_{out}^{*}(t) \pm (\alpha_{out}(t) + \beta_{out}(t))\right]. \tag{4.131}$$

Furthermore, the output and cavity mode variables are related by

$$\alpha_{out}(t) = \sqrt{\kappa}\alpha(t) - \alpha_{in}(t), \tag{4.132}$$

$$\beta_{out}(t) = \sqrt{\kappa}\beta(t) - \beta_{in}(t). \tag{4.133}$$

Upon substituting Eqs. (4.132) and (4.133) into (4.131), we have

$$\gamma_{\pm}^{out}(t) = \frac{1}{\sqrt{2}}\big[\sqrt{\kappa}\big[\alpha^*(t) + \beta^*(t) \pm (\alpha(t) + \beta(t))\big] \\ - \big[\alpha_{in}^*(t) + \beta_{in}^*(t) \pm (\alpha_{in}(t) + \beta_{in}(t))\big]\big], \tag{4.134}$$

which can also be put in the form

$$\gamma_{\pm}^{out}(t) = \sqrt{\kappa}\gamma_{\pm}(t) - \gamma_{\pm}^{in}(t), \tag{4.135}$$

where

$$\gamma_{\pm}(t) = \frac{1}{\sqrt{2}}\big[\alpha^*(t) + \beta^*(t) \pm (\alpha(t) + \beta(t))\big], \tag{4.136}$$

$$\gamma_{\pm}^{in}(t) = \frac{1}{\sqrt{2}}\big[\alpha_{in}^*(t) + \beta_{in}^*(t) \pm (\alpha_{in}(t) + \beta_{in}(t))\big]. \tag{4.137}$$

On the other hand, the input variables can be expressed in terms of the noise forces associated with the reservoir as

$$\alpha_{in}(t) = \frac{1}{\sqrt{\kappa}}F_{R\alpha}(t), \tag{4.138}$$

$$\beta_{in}(t) = \frac{1}{\sqrt{\kappa}}F_{R\beta}(t). \tag{4.139}$$

Now making use of (4.138) and (4.139), Eq. (4.137) can be written as

$$\gamma_{\pm}^{in}(t) = \frac{1}{\sqrt{\kappa}}F_{R\pm}(t), \tag{4.140}$$

where

$$F_{R\pm}(t) = \frac{1}{\sqrt{2}}\big[F_{R\alpha}^*(t) + F_{R\beta}^*(t) \pm (F_{R\alpha}(t) + F_{R\beta}(t))\big]. \tag{4.141}$$

As shown in Appendix 7.2, the noise forces $F_{Ri}(t)$ with $i = \alpha, \beta$ satisfy the correlation properties:

$$\langle F_{Ri}(t)\rangle = 0, \tag{4.142}$$

$$\langle F^*_{Ri}(t)F_{Ri}(t')\rangle = \kappa N\delta(t-t'), \tag{4.143}$$

$$\langle F_{Ri}(t)F_{Rj}(t')\rangle_{i\neq j} = \kappa M\delta(t-t'), \tag{4.144}$$

$$\langle F^*_{Ri}(t)F_{Rj}(t')\rangle_{i\neq j} = \langle F_{Ri}(t)F_{Ri}(t')\rangle = 0. \tag{4.145}$$

It is not difficult to see that the expectation value of Eq. (4.134) would be

$$\begin{aligned}\langle \gamma^{out}_{\pm}(t)\rangle = \frac{1}{\sqrt{2}}\big[\sqrt{\kappa}\big[\langle\alpha^*(t)\rangle + \langle\beta^*(t)\rangle \pm (\langle\alpha(t)\rangle + \langle\beta(t)\rangle)\big] \\ - \big[\langle\alpha^*_{in}(t)\rangle + \langle\beta^*_{in}(t)\rangle \pm (\langle\alpha_{in}(t)\rangle + \langle\beta_{in}(t)\rangle)\big]\big].\end{aligned} \tag{4.146}$$

Applying Eqs. (4.138), (4.139), and (4.142), one can readily verify that

$$\langle\alpha_{in}(t)\rangle = 0, \tag{4.147}$$

$$\langle\beta_{in}(t)\rangle = 0. \tag{4.148}$$

Upon inserting Eqs. (4.34), (4.147), and (4.148) into (4.146), we obtain

$$\langle\gamma^{out}_{\pm}(t)\rangle = 0, \tag{4.149}$$

as a result of which Eq. (4.129) becomes

$$S^{out}_{\pm}(\omega) = 1 \pm 2Re\int_0^{\infty}\langle\gamma^{out}_{\pm}(t)\gamma^{out}_{\pm}(t+\tau)\rangle_{ss}e^{i\omega\tau}d\tau. \tag{4.150}$$

Furthermore taking Eq. (4.135) into consideration, we write

$$\begin{aligned}\langle\gamma^{out}_{\pm}(t)\gamma^{out}_{\pm}(t+\tau)\rangle = \kappa\langle\gamma_{\pm}(t)\gamma_{\pm}(t+\tau)\rangle + \langle\gamma^{in}_{\pm}(t)\gamma^{in}_{\pm}(t+\tau)\rangle \\ - \sqrt{\kappa}[\langle\gamma^{in}_{\pm}(t)\gamma_{\pm}(t+\tau)\rangle + \langle\gamma_{\pm}(t)\gamma^{in}_{\pm}(t+\tau)\rangle]\end{aligned} \tag{4.151}$$

so that employing Eq. (4.140), we have

$$\begin{aligned}\langle\gamma^{out}_{\pm}(t)\gamma^{out}_{\pm}(t+\tau)\rangle = \kappa\langle\gamma_{\pm}(t)\gamma_{\pm}(t+\tau)\rangle + \frac{1}{\kappa}\langle F_{R\pm}(t)F_{R\pm}(t+\tau)\rangle \\ - [\langle F_{R\pm}(t)\gamma_{\pm}(t+\tau)\rangle + \langle\gamma_{\pm}(t)F_{R\pm}(t+\tau)\rangle].\end{aligned} \tag{4.152}$$

In view of the fact that the noise forces at $t+\tau$ do not affect the system variables at the earlier time t, we get

$$\langle\gamma_{\pm}^{out}(t)\gamma_{\pm}^{out}(t+\tau)\rangle = \kappa\langle\gamma_{\pm}(t)\gamma_{\pm}(t+\tau)\rangle + \frac{1}{\kappa}\langle F_{R\pm}(t)F_{R\pm}(t+\tau)\rangle - \langle F_{R\pm}(t)\gamma_{\pm}(t+\tau)\rangle. \tag{4.153}$$

On the basis of Eq. (4.136), we find

$$\langle\gamma_{\pm}(t)\gamma_{\pm}(t+\tau)\rangle = \frac{1}{2}[\langle\alpha(t)\alpha(t+\tau)\rangle + \langle\beta(t)\alpha(t+\tau)\rangle + \langle\alpha(t)\beta(t+\tau)\rangle + \langle\beta(t)\beta(t+\tau)\rangle \pm [\langle\alpha(t)\alpha^*(t+\tau)\rangle + \langle\beta(t)\alpha^*(t+\tau)\rangle + \langle\beta(t)\beta^*(t+\tau)\rangle + \langle\alpha(t)\beta^*(t+\tau)\rangle]] + c.c., \tag{4.154}$$

where c.c. stands for complex conjugate. We now proceed to determine the various correlation functions involved in Eq. (4.154). Using Eq. (3.92), we see that

$$\langle\alpha(t)\alpha(t+\tau)\rangle_{ss} = A_+(\tau)\langle\alpha^2(t)\rangle_{ss} + B_+(\tau)\langle\alpha(t)\beta^*(t)\rangle_{ss} + \langle\alpha(t)F_+(t+\tau)\rangle_{ss} + \langle\alpha(t)G_+(t+\tau)\rangle_{ss}. \tag{4.155}$$

Applying Eqs. (4.34) and (4.45) along with the fact that the noise forces at $t+\tau$ do not affect the system variables at the earlier times, one readily gets

$$\langle\alpha(t)\alpha(t+\tau)\rangle_{ss} = 0. \tag{4.156}$$

It can also be verified in a similar manner that

$$\langle\beta(t)\beta(t+\tau)\rangle_{ss} = 0, \tag{4.157}$$

$$\langle\alpha(t)\beta^*(t+\tau)\rangle_{ss} = 0, \tag{4.158}$$

$$\langle\alpha^*(t+\tau)\beta(t)\rangle_{ss} = 0, \tag{4.159}$$

$$\langle\alpha^*(t)\alpha(t+\tau)\rangle_{ss} = A_+(\tau)\langle\alpha^*(t)\alpha(t)\rangle_{ss} + B_+(\tau)\langle\alpha(t)\beta(t)\rangle_{ss}, \tag{4.160}$$

$$\langle\beta^*(t)\beta(t+\tau)\rangle_{ss} = A_-(\tau)\langle\beta^*(t)\beta(t)\rangle_{ss} + B_-(\tau)\langle\alpha(t)\beta(t)\rangle_{ss}, \tag{4.161}$$

$$\langle\beta(t)\alpha(t+\tau)\rangle_{ss} = A_{+}(\tau)\langle\alpha(t)\beta(t)\rangle_{ss} + B_{+}(\tau)\langle\beta(t)\beta^{*}(t)\rangle_{ss}, \tag{4.162}$$

$$\langle\alpha(t)\beta(t+\tau)\rangle_{ss} = A_{-}(\tau)\langle\alpha(t)\beta(t)\rangle_{ss} + B_{-}(\tau)\langle\alpha(t)\alpha^{*}(t)\rangle_{ss}. \tag{4.163}$$

Hence on account of Eqs. (4.154), (4.156), (4.157), (4.158), (4.159) (4.160), (4.161), (4.162), and (4.163), we arrive at

$$\begin{aligned}\langle\gamma_{\pm}(t)\gamma_{\pm}(t+\tau)\rangle_{ss} = {}& \big(A_{+}(\tau)+A_{-}(\tau)\big)\langle\alpha(t)\beta(t)\rangle_{ss} + B_{+}(\tau)\langle\beta^{*}(t)\beta(t)\rangle_{ss} \\ & + B_{-}(\tau)\langle\alpha(t)\alpha^{*}(t)\rangle_{ss} \pm \big[\big(B_{+}(\tau)+B_{-}(\tau)\big)\langle\alpha(t)\beta(t)\rangle_{ss} \\ & + A_{-}(\tau)\langle\beta^{*}(t)\beta(t)\rangle_{ss} + A_{+}(\tau)\langle\alpha(t)\alpha^{*}(t)\rangle_{ss}\big],\end{aligned} \tag{4.164}$$

which can also be put, employing Eqs. (3.94) and (3.95), in a more appealing form as

$$\langle\gamma_{\pm}(t)\gamma_{\pm}(t+\tau)\rangle_{ss} = (D_{\pm}+E_{\pm})e^{-\lambda_{1}\tau} + (D_{\pm}-E_{\pm})e^{-\lambda_{2}\tau}, \tag{4.165}$$

where

$$D_{\pm} = \langle\alpha(t)\beta(t)\rangle_{ss} \pm \frac{1}{2}\big[\langle\beta^{*}(t)\beta(t)\rangle_{ss} + \langle\alpha^{*}(t)\alpha(t)\rangle_{ss}\big], \tag{4.166}$$

$$E_{\pm} = \frac{1}{2}\big[\langle\alpha^{*}(t)\alpha(t)\rangle_{ss}(q_{-}\mp p) + \langle\beta^{*}(t)\beta(t)\rangle_{ss}(q_{+}\pm p) \pm \langle\alpha(t)\beta(t)\rangle_{ss}(q_{-}+q_{+})\big]. \tag{4.167}$$

Moreover, on the basis of Eq. (4.141), we write

$$\begin{aligned}\langle F_{R\pm}(t)F_{R\pm}(t+\tau)\rangle = {}& \frac{1}{2}[\langle F_{R\alpha}(t)F_{R\beta}(t+\tau)\rangle + \langle F_{R\beta}(t)F_{R\beta}(t+\tau)\rangle + \langle F_{R\beta}(t)F_{R\alpha}(t+\tau)\rangle \\ & + \langle F_{R\alpha}(t)F_{R\alpha}(t+\tau)\rangle \pm [\langle F_{R\alpha}(t)F^{*}_{R\beta}(t+\tau)\rangle + \langle F^{*}_{R\beta}(t)F_{R\beta}(t+\tau)\rangle \\ & + \langle F_{R\alpha}(t)F^{*}_{R\alpha}(t+\tau)\rangle + \langle F^{*}_{R\beta}(t)F_{R\alpha}(t+\tau)\rangle]] + c.c.\end{aligned} \tag{4.168}$$

so that using Eqs. (4.143), (4.144), and (4.145), we obtain

$$\langle F_{R\pm}(t)F_{R\pm}(t+\tau)\rangle = 2\kappa(M \pm N)\delta(\tau). \tag{4.169}$$

Furthermore, with the aid of Eqs. (4.136) and (4.141), we find

$$\begin{aligned}\langle F_{R\pm}(t)\gamma_{\pm}(t+\tau)\rangle = {}& \frac{1}{2}[\langle F_{R\beta}(t)\alpha(t+\tau)\rangle + \langle F_{R\alpha}(t)\alpha(t+\tau)\rangle + \langle F_{R\beta}(t)\beta(t+\tau)\rangle \\ & + \langle F_{R\alpha}(t)\beta(t+\tau)\rangle \pm [\langle F_{R\alpha}(t)\alpha^{*}(t+\tau)\rangle + \langle F^{*}_{R\beta}(t)\alpha(t+\tau)\rangle \\ & + \langle F_{R\alpha}(t)\beta^{*}(t+\tau)\rangle + \langle F^{*}_{R\beta}(t)\beta(t+\tau)\rangle]] + c.c.\end{aligned} \tag{4.170}$$

Now making use of Eq. (3.92), we see that

$$\langle F_{R\alpha}(t)\alpha^*(t+\tau)\rangle = A_+(\tau)\langle F_{R\alpha}(t)\alpha^*(t)\rangle + B_+(\tau)\langle F_{R\alpha}(t)\beta(t)\rangle + \langle F_{R\alpha}(t)F_+^*(t+\tau)\rangle + \langle F_{R\alpha}(t)G_+^*(t+\tau)\rangle. \tag{4.171}$$

In addition, in view of Eq. (3.102), we note that

$$\langle F_{R\alpha}(t)\alpha^*(t)\rangle = A_+(t)\langle F_{R\alpha}(t)\alpha^*(0)\rangle + B_+(t)\langle F_{R\alpha}(t)\beta(0)\rangle + \langle F_{R\alpha}(t)F_+^*(t)\rangle + \langle F_{R\alpha}(t)G_+^*(t)\rangle, \tag{4.172}$$

from which follows

$$\langle F_{R\alpha}(t)\alpha^*(t)\rangle = \langle F_{R\alpha}(t)F_+^*(t)\rangle + \langle F_{R\alpha}(t)G_+^*(t)\rangle. \tag{4.173}$$

Next employing Eq. (3.106), we see that

$$\langle F_{R\alpha}(t)F_+^*(t)\rangle = \frac{1}{2}\int_0^t \left[(1+p)e^{-\lambda_2(t-t')} + (1-p)e^{-\lambda_1(t-t')}\right]\langle F_{R\alpha}(t)f_\alpha^*(t')\rangle dt'. \tag{4.174}$$

We observe that the noise forces $f_i(t)$, with $i = \alpha, \beta$, can be written as

$$f_i(t) = F_{Ci}(t) + F_{Ri}(t), \tag{4.175}$$

where $F_{Ci}(t)$ is the noise force associated with the cavity radiation. It then follows using Eq. (4.175) that

$$\langle F_{R\alpha}(t)f_\alpha^*(t')\rangle = \langle F_{R\alpha}(t)F_{C\alpha}^*(t')\rangle + \langle F_{R\alpha}(t)F_{R\alpha}^*(t')\rangle. \tag{4.176}$$

On account of the fact that $F_{R\alpha}(t)$ and $F_{C\alpha}(t)$ do not correlate, we notice that

$$\langle F_{R\alpha}(t)F_{C\alpha}^*(t')\rangle = 0. \tag{4.177}$$

Now applying Eqs. (4.143) and (4.177), we obtain

$$\langle F_{R\alpha}(t)f_\alpha^*(t')\rangle = \kappa N\delta(t-t'). \tag{4.178}$$

Therefore, substituting Eq. (4.178) into (4.174) and then carrying out the integration results in

$$\langle F_{R\alpha}(t)F_+^*(t)\rangle = \frac{\kappa N}{2}. \tag{4.179}$$

Following a similar procedure it is possible to show that

$$\langle F_{R\alpha}(t)G_+^*(t)\rangle = 0. \tag{4.180}$$

Hence we see with the aid of Eqs. (4.172), (4.179), and (4.180) that

$$\langle F_{R\alpha}(t)\alpha^*(t)\rangle = \frac{\kappa N}{2}. \tag{4.181}$$

One can also find in a similar manner that

$$\langle F_{R\alpha}(t)\beta(t)\rangle = \frac{\kappa M}{2}. \tag{4.182}$$

On the other hand, taking Eq. (3.96) into consideration, we write

$$\langle F_{R\alpha}(t)F_+^*(t+\tau)\rangle = \frac{1}{2}\int_0^\tau [(1+p)e^{-\lambda_2(\tau-\tau')} + (1-p)e^{-\lambda_1(\tau-\tau')}]\langle F_{R\alpha}(t)f_\alpha^*(t+\tau')\rangle d\tau' \tag{4.183}$$

so that on taking into account Eqs. (4.143), (4.175), and (4.177), there follows

$$\langle F_{R\alpha}(t)F_+^*(t+\tau)\rangle = \frac{\kappa N}{2}\int_0^\tau [(1+p)e^{-\lambda_2(\tau-\tau')} + (1-p)e^{-\lambda_1(\tau-\tau')}]\delta(\tau')d\tau' \tag{4.184}$$

and on carrying out this integration, we get

$$\langle F_{R\alpha}(t)F_+^*(t+\tau)\rangle = \frac{\kappa N}{4}\big[(1+p)e^{-\lambda_2\tau} + (1-p)e^{-\lambda_1\tau}\big]. \tag{4.185}$$

It can also be verified in a similar way that

$$\langle F_{R\alpha}(t)G_+^*(t+\tau)\rangle = \frac{\kappa M q_+}{4}\big[e^{-\lambda_1\tau} - e^{-\lambda_2\tau}\big]. \tag{4.186}$$

Thus making use of Eqs. (3.94), (3.95), (4.171), (4.181), (4.182), (4.185), and (4.186), we find

$$\langle F_{R\alpha}(t)\alpha^*(t+\tau)\rangle = \frac{\kappa N}{2}[(1+p)e^{-\lambda_2\tau} + (1-p)e^{-\lambda_1\tau}] + \frac{\kappa M q_+}{2}[e^{-\lambda_1\tau} - e^{-\lambda_2\tau}]. \tag{4.187}$$

It is also possible to show following a similar procedure that

$$\langle F_{R\beta}^*(t)\beta(t+\tau)\rangle = \frac{\kappa N}{2}[(1-p)e^{-\lambda_2\tau} + (1+p)e^{-\lambda_1\tau}] + \frac{\kappa M q_-}{2}[e^{-\lambda_1\tau} - e^{-\lambda_2\tau}], \tag{4.188}$$

$$\langle F_{R\beta}(t)\alpha(t+\tau)\rangle = \frac{\kappa M}{2}[(1+p)e^{-\lambda_2\tau} + (1-p)e^{-\lambda_1\tau}] + \frac{\kappa N q_+}{2}[e^{-\lambda_1\tau} - e^{-\lambda_2\tau}], \tag{4.189}$$

$$\langle F_{R\alpha}(t)\beta(t+\tau)\rangle = \frac{\kappa M}{2}[(1-p)e^{-\lambda_2\tau} + (1+p)e^{-\lambda_1\tau}] + \frac{\kappa N q_-}{2}[e^{-\lambda_1\tau} - e^{-\lambda_2\tau}], \quad (4.190)$$

$$\langle F^*_{R\beta}(t)\alpha(t+\tau)\rangle = 0, \quad (4.191)$$

$$\langle F_{R\alpha}(t)\alpha(t+\tau)\rangle = 0, \quad (4.192)$$

$$\langle F_{R\beta}(t)\beta(t+\tau)\rangle = 0, \quad (4.193)$$

$$\langle F_{R\alpha}(t)\beta^*(t+\tau)\rangle = 0. \quad (4.194)$$

Hence on the basis of Eqs. (4.170), (4.187), (4.188), (4.189), (4.190), (4.191), (4.192), (4.193), and (4.194), we arrive at

$$\langle F_{R\pm}(t)\gamma_\pm(t+\tau)\rangle = \pm\kappa(N \pm M)\left[\left(1 \pm \frac{(q_+ + q_-)}{2}\right)e^{-\lambda_1\tau} + \left(1 \mp \frac{(q_+ + q_-)}{2}\right)e^{-\lambda_2\tau}\right]. \quad (4.195)$$

Now inserting Eqs. (4.165), (4.169), and (4.195) into (4.153), we obtain

$$\langle \gamma_\pm^{out}(t)\gamma_\pm^{out}(t+\tau)\rangle = 2(M \pm N)\delta(\tau) + \kappa\left[\left(D_\pm + E_\pm - \left((M \pm N)\left(1 \pm \frac{(q_+ + q_-)}{2}\right)\right)\right)e^{-\lambda_1\tau} + \left(D_\pm - E_\pm - \left((M \pm N)\left(1 \mp \frac{(q_+ + q_-)}{2}\right)\right)\right)e^{-\lambda_2\tau}\right]. \quad (4.196)$$

Therefore, the squeezing spectrum (4.150) takes the form

$$S_\pm^{out}(\omega) = 1 + 4(N \pm M)Re\int_0^\infty e^{i\omega\tau}\delta(\tau)d\tau \pm 2\kappa Re\int_0^\infty \left[D_\pm + E_\pm - \left((M \pm N)\left(1 \pm \frac{(q_+ + q_-)}{2}\right)\right)\right]e^{-(\lambda_1 - i\omega)\tau}d\tau \pm 2\kappa Re\int_0^\infty \left[D_\pm - E_\pm - \left((M \pm N)\left(1 \mp \frac{(q_+ + q_-)}{2}\right)\right)\right]e^{-(\lambda_2 - i\omega)\tau}d\tau. \quad (4.197)$$

Finally, upon carrying out the integrations in Eq. (4.197) and then taking the real part of the resulting expressions, we get

$$\begin{aligned}
S_{\pm}^{out}(\omega) = 1 + 2N \pm 2M + \frac{\kappa\lambda_1}{\lambda_1^2+\omega^2}&\left[\langle\alpha^*(t)\alpha(t)\rangle_{ss} + \langle\beta^*(t)\beta(t)\rangle_{ss} - 2(N \pm M)\right.\\
&+(\langle\alpha(t)\beta(t)\rangle_{ss} - (M \pm N))(q_+ + q_-) + (\langle\beta^*(t)\beta(t)\rangle_{ss} - \langle\alpha^*(t)\alpha(t)\rangle_{ss})p\\
&\left.\pm(2(\langle\alpha(t)\beta(t)\rangle_{ss}) + \langle\alpha^*(t)\alpha(t)\rangle_{ss}q_- + \langle\beta^*(t)\beta(t)\rangle_{ss}q_+)\right]\\
&+ \frac{\kappa\lambda_2}{\lambda_2^2+\omega^2}\left[\langle\alpha^*(t)\alpha(t)\rangle_{ss} + \langle\beta^*(t)\beta(t)\rangle_{ss} - 2(N \pm M)\right.\\
&-(\langle\alpha(t)\beta(t)\rangle_{ss} - (M \pm N))(q_+ + q_-) + (\langle\alpha^*(t)\alpha(t)\rangle_{ss} - \langle\beta^*(t)\beta(t)\rangle_{ss})p\\
&\left.\pm(2\langle\alpha(t)\beta(t)\rangle_{ss} - \langle\alpha^*(t)\alpha(t)\rangle_{ss}q_- - \langle\beta^*(t)\beta(t)\rangle_{ss}q_+)\right], \qquad (4.198)
\end{aligned}$$

which can also be put using Eqs. (4.28), (4.29), and (4.43) in the form

$$
\begin{aligned}
S_{\pm}^{out}(\omega) &= 1 + 2N \pm 2M + \frac{\kappa\lambda_1}{\lambda_1^2+\omega^2}\Bigg\{\Bigg[\left(\frac{AC}{B}+\kappa N\right)\big(1-p\pm q_-\big) + \kappa N\big(1+p\pm q_+\big) \\
&\quad - \left(\frac{AF}{2B}-\kappa M\right)\big(q_+ + q_- \pm 2\big)\Bigg]\frac{\big(\lambda_1+\lambda_2\big)^2 + 4\lambda_1\lambda_2}{8\lambda_1\lambda_2(\lambda_1+\lambda_2)} \\
&\quad + \Bigg[\left(\frac{AC}{B}+\kappa N\right)\big[p^2(1-p) + q_-^2(1\pm q_+) - q_-p(q_+ \pm (2-p))\big] \\
&\quad + \kappa N\big[q_+^2(1\pm q_-) + p^2(1+p) + q_+p(q_- \pm (2+p))\big] + \left(\frac{AF}{2B}-\kappa M\right) \\
&\quad \times\big[2p(q_+ - q_-) + (p^2 - q_+q_-)(1\pm 1) - 2p^2(q_- + q_+)\big]\Bigg]\frac{\big(\lambda_1+\lambda_2\big)^2 - 4\lambda_1\lambda_2}{8\lambda_1\lambda_2(\lambda_1+\lambda_2)} \\
&\quad + \Bigg[\left(\frac{AC}{B}+\kappa N\right)\big[p(1-p) - q_-(q_- + q_+ \pm (2-p))\big] \\
&\quad + \kappa N\big[p(p-1) - q_+(q_- + q_+ \pm (2+p))\big] \\
&\quad + \left(\frac{AF}{2B}-\kappa M\right)\big[2q_+(1-p+q_-) + 2q_-(1+p+q_+)\big]\Bigg]\frac{\lambda_1-\lambda_2}{4\lambda_1\lambda_2}\Bigg\} \\
&\quad + \frac{\kappa\lambda_2}{\lambda_2^2+\omega^2}\Bigg\{\Bigg[\left(\frac{AC}{B}+\kappa N\right)\big(1+p\mp q_-\big) + \kappa N\big(1-q_+\mp p\big) \\
&\quad + \left(\frac{AF}{2B}-\kappa M\right)\big(q_+ + q_- \mp 2\big)\Bigg]\frac{\big(\lambda_1+\lambda_2\big)^2 + 4\lambda_1\lambda_2}{8\lambda_1\lambda_2(\lambda_1+\lambda_2)} \\
&\quad + \Bigg[\left(\frac{AC}{B}+\kappa N\right)\big[q_-^2(1\mp q_+) + p^2(1+p) + q_-p(q_+ \mp (2+p))\big] \\
&\quad + \kappa N\big[q_+^2(1\mp q_-) + p^2(1-p) - q_+p(q_- \mp (2-p))\big] + \left(\frac{AF}{2B}-\kappa M\right) \\
&\quad \times\big[p(q_+ - q_-) + 2p^2(q_- + q_+) - (p^2 - q_+q_-)(1\mp 1)\big]\Bigg]\frac{\big(\lambda_1+\lambda_2\big)^2 - 4\lambda_1\lambda_2}{8\lambda_1\lambda_2(\lambda_1+\lambda_2)} \\
&\quad + \Bigg[\left(\frac{AC}{B}+\kappa N\right)\big[p(1+p) + q_-(q_- + q_+ \mp (2+p))\big] \\
&\quad + \kappa N\big[-p(p+1) + q_+(q_- + q_+ \mp (2-p))\big] \\
&\quad + \left(\frac{AF}{2B}-\kappa M\right)\big[2q_+(1-q_-+p) + 2q_-(1-p-q_+)\big]\Bigg]\frac{\lambda_1-\lambda_2}{4\lambda_1\lambda_2}\Bigg\},
\end{aligned}
\tag{4.199}
$$

where

$$
1 - p \pm q_- = 1 - \frac{1 + \frac{\Omega^2}{\gamma^2} \pm \left[\frac{\Omega}{2\gamma}\left(1+\frac{\Omega^2}{\gamma^2}\right) - \frac{3\eta\Omega}{2\gamma} + \sqrt{1-\eta^2}\left(1-\frac{\Omega^2}{2\gamma^2}\right)\right]}{\chi}, \tag{4.200}
$$

$$
1 + p \pm q_+ = 1 + \frac{1 + \frac{\Omega^2}{\gamma^2} \mp \left[\frac{\Omega}{2\gamma}\left(1+\frac{\Omega^2}{\gamma^2}\right) + \frac{3\eta\Omega}{2\gamma} - \sqrt{1-\eta^2}\left(1-\frac{\Omega^2}{2\gamma^2}\right)\right]}{\chi}, \tag{4.201}
$$

$$q_+ + q_- \pm 2 = -\frac{\Omega}{\chi\gamma}\left(1+\frac{\Omega^2}{\gamma^2}\right) \pm 2, \tag{4.202}$$

$$\begin{aligned}
&p^2(1-p) + q_-^2(1\pm q_+) - q_-p(q_+ \pm (2-p)) \\
&= \frac{1}{\chi^3}\left[\left(1+\frac{\Omega^2}{\gamma^2}\right)^2\left(\chi - \left(1+\frac{\Omega^2}{\gamma^2}\right)\right) - \left[\frac{\Omega}{2\gamma}\left(1+\frac{\Omega^2}{\gamma^2}\right) - \frac{3\eta\Omega}{2\gamma}\right.\right. \\
&\left. + \sqrt{1-\eta^2}\left(1-\frac{\Omega^2}{2\gamma^2}\right)\right]\left[\left(-\frac{\Omega}{2\gamma}\left(1+\frac{\Omega^2}{\gamma^2}\right) + \frac{3\eta\Omega}{2\gamma} - \sqrt{1-\eta^2}\left(1-\frac{\Omega^2}{2\gamma^2}\right)\right)\right. \\
&\times\left(\chi \mp \left(\frac{\Omega}{2\gamma}\left(1+\frac{\Omega^2}{\gamma^2}\right) + \frac{3\eta\Omega}{2\gamma} - \sqrt{1-\eta^2}\left(1-\frac{\Omega^2}{2\gamma^2}\right)\right)\right) - \left(1+\frac{\Omega^2}{\gamma^2}\right) \\
&\left.\left.\times\left(-\frac{\Omega}{2\gamma}\left(1+\frac{\Omega^2}{\gamma^2}\right) - \frac{3\eta\Omega}{2\gamma} + \sqrt{1-\eta^2}\left(1-\frac{\Omega^2}{2\gamma^2}\right) \pm \left(2\chi - \left(1+\frac{\Omega^2}{\gamma^2}\right)\right)\right)\right]\right],
\end{aligned} \tag{4.203}$$

$$\begin{aligned}
&p^2(1+p) + q_+^2(1\pm q_-) + q_+p(q_- \pm (2+p)) \\
&= \frac{1}{\chi^3}\left[\left(1+\frac{\Omega^2}{\gamma^2}\right)^2\left(\chi + \left(1+\frac{\Omega^2}{\gamma^2}\right)\right) - \left[\frac{\Omega}{2\gamma}\left(1+\frac{\Omega^2}{\gamma^2}\right) + \frac{3\eta\Omega}{2\gamma}\right.\right. \\
&\left. - \sqrt{1-\eta^2}\left(1-\frac{\Omega^2}{2\gamma^2}\right)\right]\left[\left(-\frac{\Omega}{2\gamma}\left(1+\frac{\Omega^2}{\gamma^2}\right) - \frac{3\eta\Omega}{2\gamma} + \sqrt{1-\eta^2}\left(1-\frac{\Omega^2}{2\gamma^2}\right)\right)\right. \\
&\times\left(\chi \mp \left(\frac{\Omega}{2\gamma}\left(1+\frac{\Omega^2}{\gamma^2}\right) - \frac{3\eta\Omega}{2\gamma} + \sqrt{1-\eta^2}\left(1-\frac{\Omega^2}{2\gamma^2}\right)\right)\right) + \left(1+\frac{\Omega^2}{\gamma^2}\right) \\
&\left.\left.\times\left(-\frac{\Omega}{2\gamma}\left(1+\frac{\Omega^2}{\gamma^2}\right) + \frac{3\eta\Omega}{2\gamma} - \sqrt{1-\eta^2}\left(1-\frac{\Omega^2}{2\gamma^2}\right) \pm \left(2\chi + \left(1+\frac{\Omega^2}{\gamma^2}\right)\right)\right)\right]\right],
\end{aligned} \tag{4.204}$$

$$\begin{aligned}
&(p^2 - q_-q_+)(1\pm 1) + 2p(q_+ - q_-) - 2p^2(q_- + q_+) \\
&= \frac{1}{\chi^3}\left[\left(\left(1+\frac{\Omega^2}{\gamma^2}\right)^2\left(1-\frac{\Omega^2}{4\gamma^2}\right) + \left(\frac{3\eta\Omega}{2\gamma} - \sqrt{1-\eta^2}\left(1-\frac{\Omega^2}{2\gamma^2}\right)\right)^2\right)(\chi \pm \chi)\right. \\
&\left. -4\chi\left(1+\frac{\Omega^2}{\gamma^2}\right)\left(\frac{3\eta\Omega}{2\gamma} - \sqrt{1-\eta^2}\left(1-\frac{\Omega^2}{2\gamma^2}\right)\right) + \frac{2\Omega}{\gamma}\left(1+\frac{\Omega^2}{\gamma^2}\right)^3\right],
\end{aligned} \tag{4.205}$$

$$\begin{aligned}
&p(1-p) - q_-(q_- + q_+ \pm (2-p)) \\
&= \frac{1}{\chi^2}\left[\left(1+\frac{\Omega^2}{\gamma^2}\right)\left(\chi - \left(1+\frac{\Omega^2}{\gamma^2}\right)\right) + \left(\frac{\Omega}{2\gamma}\left(1+\frac{\Omega^2}{\gamma^2}\right) - \frac{3\eta\Omega}{2\gamma}\right.\right. \\
&\left.\left. + \sqrt{1-\eta^2}\left(1-\frac{\Omega^2}{2\gamma^2}\right)\right)\left(-\frac{\Omega}{\gamma}\left(1+\frac{\Omega^2}{\gamma^2}\right) \pm \left(2\chi - \left(1+\frac{\Omega^2}{\gamma^2}\right)\right)\right)\right],
\end{aligned} \tag{4.206}$$

$$
\begin{aligned}
&p(p-1) - q_+(q_- + q_+ \pm (2+p)) \\
&= \frac{1}{\chi^2}\left[\left(1+\frac{\Omega^2}{\gamma^2}\right)\left(\left(1+\frac{\Omega^2}{\gamma^2}\right)-\chi\right) - \left(\frac{\Omega}{2\gamma}\left(1+\frac{\Omega^2}{\gamma^2}\right)+\frac{3\eta\Omega}{2\gamma}\right.\right. \\
&\left.\left.-\sqrt{1-\eta^2}\left(1-\frac{\Omega^2}{2\gamma^2}\right)\right)\left(-\frac{\Omega}{\gamma}\left(1+\frac{\Omega^2}{\gamma^2}\right) \pm \left(2\chi + \left(1+\frac{\Omega^2}{\gamma^2}\right)\right)\right)\right],
\end{aligned} \tag{4.207}
$$

$$
\begin{aligned}
&2q_+(1-p+q_-) + 2q_-(1+p+q_+) \\
&= -\frac{2}{\chi^2}\left[\left(\frac{\Omega}{2\gamma}\left(1+\frac{\Omega^2}{\gamma^2}\right)+\frac{3\eta\Omega}{2\gamma}-\sqrt{1-\eta^2}\left(1-\frac{\Omega^2}{2\gamma^2}\right)\right)\right. \\
&\times\left(\chi - \left(1+\frac{\Omega^2}{\gamma^2}\right)\left(1+\frac{\Omega}{2\gamma}\right)+\frac{3\eta\Omega}{2\gamma}-\sqrt{1-\eta^2}\left(1-\frac{\Omega^2}{2\gamma^2}\right)\right) \\
&+\left(\frac{\Omega}{2\gamma}\left(1+\frac{\Omega^2}{\gamma^2}\right)-\frac{3\eta\Omega}{2\gamma}+\sqrt{1-\eta^2}\left(1-\frac{\Omega^2}{2\gamma^2}\right)\right) \\
&\left.\times\left(\chi + \left(1+\frac{\Omega^2}{\gamma^2}\right)\left(1-\frac{\Omega}{2\gamma}\right)-\frac{3\eta\Omega}{2\gamma}+\sqrt{1-\eta^2}\left(1-\frac{\Omega^2}{2\gamma^2}\right)\right)\right],
\end{aligned} \tag{4.208}
$$

$$
1+p\mp q_- = 1 + \frac{1+\frac{\Omega^2}{\gamma^2} \pm \left[\frac{\Omega}{2\gamma}\left(1+\frac{\Omega^2}{\gamma^2}\right)-\frac{3\eta\Omega}{2\gamma}+\sqrt{1-\eta^2}\left(1-\frac{\Omega^2}{2\gamma^2}\right)\right]}{\chi}, \tag{4.209}
$$

$$
1-q_+\mp p = 1 + \frac{\frac{\Omega}{2\gamma}\left(1+\frac{\Omega^2}{\gamma^2}\right)+\frac{3\eta\Omega}{2\gamma}-\sqrt{1-\eta^2}\left(1-\frac{\Omega^2}{2\gamma^2}\right)\mp\left(1+\frac{\Omega^2}{\gamma^2}\right)}{\chi}, \tag{4.210}
$$

$$
\begin{aligned}
&p^2(1+p) + q_-^2(1\mp q_+) + q_-p(q_+ \mp (2+p)) \\
&= \frac{1}{\chi^3}\left[\left(1+\frac{\Omega^2}{\gamma^2}\right)^2\left(\chi+\left(1+\frac{\Omega^2}{\gamma^2}\right)\right) - \left[\frac{\Omega}{2\gamma}\left(1+\frac{\Omega^2}{\gamma^2}\right)-\frac{3\eta\Omega}{2\gamma}\right.\right. \\
&\left.+\sqrt{1-\eta^2}\left(1-\frac{\Omega^2}{2\gamma^2}\right)\right]\left[\left(-\frac{\Omega}{2\gamma}\left(1+\frac{\Omega^2}{\gamma^2}\right)+\frac{3\eta\Omega}{2\gamma}-\sqrt{1-\eta^2}\left(1-\frac{\Omega^2}{2\gamma^2}\right)\right)\right. \\
&\times\left(\chi \pm \left(\frac{\Omega}{2\gamma}\left(1+\frac{\Omega^2}{\gamma^2}\right)+\frac{3\eta\Omega}{2\gamma}-\sqrt{1-\eta^2}\left(1-\frac{\Omega^2}{2\gamma^2}\right)\right)\right)+\left(1+\frac{\Omega^2}{\gamma^2}\right) \\
&\left.\left.\times\left(-\frac{\Omega}{2\gamma}\left(1+\frac{\Omega^2}{\gamma^2}\right)-\frac{3\eta\Omega}{2\gamma}+\sqrt{1-\eta^2}\left(1-\frac{\Omega^2}{2\gamma^2}\right)\mp\left(2\chi+\left(1+\frac{\Omega^2}{\gamma^2}\right)\right)\right)\right]\right],
\end{aligned} \tag{4.211}
$$

$$
\begin{aligned}
&p^2(1-p)+q_+^2(1\mp q_-)-q_+p(q_-\mp(2-p))\\
&=\frac{1}{\chi^3}\left[\left(1+\frac{\Omega^2}{\gamma^2}\right)^2\left(\chi-\left(1+\frac{\Omega^2}{\gamma^2}\right)\right)-\left[\frac{\Omega}{2\gamma}\left(1+\frac{\Omega^2}{\gamma^2}\right)+\frac{3\eta\Omega}{2\gamma}\right.\right.\\
&\left.-\sqrt{1-\eta^2}\left(1-\frac{\Omega^2}{2\gamma^2}\right)\right]\left[\left(-\frac{\Omega}{2\gamma}\left(1+\frac{\Omega^2}{\gamma^2}\right)-\frac{3\eta\Omega}{2\gamma}+\sqrt{1-\eta^2}\left(1-\frac{\Omega^2}{2\gamma^2}\right)\right)\right.\\
&\times\left(\chi\mp\left(-\frac{\Omega}{2\gamma}\left(1+\frac{\Omega^2}{\gamma^2}\right)+\frac{3\eta\Omega}{2\gamma}-\sqrt{1-\eta^2}\left(1-\frac{\Omega^2}{2\gamma^2}\right)\right)\right)-\left(1+\frac{\Omega^2}{\gamma^2}\right)\\
&\left.\left.\times\left(-\frac{\Omega}{2\gamma}\left(1+\frac{\Omega^2}{\gamma^2}\right)+\frac{3\eta\Omega}{2\gamma}-\sqrt{1-\eta^2}\left(1-\frac{\Omega^2}{2\gamma^2}\right)\mp\left(2\chi+\left(1+\frac{\Omega^2}{\gamma^2}\right)\right)\right)\right]\right],
\end{aligned}
\tag{4.212}
$$

$$
\begin{aligned}
&(q_-q_+-p^2)(1\mp 1)+p(q_+-q_-)+2p^2(q_++q_-)\\
&=\frac{1}{\chi^3}\left[\left(\left(\frac{\Omega^2}{4\gamma^2}-1\right)\left(1+\frac{\Omega^2}{\gamma^2}\right)^2-\left(\frac{3\eta\Omega}{2\gamma}-\sqrt{1-\eta^2}\left(1-\frac{\Omega^2}{2\gamma^2}\right)\right)^2\right)(\chi\mp\chi)\right.\\
&\left.-2\chi\left(1+\frac{\Omega^2}{\gamma^2}\right)\left(\frac{3\eta\Omega}{2\gamma}-\sqrt{1-\eta^2}\left(1-\frac{\Omega^2}{2\gamma^2}\right)\right)-\frac{2\Omega}{\gamma}\left(1+\frac{\Omega^2}{\gamma^2}\right)^3\right],
\end{aligned}
\tag{4.213}
$$

$$
\begin{aligned}
&p(1+p)+q_-(q_-+q_+\mp(2+p))\\
&=\frac{1}{\chi^2}\left[\left(1+\frac{\Omega^2}{\gamma^2}\right)\left(\chi+\left(1+\frac{\Omega^2}{\gamma^2}\right)\right)-\left(\frac{\Omega}{2\gamma}\left(1+\frac{\Omega^2}{\gamma^2}\right)-\frac{3\eta\Omega}{2\gamma}\right.\right.\\
&\left.\left.+\sqrt{1-\eta^2}\left(1-\frac{\Omega^2}{2\gamma^2}\right)\right)\left(-\frac{\Omega}{\gamma}\left(1+\frac{\Omega^2}{\gamma^2}\right)\mp\left(2\chi+\left(1+\frac{\Omega^2}{\gamma^2}\right)\right)\right)\right],
\end{aligned}
\tag{4.214}
$$

$$
\begin{aligned}
&-p(p+1)+q_+(q_-+q_+\mp(2-p))\\
&=\frac{1}{\chi^2}\left[-\left(1+\frac{\Omega^2}{\gamma^2}\right)\left(\left(1+\frac{\Omega^2}{\gamma^2}\right)+\chi\right)-\left(\frac{\Omega}{2\gamma}\left(1+\frac{\Omega^2}{\gamma^2}\right)+\frac{3\eta\Omega}{2\gamma}\right.\right.\\
&\left.\left.-\sqrt{1-\eta^2}\left(1-\frac{\Omega^2}{2\gamma^2}\right)\right)\left(-\frac{\Omega}{\gamma}\left(1+\frac{\Omega^2}{\gamma^2}\right)\mp\left(2\chi-\left(1+\frac{\Omega^2}{\gamma^2}\right)\right)\right)\right],
\end{aligned}
\tag{4.215}
$$

$$
\begin{aligned}
&2q_+(1+p-q_-) + 2q_-(1-p-q_+) \\
&= -\frac{2}{\chi^2}\left[\left(\frac{\Omega}{2\gamma}\left(1+\frac{\Omega^2}{\gamma^2}\right) + \frac{3\eta\Omega}{2\gamma} - \sqrt{1-\eta^2}\left(1-\frac{\Omega^2}{2\gamma^2}\right)\right)\right. \\
&\times\left(\chi + \left(1+\frac{\Omega^2}{\gamma^2}\right)\left(1+\frac{\Omega}{2\gamma}\right) - \frac{3\eta\Omega}{2\gamma} + \sqrt{1-\eta^2}\left(1-\frac{\Omega^2}{2\gamma^2}\right)\right) \\
&+\left(\frac{\Omega}{2\gamma}\left(1+\frac{\Omega^2}{\gamma^2}\right) - \frac{3\eta\Omega}{2\gamma} + \sqrt{1-\eta^2}\left(1-\frac{\Omega^2}{2\gamma^2}\right)\right) \\
&\left.\times\left(\chi - \left(1+\frac{\Omega^2}{\gamma^2}\right)\left(1-\frac{\Omega}{2\gamma}\right) + \frac{3\eta\Omega}{2\gamma} - \sqrt{1-\eta^2}\left(1-\frac{\Omega^2}{2\gamma^2}\right)\right)\right]. \qquad (4.216)
\end{aligned}
$$

In order to study the dependence of the squeezing spectrum on the linear gain coefficient, amplitude of the driving radiation, initial preparation of the atoms, and squeeze parameter, we plot the squeezing spectrum versus these parameters by alternatively fixing two of them. We first plot the squeezing spectrum versus Ω/γ and η for $A = 1.3$ and $r = 0.75$. We take similar parameters as in Section 4.1.1 so that comparison of the squeezing inside and outside the cavity can be made.

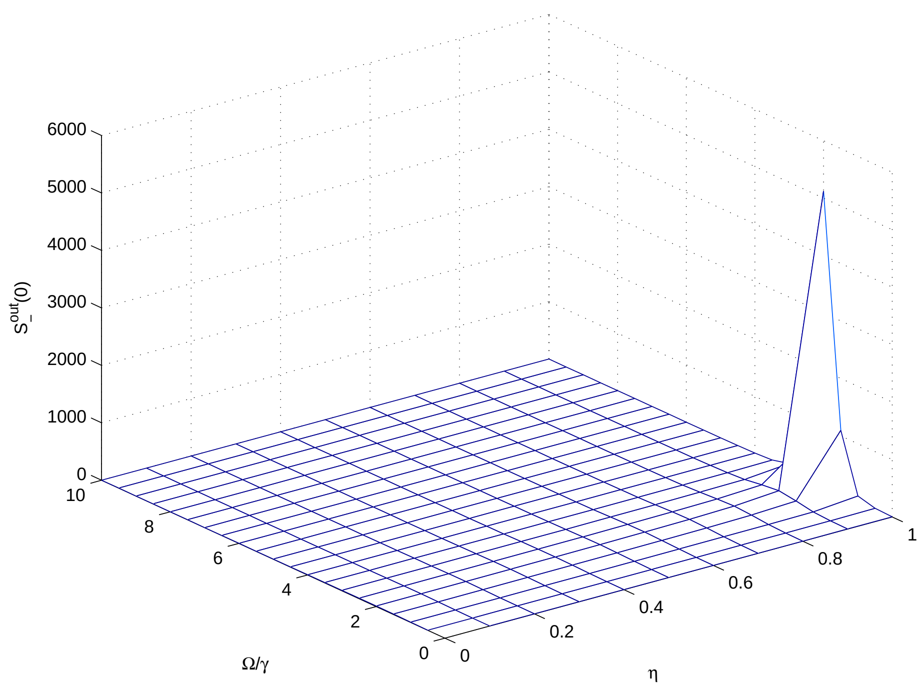

Fig. 4.22: Plot of the squeezing spectrum $S_-^{out}(0)$ (Eq. (4.199)) of the two-mode output radiation at steady state for $\kappa = 0.5$, $r = 0.75$, and $A = 1.3$.

It is clearly shown in Fig. 4.22 that the two-mode radiation generated by the system under consideration does not exhibit squeezing outside the cavity even when the cavity is coupled to a two-mode squeezed vacuum reservoir for certain values of Ω/γ and η. Like for the cavity radiation, the maximum squeezing of the output radiation occurs for $\eta = 0$ and $\Omega = 0.1\gamma$. It is also found that the squeezing, for example, does not occur for values of Ω less than 6.6γ when $\eta = 1$, $r = 0.75$, $\kappa = 0.5$, and $A = 1.3$.

We next plot the squeezing spectrum versus A and η, where the amplitude of the driving radiation is fixed to the value for which the maximum squeezing is obtained in the previous case ($\Omega = 0.1\gamma$).

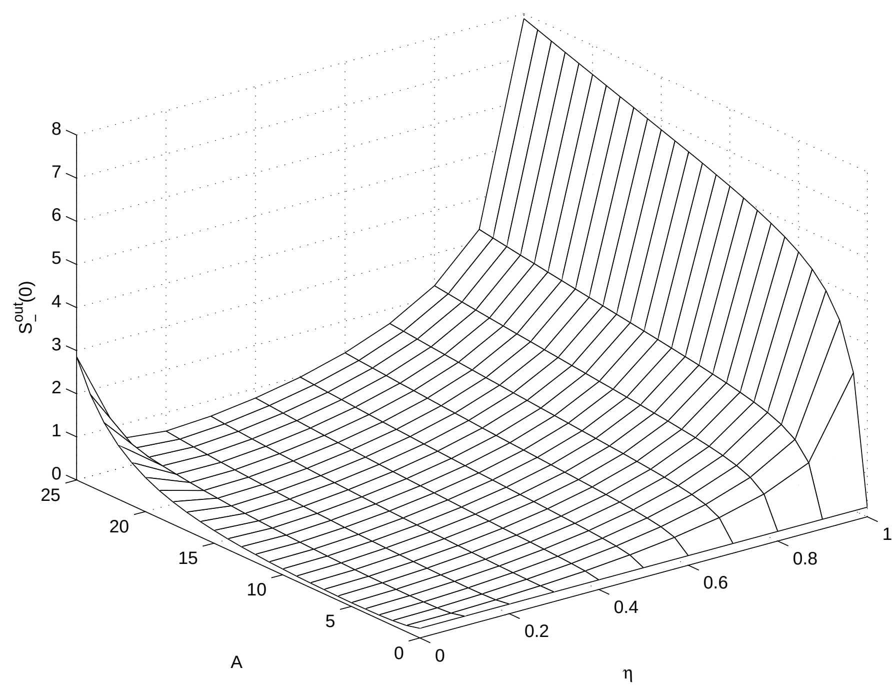

Fig. 4.23: Plot of the squeezing spectrum $S_{-}^{out}(0)$ (Eq. (4.199)) of the two-mode output radiation at steady state for $\kappa = 0.5$, $r = 0.75$, and $\Omega = 0.1\gamma$.

It is not difficult to see from Fig. 4.23 that the two-mode output radiation does not exhibit squeezing for certain values of A and η. It is also possible to see that the degree of squeezing decreases with the linear gain coefficient for some values of η. It is found that the maximum squeezing occurs for $\eta = 0$ and $A = 5$. We hence come to understand that the maximum squeezing for the output and cavity radiation occurs for the same value of η, but for different linear gain coefficient.

We now plot the squeezing spectrum versus Ω/γ and A. Here η is fixed arbitrarily to 0.1.

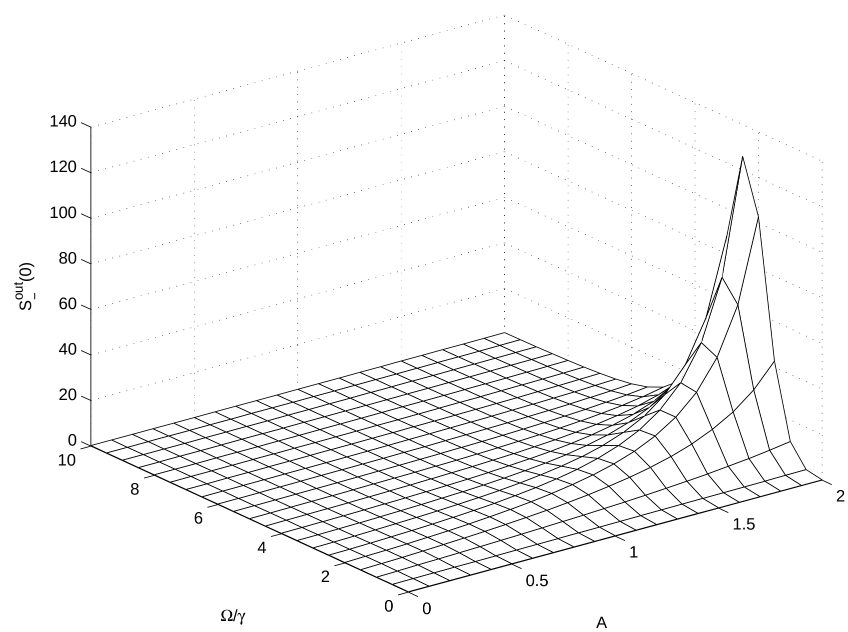

Fig. 4.24: Plot of the squeezing spectrum $S_{-}^{out}(0)$ (Eq. (4.199)) of the two-mode output radiation at steady state for $\kappa = 0.5$, $r = 0.75$, and $\eta = 0.1$.

One can clearly see from Fig. 4.24 that the two-mode output radiation does not exhibit squeezing for certain values of A and Ω/γ. As in the case of the cavity radiation, the degree of squeezing is found to decrease with the linear gain coefficient for some values of Ω/γ. We also found that the maximum squeezing occurs for some values of Ω/γ when $A = 0$. This indicates that the squeezing for the output radiation is less than what it would be when we have the squeezed vacuum reservoir with squeeze parameter of $r = 0.75$.

In order to study the dependence of the squeezing spectrum particularly on the squeeze parameter, we plot the squeezing spectrum versus the linear gain coefficient, initial preparation of the atoms, and amplitude of the driving radiation for different values of r. We fix two of these parameters to the values we have taken while studying the squeezing of the cavity radiation so that comparison of the squeezing inside and outside the cavity can be made. To this end, we first plot the squeezing spectrum versus the linear gain coefficient. We take $\Omega = 0.1\gamma$ and $\eta = 0.1$.

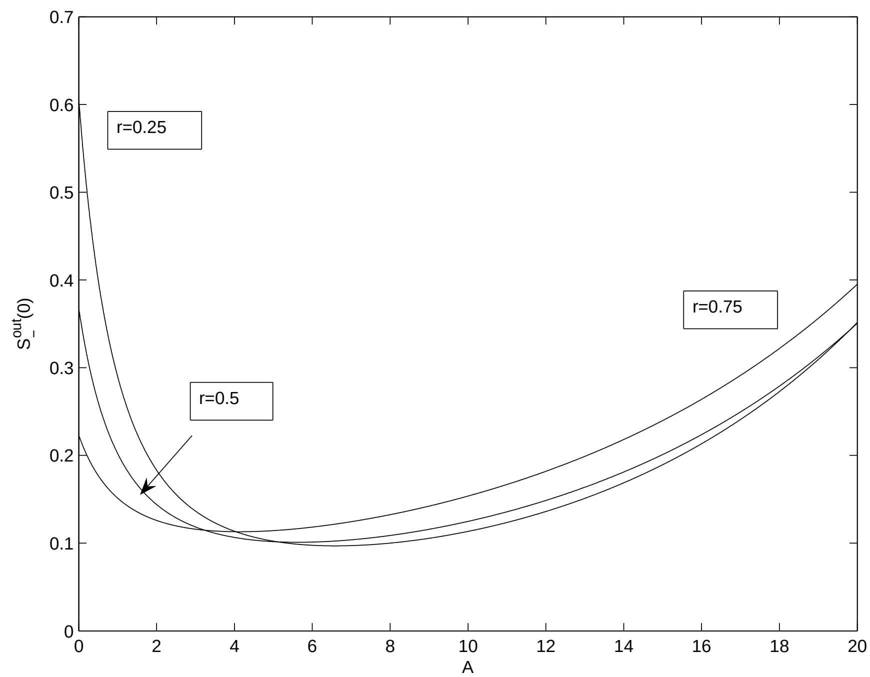

Fig. 4.25: Plots of the squeezing spectrum $S_{-}^{out}(0)$ (Eq. (4.199)) of the two-mode output radiation at steady state for $\kappa = 0.5$, $\Omega = 0.1\gamma$, and $\eta = 0.1$ and different values of r.

We see from Fig. 4.25 that the squeezing of the output radiation increases with the squeeze parameter for smaller values of A, but decreases for larger values. It is found that the maximum squeezing occurs for $r = 0.25$ and $A = 6.7$. Moreover, as clearly shown in Figs. 4.4 and 4.25, the minimum value of the squeezing spectrum is less than the corresponding minimum value of the quadrature variance, in spite of the unbiased noise introduced while the radiation crosses the mirror.

We next plot the squeezing spectrum versus η. We take $\Omega = 0.1\gamma$ and $A = 1$.

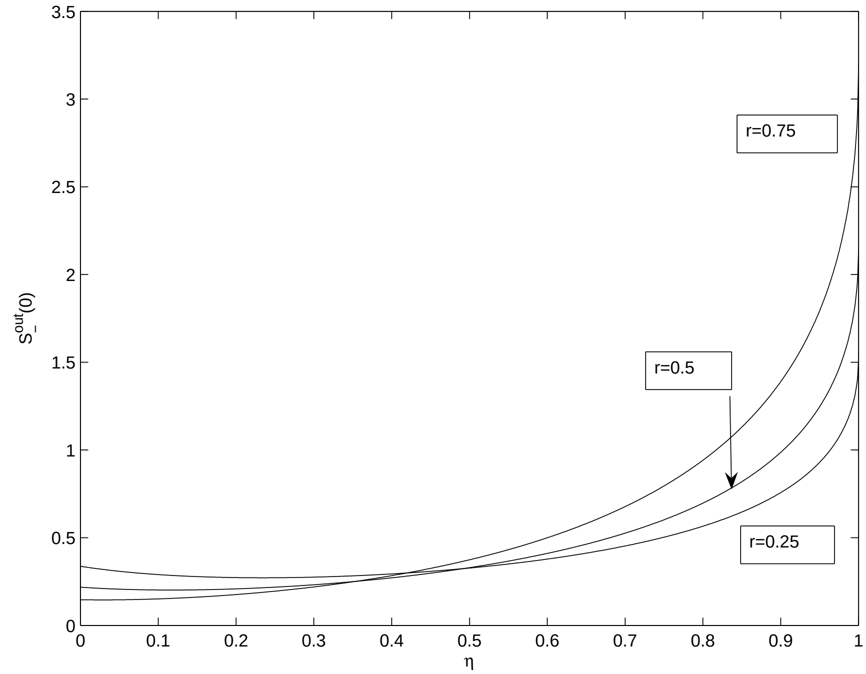

Fig. 4.26: Plots of the squeezing spectrum $S_{-}^{out}(0)$ (Eq. (4.199)) of the two-mode output radiation at steady state for $\kappa = 0.5$, $\Omega = 0.1\gamma$, and $A = 1$.

According to the result given in Fig. 4.26 the squeezing spectrum decreases with the squeeze parameter for smaller values of η, but increases with larger values. It is also found that the minimum value of the squeezing spectrum is less than the corresponding minimum value of the quadrature variance.

We now plot the squeezing spectrum versus Ω/γ for different values of r. We take $\eta = 0.1$ and $A = 2.3$.

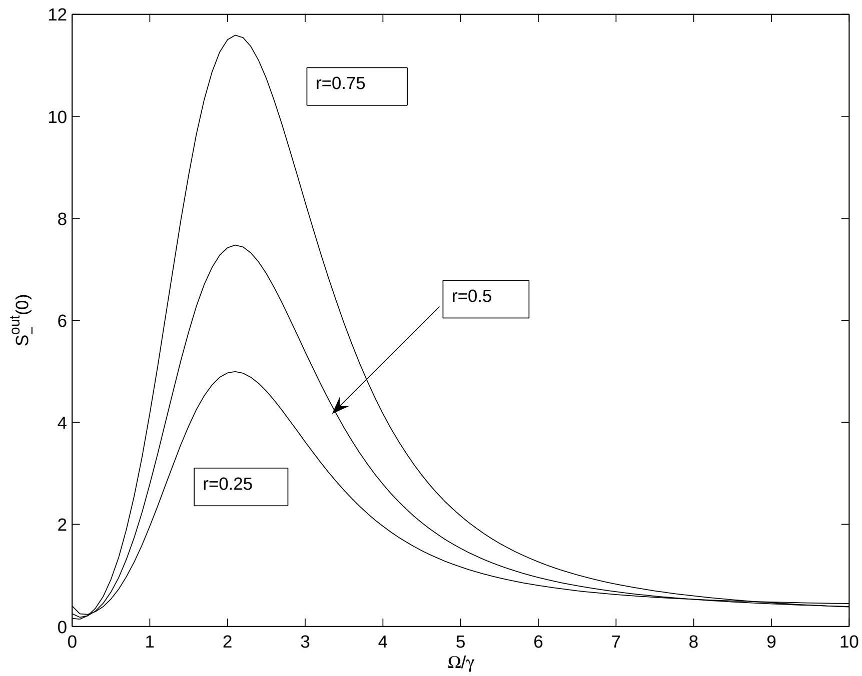

Fig. 4.27: Plots of the squeezing spectrum $S_{-}^{out}(0)$ (Eq. (4.199)) of the two-mode output radiation at steady state for $\kappa = 0.5$, $\eta = 0.1$, and $A = 1$.

As in the case of the cavity radiation, the squeezing of the output radiation occurs either for smaller or larger values of Ω/γ. We also see from Fig. 4.27 that the squeezing increases with the squeeze parameter for some values of Ω/γ.

In order to study the squeezing of the output radiation more closely, we consider various cases of interest. In the first place, when there is no driving radiation ($\Omega = 0$), we see that

$$1 - p \pm q_{-} = 1 - \frac{1 \pm \sqrt{1-\eta^2}}{\eta}, \tag{4.217}$$

$$1 + p \pm q_{+} = 1 + \frac{1 \pm \sqrt{1-\eta^2}}{\eta}, \tag{4.218}$$

$$q_{+} + q_{-} \pm 2 = \pm 2, \tag{4.219}$$

$$\begin{aligned} &p^2(1-p) + q_-^2(1 \pm q_+) - q_- p(q_+ \pm (2-p)) \\ &= \frac{1}{\eta^3}\left[\eta - 1 + (1-\eta^2)(\eta \pm \sqrt{1-\eta^2}) - \sqrt{1-\eta^2} \mp (2\eta - 1)\right], \end{aligned} \tag{4.220}$$

$$\begin{aligned} &p^2(1+p) + q_+^2(1 \pm q_-) + q_+ p(q_- \pm (2+p)) \\ &= \frac{1}{\eta^3}\left[\eta + 1 + (1-\eta^2)(\eta \mp \sqrt{1-\eta^2}) - \sqrt{1-\eta^2} \pm (2\eta - 1)\right], \end{aligned} \tag{4.221}$$

$$\begin{aligned} &(p^2 - q_- q_+)(1 \pm 1) + 2p(q_+ - q_-) - 2p^2(q_- + q_+) \\ &= \frac{1}{\eta^2}\left[(2-\eta^2)(1 \pm 1) + 2\sqrt{1-\eta^2}\right], \end{aligned} \tag{4.222}$$

$$p(1-p) - q_-(q_- + q_+ \pm (2-p)) = \frac{1}{\eta^2}\left[\eta - 1 \pm \sqrt{1-\eta^2}(2\eta - 1)\right], \tag{4.223}$$

$$p(p-1) - q_+(q_- + q_+ \pm (2+p)) = \frac{1}{\eta^2}\left[1 - \eta \pm \sqrt{1-\eta^2}(2\eta + 1)\right], \tag{4.224}$$

$$2q_+(1 - p + q_-) + 2q_-(1 + p + q_+) = -\frac{4\sqrt{1-\eta^2}}{\eta^2}(1 + \sqrt{1-\eta^2}), \tag{4.225}$$

$$1 + p \mp q_- = 1 + \frac{1 \pm \sqrt{1-\eta^2}}{\eta}, \tag{4.226}$$

$$1 - q_+ \mp p = 1 - \frac{\sqrt{1-\eta^2} \pm 1}{\eta}, \tag{4.227}$$

$$\begin{aligned} &p^2(1+p) + q_-^2(1 \mp q_+) + q_- p(q_+ \mp (2+p)) \\ &= \frac{1}{\eta^3}\left[\eta + 1 + (1-\eta^2)(\eta \mp \sqrt{1-\eta^2}) + \sqrt{1-\eta^2} \mp (2\eta + 1)\right], \end{aligned} \tag{4.228}$$

$$\begin{aligned} &p^2(1-p) + q_+^2(1 \mp q_-) - q_+ p(q_- \mp (2-p)) \\ &= \frac{1}{\eta^3}\left[\eta - 1 - (1-\eta^2)(\eta \pm \sqrt{1-\eta^2}) + \sqrt{1-\eta^2} \mp (2\eta + 1)\right], \end{aligned} \tag{4.229}$$

$$(q_- q_+ - p^2)(1 \mp 1) + p(q_+ - q_-) + 2p^2(q_+ + q_-) = \frac{1}{\eta^2}\left[\eta^2(1 \mp 1) + 2\sqrt{1-\eta^2}\right], \tag{4.230}$$

$$p(1+p)+q_-(q_-+q_+\mp(2+p))=\frac{1}{\eta^2}\left[\eta+1\pm\sqrt{1-\eta^2}(2\eta+1)\right], \tag{4.231}$$

$$-p(p+1)+q_+(q_-+q_+\mp(2-p))=\frac{1}{\eta^2}\left[-\eta-1\mp\sqrt{1-\eta^2}(2\eta-1)\right], \tag{4.232}$$

$$2q_+(1+p-q_-)+2q_-(1-p-q_+)=\frac{4}{\eta^2}\left[\sqrt{1-\eta^2}(1+\sqrt{1-\eta^2})\right]. \tag{4.233}$$

Now making use of Eqs. (4.83), (4.84), (4.85), (4.86), (4.87), (4.94), (4.95), (4.96), (4.217), (4.218), (4.219), (4.220), (4.221), (4.222), (4.223), (4.224), (4.225), (4.226), (4.227), (4.228), (4.229), (4.230), (4.231), (4.232), and (4.233), we obtain

$$\begin{aligned}
S_{\pm}^{out}(0) &= 1+\frac{\kappa}{2\eta\big((\kappa+A\eta)^2+4\omega^2\big)(2\kappa+A\eta)}\big[2(N\pm M)\big(8\kappa\eta(\kappa+A\eta)+A^2\eta^3\big)\\
&+2NA^2\big(2-\eta^3\pm\sqrt{1-\eta^2}(2\eta-1)\big)-MA^2\eta\big((2\eta-\eta^2)(1\pm 1)\\
&+4\sqrt{1-\eta^2}\big)+8A\sqrt{1-\eta^2}\big(M(1+\sqrt{1-\eta^2})\pm N\eta\big)(2\kappa+A\eta)\big]\\
&+\frac{\kappa}{2\eta(\kappa+A\eta)(2\kappa+A\eta)(\kappa^2++4\omega^2)}\big[2(N\pm M)\big(8\kappa\eta(\kappa+A\eta)+A^2\eta^3\big)\\
&+2NA^2\big(2\eta-\eta^3\pm\sqrt{1-\eta^2}(2\eta+1)\big)-MA^2\big(\eta^3(1\pm 1)+2\sqrt{1-\eta^2}\big)\\
&\pm 4NA\sqrt{1-\eta^2}(2\kappa+A\eta)-8MA\sqrt{1-\eta^2}\big(1+\sqrt{1-\eta^2}\big)(2\kappa+A\eta)\big]\\
&+\frac{A}{4\eta\big((\kappa+A\eta)^2+4\omega^2\big)(2\kappa+A\eta)}\big[\big(8\kappa(\kappa+A\eta)+A^2\eta^2\big)\big(2\eta-1\pm\eta^2\sqrt{1-\eta^2}\big)\\
&+A^2\big[(1-\eta)\big(\eta-\eta^2+(1-\eta^2)(\eta\pm\sqrt{1-\eta^2})\big)\pm\sqrt{1-\eta^2}(2\eta-1)\\
&-\frac{\eta\sqrt{1-\eta^2}}{2}\big((2-\eta^2)(1\pm 1)+4\sqrt{1-\eta^2}\big)\big]+2A(2\kappa+A\eta)\\
&\times\big((2-\eta)\big(\eta-1\pm\sqrt{1-\eta^2}(2\eta-1)+2(1-\eta^2)(1+\sqrt{1-\eta^2})\big)\big)\big]\\
&+\frac{A}{8\eta(\kappa+A\eta)(2\kappa+A\eta)(\kappa+4\omega^2)}\big[\big(8\kappa(\kappa+A\eta)+A^2\eta^2\big)\\
&\times\big((1-\eta)(1+\eta\pm\sqrt{1-\eta^2})\pm\eta\sqrt{1-\eta^2}\big)+A^2\big[(1-\eta)\big(\eta+\eta^2\\
&+(1-\eta^2)(\eta\pm\sqrt{1-\eta^2})\pm\sqrt{1-\eta^2}(2\eta+1)-\eta\sqrt{1-\eta^2}(\eta^2(1\pm 1)\\
&+2\sqrt{1-\eta^2})\big)\big]+2A(2\kappa+A\eta)\big((1-\eta)(\eta+1\pm\sqrt{1-\eta^2}(2\eta+1)\\
&+\sqrt{1-\eta^2}(1+\eta\pm\sqrt{1-\eta^2}(2\eta-1))\big)\big)\big].
\end{aligned} \tag{4.234}$$

In the following, we seek to analyze the dependence of the squeezing spectrum on the linear gain coefficient, initial preparation of the atoms, and squeeze parameter. To this end, we first plot the squeezing spectrum versus η for different values of A and $r = 0$. The values of A are arbitrarily chosen.

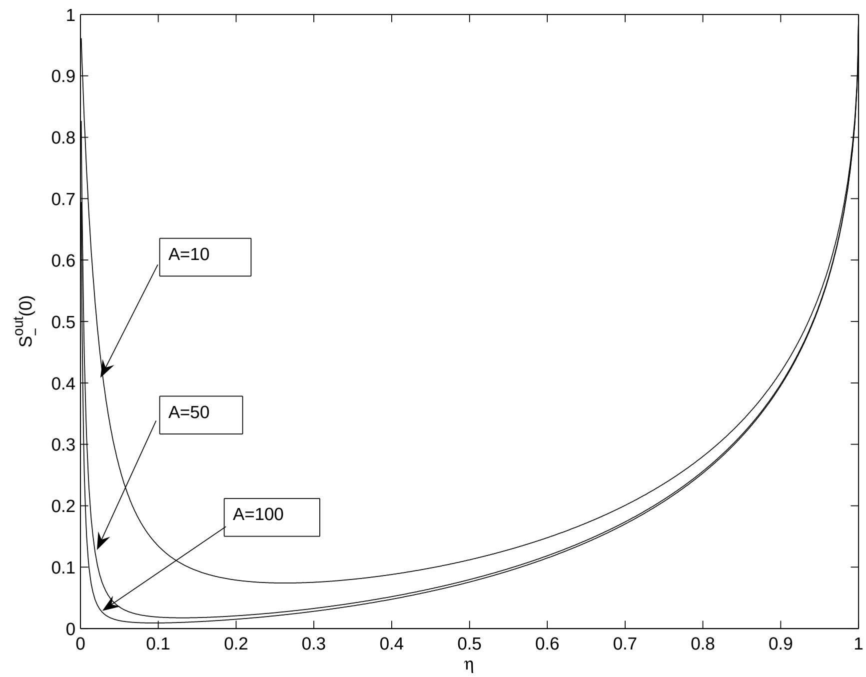

Fig. 4.28: Plots of the squeezing spectrum $S_-^{out}(0)$ (Eq. (4.234)) of the two-mode output radiation at steady state for $\omega = 0$, $\kappa = 0.5$, $r = 0$, $\Omega = 0$, and different values of A.

We see from Fig. 4.28 that the output radiation exhibits squeezing for values of η between 0 and 1. We also notice that the squeezing spectrum decreases with the linear gain coefficient. Moreover, it is found that a maximum squeezing occurs for values of η near 0.1 for $A = 100$. Comparison of the results given in Figs. 4.14 and 4.28 reveals that the minimum squeezing spectrum of the output radiation is less than the corresponding quadrature variance of the cavity radiation.

We next plot the squeezing spectrum versus η for different values of r. Here $A = 1$ is taken for convenience.

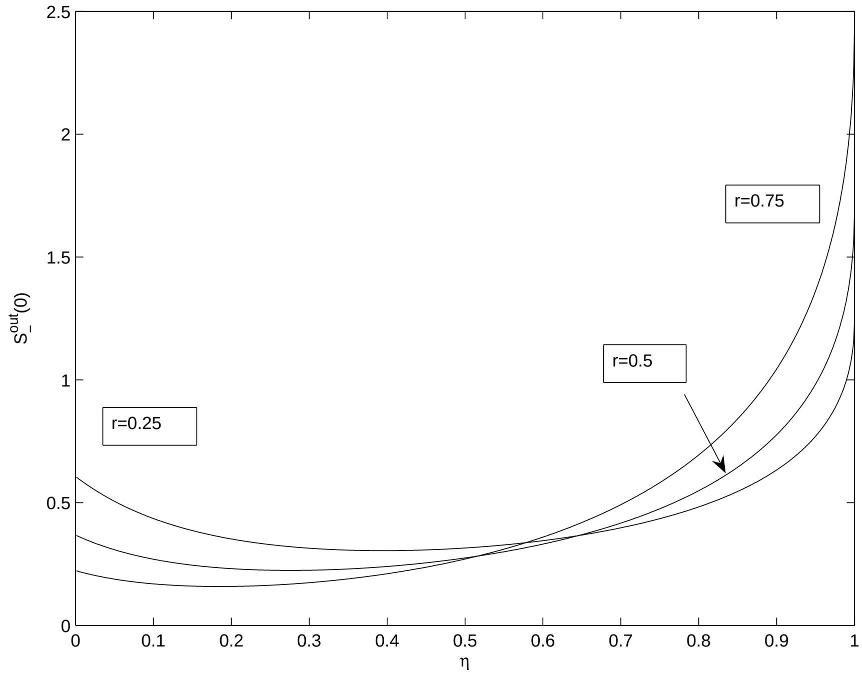

Fig. 4.29: Plots of the squeezing spectrum $S_{-}^{out}(0)$ (Eq. (4.234)) of the two-mode output radiation at steady state for $\omega = 0$, $\kappa = 0.5$, $A = 1$, $\Omega = 0$, and different values r.

According to the result given in Fig. 4.29 the squeezing spectrum decreases with the squeeze parameter for smaller values of η, but increases for larger values. As shown in Fig. 4.15, similar effect of the squeezed parameter is also observed for the cavity radiation. It is found that a maximum squeezing occurs at $\eta = 0.19$.

We now seek to study the dependence of the squeezing spectrum on the amplitude of the driving radiation, linear gain coefficient, and squeeze parameter when half of the atoms are initially prepared to be in the upper level ($\eta = 0$). To this effect, we first plot the squeezing spectrum versus Ω/γ for different values of A. We consider very small values of Ω/γ.

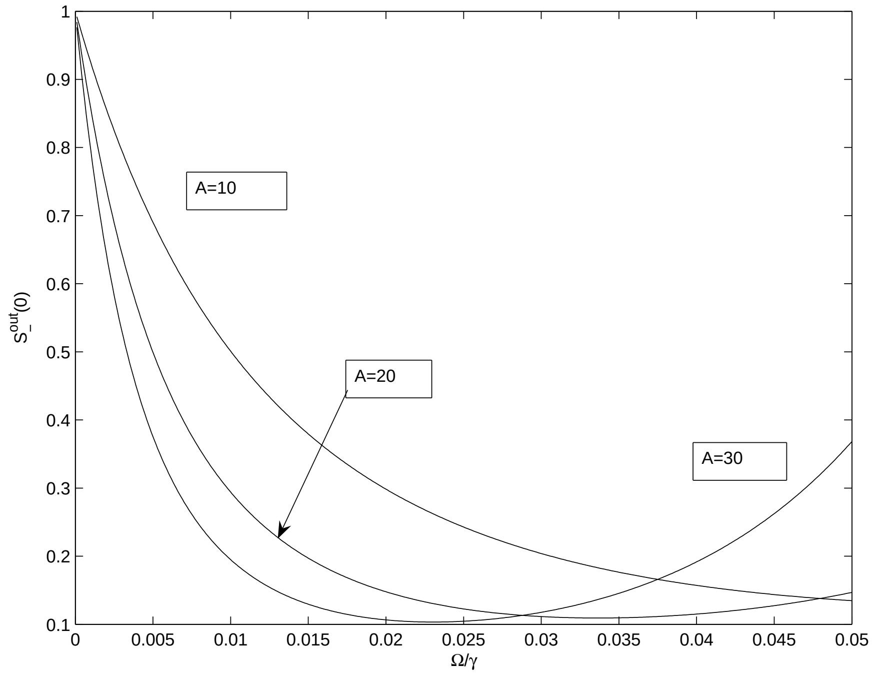

Fig. 4.30: Plots of the squeezing spectrum $S_{-}^{out}(0)$ (Eq. (4.199)) of the two-mode output radiation at steady state for $\omega = 0$, $\eta = 0$, $\kappa = 0.5$, $r = 0$, and different values of A.

We clearly see from Fig. 4.30 that the squeezing spectrum decreases with the linear gain coefficient for smaller values of Ω/γ, but increases for larger values. As shown in Fig. 4.8, similar effect of the amplitude of the driving radiation on squeezing for cavity radiation is observed. It is found that a maximum squeezing occurs for $A = 40$ and $\Omega = 0.017\gamma$. On the other hand, comparison of Figs. 4.28 and 4.30 reveals that coupling the top and bottom levels of the atoms by an external coherent radiation significantly enhances the squeezing of the output radiation for $\eta = 0$.

We next plot the squeezing spectrum versus Ω/γ for different values of r. The linear gain coefficient is taken to be $A = 40$.

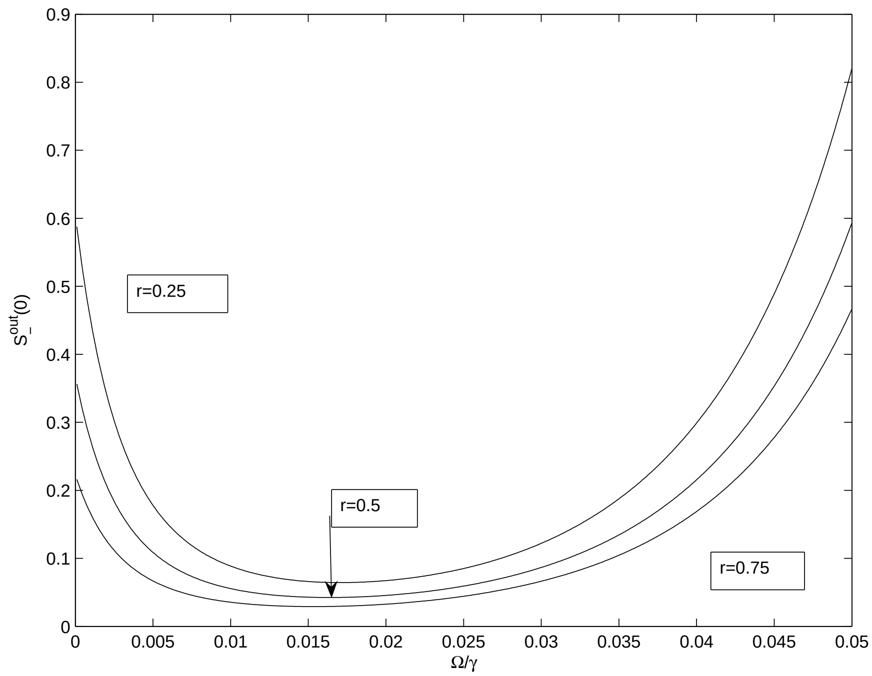

Fig. 4.31: Plots of the squeezing spectrum $S_{-}^{out}(0)$ (Eq. (4.199)) of the two-mode output radiation at steady state for $\omega = 0$, $\eta = 0$, $\kappa = 0.5$, $A = 40$, and different values of r.

It is not difficult to see from Fig. 4.31 that the squeezing spectrum decreases with the squeeze parameter. It turns out that a maximum squeezing occurs for $\Omega = 0.015\gamma$ and $r = 0.75$. Just like in the cavity radiation, the maximum squeezing for the output radiation is found to occur for nearly the same values of Ω/γ for different values of r.

Finally, in order to study the dependence of the squeezing spectrum on the amplitude of the driving radiation, linear gain coefficient, and squeezing parameter when all the atoms are initially prepared to be in the bottom level ($\eta = 1$), we first plot the squeezing spectrum versus Ω/γ for different values of A. We consider the case when Ω/γ is large.

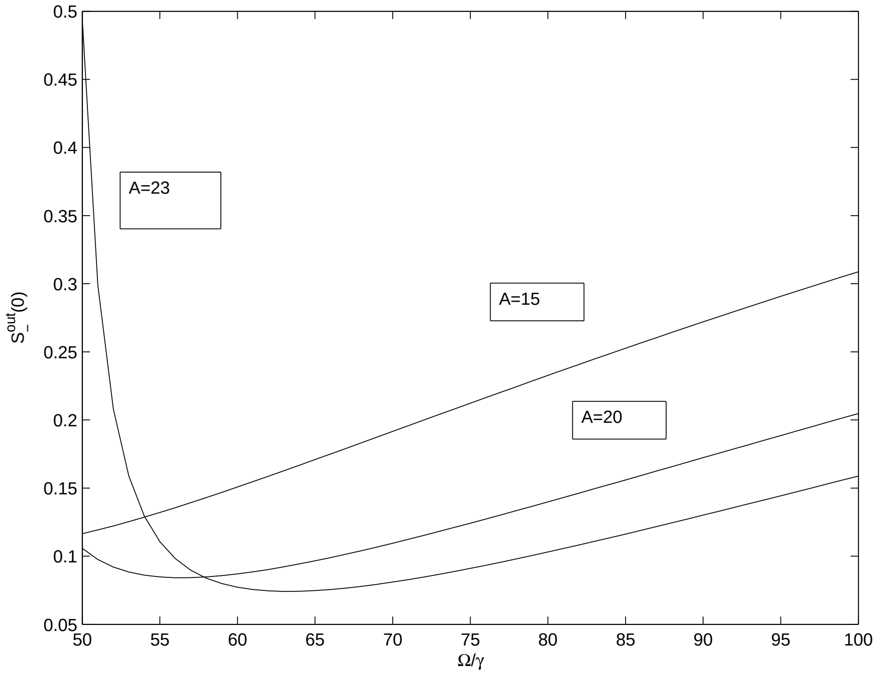

Fig. 4.32: Plots of the squeezing spectrum $S_{-}^{out}(0)$ (Eq. (4.199)) of the two-mode output radiation at steady state for $\omega = 0$, $\eta = 1$, $\kappa = 0.5$, $r = 0$, and different values of A.

As clearly shown in Fig. 4.32, the squeezing spectrum decreases with the linear gain coefficient for relatively larger values of Ω/γ, but increases for smaller values. It is found that a maximum squeezing occurs for $A = 23$ and $\Omega = 62.5\gamma$. On the other hand, comparison of Figs. 4.28 and 4.32 reveals that the degree of squeezing of the output radiation is substantially increased for $\eta = 1$, if the top and bottom levels of the atoms are coupled externally by a strong external radiation.

We next plot the squeezing spectrum versus Ω/γ for different values of r. We take the linear gain coefficient to be $A = 23$.

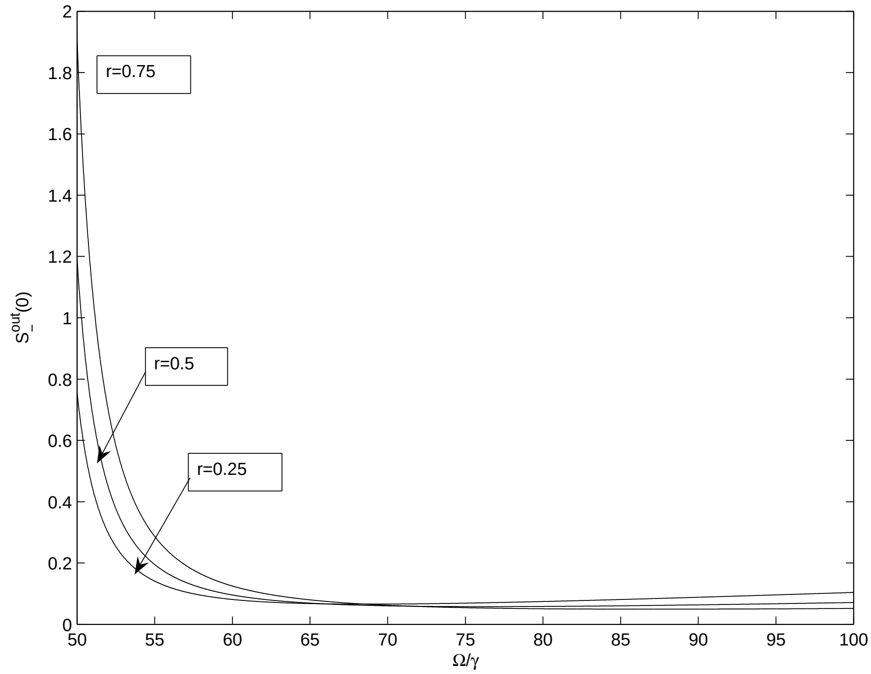

Fig. 4.33: Plots of the squeezing spectrum $S_{-}^{out}(0)$ (Eq. (4.199)) of the two-mode output radiation at steady state for $\omega = 0$, $\eta = 1$, $\kappa = 0.5$, $A = 23$, and different values of r.

It is possible to see from Fig. 4.33 that the squeezing spectrum decreases with the squeeze parameter for relatively larger values of Ω/γ, but increases for smaller values. It is found that a maximum squeezing occurs for $r = 0.75$ near $\Omega = 90\gamma$.

5

Photon Statistics

5.1 Mean number of photon pairs

We now seek to determine the mean number of photon pairs of a two-mode cavity radiation. To this end, we first write based on Eq. (4.1) that

$$\langle \hat{c}^\dagger(t)\hat{c}(t)\rangle = \frac{1}{2}\big[\langle \hat{a}^\dagger(t)\hat{a}(t)\rangle + \langle \hat{b}^\dagger(t)\hat{b}(t)\rangle + \langle \hat{a}^\dagger(t)\hat{b}(t)\rangle + \langle \hat{b}^\dagger(t)\hat{a}(t)\rangle\big]. \tag{5.1}$$

We notice that the operators in Eq. (5.1) are in the normal order. Hence it is possible to express Eq. (5.1) in terms of the c-number variables associated with the normal ordering as

$$\langle \hat{c}^\dagger(t)\hat{c}(t)\rangle = \frac{1}{2}\big[\langle \alpha^*(t)\alpha(t)\rangle + \langle \beta^*(t)\beta(t)\rangle + \langle \alpha^*(t)\beta(t)\rangle + \langle \beta^*(t)\alpha(t)\rangle\big], \tag{5.2}$$

which can be written in a more compact form as

$$\langle \hat{c}^\dagger(t)\hat{c}(t)\rangle = \langle \gamma^*(t)\gamma(t)\rangle. \tag{5.3}$$

It is not difficult to see using Eq. (4.45) that

$$\langle \hat{c}^\dagger(t)\hat{c}(t)\rangle = \frac{1}{2}\big[\langle \alpha^*(t)\alpha(t)\rangle + \langle \beta^*(t)\beta(t)\rangle\big]. \tag{5.4}$$

Therefore, $\langle \hat{c}^\dagger(t)\hat{c}(t)\rangle$ can be interpret as the mean number of photon pairs $\bar{n}$. On account of Eqs. (4.28) and (4.29), we find

$$\begin{aligned}\bar{n} =& \frac{\left(\frac{AC}{B}+\kappa N\right)\left(1-2p+p^2+q_-^2\right)+\kappa N\left(1+2p+p^2+q_+^2\right)}{16\lambda_1}\left[1-e^{-2\lambda_1 t}\right]\\ &-\frac{\left(\frac{AF}{B}-2\kappa M\right)\left(q_-+q_++p\left(q_--q_+\right)\right)}{16\lambda_1}\left[1-e^{-2\lambda_1 t}\right]\\ &+\frac{\left(\frac{AC}{B}+\kappa N\right)\left(1+2p+p^2+q_-^2\right)+\kappa N\left(1-2p+p^2+q_+^2\right)}{16\lambda_2}\left[1-e^{-2\lambda_2 t}\right]\\ &+\frac{\left(\frac{AF}{B}-2\kappa M\right)\left(q_-+q_+-p\left(q_--q_+\right)\right)}{16\lambda_2}\left[1-e^{-2\lambda_2 t}\right]\\ &+\frac{\left(\frac{AC}{B}+\kappa N\right)\left(1-p^2-q_-^2\right)+\kappa N\left(1-p^2-q_+^2\right)}{4(\lambda_1+\lambda_2)}\left[1-e^{-(\lambda_1+\lambda_2)t}\right]\\ &+\frac{\left(\frac{AF}{B}-2\kappa M\right)p\left(q_--q_+\right)}{4(\lambda_1+\lambda_2)}\left[1-e^{-(\lambda_1+\lambda_2)t}\right],\end{aligned} \tag{5.5}$$

which reduces at steady state to

$$\begin{aligned}\bar{n} =& \left(\frac{AC}{B}+2\kappa N\right)\frac{(\lambda_1+\lambda_2)^2+4\lambda_1\lambda_2}{16\lambda_1\lambda_2(\lambda_1+\lambda_2)}+\left[\frac{AC}{B}(p^2+q_-^2)\right.\\ &\left.+\kappa N(2p^2+q_-^2+q_+^2)+\left(\frac{AF}{B}-2\kappa M\right)p(q_+-q_-)\right]\frac{(\lambda_1+\lambda_2)^2-4\lambda_1\lambda_2}{16\lambda_1\lambda_2(\lambda_1+\lambda_2)}\\ &+\left[\frac{AC}{B}p+\left(\frac{AF}{2B}-\kappa M\right)(q_++q_-)\right]\frac{\lambda_1-\lambda_2}{8\lambda_1\lambda_2},\end{aligned} \tag{5.6}$$

in which

$$\begin{aligned}p^2+q_-^2 =& \frac{1}{\chi^2}\left[\left(1+\frac{\Omega^2}{\gamma^2}\right)^2\left(1+\frac{\Omega^2}{4\gamma^2}\right)-\frac{\Omega}{\gamma}\left(1+\frac{\Omega^2}{\gamma^2}\right)\left[\frac{3\eta\Omega}{2\gamma}-\sqrt{1-\eta^2}\left(1-\frac{\Omega^2}{2\gamma^2}\right)\right]\right.\\ &\left.+\left[\frac{3\eta\Omega}{2\gamma}-\sqrt{1-\eta^2}\left(1-\frac{\Omega^2}{2\gamma^2}\right)\right]^2\right],\end{aligned} \tag{5.7}$$

$$2p^2+q_-^2+q_+^2 = \frac{2}{\chi^2}\left[\left(1+\frac{\Omega^2}{\gamma^2}\right)^2\left(1+\frac{\Omega^2}{4\gamma^2}\right)+\left[\frac{3\eta\Omega}{2\gamma}-\sqrt{1-\eta^2}\left(1-\frac{\Omega^2}{2\gamma^2}\right)\right]^2\right], \tag{5.8}$$

$$p(q_+-q_-) = -\frac{2}{\chi^2}\left[\left(1+\frac{\Omega^2}{\gamma^2}\right)\left[\frac{3\eta\Omega}{2\gamma}-\sqrt{1-\eta^2}\left(1-\frac{\Omega^2}{2\gamma^2}\right)\right]\right]. \tag{5.9}$$

In the following, we seek to study the dependence of the mean number of photon pairs on the amplitude of the driving radiation, linear gain coefficient, initial preparation of the atoms, and squeeze parameter. To this end, we plot the mean number of photon pairs versus Ω/γ, A, and η by alternatively fixing one of them and taking $r = 0.75$ for convenience. We first consider the dependence of the mean number of photon pairs on the amplitude of the driving radiation and initial preparation of the atoms for $A = 1.3$. It is found using Eq. (4.51) that $\lambda_2 \geq 0$ for $0 \leq \eta \leq 1$ and $0 \leq \Omega \leq 10\gamma$ when $A \leq 1.3$ for which the mean number of photon pairs takes physically acceptable values ($\bar{n} \geq 0$) at steady state.

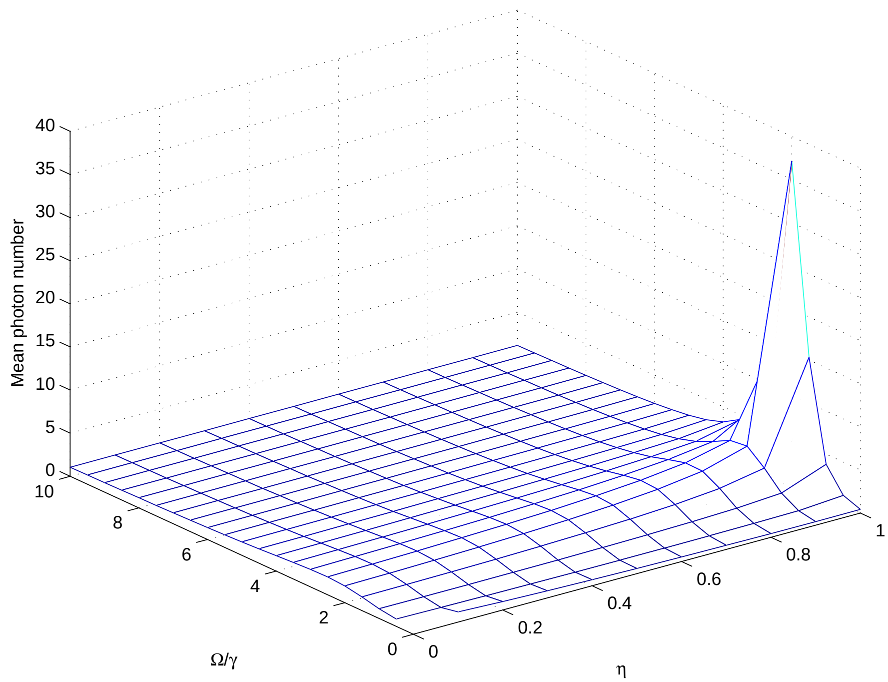

Fig. 5.1: Plot of the mean number of photon pairs of the cavity radiation (Eq. (5.6)) at steady state for $\kappa = 0.5$, $r = 0.75$, and $A = 1.3$.

We see from Fig. 5.1 that the mean number of photon pairs is larger for certain values of η and Ω/γ. It is found that the mean number of photon pairs takes its maximum value when $\eta = 1$ and $\Omega = 2\gamma$. From the results shown in Figs. 4.1 and 5.1, we observe that the mean number of photon pairs would be larger for values of Ω/γ and η for which there is no squeezing. Moreover, for $\eta = 0$, $A = 1.3$, $r = 0.75$, and $\Omega = 0.1\gamma$ the mean number of photon pairs is found to be $\bar{n} = 1.17$. We recall that the squeezing is maximum for these values of the involved parameters.

We next plot the mean number of photon pairs versus A and η. Here the amplitude of the driving radiation is fixed at the value for which the degree of squeezing is found to be maximum with the linear gain coefficient and initial preparation of the atoms.

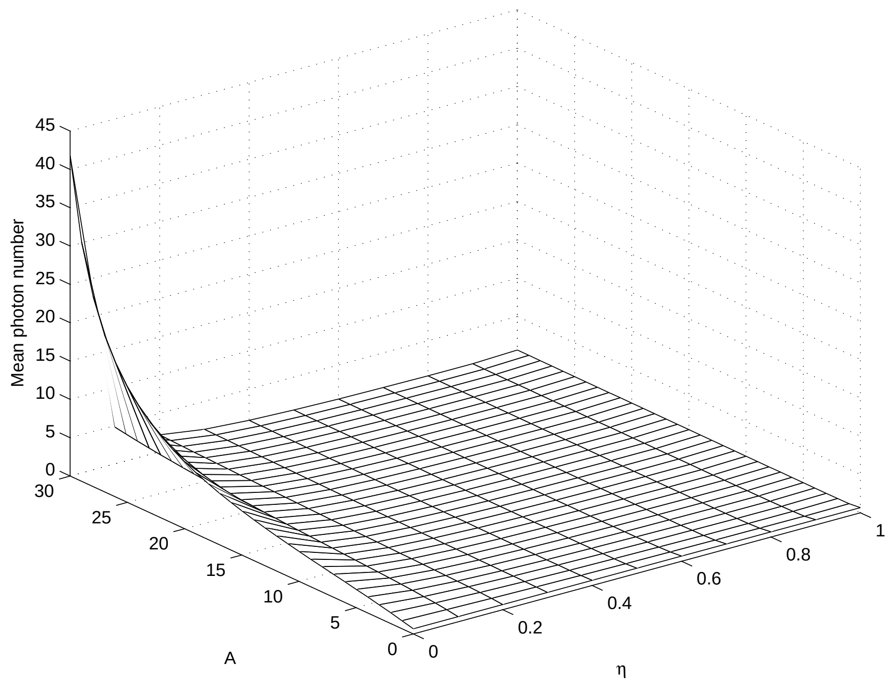

Fig. 5.2: Plot of the mean number of photon pairs of the cavity radiation (Eq. (5.6)) at steady state for $\kappa = 0.5$, $r = 0.75$, and $\Omega = 0.1\gamma$.

According to the result shown in Fig. 5.2, the mean number of photon pairs increases with the linear gain coefficient. Particularly, the mean number of photon pairs rapidly increases with the linear gain coefficient when the atoms are initially prepared in such a way that there are nearly half of them in the top level. The mean number of photon pairs turns out to be $\bar{n} = 3.67$ for $\eta = 0$, $r = 0.75$, $\Omega = 0.1\gamma$, and $A = 9.2$ at which the squeezing is maximum.

We now plot the mean number of photon pairs versus A and Ω/γ. The initial preparation of the atoms is represented by $\eta = 0.1$ so that comparison with the corresponding degree of squeezing of the cavity radiation can be made.

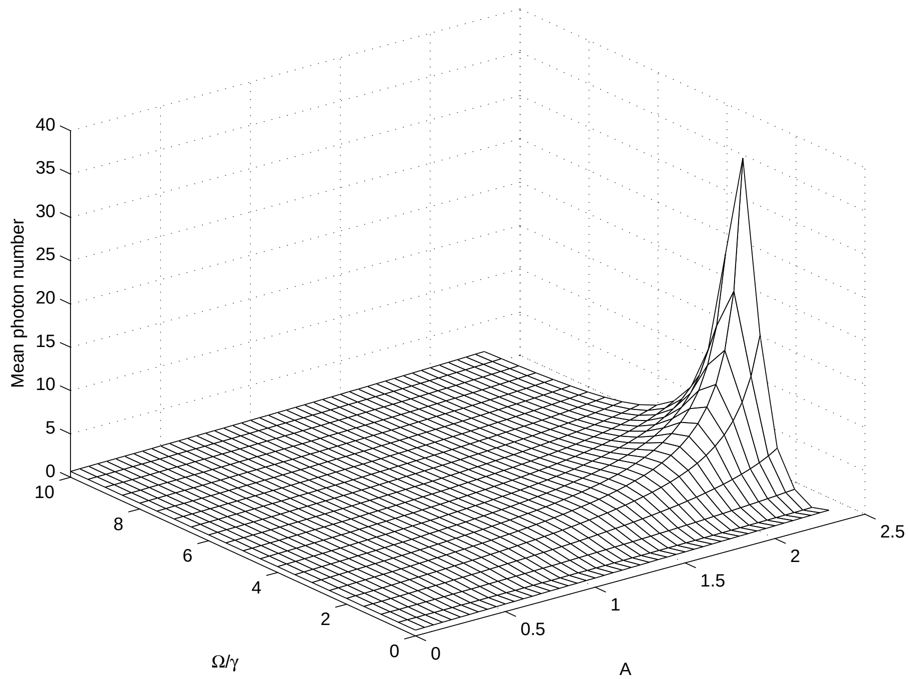

Fig. 5.3: Plot of the mean number of photon pairs of the cavity radiation (Eq. (5.6)) at steady state for $\kappa = 0.5$, $r = 0.75$, and $\eta = 0.1$.

It is found that the mean number of photon pairs attains a maximum value of $\bar{n} = 34.9$ for $\Omega = 2.5\gamma$ and $A = 2.3$. We see from Figs. 4.3 and 5.3 that the mean number of photon pairs is maximum for values of Ω/γ and A for which there is no squeezing. Moreover, a mean number of photon pairs of $\bar{n} = 1.15$ is obtained at $\Omega = 0.1\gamma$ and $A = 2.3$ where the squeezing is maximum. As can readily be inferred from Figs. 5.1, 5.2, and 5.3, the mean number of photon pairs of the cavity radiation strongly depends on the linear gain coefficient, amplitude of the driving radiation, and initial preparation of the atoms. Therefore, we next seek to consider various specific cases to analyze the dependence of the mean number of photon pairs of the two-mode cavity radiation on Ω/γ, A, η, and r in detail. To this effect, we first plot the mean number of photon pairs versus A for different values of r, $\Omega = 0.1\gamma$, and $\eta = 0.1$.

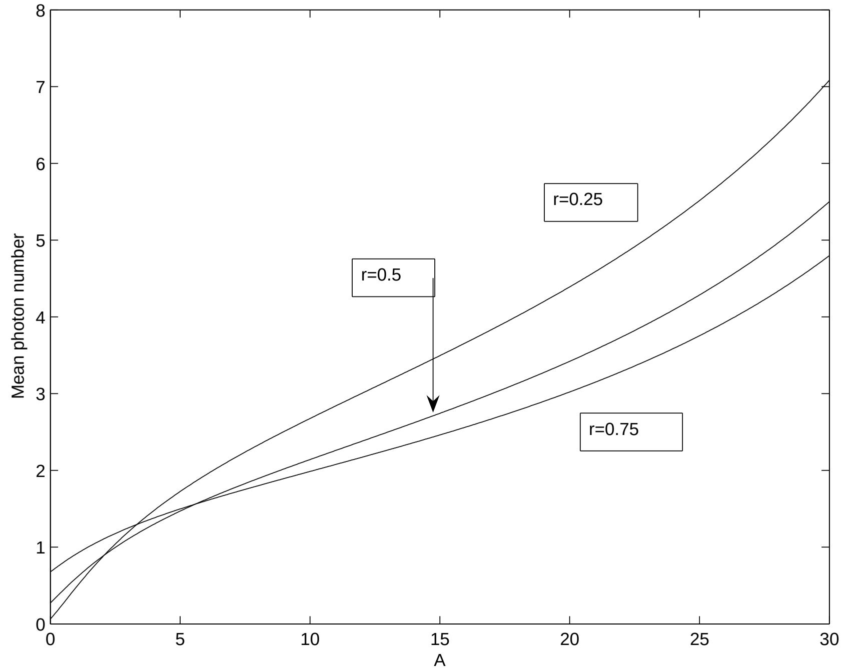

Fig. 5.4: Plots of the mean number of photon pairs of the cavity radiation (Eq. (5.6)) at steady state for $\eta = 0.1$, $\kappa = 0.5$, $\Omega = 0.1\gamma$, and different values of r.

As clearly shown in Fig. 5.4 the mean number of photon pairs increases with the squeeze parameter for smaller values of the linear gain coefficient, but decreases for larger values. One can also see that the mean number of photon pairs increases with the linear gain coefficient. We notice that the mean number of photon pairs for $A = 0$ is entirely associated with the two-mode squeezed radiation entering the cavity.

We next plot the mean number of photon pairs versus η for different values of r. We take $A = 14$ and $\Omega = 0.1\gamma$.

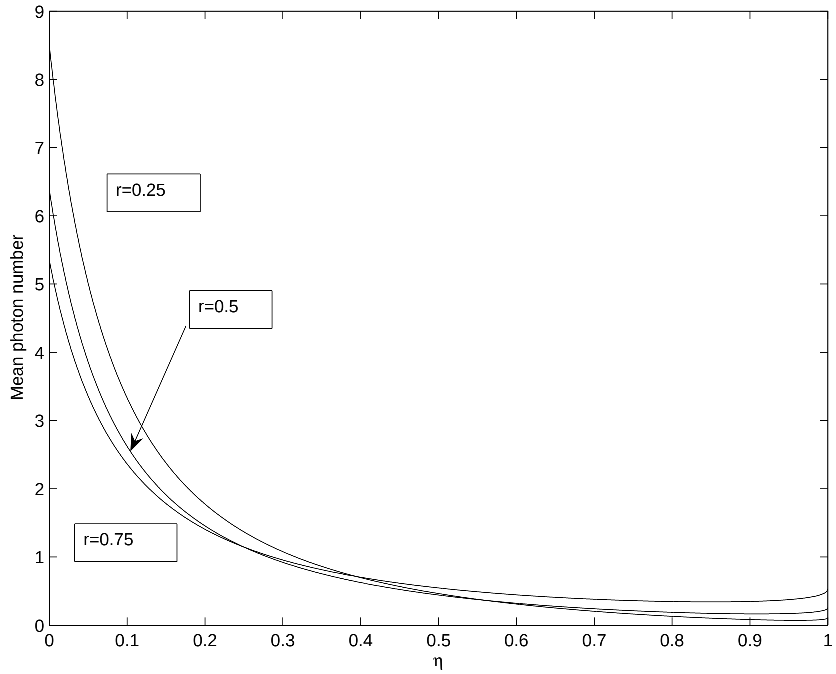

Fig. 5.5: Plots of the mean number of photon pairs of the cavity radiation (Eq. (5.6)) at steady state for $A = 14$, $\kappa = 0.5$, $\Omega = 0.1\gamma$, and different values of r.

We see from Fig. 5.5 that the mean number of photon pairs decreases with the squeeze parameter for smaller values of η, but increases for larger values. We also notice that the mean number of photon pairs is larger for values of η at which the squeezing is found to be relatively higher. However, the mean number of photon pairs near $\eta = 0$ decreases with the squeeze parameter contrary to the degree of squeezing which increases with the squeeze parameter in this case. We obtain $\bar{n} = 5.3$ for $A = 14$, $\Omega = 0.1\gamma$, $\eta = 0$, and $r = 0.75$ at which the squeezing is found to be maximum.

We now plot the mean number of photon pairs versus Ω/γ for different values of A. Here we take $\eta = 0.1$ so that comparison with the previous results can be made when required.

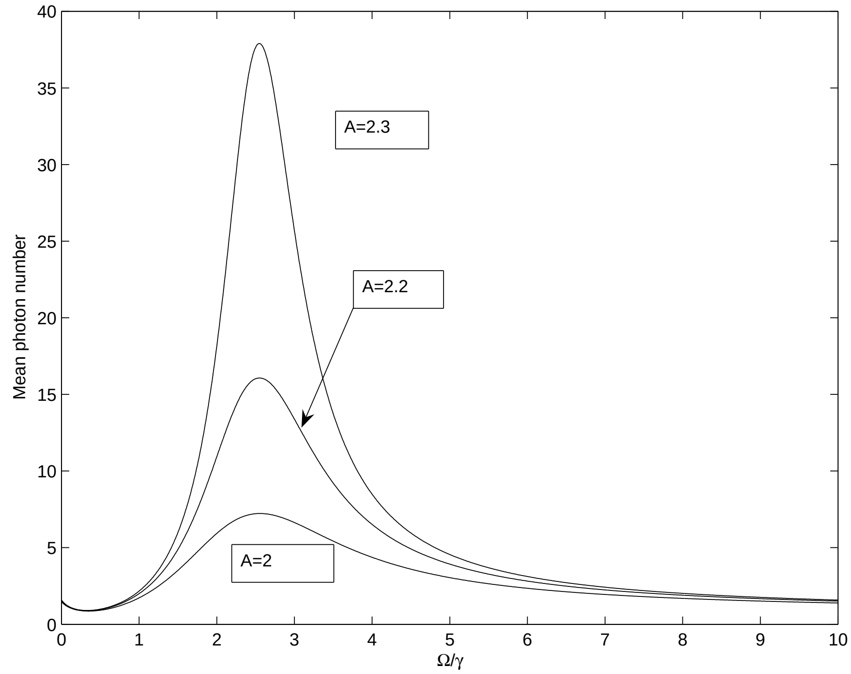

Fig. 5.6: Plots of the mean number of photon pairs of the cavity radiation (Eq. (5.6)) at steady state for $\eta = 0.1$, $\kappa = 0.5$, $r = 0.75$, and different values of A.

As clearly indicated in Fig. 5.6, the mean number of photon pairs increases with the linear gain coefficient. It is also possible to infer from Figs. 4.6 and 5.6 that the mean number of photon pairs is larger for values of Ω/γ for which there is no squeezing. Moreover, the mean number of photon pairs is found to be $\bar{n} = 1.24$ for $A = 2.3$, $\eta = 0.1$, $r = 0.75$, and $\Omega = 0.07\gamma$ at which the squeezing is maximum.

We next plot the mean number of photon pairs versus Ω/γ for different values of r. $A = 2.3$ and $\eta = 0.1$ are also taken so that a relation with the corresponding squeezing can be made.

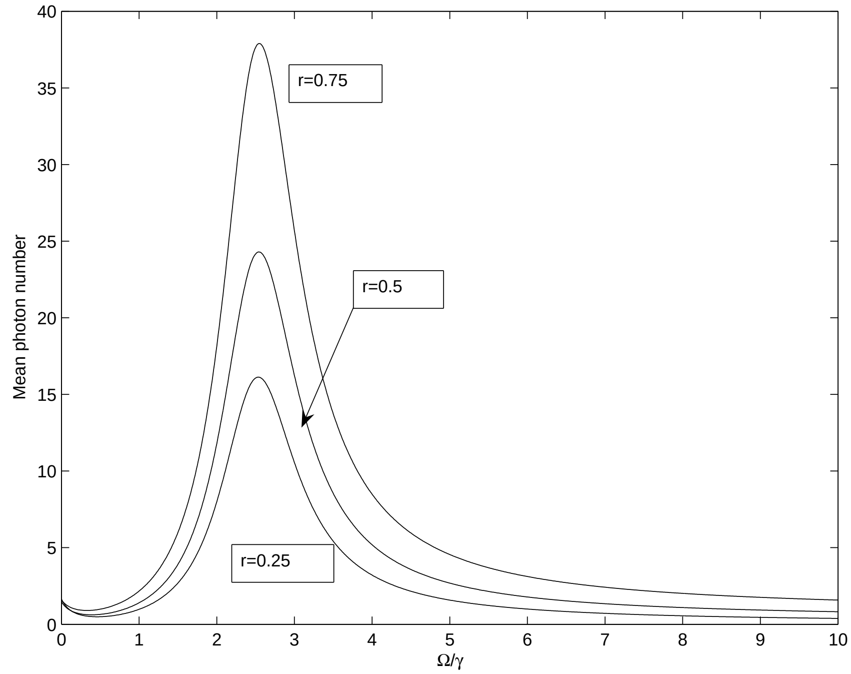

Fig. 5.7: Plots of the mean number of photon pairs of the cavity radiation (Eq. (5.6)) at steady state for $A = 2.3$, $\kappa = 0.5$, $\eta = 0.1$, and different values of r.

According to the result given in Fig. 5.7, the mean number of photon pairs turns out to increase with the squeeze parameter. Although the mean number of photon pairs is smaller for values of Ω/γ for which there is squeezing (See the results shown in Figs. 4.7 and 5.7), it is found to be larger for values of the squeeze parameter for which the squeezing is higher. It is possible to deduce from what we have discussed so far that the system under consideration can generate a relatively strong radiation. We also realize that the mean number of photon pairs can be optimized by properly choosing the values of the linear gain coefficient, initial preparation of the atoms, amplitude of the driving radiation, and squeeze parameter. In order to study the dependence of the mean number of photon pairs on these parameters more closely, we seek to consider special cases of interest.

5.1.1 When half of the atoms are initially in the top level

When half of the atoms are initially in the top level ($\eta = 0$), Eq. (5.6) takes the form

$$\bar{n} = \left(\frac{AC'}{B} + 2\kappa N\right)\frac{(\lambda_1' + \lambda_2')^2 + 4\lambda_1'\lambda_2'}{16\lambda_1'\lambda_2'(\lambda_1' + \lambda_2')} + \left[\frac{AC'}{B}(p'^2 + q_-'^2) + \kappa N(2p'^2 + q_-'^2 + q_+'^2) + \left(\frac{AF'}{B} - 2\kappa M\right)p'(q_+' - q_-')\right]\frac{(\lambda_1' + \lambda_2')^2 - 4\lambda_1'\lambda_2'}{16\lambda_1'\lambda_2'(\lambda_1' + \lambda_2')} + \left[\frac{AC'}{B}p' + \left(\frac{AF'}{2B} - \kappa M\right)(q_+' + q_-')\right]\frac{\lambda_1' - \lambda_2'}{8\lambda_1'\lambda_2'}, \tag{5.10}$$

with

$$p'^2 + q_-'^2 = \frac{1}{\chi'^2}\left[\left(1 + \frac{\Omega^2}{\gamma^2}\right)^2\left(1 + \frac{\Omega^2}{4\gamma^2}\right) + \frac{\Omega}{\gamma}\left(1 + \frac{\Omega^2}{\gamma^2}\right)\left(1 - \frac{\Omega^2}{2\gamma^2}\right) + \left(1 - \frac{\Omega^2}{2\gamma^2}\right)^2\right], \tag{5.11}$$

$$2p'^2 + q_-'^2 + q_+'^2 = \frac{2}{\chi'^2}\left[\left(1 + \frac{\Omega^2}{\gamma^2}\right)^2\left(1 + \frac{\Omega^2}{4\gamma^2}\right) + \left(1 - \frac{\Omega^2}{2\gamma^2}\right)^2\right], \tag{5.12}$$

$$p'(q_+' - q_-') = \frac{2}{\chi'^2}\left[\left(1 + \frac{\Omega^2}{\gamma^2}\right)\left(1 - \frac{\Omega^2}{2\gamma^2}\right)\right]. \tag{5.13}$$

$$p' = \frac{1}{\chi'}\left(1 + \frac{\Omega^2}{\gamma^2}\right). \tag{5.14}$$

In the following, we seek to investigate the dependence of the mean number of photon pairs on the amplitude of the driving radiation, linear gain coefficient, and squeeze parameter in detail when half of the atoms are initially prepared to be in the top level. To this end, we first plot the mean number of photon pairs versus Ω/γ for different values of A and $r = 0$. It is found using Eq. (4.63) that the mean number of photon pairs takes physically admissible values for $\eta = 0$ and $0 \leq \Omega \leq 50\gamma$ when $A \leq 2.35$.

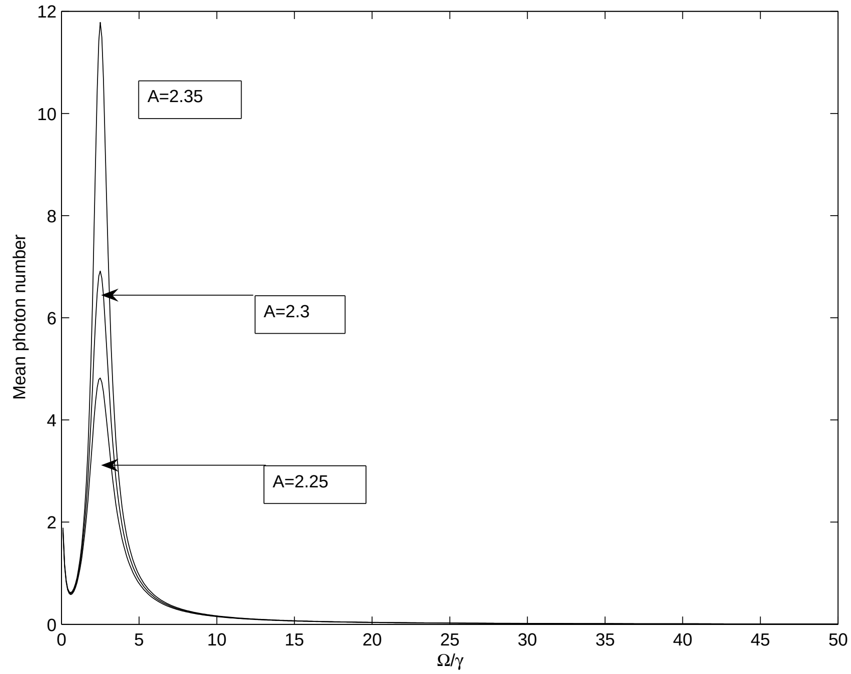

Fig. 5.8: Plots of the mean number of photon pairs of the cavity radiation (Eq. (5.10)) at steady state for $\eta = 0$, $\kappa = 0.5$, $r = 0$, and different values A.

As shown in Fig. 5.8, the mean number of photon pairs increases with the linear gain coefficient. We also see with the aid of Fig. 4.1 that the mean number of photon pairs would be larger for values of Ω/γ for which there is no squeezing. We notice that the mean number of photon pairs is quite small for larger values of Ω/γ regardless of the values of A. The mean number of photon pairs is found to be $\bar{n} = 21.4$ for $\eta = 0$, $A = 30$, $r = 0.75$, and $\Omega = 0.03\gamma$ at which the squeezing is maximum.

We next plot the mean number of photon pairs versus the squeeze parameter and Ω/γ. The value of the linear gain coefficient is arbitrarily taken to be $A = 2.25$ so that the dependence of the mean number of photon pairs on parameters under consideration is directly evident from the figure.

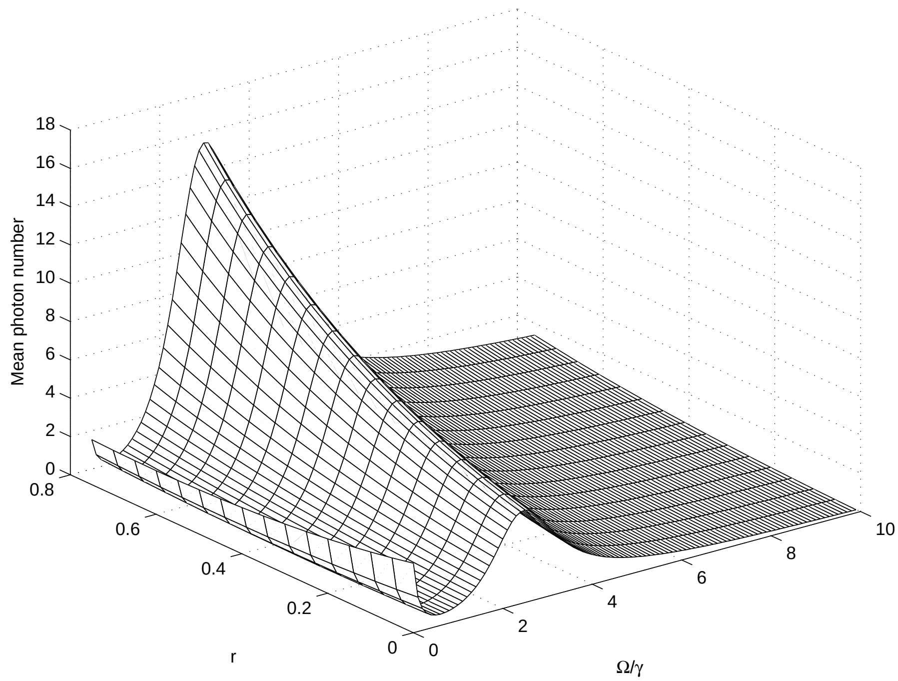

Fig. 5.9: Plot of the mean number of photon pairs of the cavity radiation (Eq. (5.10)) at steady state for $\eta = 0$, $\kappa = 0.5$, and $A = 2.25$.

It is not difficult to see from Fig. 5.9 that the mean number of photon pairs of the cavity radiation decreases with the squeeze parameter for certain values of Ω/γ. We also notice that the mean number of photon pairs decreases with the amplitude of the driving radiation for smaller and larger values of Ω/γ, but increases for other values.

5.1.2 When all the atoms are initially in the bottom level

When all the atoms are initially in the bottom level ($\eta = 1$), it is possible to put Eq. (5.6) in the form

$$\bar{n} = \left(\frac{AC''}{B} + 2\kappa N\right)\frac{(\lambda_1'' + \lambda_2'')^2 + 4\lambda_1''\lambda_2''}{16\lambda_1''\lambda_2''(\lambda_1'' + \lambda_2'')} + \left[\frac{AC''}{B}(p''^2 + q_-''^2)\right.$$
$$\left. + \kappa N(2p''^2 + q_-''^2 + q_+''^2) + \left(\frac{AF''}{B} - 2\kappa M\right)p''(q_+'' - q_-'')\right]\frac{(\lambda_1'' + \lambda_2'')^2 - 4\lambda_1''\lambda_2''}{16\lambda_1''\lambda_2''(\lambda_1'' + \lambda_2'')}$$
$$+ \left[\frac{AC''}{B}p'' + \left(\frac{AF''}{2B} - \kappa M\right)(q_+'' + q_-'')\right]\frac{\lambda_1'' - \lambda_2''}{8\lambda_1''\lambda_2''}, \tag{5.15}$$

where

$$p''^2 + q''^2_- = \frac{1}{\chi''^2}\left[\left(1+\frac{\Omega^2}{\gamma^2}\right)^2\left(1+\frac{\Omega^2}{4\gamma^2}\right)+\frac{3\Omega^2}{4\gamma^2}\left(1-\frac{2\Omega^2}{\gamma^2}\right)\right], \tag{5.16}$$

$$2p''^2 + q''^2_- + q''^2_+ = \frac{2}{\chi''^2}\left[\left(1+\frac{\Omega^2}{\gamma^2}\right)^2\left(1+\frac{\Omega^2}{4\gamma^2}\right)+\frac{9\Omega^2}{4\gamma^2}\right], \tag{5.17}$$

$$p''(q''_+ - q''_-) = -\frac{3\Omega}{\gamma\chi''^2}\left(1+\frac{\Omega^2}{\gamma^2}\right). \tag{5.18}$$

$$p'' = \frac{1}{\chi''}\left(1+\frac{\Omega^2}{\gamma^2}\right). \tag{5.19}$$

We now seek to evaluate the dependence of the mean number of photon pairs on the amplitude of the driving radiation, linear gain coefficient, and squeeze parameter in detail when all the atoms are initially prepared to be in the bottom level. We first plot the mean number of photon pairs versus Ω/γ for different values of A and $r = 0$. The values of the linear gain coefficient are arbitrarily fixed in such a way that the dependence of the mean number of photon pairs on parameters under consideration is clearly seen from the figure.

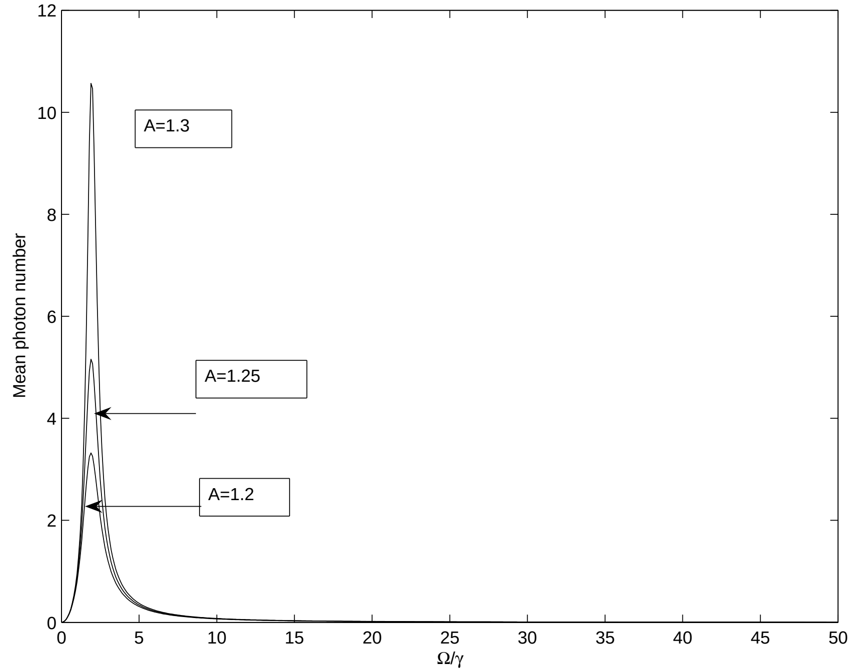

Fig. 5.10: Plots of the mean number of photon pairs of the cavity radiation (Eq. (5.15)) at steady state for $\eta = 1$, $\kappa = 0.5$, $r = 0$, and different values A.

It is possible to see from Fig. 5.10 that the mean number of photon pairs is very small for larger values of Ω/γ. We also notice that the mean number of photon pairs is zero when there is no external driving radiation and in the absence of the squeezed vacuum reservoir for all admissible values of A. In relation to the result shown in Fig. 4.1 we observe that although a strong radiation can be generated near $\Omega = 1.8\gamma$ for $\eta = 1$, the mean number of photon pairs for values of Ω/γ at which the squeezing exists is still small. The mean number of photon pairs is found to be $\bar{n} = 1.3$ for $\eta = 1$, $A = 5$, $\Omega = 31\gamma$, and $r = 0.75$ at which the squeezing is maximum.

Next the mean number of photon pairs versus Ω/γ and r is plotted when all the atoms are initially prepared to be in the bottom level. The linear gain coefficient is arbitrarily taken to be $A = 1.25$ so that the dependence of the mean number of photon pairs on parameters under consideration can easily be seen from the figure.

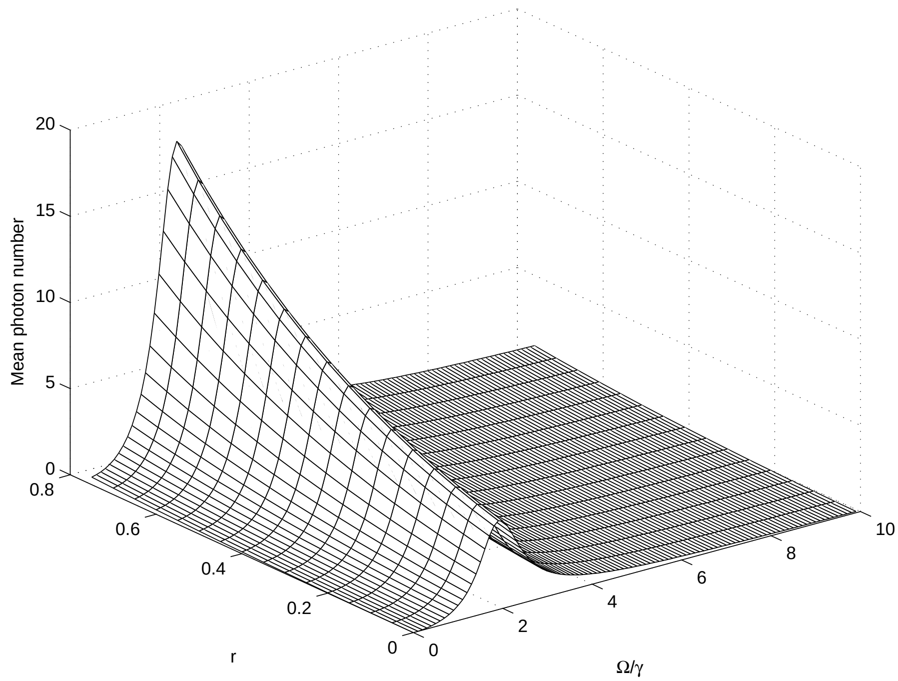

Fig. 5.11: Plot of the mean number of photon pairs of the cavity radiation (Eq. (5.15)) at steady state for $\eta = 1$, $\kappa = 0.5$, and $A = 1.25$.

As indicated in Fig. 5.11 the mean number of photon pairs increases with the squeeze parameter and amplitude of the driving radiation for smaller values of Ω/γ, contrary to what we have obtained for $\eta = 0$ case. Moreover, one can easily see from Fig. 5.11 that the mean number of photon pairs increases with the squeeze parameter for all values of Ω/γ.

5.1.3 In the absence of the external driving radiation

Now we consider the case when the top and bottom levels of the atoms are not externally coupled. We note for $\Omega = 0$ that

$$p^2 + q_-^2 = \frac{2 - \eta^2}{\eta^2}, \tag{5.20}$$

$$2p^2 + q_-^2 + q_+^2 = \frac{2(2 - \eta^2)}{\eta^2}, \tag{5.21}$$

$$p(q_+ - q_-) = \frac{2\sqrt{1-\eta^2}}{\eta^2}, \tag{5.22}$$

$$p = \frac{1}{\eta}. \tag{5.23}$$

Thus on account of Eqs. (4.83), (4.84), (4.85), (4.93), (4.94), (4.95), (4.96), (5.6), (5.20), (5.21), (5.22), and (5.23), we reach at

$$\bar{n} = A(1-\eta)\frac{4\kappa(\kappa+A\eta)+A^2+A(2\kappa+A\eta)}{8\kappa(2\kappa+A\eta)(\kappa+A\eta)} + \kappa N\frac{4\kappa(\kappa+A\eta)+A^2}{2\kappa(2\kappa+A\eta)(\kappa+A\eta)} - \frac{\left(A\sqrt{1-\eta^2}+4\kappa M\right)A^2\sqrt{1-\eta^2}}{8\kappa(2\kappa+A\eta)(\kappa+A\eta)}. \tag{5.24}$$

In order to study the dependence of the mean number of photon pairs on the linear gain coefficient, squeeze parameter, and initial preparation of the atoms more closely, we first plot the mean number of photon pairs versus η for different values of A. The values of A are arbitrarily chosen.

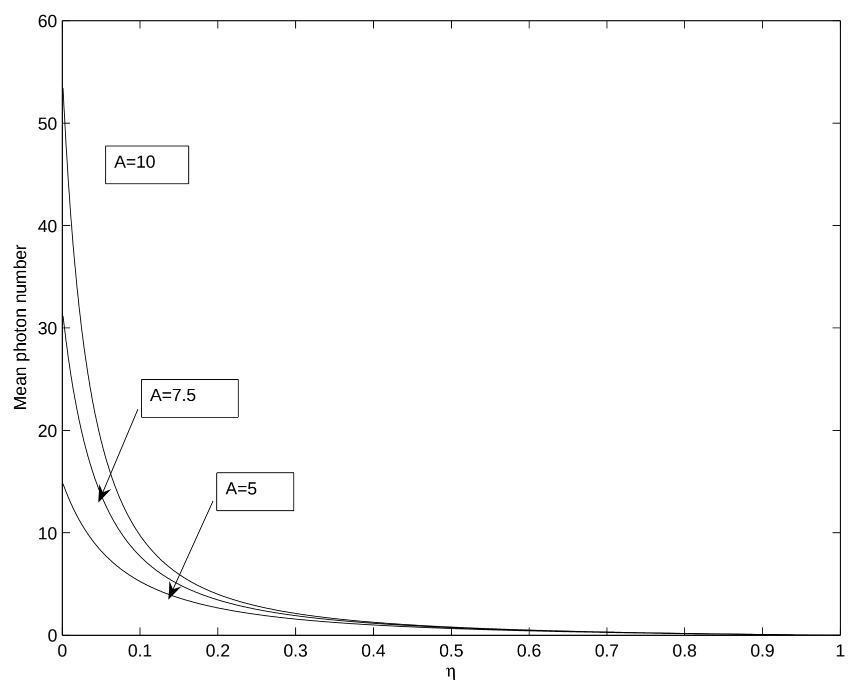

Fig. 5.12: Plots of the mean number of photon pairs of the cavity radiation (Eq. (5.24)) at steady state for $\Omega = 0$, $\kappa = 0.5$, $r = 0$, and different values A.

When $\Omega = 0$ a strong radiation can be generated in principle for $\eta = 0$, since the mean number of photon pairs increases with the linear gain coefficient as clearly shown in Fig. 5.12 and there is no limit on the values of the linear gain coefficient in this case. For instance, the mean number of photon pairs is found to be $\bar{n} = 101.5$ when $A = 1000$, $\eta = 0.05$, $\Omega = 0$, and $r = 0$ at which the squeezing is maximum. We also see from Fig. 5.12 that the mean number of photon pairs is zero when $\eta = 1$ for all values of A when $r = 0$.

We next plot the mean number of photon pairs versus the squeeze parameter and η. The linear gain coefficient is arbitrarily taken to be $A = 3.5$.

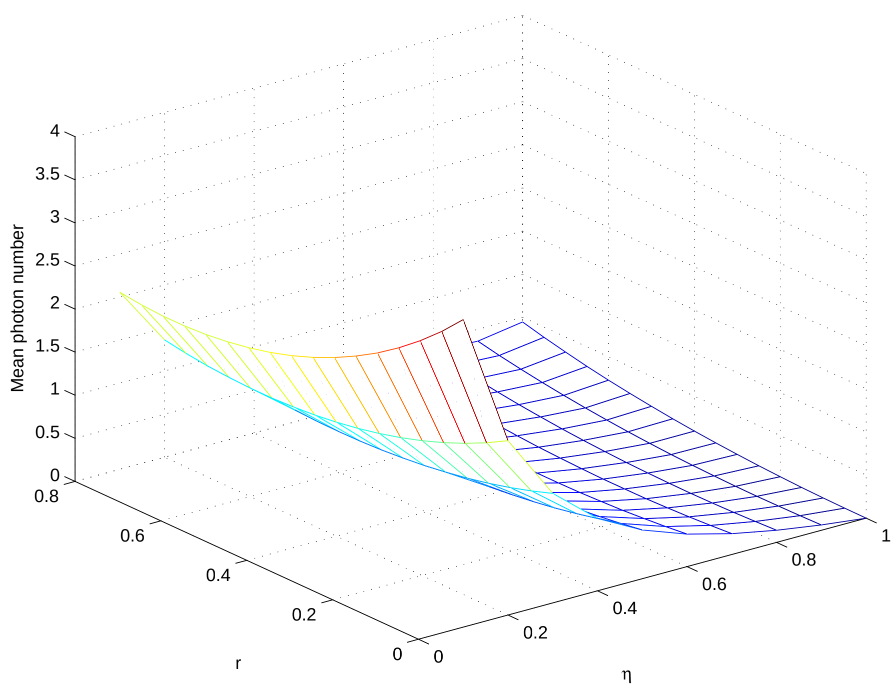

Fig. 5.13: Plot of the mean number of photon pairs of the cavity radiation (Eq. (5.24)) at steady state for $\Omega = 0$, $\kappa = 0.5$, and $A = 3.5$.

One can see from Fig. 5.13 that the mean number of photon pairs decreases with the squeeze parameter for certain values of the squeeze parameter and η. We also found that a similar situation exists except for very small values of the linear gain coefficient, where the mean number of photon pairs increases with r for all values of η. The mean number of photon pairs is found to be $\bar{n} = 141.6$ for $r = 0.75$, $\eta = 0.02$, $\Omega = 0$, and $A = 1000$ where the degree of squeezing is maximum.

5.1.4 For a weak driving radiation

In the weak driving limit ($\Omega \ll \gamma$), we note that

$$\begin{aligned}\bar{n} = &\left(\frac{AC'''}{B} + 2\kappa N\right)\frac{(\lambda_1''' + \lambda_2''')^2 + 4\lambda_1'''\lambda_2'''}{16\lambda_1'''\lambda_2'''(\lambda_1''' + \lambda_2''')} + \left[\frac{AC'''}{B}(p'''^2 + q_-'''^2)\right. \\ &\left. + \kappa N(2p'''^2 + q_-'''^2 + q_+'''^2) + \left(\frac{AF'''}{B} - 2\kappa M\right)p'''(q_+''' - q_-''')\right]\frac{(\lambda_1''' + \lambda_2''')^2 - 4\lambda_1'''\lambda_2'''}{16\lambda_1'''\lambda_2'''(\lambda_1''' + \lambda_2''')} \\ &+ \left[\frac{AC'''}{B}p''' + \left(\frac{AF'''}{2B} - \kappa M\right)(q_+''' + q_-''')\right]\frac{\lambda_1''' - \lambda_2'''}{8\lambda_1'''\lambda_2'''}, \end{aligned} \tag{5.25}$$

where

$$p'''^2 + q_-'''^2 = \frac{2 - \eta^2 - \frac{\Omega}{\gamma}\sqrt{1-\eta^2}(3\eta - 1)}{\eta^2 + \frac{3\eta\Omega}{\gamma}\sqrt{1-\eta^2}}, \tag{5.26}$$

$$2p'''^2 + q_-'''^2 + q_+'''^2 = \frac{2\left[2 - \eta^2 - \frac{3\eta\Omega}{\gamma}\sqrt{1-\eta^2}\right]}{\eta^2 + \frac{3\eta\Omega}{\gamma}\sqrt{1-\eta^2}}, \tag{5.27}$$

$$p'''(q_+''' - q_-''') = -\frac{2\left(\frac{3\eta\Omega}{2\gamma} - \sqrt{1-\eta^2}\right)}{\eta^2 + \frac{3\eta\Omega}{\gamma}\sqrt{1-\eta^2}}, \tag{5.28}$$

$$p''' = \frac{1}{\left[\eta^2 + \frac{3\eta\Omega}{\gamma}\sqrt{1-\eta^2}\right]^{\frac{1}{2}}}. \tag{5.29}$$

We now seek to analyze the dependence of the mean number of photon pairs on the amplitude of the driving radiation, initial preparation of the atoms, linear gain coefficient, and squeeze parameter in the weak driving limit more closely. To this end, we first plot the mean number of photon pairs versus Ω/γ and η. The linear gain coefficient and squeeze parameter are taken to be $A = 32$ and $r = 0.75$ so that comparison with the squeezing of the cavity can be made.

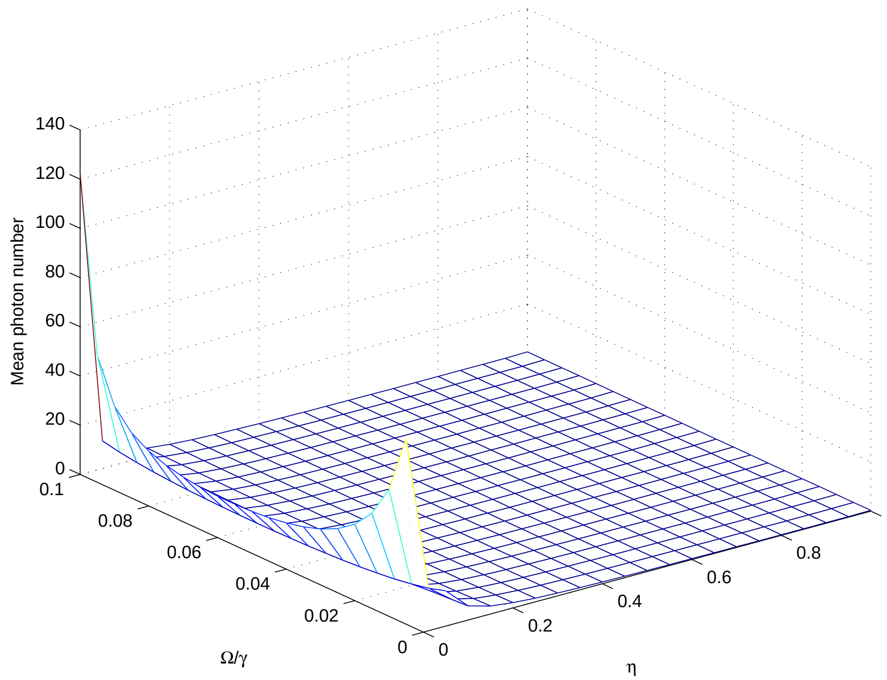

Fig. 5.14: Plot of the mean number of photon pairs of the cavity radiation (Eq. (5.25)) at steady state for $\Omega \ll \gamma$, $\kappa = 0.5$, $r = 0.75$, and $A = 32$.

As clearly indicated in Fig. 5.14, the mean number of photon pairs significantly depends on the amplitude of the driving radiation for very small values of η. The mean number of photon pairs is found to be $\bar{n} = 2.2$ for $A = 32$, $\eta = 0.06$ and $\Omega = 0.02\gamma$ at which the squeezing is maximum.

We next plot the mean number of photon pairs versus A and Ω/γ. We fix the initial preparation of the atoms to the value at which the squeezing is maximum for the same choice of other parameters ($\eta = 0.06$).

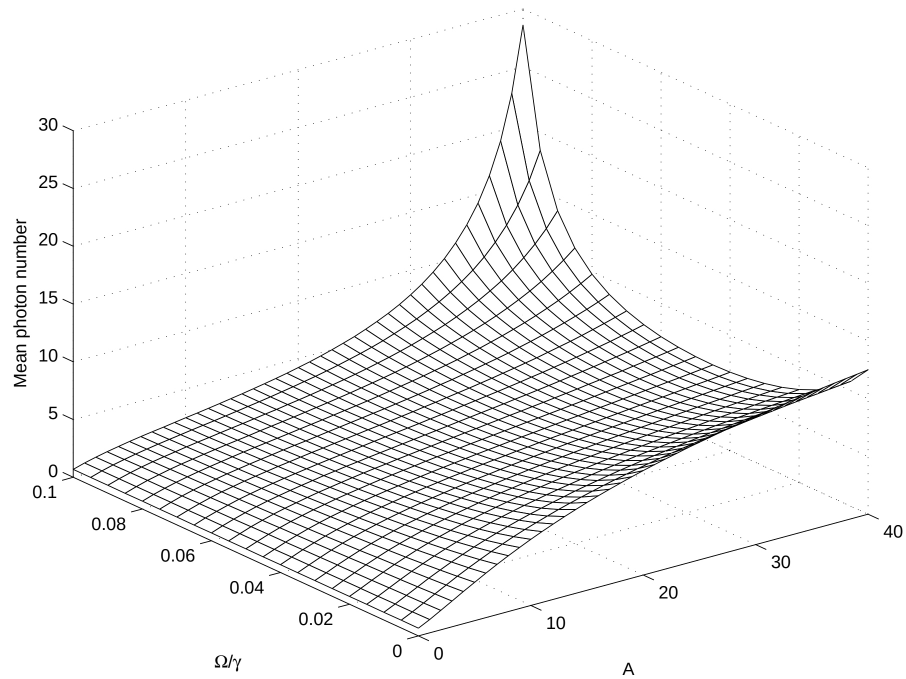

Fig. 5.15: Plot of the mean number of photon pairs of the cavity radiation (Eq. (5.25)) at steady state for $\Omega \ll \gamma$, $\kappa = 0.5$, $r = 0.75$, and $\eta = 0.06$.

It is not difficult to see from Fig. 5.15 that the mean number of photon pairs increases with the linear gain coefficient for smaller values of Ω/γ. Moreover, the mean number of photon pairs is found to be $\bar{n} = 8$ for $A = 40$, $\eta = 0.06$, $r = 0.075$, and $\Omega = 0.02\gamma$ at which the squeezing is maximum.

We next plot the mean number of photon pairs versus Ω/γ for different values of r. We take $A = 40$ and $\eta = 0.06$, the values for which the squeezing is maximum.

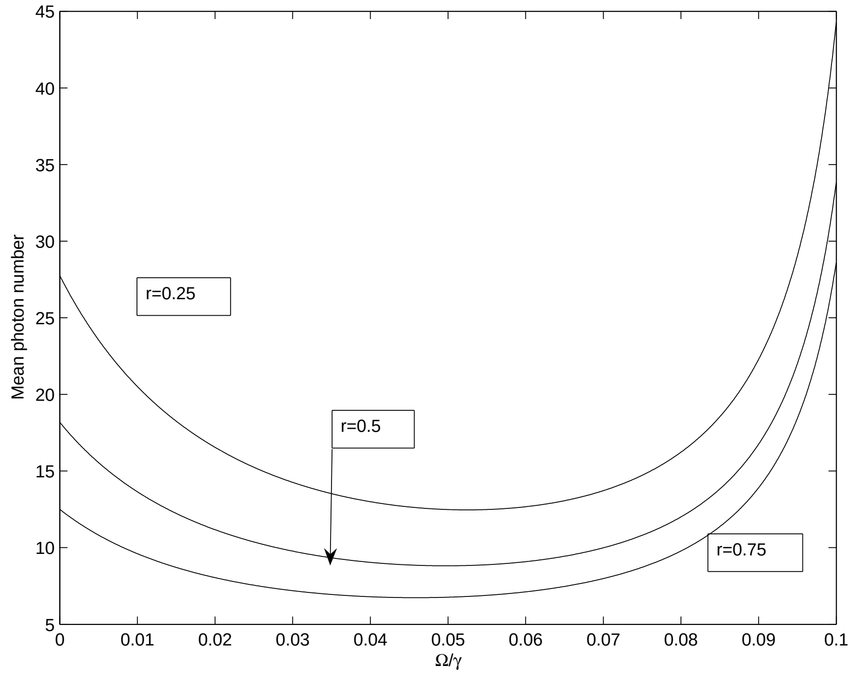

Fig. 5.16: Plots of the mean number of photon pairs of the cavity radiation (Eq. (5.25)) at steady state for $\Omega \ll \gamma$, $\kappa = 0.5$, $\eta = 0.06$, $A = 40$, and different values of r.

According to the result given in Fig. 5.16, the mean number of photon pairs decreases with the squeeze parameter for smaller values of Ω/γ. As can be inferred from Fig. 5.9 similar effect of the squeezed vacuum reservoir is observed for $\eta = 0$.

5.1.5 For a strong driving radiation

On the other hand, when the driving radiation is taken to be very large ($\Omega \gg \gamma$), we see that

$$p^2 + q_-^2 = 1, \tag{5.30}$$

$$2p^2 + q_-^2 + q_+^2 = 2, \tag{5.31}$$

$$p(q_+ - q_-) = -\frac{4\gamma^2}{\Omega^2}\sqrt{1-\eta^2}, \tag{5.32}$$

$$p = \frac{2\gamma}{\Omega}. \tag{5.33}$$

Hence making use of Eqs. (4.110), (4.111), (4.112), (4.120), (4.121),(4.122), (4.123), (5.6), (5.30), (5.31), (5.32), and (5.33), we find

$$\begin{aligned}\bar{n} = & \left(\frac{A\gamma^2}{\Omega^2}(2+\eta) + 2\kappa N\right)\frac{\Omega^2}{2(\kappa^2\Omega^2 - A^2\gamma^2)} \\ & + \left[\left(\frac{A\gamma}{\Omega} + 2\kappa M\right)\frac{\gamma^2}{\Omega^2}\sqrt{1-\eta^2}\right]\frac{A^2\gamma^2}{\kappa(\kappa^2\Omega^2 - A^2\gamma^2)} \\ & - \left[\frac{A\gamma^3}{\Omega^3}(2+\eta) + \left(\frac{A\gamma}{2\Omega} + \kappa M\right)\right]\frac{A\gamma\Omega}{(\kappa^2\Omega^2 - A^2\gamma^2)}.\end{aligned} \tag{5.34}$$

In order to study the dependence of the mean number of photon pairs on the amplitude of the driving radiation, initial preparation of the atoms, linear gain coefficient, and squeeze parameter more closely in the strong driving limit, we first plot the mean number of photon pairs versus Ω/γ and η. We fix the linear gain coefficient and squeeze parameter to $A = 48$ and $r = 0.75$ so that comparison with the corresponding squeezing can be made.

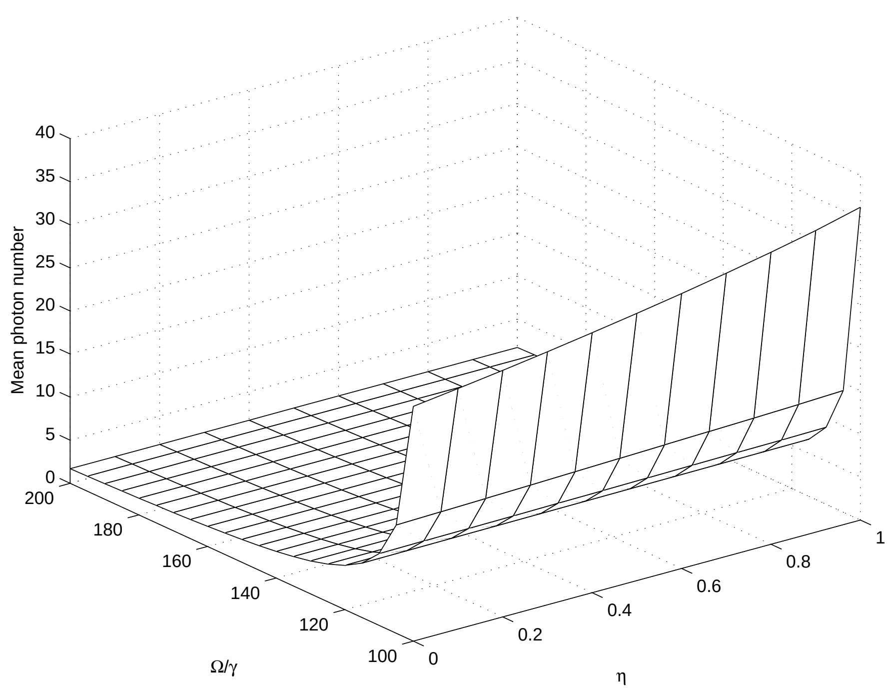

Fig. 5.17: Plot of the mean number of photon pairs of the cavity radiation (Eq. (5.34)) at steady state for $\Omega \gg \gamma$, $\kappa = 0.5$, $r = 0.75$, and $A = 48$.

As one can easily see from Fig. 5.17, the mean number of photon pairs decreases with the amplitude of the driving radiation in the same manner regardless of how the atoms are initially prepared. We also see that the mean number of photon pairs increases with η. Moreover, the mean number of photon pairs is found to be $\bar{n} = 10.4$ for $\eta = 1$, $A = 48$, $r = 0.75$, and $\Omega = 108\gamma$ at which the squeezing is maximum.

We next plot the mean number of photon pairs versus Ω/γ and A. Hence we take $\eta = 1$ so that comparison with the squeezing for the strong driving limit can be made.

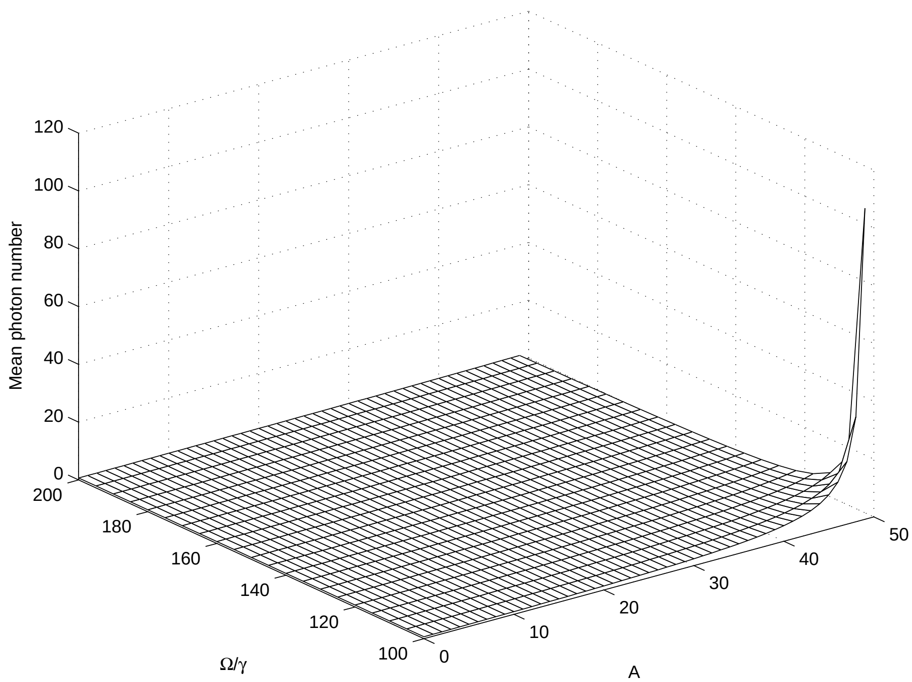

Fig. 5.18: Plot of the mean number of photon pairs of the cavity radiation (Eq. (5.34)) at steady state for $\Omega \gg \gamma$, $\kappa = 0.5$, $r = 0.75$, and $\eta = 1$.

We clearly see from Fig. 5.18 that a large mean number of photon pairs is obtained for some values of A and Ω/γ. In particular, the mean number of photon pairs is found to be $\bar{n} = 11.5$ for $A = 49.4$, $\eta = 1$, $r = 0.75$, and $\Omega = 110\gamma$ at which the squeezing is maximum.

We next plot the mean number of photon pairs versus Ω/γ for different values of r. A and η are taken to be 49.4 and 1 so that comparison with the squeezing can be made.

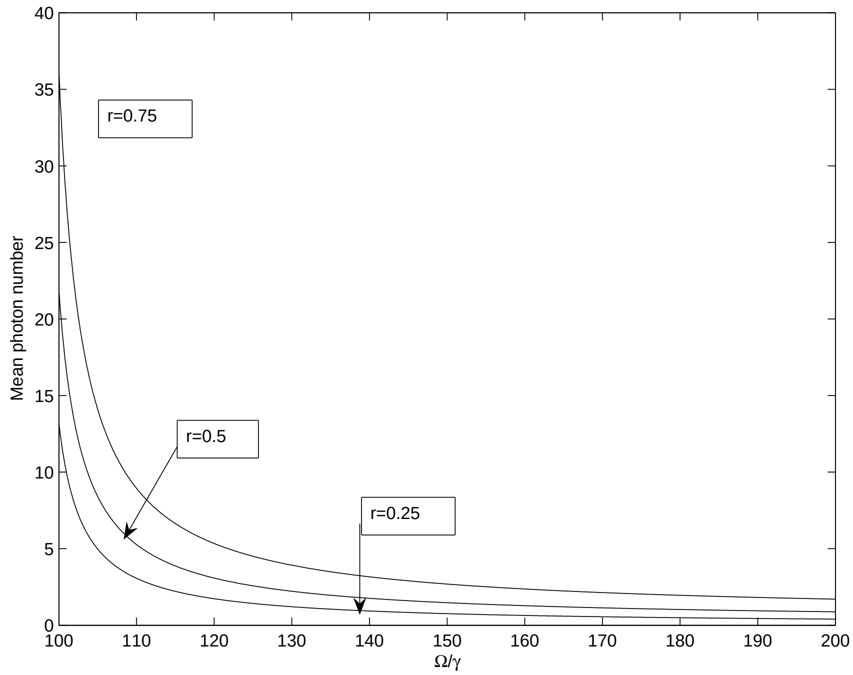

Fig. 5.19: Plots of the mean number of photon pairs of the cavity radiation (Eq. (5.34)) at steady state for $\Omega \gg \gamma$, $\kappa = 0.5$, $A = 49.4$, $\eta = 1$, and different values of A.

We see from Fig. 5.19 that the mean number of photon pairs increases with the squeeze parameter in the strong driving limit. As in previous cases, the mean number of photon pairs decreases with the amplitude of the driving radiation for a given value of A.

5.2 Variance of the number of photon pairs

The variance of the photon number is defined as

$$\Delta n^2 = \langle \hat{n}^2(t) \rangle - \langle \hat{n}(t) \rangle^2, \tag{5.35}$$

where

$$\hat{n} = \hat{c}^\dagger(t)\hat{c}(t). \tag{5.36}$$

Using the boson commutation relation (4.7), it is possible to rewrite Eq. (5.35) in the normal order as

$$\Delta n^2 = \langle \hat{c}^{\dagger^2}(t)\hat{c}^2(t)\rangle + \langle \hat{c}^\dagger(t)\hat{c}(t)\rangle - \langle \hat{c}^\dagger(t)\hat{c}(t)\rangle^2. \tag{5.37}$$

Therefore, we express Eq. (5.37) in terms of the c-number variables associated with the normal ordering as

$$\Delta n^2 = \langle \gamma^{*^2}(t)\gamma^2(t)\rangle + \langle \gamma^*(t)\gamma(t)\rangle - \langle \gamma^*(t)\gamma(t)\rangle^2. \tag{5.38}$$

We realize that $\gamma(t)$ is a Gaussian variable with zero mean, since $\alpha(t)$ and $\beta(t)$ are Gaussian variables with zero mean. As a result, we can write [34]

$$\langle \gamma^{*^2}(t)\gamma^2(t)\rangle = \langle \gamma^{*^2}(t)\rangle\langle \gamma^2(t)\rangle + 2\langle \gamma^*(t)\gamma(t)\rangle^2. \tag{5.39}$$

Hence substitution of (5.39) into Eq. (5.38) yields

$$\Delta n^2 = \langle \gamma^{*^2}(t)\rangle\langle \gamma^2(t)\rangle + \langle \gamma^*(t)\gamma(t)\rangle + \langle \gamma^*(t)\gamma(t)\rangle^2. \tag{5.40}$$

Next we proceed to calculate the correlations involved in Eq. (5.40). In view of Eq. (4.2), we see that

$$\langle \gamma^2(t)\rangle = \frac{1}{2}\left[\langle \alpha^2(t)\rangle + 2\langle \alpha(t)\beta(t)\rangle + \langle \beta^2(t)\rangle\right], \tag{5.41}$$

in which taking Eqs. (4.34) and (4.35) into consideration leads to

$$\langle \gamma^2(t)\rangle = \langle \alpha(t)\beta(t)\rangle. \tag{5.42}$$

On the basis of Eqs. (5.2), (5.40), and (5.42), we get

$$\Delta n^2 = \langle \alpha(t)\beta(t)\rangle^2 + \bar{n} + \bar{n}^2. \tag{5.43}$$

Since $\langle \alpha(t)\beta(t)\rangle^2$ is positive, $\Delta n^2 \geq \bar{n}$. We hence observe that the cavity radiation exhibits a super-Poissonian photon statistics for all cases. The super-Poissonian photon statistics has been also reported for the cavity radiation of a degenerate three-level cascade laser in which the atoms are initially prepared in a coherent superposition of the top and bottom levels [15].

5.3 Photon number distribution

5.3.1 Probability for finding n photon pairs

In this section, we seek to determine the probability for finding n photon pairs in the cavity. It is a well established fact that the photon number distribution for the superimposed cavity radiation can be expressed in terms of the corresponding Q-function as

$$P(n,t) = \frac{\pi}{n!}\frac{\partial^{2n}}{\partial\gamma^n\partial\gamma^{*n}}\left[Q(\gamma,t)\exp\left(\gamma^*\gamma\right)\right]_{\gamma=\gamma^*=0}, \tag{5.44}$$

in which the Q-function for the cavity radiation is defined as

$$Q(\gamma,t) = \frac{1}{\pi^2}\int d^2z\,\zeta(z,t)\exp(z^*\gamma - z\gamma^*), \tag{5.45}$$

where

$$\zeta(z,t) = Tr\left[\hat{\rho}(0)e^{-z^*\hat{c}(t)}e^{z\hat{c}^\dagger(t)}\right], \tag{5.46}$$

is the antinormally ordered characteristic function. Now making use of the operator identity,

$$e^{\hat{A}}e^{\hat{B}} = e^{\hat{B}}e^{\hat{A}}e^{[\hat{A},\,\hat{B}]}, \tag{5.47}$$

it is possible to put Eq. (5.46) in the form

$$\zeta(z,t) = e^{-z^*z}Tr\left[\hat{\rho}(0)e^{z\hat{c}^\dagger(t)}e^{-z^*\hat{c}(t)}\right] \tag{5.48}$$

that can also be expressed in terms of the c-number variables associated with the normal ordering as

$$\zeta(z,t) = e^{-z^*z}\big\langle\exp\left(z\gamma^*(t) - z^*\gamma(t)\right)\big\rangle. \tag{5.49}$$

On the other hand, since $\gamma(t)$ is a Gaussian variable with zero mean, one can verify [35] that

$$\big\langle\exp\left(z\gamma^*(t) - z^*\gamma(t)\right)\big\rangle = \exp\left[\frac{1}{2}\big\langle\left(z\gamma^*(t) - z^*\gamma(t)\right)^2\big\rangle\right], \tag{5.50}$$

as a result

$$\zeta(z,t) = e^{-z^*z}\exp\left[\frac{1}{2}\left(z^2\langle\gamma^{*^2}(t)\rangle + z^{*^2}\langle\gamma^2(t)\rangle - 2z^*z\langle\gamma^*(t)\gamma(t)\rangle\right)\right]. \tag{5.51}$$

Moreover, in view of Eqs. (4.2), (4.34), (4.35), (5.2), (5.42), and (5.51), we see that

$$\zeta(z,t) = \exp\left[-az^*z + \frac{b}{2}(z^2 + z^{*^2})\right], \tag{5.52}$$

where

$$a = 1 + \bar{n}, \tag{5.53}$$

$$b = \langle\alpha(t)\beta(t)\rangle. \tag{5.54}$$

Therefore, substitution of Eq. (5.52) into (5.45) results in

$$Q(\gamma,t) = \frac{1}{\pi^2}\int d^2z \exp\left[-az^*z + \frac{b}{2}\left(z^2 + z^{*^2}\right) + z^*\gamma - z\gamma^*\right] \tag{5.55}$$

so that carrying out the integration yields

$$Q(\gamma,t) = \frac{\sqrt{u^2 - v^2}}{\pi}\exp\left[-u\gamma^*\gamma + \frac{v}{2}\left(\gamma^2 + \gamma^{*^2}\right)\right], \tag{5.56}$$

in which

$$u = \frac{a}{a^2 - b^2}, \tag{5.57}$$

$$v = \frac{b}{a^2 - b^2}. \tag{5.58}$$

Furthermore, with the aid of Eq. (5.56) the photon number distribution (5.44) can be rewritten in the form

$$P(n,t) = \frac{\sqrt{u^2 - v^2}}{n!}\frac{\partial^{2n}}{\partial\gamma^n\partial\gamma^{*^n}}\exp\left[\left(1-u\right)\gamma^*\gamma + \frac{v}{2}\left(\gamma^2 + \gamma^{*^2}\right)\right]_{\gamma=\gamma^*=0}. \tag{5.59}$$

This can be expressed in power series as

$$P(n,t) = \frac{\sqrt{u^2 - v^2}}{n!}\frac{\partial^{2n}}{\partial\gamma^n\partial\gamma^{*^n}}\sum_{i,j,k=0}^{\infty}\frac{(1-u)^i v^{j+k}}{2^{j+k}i!j!k!}\gamma^{i+2j}\gamma^{*^{(i+2k)}}|_{\gamma=\gamma^*=0}. \tag{5.60}$$

Performing these differentiations leads to

$$P(n,t) = \frac{\sqrt{u^2 - v^2}}{n!} \times \sum_{i,j,k=0}^{\infty} \frac{(1-u)^i v^{j+k}}{2^{j+k} i! j! k!} \frac{(i+2j)!}{(i+2j-n)!} \frac{(i+2k)!}{(i+2k-n)!} \gamma^{i+2j-n} \gamma^{*(i+2k-n)}|_{\gamma=\gamma^*=0}. \quad (5.61)$$

Next employing the condition

$$\gamma = \gamma^* = 0, \quad (5.62)$$

we see that

$$P(n,t) = \frac{\sqrt{u^2 - v^2}}{n!} \sum_{i,j,k=0}^{\infty} \frac{(1-u)^i v^{j+k}}{2^{j+k} i! j! k!} \frac{(i+2j)!}{(i+2j-n)!} \frac{(i+2k)!}{(i+2k-n)!} \delta_{i+2k,n} \delta_{i+2j,n}. \quad (5.63)$$

We realize that $P(n,t) \neq 0$ provided that

$$2j = n - i, \quad (5.64)$$

$$2k = n - i, \quad (5.65)$$

which implies that

$$j = k, \quad (5.66)$$

$$j = \frac{n-i}{2}. \quad (5.67)$$

Now upon taking Eqs. (5.66) and (5.67) into consideration, we get

$$P(n,t) = n! \sqrt{u^2 - v^2} \sum_{i=0}^{\infty} \frac{(1-u)^i v^{n-i}}{2^{n-i} i! \left[\left(\frac{n-i}{2} \right)! \right]^2} \quad (5.68)$$

that can also be written using Eqs. (5.53), (5.54), (5.57), and (5.58) at steady state as

$$P(n,t) = \frac{n!}{\left[1 + 2\bar{n} + \bar{n}^2 - C_{\alpha\beta}^2\right]^{\frac{1}{2}}} \left(\frac{C_{\alpha\beta}}{1 + 2\bar{n} + \bar{n}^2 - C_{\alpha\beta}^2} \right)^n \times \sum_{i=0}^{\infty} \frac{1}{2^{n-i} i! \left[\left(\frac{n-i)}{2} \right)! \right]^2} \left(\frac{\bar{n} + \bar{n}^2 - C_{\alpha\beta}^2}{C_{\alpha\beta}} \right)^i, \quad (5.69)$$

$$C_{\alpha\beta} = -\left(\frac{AF}{B} - \kappa M\right)\frac{(\lambda_1+\lambda_2)^2 + 4\lambda_1\lambda_2}{8\lambda_1\lambda_2(\lambda_1+\lambda_2)}$$
$$+\left[\kappa N p(q_+ - q_-) - \frac{AC}{B}pq_- + \left(\frac{AF}{2B} - \kappa M\right)(p^2 - q_-q_+)\right]\frac{(\lambda_1+\lambda_2)^2 - 4\lambda_1\lambda_2}{8\lambda_1\lambda_2(\lambda_1+\lambda_2)}$$
$$-\left[\left(\frac{AC}{B}q_- + \kappa N(q_+ + q_-)\right)\right]\frac{\lambda_1 - \lambda_2}{4\lambda_1\lambda_2}, \tag{5.70}$$

with

$$pq_- = \frac{1}{\chi^2}\left(1+\frac{\Omega^2}{\gamma^2}\right)\left[\frac{\Omega}{2\gamma}\left(1+\frac{\Omega^2}{\gamma^2}\right) - \left[\frac{3\eta\Omega}{2\gamma} - \sqrt{1-\eta^2}\left(1-\frac{\Omega^2}{2\gamma^2}\right)\right]\right], \tag{5.71}$$

$$q_- - q_+ = \frac{2}{\chi}\left[\frac{3\eta\Omega}{2\gamma} - \sqrt{1-\eta^2}\left(1-\frac{\Omega^2}{2\gamma^2}\right)\right], \tag{5.72}$$

$$q_-q_+ - p^2 = \frac{1}{\chi^2}\left[\left(1+\frac{\Omega^2}{\gamma^2}\right)\left(\frac{\Omega^2}{4\gamma^2} - 1\right) - \left[\frac{3\eta\Omega}{2\gamma} - \sqrt{1-\eta^2}\left(1-\frac{\Omega^2}{2\gamma^2}\right)\right]^2\right], \tag{5.73}$$

and $q_- + q_+$ and χ are given in Eqs. (4.57) and (4.58). We notice that the factorials are defined for nonnegative integers, which implies that

$$i \leq n \tag{5.74}$$

and i should take odd values when n is odd and even values when n is even. To ensure these conditions, we define $i = 2p$ when n is even and $i = 2q+1$ when n is odd. In view of Eq. (5.74) and these restrictions Eq. (5.69) can be put for even n in the form

$$P(n,t) = \frac{n!}{\left[1+2\bar{n}+\bar{n}^2 - C_{\alpha\beta}^2\right]^{\frac{1}{2}}}\left(\frac{C_{\alpha\beta}}{1+2\bar{n}+\bar{n}^2 - C_{\alpha\beta}^2}\right)^n$$
$$\times\sum_{p=0}^{n/2}\frac{1}{2^{n-2p}(2p)!\left[\left(\frac{n-2p}{2}\right)!\right]^2}\left(\frac{\bar{n}+\bar{n}^2 - C_{\alpha\beta}^2}{C_{\alpha\beta}}\right)^{2p} \tag{5.75}$$

and

$$P(n,t) = \frac{n!}{\left[1+2\bar{n}+\bar{n}^2 - C_{\alpha\beta}^2\right]^{\frac{1}{2}}}\left(\frac{C_{\alpha\beta}}{1+2\bar{n}+\bar{n}^2 - C_{\alpha\beta}^2}\right)^n$$
$$\times\sum_{q=0}^{(n-1)/2}\frac{1}{2^{n-(2q+1)}(2q+1)!\left[\left(\frac{n-(2q+1)}{2}\right)!\right]^2}\left(\frac{\bar{n}+\bar{n}^2 - C_{\alpha\beta}^2}{C_{\alpha\beta}}\right)^{2q+1}, \tag{5.76}$$

for odd n.

We now seek to study the probability for finding n pairs of photons generated by the system under consideration. To this end, we investigate the dependence of the photon number distribution on the linear gain coefficient, squeeze parameter, and amplitude of the driving radiation by alternatively varying these parameters. We first plot the photon number distribution versus the number of photons to be counted for different values of r when $\Omega = 0$. The values of the squeeze parameter are arbitrarily chosen so that the dependence of the photon number distribution is evident from the figure. Moreover, we take $A = 10$ and $\eta = 0.1$.

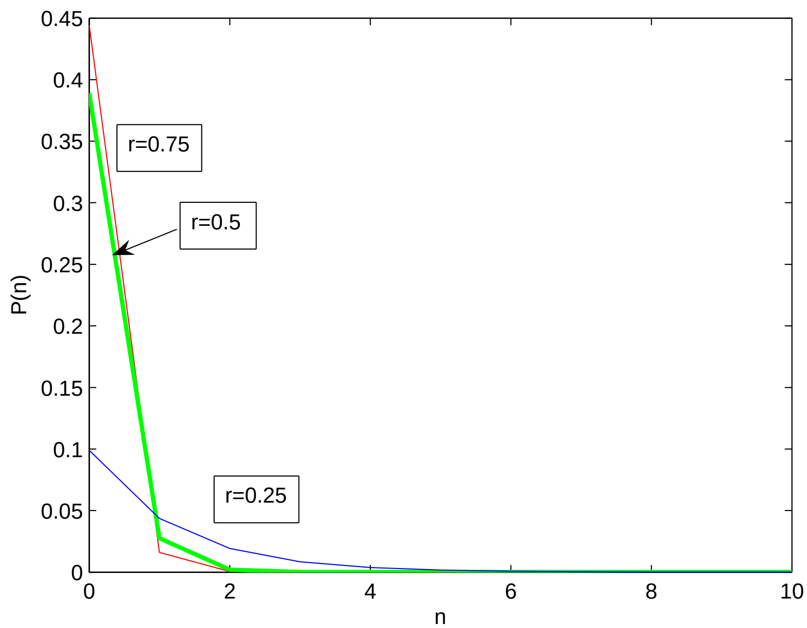

Fig. 5.20: Plots of the photon number distribution of the cavity radiation (Eq. (5.75) and (5.76)) at steady state for $\kappa = 0.5$, $\Omega = 0$, $A = 10$, $\eta = 0.1$, and different values of r.

We clearly see from Fig. 5.20 that the photon number distribution decreases rapidly with the pairs of photons to be counted. We notice that there is no distinct difference in the probability for finding even and odd pairs of photon numbers in the cavity. The photon number distribution increases with the squeeze parameter for $n = 0$, but decreases for $n \neq 0$.

We next plot the photon number distribution versus the number of photons to be counted for different values of r when $\Omega \neq 0$. The values of r, A, and η are taken to be the same as the previous case so that comparison can be made.

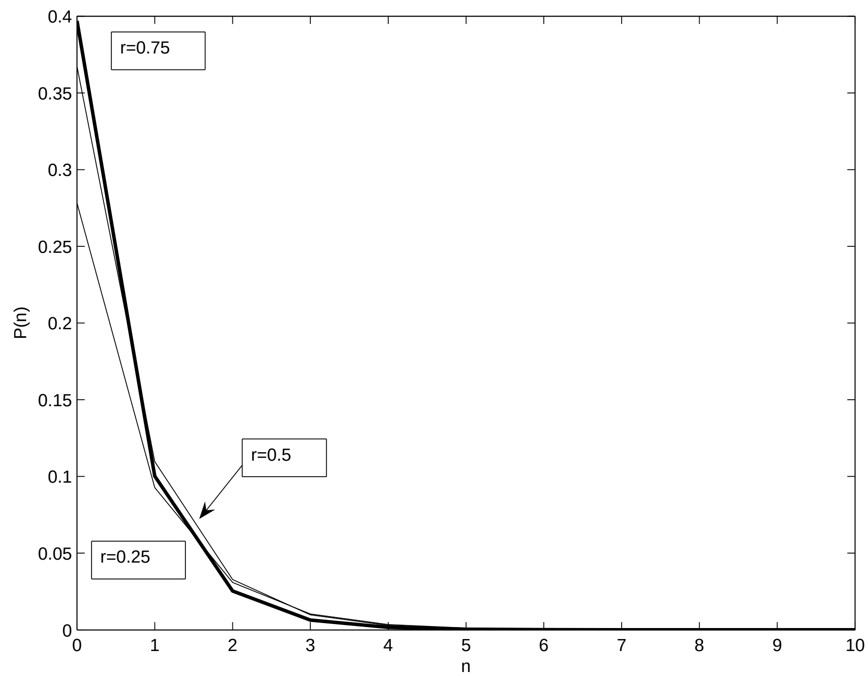

Fig. 5.21: Plots of the photon number distribution of the cavity radiation (Eq. (5.75) and (5.76)) at steady state for $\kappa = 0.5$, $\Omega = 0.1\gamma$, $A = 10$, $\eta = 0.1$, and different values of r.

It is not difficult to see from Fig. 5.21 that the probability for finding n pairs of photons in the cavity decreases rapidly with n. Moreover, comparison of Figs. 5.20 and 5.21 reveals that the probability for finding larger number of photons is lesser in the absence of an external driving radiation.

In the following, we plot the photon number distribution versus the number of pairs of photons to be counted for different values of A, $r = 0.5$, and $\eta = 0.1$. We first consider the case in which $\Omega = 0$.

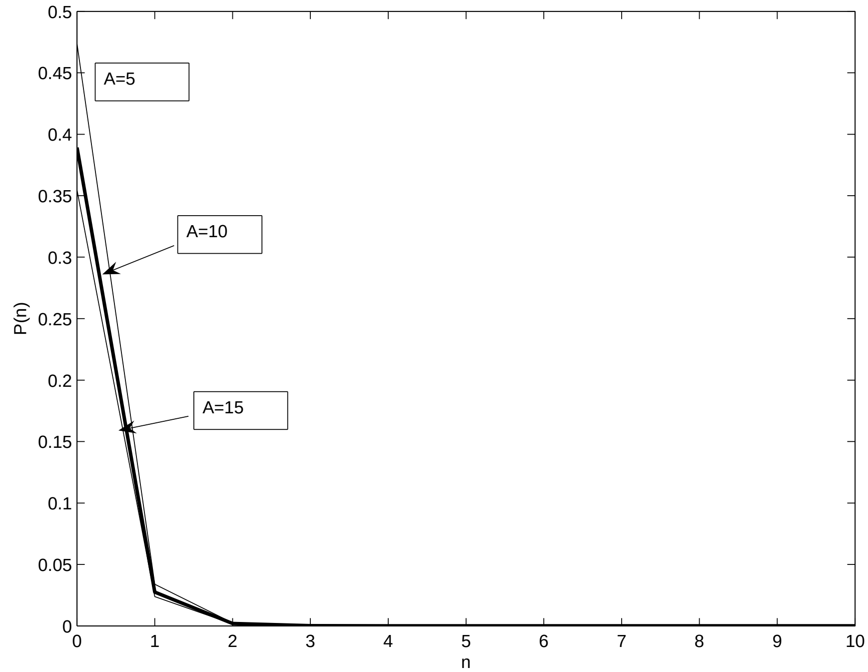

Fig. 5.22: Plots of the photon number distribution of the cavity radiation (Eq. (5.75) and (5.76)) at steady state for $\kappa = 0.5$, $\Omega = 0$, $r = 0.5$, $\eta = 0.1$, and different values of A.

According to the result given in Fig. 5.22, the probability for finding no photon pairs in the cavity decreases with the linear gain coefficient.

We next plot the photon number distribution for similar values of r, A, and η, but $\Omega = 0.1\gamma$.

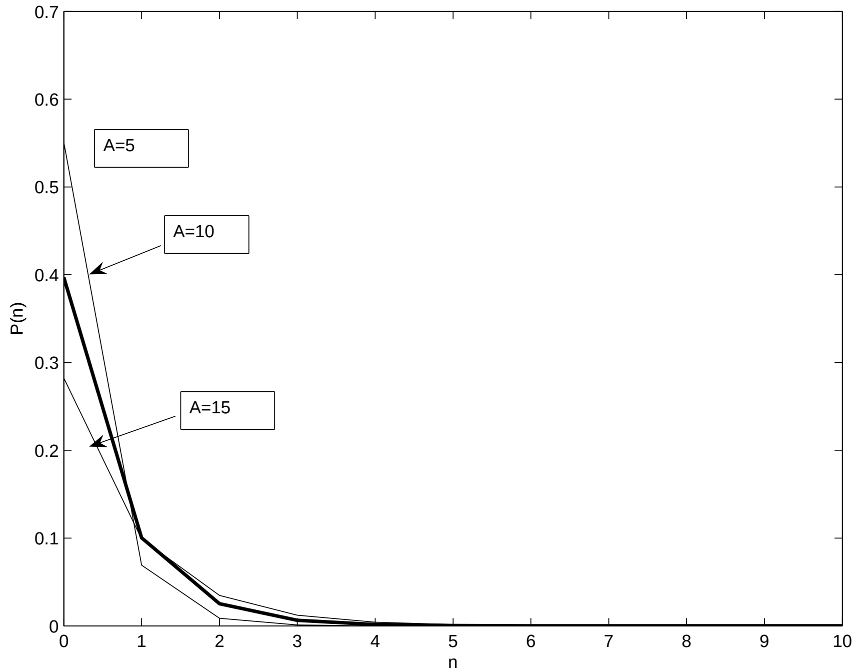

Fig. 5.23: Plots of the photon number distribution of the cavity radiation (Eq. (5.75) and (5.76)) at steady state for $\kappa = 0.5$, $\Omega = 0.1\gamma$, $r = 0.5$, $\eta = 0.1$, and different values of A.

It is possible to see from Figs. 5.22 and 5.23 that the probability for finding larger numbers of photons is larger when there is an external driving radiation. Moreover, we notice that the probability distribution decreases with the number of photons to be counted relatively faster for smaller values of the linear gain coefficient.

5.3.2 Joint probability for finding n photons of mode a and m photons of mode b

We now seek to determine the joint probability for finding n and m photons in a and b cavity modes, respectively, which can be expressed in terms of the corresponding Q-function as

$$P(n,m,t) = \frac{\pi^2}{n!m!}\frac{\partial^{2n}}{\partial\alpha^{*n}\partial\alpha^n}\frac{\partial^{2m}}{\partial\beta^{*m}\partial\beta^m}\left[Q(\alpha,\beta,t)\exp\left(\alpha^*\alpha+\beta^*\beta\right)\right]_{\alpha^*=\alpha=\beta^*=\beta=0}. \quad (5.77)$$

The Q-function for a two-mode radiation, on the other hand, can be defined as

$$Q(\alpha,\beta,t) = \frac{1}{\pi^4}\int d^2z d^2\eta\, \zeta(z,\eta,t)\exp\left[z^*\alpha + \eta^*\beta - z\alpha^* - \eta\beta^*\right], \tag{5.78}$$

where the antinormally ordered characteristic function $\zeta(z,\eta,t)$ for the two-mode radiation is

$$\zeta(z,\eta,t) = Tr\big\{\hat{\rho}(0)e^{-z^*\hat{a}(t)}e^{-\eta^*\hat{b}(t)}e^{z\hat{a}^\dagger(t)}e^{\eta\hat{b}^\dagger(t)}\big\}. \tag{5.79}$$

Using the operator identity (5.47), it is possible to express Eq. (5.79) in terms of c-number variables associated with the normal ordering as

$$\zeta(z,\eta,t) = e^{-z^*z-\eta^*\eta}\big\langle \exp\left[z\alpha^*(t) + \eta\beta^*(t) - z^*\alpha(t) - \eta^*\beta(t)\right]\big\rangle. \tag{5.80}$$

Since $\alpha(t)$ and $\beta(t)$ are Gaussian variables with zero mean, one can verify that [35]

$$\begin{aligned}&\big\langle \exp\left[z\alpha^*(t) + \eta\beta^*(t) - z^*\alpha(t) - \eta^*(t)\beta(t)\right]\big\rangle\\ &= \exp\left[\frac{1}{2}\big\langle(z\alpha^*(t) + \eta\beta^*(t) - z^*\alpha(t) - \eta^*\beta(t))^2\big\rangle\right],\end{aligned} \tag{5.81}$$

as a result

$$\begin{aligned}\zeta(z,\eta,t) = e^{-z^*z-\eta^*\eta}\exp\Bigg[\frac{1}{2}\big(&z^2\langle\alpha^{*^2}(t)\rangle + z^{*^2}\langle\alpha^2(t)\rangle + \eta^2\langle\beta^{*^2}(t)\rangle + \eta^2\langle\beta^2(t)\rangle\\ &-2z^*z\langle\alpha^*(t)\alpha(t)\rangle - 2\eta^*\eta\langle\beta^*(t)\beta(t)\rangle + 2z\eta\langle\alpha^*(t)\beta^*(t)\rangle + 2z^*\eta^*\langle\alpha(t)\beta(t)\rangle\\ &-2z\eta^*\langle\alpha^*(t)\beta(t)\rangle - 2z^*\eta\langle\alpha(t)\beta^*(t)\rangle\big)\Bigg].\end{aligned} \tag{5.82}$$

On account of (4.34), (4.35), (4.44), and (4.45), Eq. (5.82) turns out to be

$$\zeta(z,\eta,t) = \exp\left[-az^*z - b\eta^*\eta + c(z\eta + z^*\eta^*)\right], \tag{5.83}$$

where

$$a = 1 + \langle\alpha^*(t)\alpha(t)\rangle, \tag{5.84}$$

$$b = 1 + \langle\beta^*(t)\beta(t)\rangle, \tag{5.85}$$

$$c = \langle\alpha(t)\beta(t)\rangle. \tag{5.86}$$

Substituting Eq. (5.83) into (5.78) and then carrying out the integration yield

$$Q(\alpha,\beta)=\frac{uv-w^2}{\pi^2}\exp\left[-u\alpha^*\alpha-v\beta^*\beta+w(\alpha\beta+\alpha^*\beta^*)\right], \tag{5.87}$$

in which

$$u=\frac{b}{ab-c^2}, \tag{5.88}$$

$$v=\frac{a}{ab-c^2}, \tag{5.89}$$

$$w=\frac{c}{ab-c^2}. \tag{5.90}$$

Upon inserting Eq. (5.87) into (5.77), the joint probability distribution function can be expressed in power series as

$$P(n,m,t)=\frac{uv-w^2}{n!m!}\frac{\partial^{2n}}{\partial\alpha^{*n}\partial\alpha^n}\frac{\partial^{2m}}{\partial\beta^{*m}\partial\beta^m} \times\sum_{i,j,k,l=0}^{\infty}\frac{(1-u)^i(1-v)^j w^{k+l}}{i!j!k!l!}\alpha^{i+k}\alpha^{*i+l}\beta^{j+k}\beta^{*j+l}|_{\alpha=\alpha^*=\beta=\beta^*=0}. \tag{5.91}$$

Then performing the differentiation and employing the condition

$$\alpha=\alpha^*=\beta=\beta^*=0, \tag{5.92}$$

we find

$$P(n,m,t)=n!m!(uv-w^2)\sum_{i=n-m}^{n}\frac{(1-u)^i(1-v)^{i+m-n}w^{2(n-i)}}{i!(i+m-n)![(n-i)!]^2}. \tag{5.93}$$

This result indicates that there is no finite joint probability for finding more photons in mode b than mode a in the cavity. For $n=m$, we see that

$$P(n,n)=(n!)^2(uv-w^2)\sum_{i=0}^{n}\frac{[(1-u)(1-v)]^i w^{2(n-i)}}{(i!)^2[(n-i)!]^2}. \tag{5.94}$$

It is possible to infer that there is a finite probability for getting equal number of photons in the two modes.

5.4 Variance of the photon number difference

The variance of the photon number difference can be expressed as

$$\Delta I_D^2 = \langle \hat{I}_D^2 \rangle - \langle \hat{I}_D \rangle^2, \tag{5.95}$$

where the photon number difference $\hat{I}_D$ is defined as

$$\hat{I}_D = \hat{a}^\dagger(t)\hat{a}(t) - \hat{b}^\dagger(t)\hat{b}(t). \tag{5.96}$$

One can easily see using Eq. (5.96) that

$$\langle \hat{I}_D^2 \rangle = \langle \hat{a}^\dagger(t)\hat{a}(t)\hat{a}^\dagger(t)\hat{a}(t)\rangle + \langle \hat{b}^\dagger(t)\hat{b}(t)\hat{b}^\dagger(t)\hat{b}(t)\rangle - 2\langle \hat{a}^\dagger(t)\hat{a}(t)\hat{b}^\dagger(t)\hat{b}(t)\rangle, \tag{5.97}$$

which can also be put applying the boson commutation relation (4.3) in the form

$$\langle \hat{I}_D^2 \rangle = \langle \hat{a}^{\dagger^2}(t)\hat{a}^2(t)\rangle + \langle \hat{b}^{\dagger^2}(t)\hat{b}^2(t)\rangle - 2\langle \hat{a}^\dagger(t)\hat{a}(t)\hat{b}^\dagger(t)\hat{b}(t)\rangle$$
$$+ \langle \hat{a}^\dagger(t)\hat{a}(t)\rangle + \langle \hat{b}^\dagger(t)\hat{b}(t)\rangle. \tag{5.98}$$

We notice that the operators in Eq. (5.98) are in the normal order. Hence Eq. (5.98) is expressible in terms of the c-number variables associated with the normal ordering as

$$\langle \hat{I}_D^2 \rangle = \langle \alpha^{*^2}(t)\alpha^2(t)\rangle + \langle \beta^{*^2}(t)\beta^2(t)\rangle - 2\langle \alpha^*(t)\alpha(t)\beta^*(t)\beta(t)\rangle$$
$$+ \langle \alpha^*(t)\alpha(t)\rangle + \langle \beta^*(t)\beta(t)\rangle. \tag{5.99}$$

Since $\alpha(t)$ and $\beta(t)$ are the Gaussian variables with zero mean, one can readily see that

$$\langle \hat{I}_D^2 \rangle = \langle \alpha^{*^2}(t)\rangle\langle \alpha^2(t)\rangle + 2\langle \alpha^*(t)\alpha(t)\rangle^2 + \langle \beta^{*^2}(t)\rangle\langle \beta^2(t)\rangle + 2\langle \beta^*(t)\beta(t)\rangle^2 - 2\langle \alpha(t)\beta(t)\rangle^2$$
$$- 2\langle \alpha^*(t)\alpha(t)\rangle\langle \beta^*(t)\beta(t)\rangle - 2\langle \alpha^*(t)\beta(t)\rangle^2 + \langle \alpha^*(t)\alpha(t)\rangle + \langle \beta^*(t)\beta(t)\rangle. \tag{5.100}$$

It is also possible to express Eq. (5.96) in terms of the c-number variables associated with the normal ordering as

$$\langle \hat{I}_D \rangle = \langle \alpha^*(t)\alpha(t)\rangle - \langle \beta^*(t)\beta(t)\rangle, \tag{5.101}$$

from which follows

$$\langle \hat{I}_D \rangle^2 = \langle \alpha^*(t)\alpha(t)\rangle^2 + \langle \beta^*(t)\beta(t)\rangle^2 - 2\langle \alpha^*(t)\alpha(t)\rangle\langle \beta^*(t)\beta(t)\rangle. \tag{5.102}$$

Now making use of Eqs. (5.95), (5.100), and (5.102), we get

$$\Delta I_D^2 = \langle \alpha^{*^2}(t)\rangle\langle \alpha^2(t)\rangle + \langle \alpha^*(t)\alpha(t)\rangle^2 + \langle \beta^{*^2}(t)\rangle\langle \beta^2(t)\rangle + \langle \beta^*(t)\beta(t)\rangle^2$$
$$- 2\langle \alpha(t)\beta(t)\rangle^2 - 2\langle \alpha^*(t)\beta(t)\rangle^2 + \langle \alpha^*(t)\alpha(t)\rangle + \langle \beta^*(t)\beta(t)\rangle. \qquad (5.103)$$

Therefore, application of Eqs. (4.34), (4.35), and (4.45) finally leads at steady state to

$$\Delta I_D^2 = N_\alpha\big(1+N_\alpha\big) + N_\beta\big(1+N_\beta\big) - 2C_{\alpha\beta}^2, \qquad (5.104)$$

where

$$N_\alpha = \left(\frac{AC}{B} + \kappa N\right)\frac{(\lambda_1+\lambda_2)^2 + 4\lambda_1\lambda_2}{8\lambda_1\lambda_2(\lambda_1+\lambda_2)}$$
$$+ \left[\frac{AC}{B}p^2 + \kappa N(p^2+q_+^2) + \left(\frac{AF}{B} - 2\kappa M\right)pq_+\right]\frac{(\lambda_1+\lambda_2)^2 - 4\lambda_1\lambda_2}{8\lambda_1\lambda_2(\lambda_1+\lambda_2)}$$
$$+ \left[\left(\frac{AC}{B} + \kappa N\right)p + \left(\frac{AF}{2B} - \kappa M\right)q_+\right]\frac{\lambda_1-\lambda_2}{4\lambda_1\lambda_2}, \qquad (5.105)$$

$$N_\beta = \kappa N\frac{(\lambda_1+\lambda_2)^2 + 4\lambda_1\lambda_2}{8\lambda_1\lambda_2(\lambda_1+\lambda_2)}$$
$$+ \left[\frac{AC}{B}q_-^2 + \kappa N(p^2+q_-^2) - \left(\frac{AF}{B} - 2\kappa M\right)pq_-\right]\frac{(\lambda_1+\lambda_2)^2 - 4\lambda_1\lambda_2}{8\lambda_1\lambda_2(\lambda_1+\lambda_2)}$$
$$- \left[\kappa N p - \left(\frac{AF}{2B} - \kappa M\right)q_-\right]\frac{\lambda_1-\lambda_2}{4\lambda_1\lambda_2}, \qquad (5.106)$$

with

$$p^2 = \frac{1}{\chi^2}\left(1+\frac{\Omega^2}{\gamma^2}\right)^2, \qquad (5.107)$$

$$q_+^2 + p^2 = \frac{1}{\chi^2}\left[\left(1+\frac{\Omega^2}{\gamma^2}\right)^2\left(1+\frac{\Omega^2}{4\gamma^2}\right) + \left[\frac{3\eta\Omega}{2\gamma} - \sqrt{1-\eta^2}\left(1-\frac{\Omega^2}{2\gamma^2}\right)\right]^2\right.$$
$$\left. + \frac{\Omega}{\gamma}\left(1+\frac{\Omega^2}{\gamma^2}\right)\left[\frac{3\eta\Omega}{2\gamma} - \sqrt{1-\eta^2}\left(1-\frac{\Omega^2}{2\gamma^2}\right)\right]\right], \qquad (5.108)$$

$$pq_\pm = \frac{1}{\chi^2}\left(1+\frac{\Omega^2}{\gamma^2}\right)\left[-\frac{\Omega}{2\gamma}\left(1+\frac{\Omega^2}{\gamma^2}\right) \mp \left[\frac{3\eta\Omega}{2\gamma} - \sqrt{1-\eta^2}\left(1-\frac{\Omega^2}{2\gamma^2}\right)\right]\right], \qquad (5.109)$$

$$q_-^2 = \frac{1}{\chi^2}\left[\frac{\Omega^2}{4\gamma^2}\left(1+\frac{\Omega^2}{\gamma^2}\right)^2 + \left[\frac{3\eta\Omega}{2\gamma} - \sqrt{1-\eta^2}\left(1-\frac{\Omega^2}{2\gamma^2}\right)\right]^2\right.$$
$$\left. - \frac{\Omega}{\gamma}\left(1+\frac{\Omega^2}{\gamma^2}\right)\left[\frac{3\eta\Omega}{2\gamma} - \sqrt{1-\eta^2}\left(1-\frac{\Omega^2}{2\gamma^2}\right)\right]\right]. \qquad (5.110)$$

In the following, we seek to study the dependence of the variance of the photon number difference on the linear gain coefficient, initial preparation of the atoms, amplitude of the driving radiation, and squeeze parameter by alternatively fixing these parameters. We first plot the variance of the photon number difference versus A for different values of r. $\eta = 0.1$ and $\Omega = 0.1\gamma$ are taken so that comparison with the previous discussions can be made.

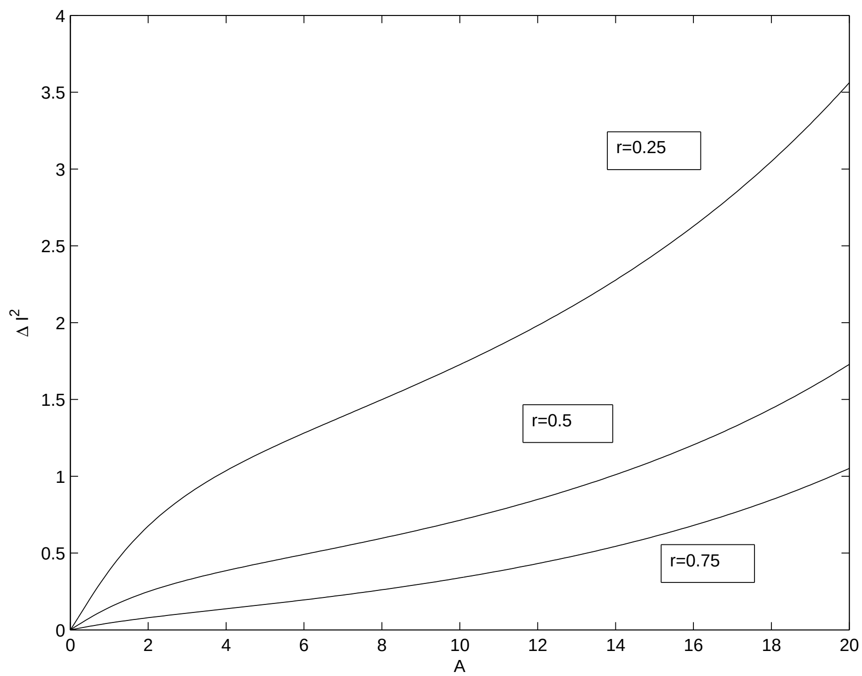

Fig. 5.24: Plots of the variance of the photon number difference of the cavity radiation (Eq. (5.104)) at steady state for $\kappa = 0.5$, $\eta = 0.1$, $\Omega = 0.1$, and different values of r

It is clearly shown in Fig. 5.24 that the variance of the photon number difference increases with the linear gain coefficient, but decreases with the squeeze parameter. Comparison of Figs. 5.4 and 5.24 reveals that the mean number of photon pairs and variance of the photon number difference depend on the squeeze parameter and linear gain coefficient in a similar manner for larger values of A. On the other hand, we observe that the degree of squeezing and variance of the photon number difference increases with the linear gain coefficient for smaller values of A. However, the variance of the photon number difference decreases with the squeeze parameter as opposed to the degree of squeezing.

We next plot the variance of the photon number difference versus the initial preparation of the atoms for different values of A. The squeeze parameter and amplitude of the driving radiation are taken to be $r = 0.75$ and $\Omega = 0.1\gamma$.

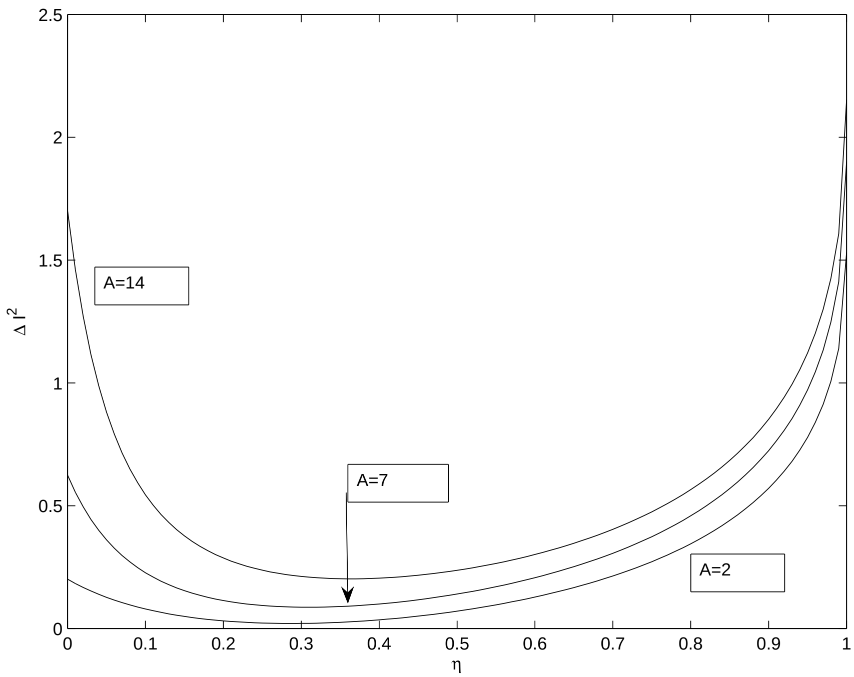

Fig. 5.25: Plots of the variance of the photon number difference of the cavity radiation (Eq. (5.104)) at steady state for $\kappa = 0.5$, $\Omega = 0.1\gamma$, $r = 0.75$, and different values of A.

Fig. 5.25 indicates that the variance of the photon number difference increases with the linear gain coefficient as in the previous case. One can see that the variance of the photon number difference is larger for a maximum or minimum atomic coherence. On the basis of the result given in Fig. 4.2, we notice that the quadrature variance and variance of the photon number difference depend on the linear gain coefficient and initial preparation of the atoms in a similar manner in the given ranges.

We next plot the variance of the photon number difference versus Ω/γ for different values of r. We take $\eta = 0.1$ and $A = 1.3$.

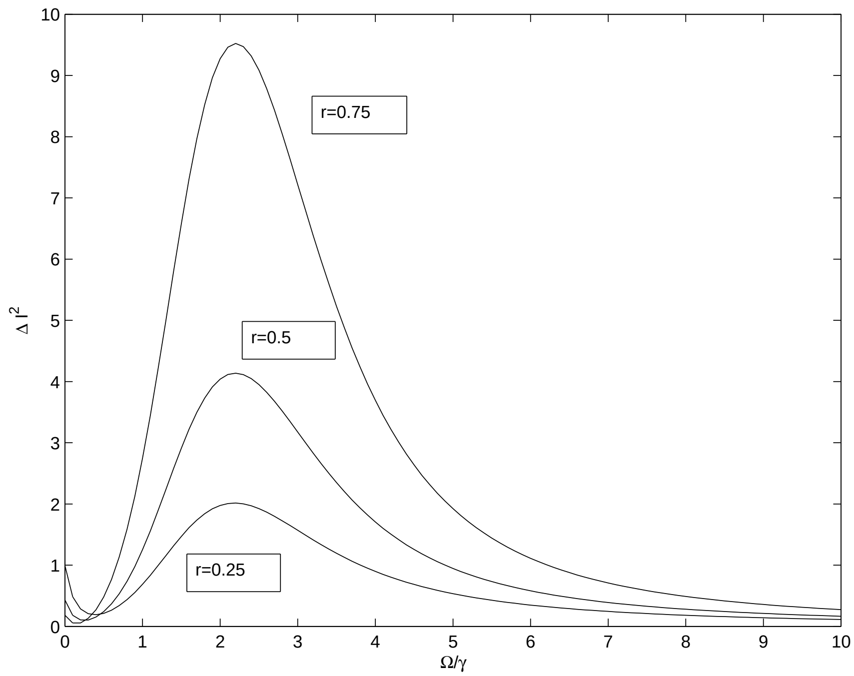

Fig. 5.26: Plots of the variance of the photon number difference of the cavity radiation (Eq. (5.104)) at steady state for $\kappa = 0.5$, $A = 1.3$, $\eta = 0.1$, and different values of r

As clearly shown in Fig. 4.7, the degree of squeezing increases with the squeeze parameter for smaller values of Ω/γ, unlike the variance of the photon number difference. It is not difficult to see from Figs. 5.7 and 5.26 that the mean number of photon pairs and variance of the photon number difference take large values for the same range of Ω/γ and both increase with the squeeze parameter when there is no squeezing.

We next plot the variance of the photon number difference versus η for different values of A when $\Omega = 0$. The squeeze parameter is taken to be $r = 0.75$.

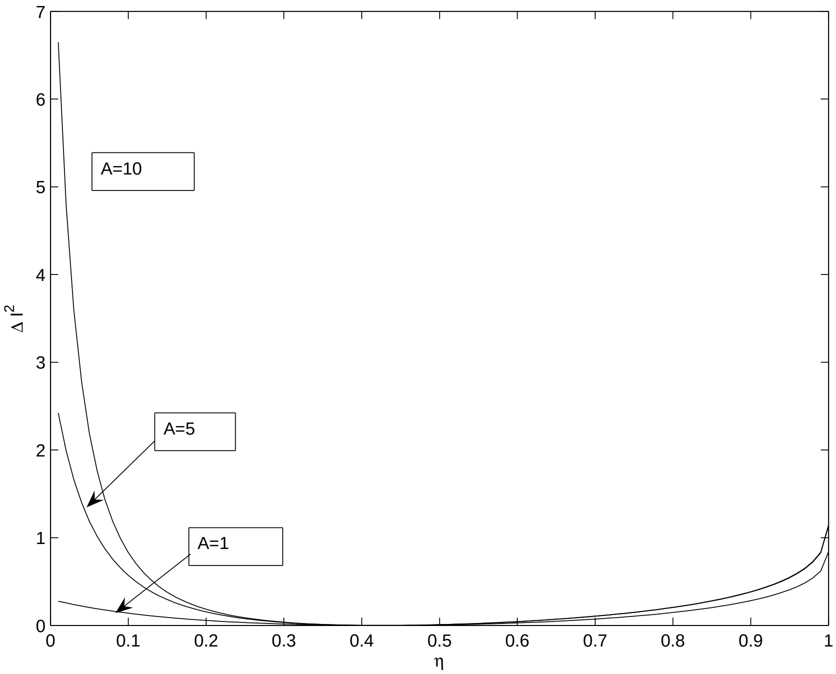

Fig. 5.27: Plots of the variance of the photon number difference of the cavity radiation (Eq. (5.104)) at steady state for $\kappa = 0.5$, $\Omega = 0$, $r = 0.75$, and different values of A.

We see from Fig. 5.27 that the variance of the photon number difference increases with the linear gain coefficient. It is not difficult to see that the variance of the photon number difference near $\eta = 0.4$ is zero for all values of A when $r = 0.75$.

We next plot the variance of the photon number difference versus η for different values of r when $\Omega = 0$. The linear gain coefficient is taken to be $A = 1$ so that the dependence of the variance of the photon number difference is evident from the figure.

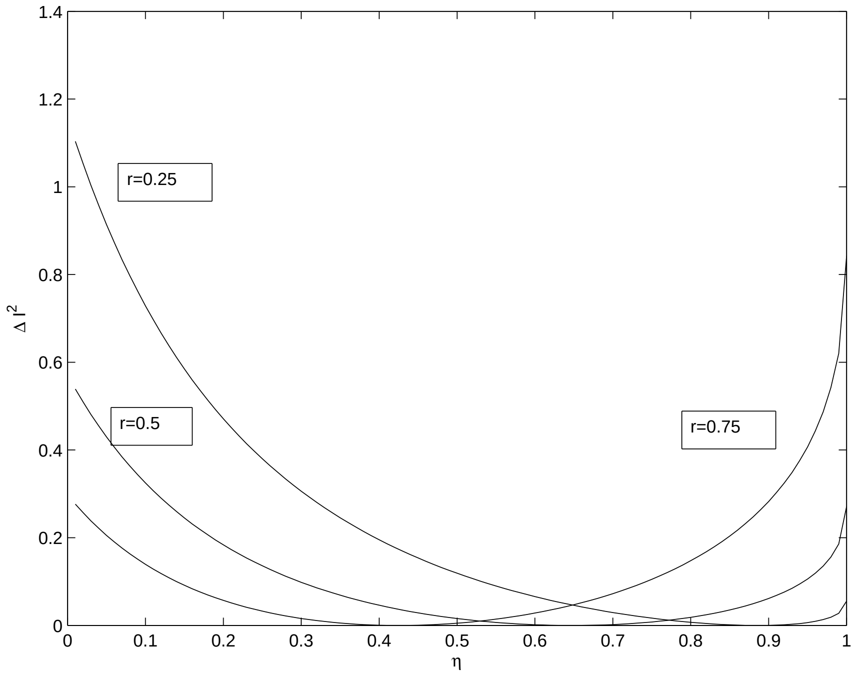

Fig. 5.28: Plots of the variance of the photon number difference of the cavity radiation (Eq. (5.104)) at steady state for $\kappa = 0.5$, $\Omega = 0$, $A = 1$, and different values of r.

As clearly shown in Fig. 5.28, the variance of the photon number difference turns out to be zero for specific values of η corresponding to each squeeze parameter. The larger the squeeze parameter, the smaller the value of η for which the variance of the photon number difference would be zero.

We next plot the variance of the photon number difference versus Ω/γ for different values of A when $\eta = 0$ and $r = 0$.

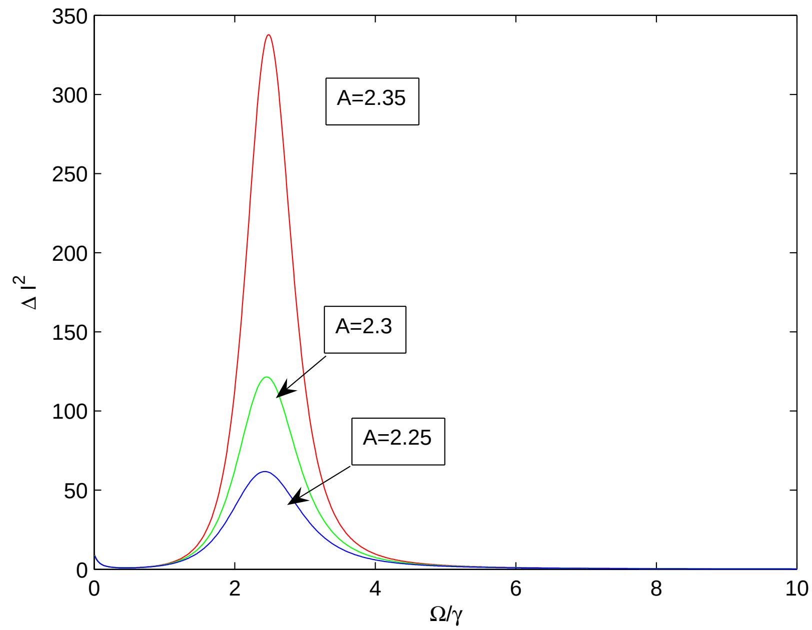

Fig. 5.29: Plots of the variance of the photon number difference of the cavity radiation (Eq. (5.104)) at steady state for $\kappa = 0.5$, $\eta = 0$, $r = 0$, and different values of A.

It is not difficult to see from Fig. 5.29 that the variance of the photon number difference generally increases with the linear gain coefficient. Moreover, comparison of Figs. 5.8 and 5.29 shows that the variance of the photon number difference can be greater than the corresponding mean number of the photon number.

We next plot the variance of the photon number difference versus Ω/γ for different values of r when $\eta = 0$ and $A = 2.35$.

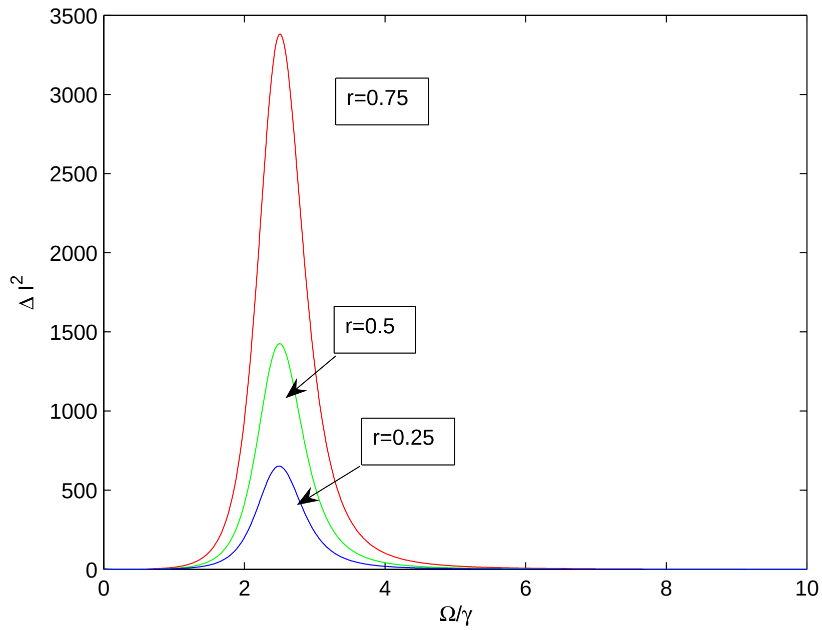

Fig. 5.30: Plots of the variance of the photon number difference of the cavity radiation (Eq. (5.104)) at steady state for $\kappa = 0.5$, $\eta = 0$, $A = 2.35$, and different values of r.

As clearly shown in Fig. 5.30, the variance of the photon number difference turns out to be very large for some values of the amplitude of the driving radiation. It is also possible to observe that the variance of the photon number difference can increase with the squeeze parameter.

We next plot the variance of the photon number difference versus Ω/γ and η. The linear gain coefficient and squeeze parameter are taken to be $A = 48$ and $r = 0.75$.

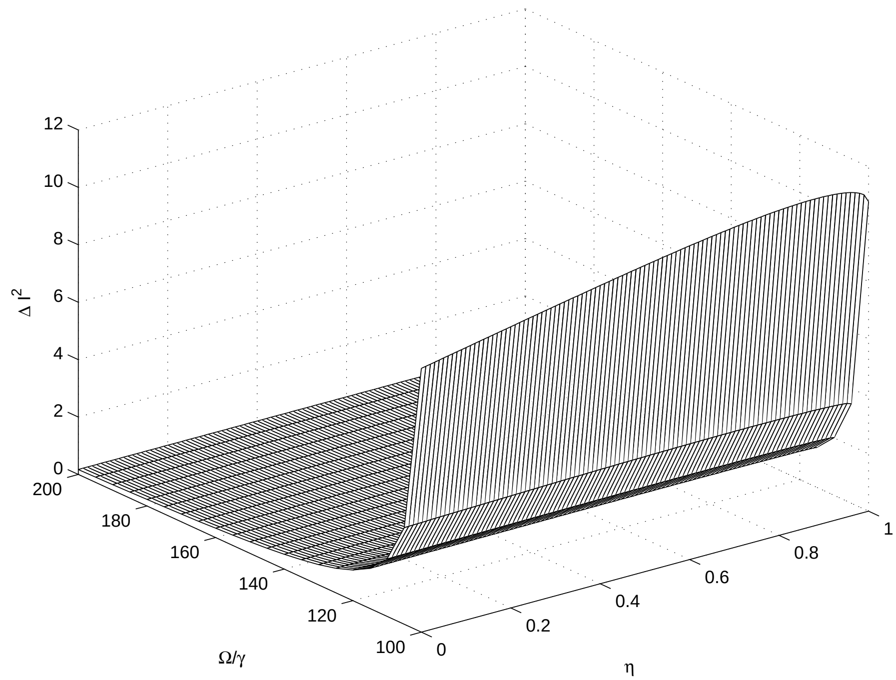

Fig. 5.31: Plot of the variance of the photon number difference of the cavity radiation (Eq. (5.104)) at steady state for $\kappa = 0.5$, $A = 48$, and $r = 0.75$

We see from Fig. 5.31 that the variance of the photon number difference decreases with the amplitude of the driving radiation in the strong driving limit. We notice that the dependence of the variance of the photon number difference on the way the atoms are initial prepared is insignificant in this case. Comparison of the results shown in Figs. 5.17 and 5.31 reveals that the mean number of photon pairs and variance of the photon number difference depend on the initial preparation of the atoms and amplitude of the driving radiation in a similar manner.

6

Conclusion

In this dissertation the squeezing of the cavity radition as well as the output radiation and the statistical properties of the cavity radiation of a nondegenerate three-level cascade laser, in which the tope and bottom levels of the atoms are coupled by a strong radiation and the cavity is coupled to a two-mode squeezed vacuum reservoir, are analyzed. It is found that a strong squeezed radiation can be generated either for a weak or strong driving radiation for certain values of A, r, and η, whereas the cavity radiation exhibits super-Poissonian photon statistics for all values of the amplitude of the driving radiation. Even though the squeezing of the cavity radiation and the mean number of photon pairs in general increase with A, the values of A cannot be arbitrarily large when there is an external coherent radiation. However one can produce a strong squeezed radiation in the absence of an external coherent radiation, since there is no limit to the values of A in this case.

The mean number of photon pairs is relatively small for many cases for which the degree of squeezing is relatively high. But this does not hold true when there is no external coherent radiation. Although the degree of squeezing and mean number of photon pairs increase with r under various conditions, it turns out that the degree of squeezing decreases with r when η is close to 1 and the mean number of photon pairs decreases with r when η is close to 0. Moreover, it is found that there is no distinct difference in the probability for finding odd and even pairs of photons in the cavity which agrees with the result obtained by Ansari [10] for the degenerate case. In addition, the mean number of photons in mode a turns out to be greater than that in mode b.

The variance of the photon number difference turns out to be zero for certain values of η, A, and r when $\Omega = 0$. On top of this, there is an indication that Δc_{-}^2 can be related to ΔI_D^2. If this claim is proved to be correct, the quantification of the available degree of squeezing can be carried out by ordinary photon counting techniques which is far more easy when compared to the otherwise employed hetrodyne measurement. In general terms, this study at large demonstrates that the degree of squeezing and $\bar{n}$ can be increased by carefully selecting the involved parameters. It is, hence, hoped that the versatility in the system under consideration perhaps makes it an attractive viable scheme to produce a bright two-mode squeezed light that can be applied in testing of various continuous variable nonclassical correlations.

7

Appendix

7.1 Expectation values of reservoir modes

In this appendix we seek to obtain various expectation values involving the squeezed vacuum reservoir modes following the procedure introduced by Fesseha [29]. In particular, we consider the case in which a two-mode squeezed vacuum is incident on a single-port mirror. The reservoir modes in this case can be described by

$$|r\rangle_k = \hat{S}_k(r)|0,0\rangle, \tag{A1}$$

where

$$\hat{S}_k(r) = e^{r(\hat{a}_k^\dagger \hat{b}_k^\dagger - \hat{a}_k \hat{b}_k)} \tag{A2}$$

is the two-mode squeeze operator. Here k varies around $(k_a + k_b)/2$, in which k_a and k_b are the wave numbers of the cavity modes. We note that the corresponding density operator is expressible as

$$\hat{\rho}_k = \hat{S}_k(r)|0,0\rangle\langle 0,0|\hat{S}_k^\dagger(r). \tag{A3}$$

Applying this density operator, one can write

$$\langle \hat{a}_k \rangle = \langle 0,0|\hat{a}_k(r)|0,0\rangle, \tag{A4}$$

$$\langle \hat{b}_k \rangle = \langle 0,0|\hat{b}_k(r)|0,0\rangle, \tag{A5}$$

where

$$\hat{a}_k(r) = \hat{S}_k^\dagger(r)\hat{a}_k\hat{S}_k(r), \tag{A6}$$

$$\hat{b}_k(r) = \hat{S}_k^\dagger(r)\hat{b}_k\hat{S}_k(r). \tag{A7}$$

Now with the aid of Eqs. (A2), (A6), and (A7), one can verify that

$$\hat{a}_k(r) = \hat{a}_k \cosh r + \hat{b}_k^\dagger \sinh r, \tag{A8}$$

$$\hat{b}_k(r) = \hat{b}_k \cosh r + \hat{a}_k^\dagger \sinh r, \tag{A9}$$

in which

$$\hat{a}_k = \hat{a}_k(0), \tag{A10}$$

$$\hat{b}_k = \hat{b}_k(0). \tag{A11}$$

Substituting (A8) into Eq. (A4), we have

$$\langle \hat{a}_k \rangle = \cosh r \langle 0,0|\hat{a}_k|0,0\rangle + \sinh r \langle 0,0|\hat{b}_k^\dagger|0,0\rangle, \tag{A12}$$

from which follows

$$\langle \hat{a}_k \rangle = 0. \tag{A13}$$

Furthermore, using the fact that

$$\hat{S}_k^\dagger(r)\hat{S}_k(r) = \hat{I} \tag{A14}$$

along with Eqs. (A3), (A6), and (A14), we obtain

$$\langle \hat{a}_k^\dagger \hat{a}_{k'} \rangle = \langle 0,0|\hat{a}_k^\dagger(r)\hat{a}_{k'}(r)|0,0\rangle. \tag{A15}$$

With the aid of Eq. (A8), one can put (A15) in the form

$$\langle \hat{a}_k^\dagger \hat{a}_{k'} \rangle = \cosh^2 r \langle 0,0|\hat{a}_k^\dagger \hat{a}_{k'}|0,0\rangle + \sinh^2 r \langle 0,0|\hat{b}_k \hat{b}_{k'}^\dagger|0,0\rangle$$

$$+ \cosh r \sinh r \langle 0,0|\hat{b}_k \hat{a}_{k'}|0,0\rangle + \cosh r \sinh r \langle 0,0|\hat{a}_k^\dagger \hat{b}_{k'}^\dagger|0,0\rangle. \tag{A16}$$

It then follows that

$$\langle \hat{a}_k^\dagger \hat{a}_{k'} \rangle = N\delta_{kk'}, \tag{A17}$$

where

$$N = \sinh^2 r. \tag{A18}$$

Now employing the commutation relation

$$[\hat{a}_k, \hat{a}^\dagger_{k'}] = \delta_{kk'}, \tag{A19}$$

and Eq. (A17), one readily obtains

$$\langle \hat{a}_k \hat{a}^\dagger_{k'} \rangle = (N+1)\delta_{kk'}. \tag{A20}$$

Following the same procedure, one can easily verify that

$$\langle \hat{a}_k \hat{a}_{k'} \rangle = 0. \tag{A21}$$

It can also be established in a similar manner that

$$\langle \hat{b}_k \rangle = 0, \tag{A22}$$

$$\langle \hat{b}^\dagger_k \hat{b}_{k'} \rangle = N\delta_{kk'}, \tag{A23}$$

$$\langle \hat{b}_k \hat{b}^\dagger_{k'} \rangle = (N+1)\delta_{kk'}, \tag{A24}$$

$$\langle \hat{b}_k \hat{b}_{k'} \rangle = 0. \tag{A25}$$

Moreover, applying Eqs. (A8) and (A9), one can write

$$\langle \hat{a}_k \hat{b}_{k'} \rangle = \cosh^2 r \langle 0,0|\hat{a}_k \hat{b}_{k'}|0,0\rangle + \sinh^2 r \langle 0,0|\hat{b}^\dagger_k \hat{a}^\dagger_{k'}|0,0\rangle$$

$$+ \cosh r \sinh r \langle 0,0|\hat{a}_k \hat{a}^\dagger_{k'}|0,0\rangle + \cosh r \sinh r \langle 0,0|\hat{b}^\dagger_k \hat{b}_{k'}|0,0\rangle, \tag{A26}$$

from which follows

$$\langle \hat{a}_k \hat{b}_{k'} \rangle = M\delta_{kk'}, \tag{A27}$$

where

$$M = \cosh r \sinh r. \tag{A28}$$

It can also be shown in a similar manner that

$$\langle \hat{a}_k \hat{b}^\dagger_{k'} \rangle = 0. \tag{A29}$$

We assume that k varies very little around $(k_a + k_b)/2$. We can then write

$$k \approx k_a + k_b - k. \tag{A30}$$

Hence on the basis of (A30), Eq. (A27) can be put in form

$$\langle \hat{a}_k \hat{b}_{k'} \rangle = M\delta_{k_a+k_b-k,k'}. \tag{A31}$$

7.2 Correlation properties of the noise operators

The noise operators associated with a two-mode squeezed vacuum reservoir are defined by

$$\hat{F}_{Ra}(t) = \sum_k \lambda_k \hat{a}_k e^{i(\omega_a - \omega_k)t}, \qquad (B1)$$

$$\hat{F}_{Rb}(t) = \sum_j \lambda_j \hat{b}_j e^{i(\omega_b - \omega_j)t}, \qquad (B2)$$

where λ_k and λ_j are the coupling constants. It is not difficult to see from Eqs. (A13) and (A22) that

$$\langle \hat{F}_{Ra}(t') \rangle = \langle \hat{F}_{Rb}(t') \rangle = 0. \qquad (B3)$$

With the aid of Eq. (B1), it is possible to write

$$\langle \hat{F}^\dagger_{Ra}(t)\hat{F}_{Ra}(t') \rangle = \sum_{k,k'} \lambda_k \lambda_{k'} \langle \hat{a}^\dagger_k \hat{a}_{k'} \rangle e^{-i(\omega_a - \omega_k)t + i(\omega_a - \omega_k)t'}. \qquad (B4)$$

It then follows from the application of Eq. (A17) that

$$\langle \hat{F}^\dagger_{Ra}(t)\hat{F}_{Ra}(t') \rangle = N \sum_k \lambda_k^2 e^{-i(\omega_a - \omega_k)(t-t')}. \qquad (B5)$$

On account of Eq. (2.77), one readily gets

$$\langle \hat{F}^\dagger_{Ra}(t)\hat{F}_{Ra}(t') \rangle = \kappa N \delta(t - t'). \qquad (B6)$$

It can be verified in a similar manner that

$$\langle \hat{F}_{Ra}(t)\hat{F}^\dagger_{Ra}(t') \rangle = \langle \hat{F}_{Rb}(t)\hat{F}^\dagger_{Rb}(t') \rangle = \kappa(N+1)\delta(t - t'), \qquad (B7)$$

$$\langle \hat{F}_{Ra}(t)\hat{F}_{Ra}(t') \rangle = \langle \hat{F}_{Rb}(t)\hat{F}_{Rb}(t') \rangle = 0, \qquad (B8)$$

$$\langle \hat{F}^\dagger_{Rb}(t)\hat{F}_{Rb}(t') \rangle = \kappa N \delta(t - t'), \qquad (B9)$$

where the mean photon numbers for the two modes are taken to be the same. Furthermore, making use of Eqs. (B1) and (B2), we see that

$$\langle \hat{F}_{Rb}(t)\hat{F}_{Ra}(t') \rangle = \sum_{k,j} \lambda_k \lambda_j \langle \hat{a}_k \hat{b}_j \rangle e^{i(\omega_a - \omega_k)t + i(\omega_b - \omega_j)t'}. \qquad (B10)$$

Hence in view of Eq. (A23), we find

$$\langle \hat{F}_{Rb}(t)\hat{F}_{Ra}(t')\rangle = \kappa M\delta(t-t'). \qquad (B11)$$

It can also be obtained in a similar manner that

$$\langle \hat{F}^{\dagger}_{Rb}(t)\hat{F}_{Ra}(t')\rangle = 0, \qquad (B12)$$

$$\langle \hat{F}_{Ra}(t)\hat{F}_{Rb}(t')\rangle = \kappa M\delta(t-t'). \qquad (B13)$$

Bibliography

[1] M. O. Scully, Phys. Rev. Lett. **55**, 2802 (1985).

[2] M. O. Scully and M. S. Zubairy, Phys. Rev. A **35**, 752 (1987).

[3] M. O. Scully and M. S. Zubairy, Opt. Commun. **66**, 303 (1988).

[4] M. O. Scully, K. Wodkiewicz, M. S. Zubairy, J. Bergou, N. Lu, and J. Meyer ter Van, Phys. Rev. lett. **60**, 1832 (1988).

[5] J. Anwar and M. S. Zubairy, Phys. Rev. A **49**, 481 (1994).

[6] Mesfin Abayneh (MSc Thesis, Addis Ababa University, 2001).

[7] N. A. Ansari, J. G. Banacloche, and M. S. Zubairy, Phys. Rev. A **41**, 5179 (1990).

[8] N. A. Ansari, Phys. Rev. A **46**, 1560 (1992).

[9] C. A. Blockley and D. F. Walls, Phys. Rev. A **43**, 5049 (1991).

[10] N. A. Ansari, Phys. Rev. A **48**, 4686 (1993).

[11] H. Xiong, M. O. Scully, and M. S. Zubairy, Phys. Rev. Lett. **94**, 023601 (2005).

[12] Driba Demissie (MSc Thesis, Addis Ababa University, 2001).

[13] Adane Samuel (MSc Thesis, Addis Ababa University, 2003).

[14] Eyob Alebachew (MSc Thesis, Addis Ababa University, 2003).

[15] N. Lu, Phys. Rev. A **42**, 6756 (1990).

[16] K. Fesseha, Phys. Rev. A **63**, 033811 (2001).

[17] S. An and M. Sargent III, Phys. Rev. A **39**, 1841 (1989).

[18] C. J. Villas-Boas and M. H. Y. Moussa, Eur. Phys. J. D **32**, 147 (2005).

[19] X. Hu and Z. Xu, J. Phys. B: At. Mol. Opt. Phys. **34**, 787 (2001).

[20] V. Buhner and C. Tamm, Phys. Rev. A **61**, 061801(R) (2000).

[21] J. Evers and C. H. Keitel, Phys. Rev. A **65**, 033813 (2002).

[22] A. Einstein, B. Podolsky, and R. Rosen, Phys. Rev. **47**, 777 (1935).

[23] P. Lodahl, Phys. Rev. A **68**, 023806 (2003).

[24] H. Jeong, J. Lee, and M. S. Kim, Phys. Rev. A **61**, 052101 (2000).

[25] Z. B. Chen, J. W. Pan, G. Hou, and Y. D. Zhang, Phys. Rev. Lett. **88**, 040406 (2002).

[26] K. Fesseha, Opt. Commun. **156**, 145 (1998).

[27] R. E. Slusher, B. Yurke, P. Grangier, A. Laporta, D. F. Walls, and M. Reid, J. Opt. Soc. Am. B **4**, 1453 (1987).

[28] G. J. Milburn, M. D. Levenson, M. R. Shelby, S. H. Perlmutter, R. G. Devoe, and D. F. Walls, J. Opt. Soc. Am. B **4**, 1476 (1987).

[29] Fesseha kassahun, *Fundamentals of Quantum Optics* (Lulu, North Carolina, 2008).

[30] M. O. Scully and M. S. Zubairy, *Quantum Optics* (Cambridge University Press, Cambridge, 1997).

[31] L. S. Terreros and F. J. Bermejo, Phys. Rev. A **45**, 1906 (1992).

[32] C. W. Gardiner and M. J. Collett, Phys. Rev. A **31**, 3761 (1985).

[33] W. H. Louisell, *Quantum statistical properties of radiation* (Wiley, Newyork, 1973).

[34] S. M. Barnett and P. M. Badmore, *Methods in theoretical quantum optics* (Oxford University Press, New York 1997).

[35] W. Chow, W. Koch, and M. Sargent III, *Semiconductor Laser Physics* (Springer-Verlag, Berline, 1994).